

https://dspace.org/

Investigation of the Pt-Al-Cr system as part of the development of the Pt-Al-Cr-Ru thermodynamic database

Suss, Rainer

2008-09-03T11:52:13Z
http://hdl.handle.net/10539/5591

Downloaded from a DSpace repository. https://dspace.org/

PART TWO: PHASE ANALYSES OF THE Pt-Al-Cr SYSTEM

1. EXPERIMENTAL PROCEDURE

The alloys were prepared by arc-melting the pure (at least 99.9%) elements several times to attempt homogeneity. The as-cast samples were cut in half with an Accutom® cutting wheel, mounted and ground to 1200 grit on SiC paper. The samples were then polished using an oxide polishing (OP-S) system, by which polishing is achieved through a combination of chemical treatment (the solution has a pH of 8) and gentle abrasive action. It allows selective polishing of softer phases and makes subsequent etching of the sample superfluous. The other halves were heat treated in air in a muffle furnace at 1000°C for 1000 hours and quenched in water. Metallographic sample preparation was carried out as before. The microstructure was examined using a JEOL JSM-840 scanning electron microscope (SEM) and, where possible (i.e. where the phases were larger than 3 μm), the phase- and overall compositions of the samples were analysed using a Tracor Northern energy dispersive X-ray spectrometer (EDS) with Vantage software. Pure element standards were used. The energy dispersive X-ray spectrometry (EDX) analyses were carried out at an accelerating voltage of 20kV, and at least four analyses were carried out to obtain an average composition. Samples were usually imaged in the backscattered electron (BSE) imaging mode. The BSE detector used was a Si P-N junction (divided annular type). X-ray diffraction (XRD) analyses were conducted on the polished samples using a Siemens Kristalloflex with Mo Kα radiation. Although powder diffraction would have been preferred, the number of samples, availability of equipment, and the different nature of alloys with regard to brittleness/toughness which would affect ease of sample preparation for powder diffraction, made the use of bulk samples more convenient. Computer modelling, using the *Crystallographica* package, available from Oxford Cryosystems, was used to predict XRD patterns of some phases that were in Pearson's handbook [1985Vil] but not in the JCPDS database [2000Jcp]. After examination, the as-cast samples were heat treated intermittently (due to power failures) in air in a muffle furnace at 600°C for a total of 2500 hours (the last continuous period being ~1000h) and quenched in water. Metallographic preparation and microscopic examination were carried out as before.

2. RESULTS AND DISCUSSION

2.1. Phase analysis – as cast

2.1.1. Nominal $Pt_{10}:Al_{10}:Cr_{80}$

Alloy $Pt_{10}:Al_{10}:Cr_{80}$ comprised dark dendrites with a mixture of light and dark located interdendritically (Figure 2.1). The EDX analyses are given in Table 2.1 and also shown graphically in Figure 2.2. The sample cracked heavily in the sectioning process and not enough material was available for XRD analysis. However, the alloy's resemblance both in microstructure and EDX analyses to that of alloy $Pt_{20}:Al_{20}:Cr_{60}$ (Figures 2.12 and 13) made it possible to confirm the identities of the phases. From the XRD analysis of alloy $Pt_{20}:Al_{20}:Cr_{60}$ (Figure 2.14) and the position of its phases on the ternary diagram (Figure 2.13) it would appear that the light phase was ~PtAl and the dark phase (Cr) (W-type). In both these alloys there was a suggestion of a fine eutectic mixture. The XRD pattern for PtAl was modelled with *Crystallographica*, and the cubic FeSi-type's pattern (B20) seemed to be a good fit to some of the measured peaks (Figure 2.14). The microstructure formed by:

$$L \rightarrow (Cr)$$

followed by an eutectic reaction

$$L \rightarrow (Cr) + \sim PtAl.$$

The standard deviation in composition of the white phase was quite large (Table 2.1), probably because the white regions were very small and its analyses probably affected by the surrounding dark phase. The composition for the light phase in alloy $Pt_{20}:Al_{20}:Cr_{60}$ (Figure 2.13) is likely to be more accurate, since its standard deviation was smaller.

The XRD peaks of W-type Cr was used throughout this investigation for the identification of (Cr). Also, B20 PtAl was used throughout.

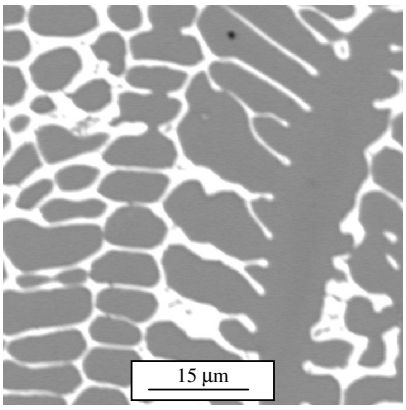

Figure 2.1. BSE-SEM image of nominal $Pt_{10}:Al_{10}:Cr_{80}$ in the as-cast condition: (Cr) dark; ~PtAl light.

Table 2. 1. Phase analyses for nominal $Pt_{10}:Al_{10}:Cr_{80}$ (at.%) in the as-cast condition.

Phase description	**Pt**	**Al**	**Cr**	**Phase**
Overall	9.2 ± 1.2	9.3 ± 1.3	81.5 ± 2.5	-
Dark	4.0 ± 0.1	3.9 ± 0.1	92.1 ± 0.1	(Cr)
Light	39.4 ± 1.2	37.6 ± 1.4	23.0 ± 2.6	~PtAl

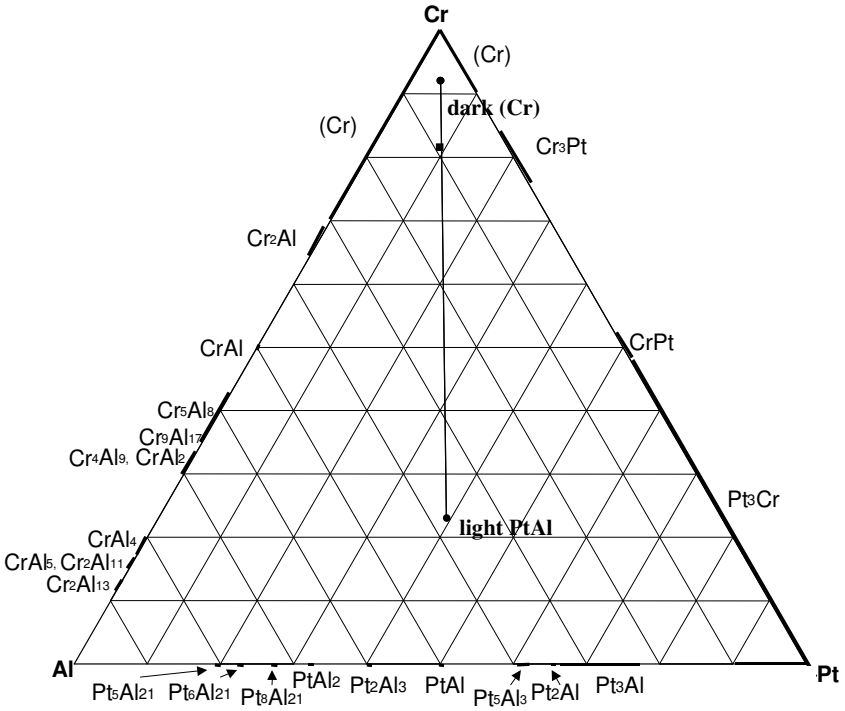

Figure 2.2. EDX analyses of nominal $Pt_{10}:Al_{10}:Cr_{80}$ (at.%) in the as-cast condition.

(■ overall composition; ● phases)

2.1.2. Nominal $Pt_{10}:Al_{30}:Cr_{60}$

Alloy $Pt_{10}:Al_{30}:Cr_{60}$ comprised dark (Cr) (W type) dendrites with fine grey precipitates inside, as well as an interdendritic eutectic mixture of dark (Cr) and light ~$PtAl_2$ (Figure 2.3). The results of the EDX analyses are given in Table 2.2 and shown graphically in Figure 2.4. The standard deviation in the overall composition was very large which could mean that the alloy was not very homogeneous. Furthermore, the light phase was very small (smaller than the potential ~3µm size of beam spread on interaction) and its analyses were definitely affected by the surrounding phase. Its composition could therefore be extrapolated along the tie-line to lower levels of Cr, but only subsequent alloys would tell to what extent. The dark analysis would also incorporate both the dark phase and the precipiates. The peaks for (Cr) and ~$PtAl_2$ were an excellent fit for the measured XRD pattern (Figure 2.5), although slightly shifted. (Note that the shift has already been incorporated in Figure 2.5. The same is done throughout this thesis where peaks have shifted). This structure formed by the following reaction sequence:

$$L \rightarrow (Cr)$$

$$L \rightarrow (Cr) + \sim PtAl_2.$$

This was followed by a solid state precipitation reaction. Taking the position of the dark component into account, the precipitates would probably be ~Cr_2Al.

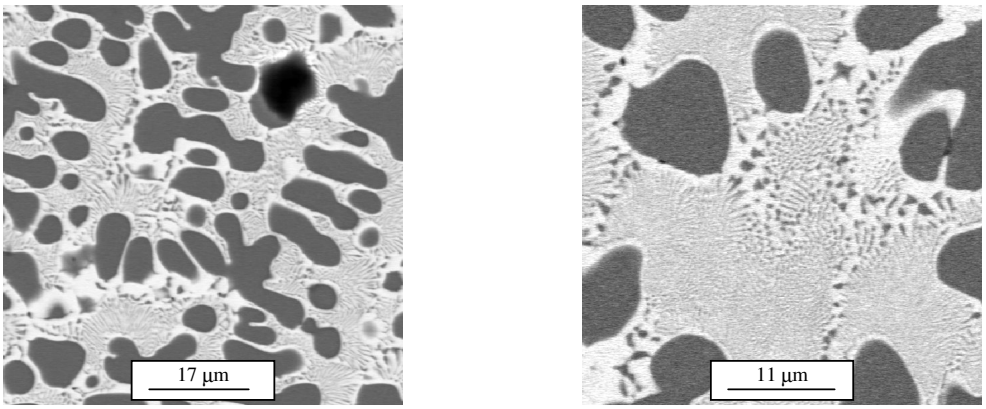

Figure 2.3. BSE-SEM image of nominal $Pt_{10}:Al_{30}:Cr_{60}$ in the as-cast condition: (Cr) dark; ~$PtAl_2$ light; ~Cr_2Al grey?

Table 2.2. Phase analyses for nominal $Pt_{10}:Al_{30}:Cr_{60}$ (at.%) in the as-cast condition.

Phase description	**Pt**	**Al**	**Cr**	**Phase**
Overall	9.4 ± 1.4	28.3 ± 2.9	62.3 ± 4.3	-
Dark	1.8 ± 0.0	18.6 ± 0.0	79.6 ± 0.1	(Cr)
Light	27.6 ± 0.1	56.5 ± 0.0	15.9 ± 0.0	~$PtAl_2$
Eutectic dark + light	20.7 ± 0.8	44.7 ± 0.5	34.6 ± 1.3	(Cr) + ~$PtAl_2$

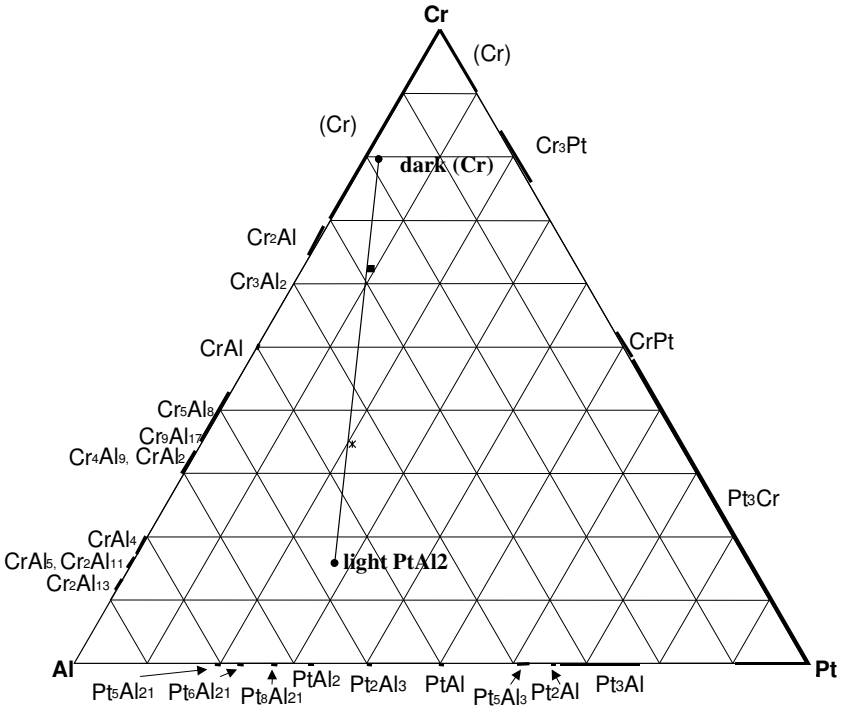

Figure 2.4. EDX analyses of nominal $Pt_{10}:Al_{30}:Cr_{60}$ (at.%) in the as-cast condition.

(■ overall composition; ● phases; ✶ eutectic)

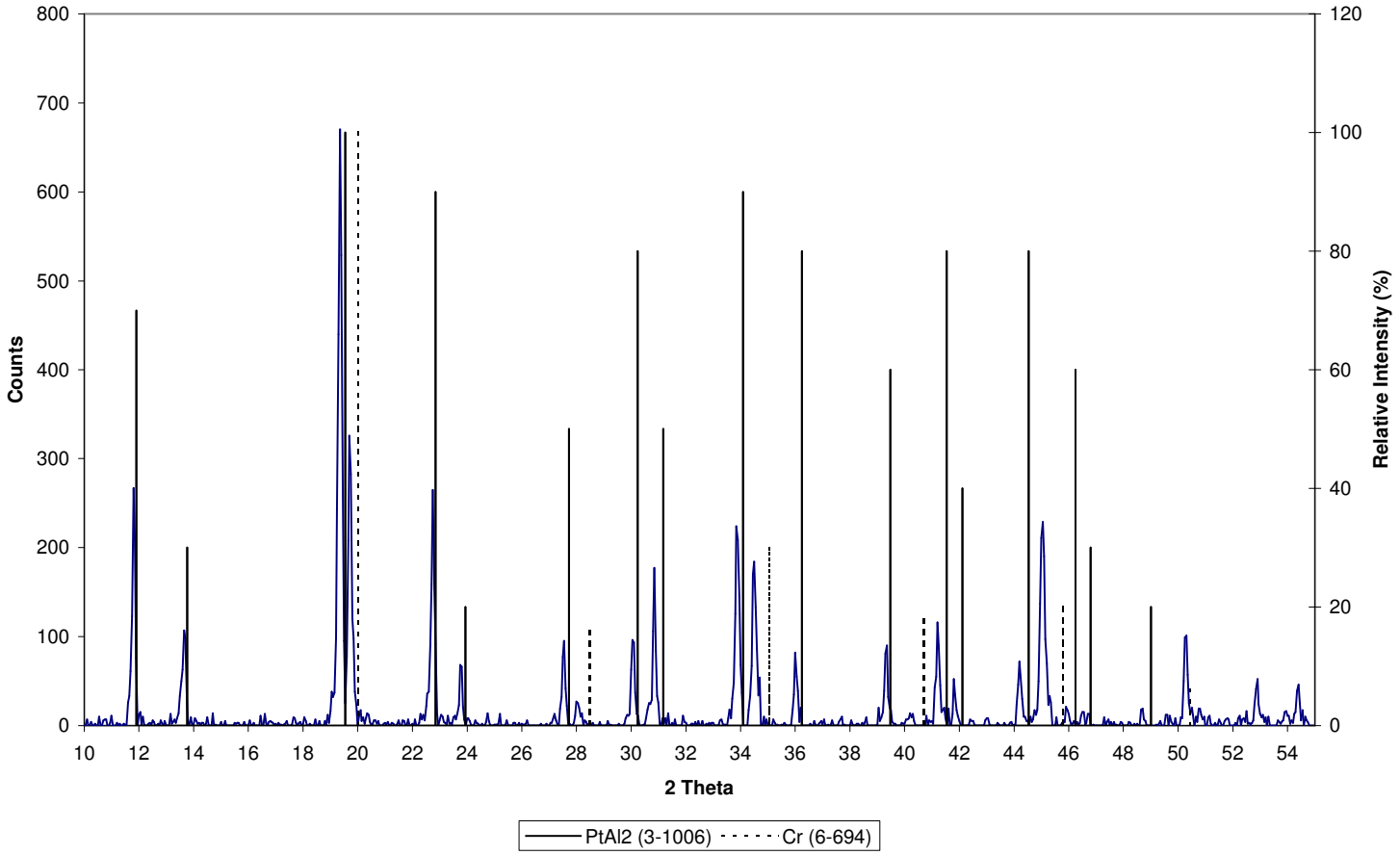

Figure 2.5. XRD pattern for nominal Pt_{10}:Al_{30}:Cr_{60} in the as-cast condition.

2.1.3. Nominal $Pt_{10}:Al_{60}:Cr_{30}$

Alloy $Pt_{10}:Al_{60}:Cr_{30}$ comprised light dendrites with a dark interdendritic phase in some areas, while in other areas the interdendritic areas comprised an eutectic mixture of dark and light (Figure 2.6). Other small areas of different contrast, appearing out-of-focus, are edge effects. The EDX analyses are given in Table 2.3 and Figure 2.7. XRD analysis clearly confirmed that the one phase – the light one – was ~$PtAl_2$ (Figure 2.8). Taking into account the position of the dark phase on the ternary diagram (Figure 2.7), one would expect that it was ~Cr_5Al_8, but the XRD analysis showed that the remaining experimental peaks (not matching with those of ~$PtAl_2$) coincided with a combination of that of shifted peaks for ~$CrAl_2$ (a compound listed in the JCPDS database but not shown in the binary Cr-Al phase diagram) and ~Cr_5Al_8 (Figure 2.8). Taking into account the microstructure of alloy $Pt_{10}:Al_{60}:Cr_{30}$ after being annealed at 600°C, where a second phase was clearly resolved by SEM, ~Cr_4Al_9 or ~$CrAl_2$ might have been present as the result of a solid state reaction. The phase was, however, never observed in the as-cast state. The compositions and diffraction patterns of all the Al-rich Cr-Al intermetallic compounds are very similar, making it difficult to decide on the most correct one. From the position of the dark phase on the diagram mentioned before, as well as the fact that ~$CrAl_2$ is not found in the binary Cr-Al diagram, it was accepted that the phase was most probably ~Cr_5Al_8.

The structure formed by the following reactions:

$$L \rightarrow \sim PtAl_2$$

$$L \rightarrow \sim PtAl_2 + \sim Cr_5Al_8$$

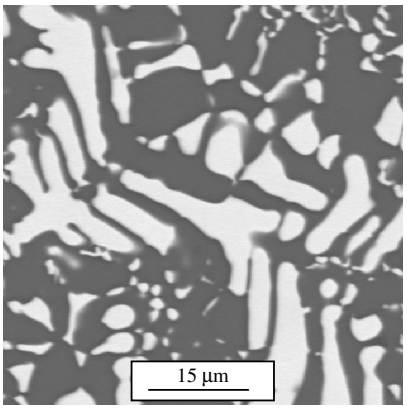

Figure 2.6. BSE-SEM image of nominal $Pt_{10}:Al_{60}:Cr_{30}$ in the as-cast condition:~Cr_5Al_8 dark; ~$PtAl_2$ light.

Table 2.3. Phase analyses for nominal $Pt_{10}:Al_{60}:Cr_{30}$ (at.%) in the as-cast condition.

Phase description	**Pt**	**Al**	**Cr**	**Phase**
Overall	7.7 ± 0.2	59.3 ± 0.2	33.0 ± 0.3	-
Dark	0.8 ± 0.0	59.8 ± 0.6	39.4 ± 0.6	~Cr_5Al_8
Light	28.1 ± 0.2	58.8 ± 0.1	13.1 ± 0.3	~$PtAl_2$

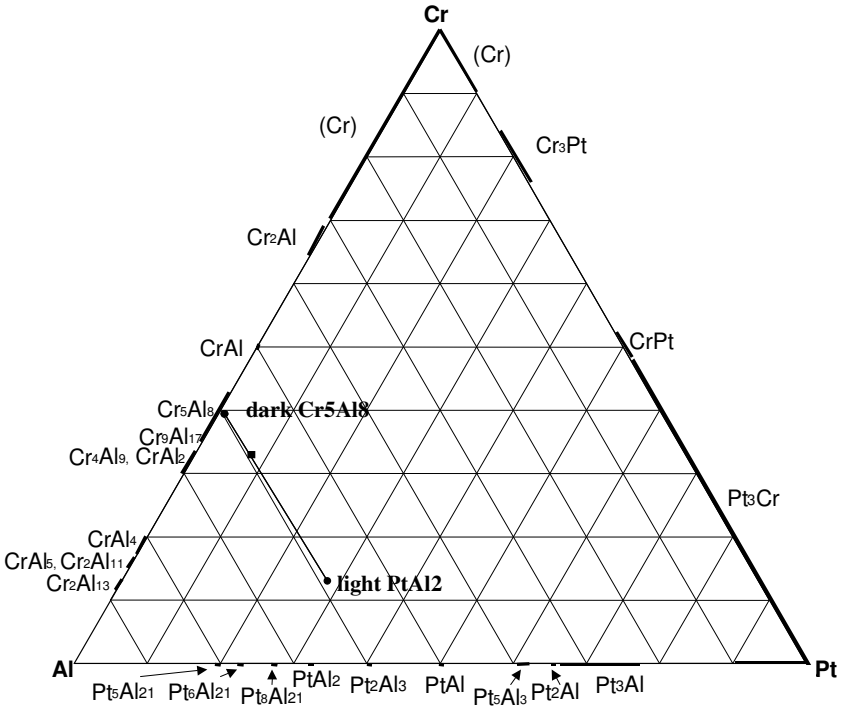

Figure 2.7. EDX analyses of nominal $Pt_{10}:Al_{60}:Cr_{30}$ (at.%) in the as-cast condition.

(■ overall composition; ● phases)

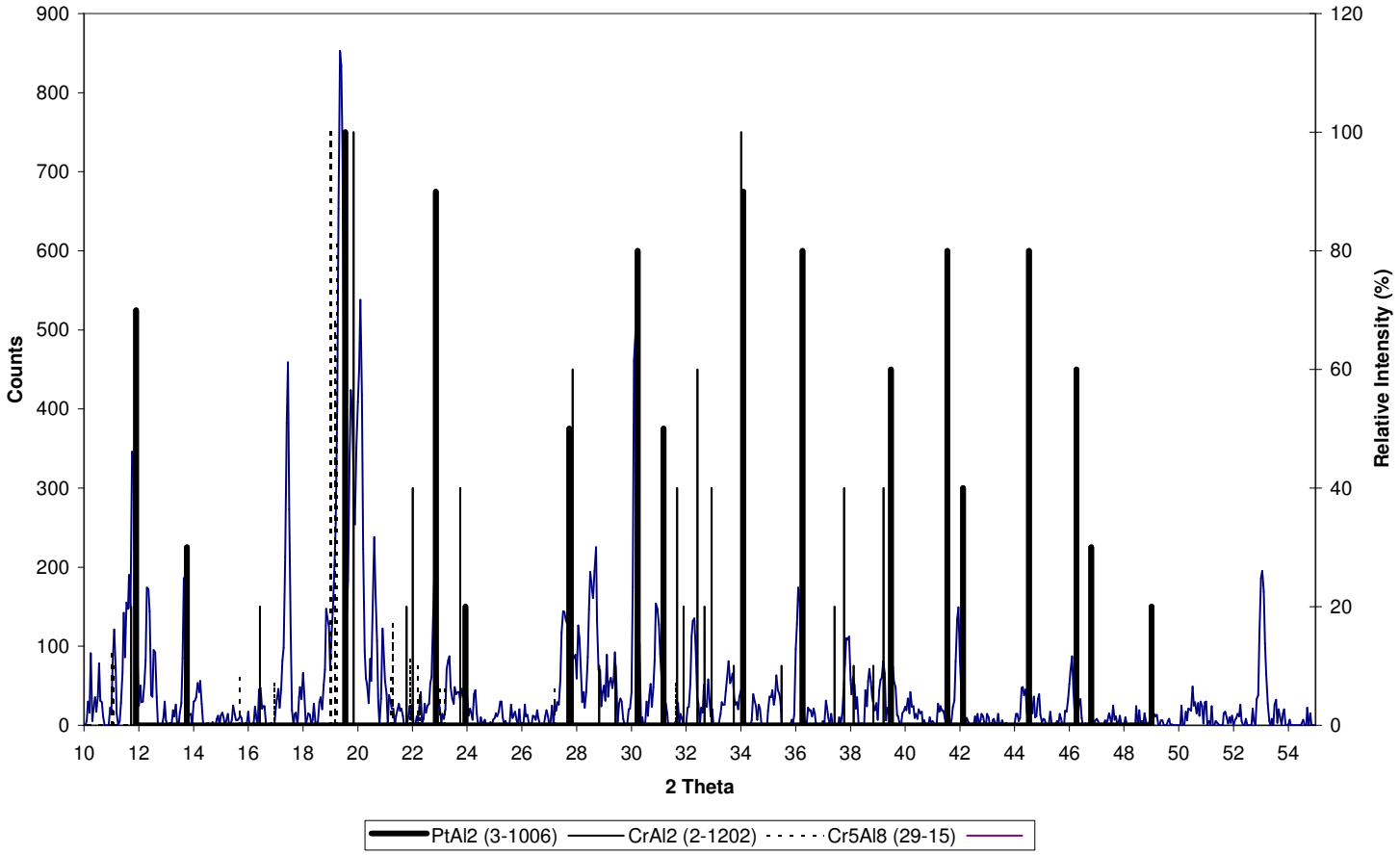

Figure 2.8. XRD pattern for nominal Pt_{10}:Al_{60}:Cr_{30} in the as-cast condition.

2.1.4. Nominal Pt_{10}:Al_{80}:Cr_{10}

Alloy Pt_{10}:Al_{80}:Cr_{10} had a very complicated structure, comprising four phases (Figure 2.9). The EDX analyses of the alloy and all its phases are given in Table 2.4 and shown graphically in Figure 2.10. Note that, as the very light phase was very small, its analysis was probably affected by the surrounding phases, so it could actually be more Pt-rich. The reason for the variation in composition of the dark phase was unclear, unless some EDX measurements had been done in small areas where the analyses could have been affected by the surrounding phase(s). From Figure 2.10, the very dark phase (inside the dark phase) was obviously (Al) as part of a sparse euetctci, and this was confirmed by XRD analyses (Figure 2.11). The very light phase (inside the light phase) was clearly identified as ~$PtAl_2$. The light phase was most probably either ~Pt_8Al_{21} or ~Pt_6Al_{21} (a compound in the JCPDS database but not found in the Pt-Al binary phase diagram), and therefore probably the former. The dark phase was more difficult to identify, the range of possible phases being quite large: ~$CrAl_4$, ~$CrAl_5$ (a JCPDS compound, and as mentioned in §1, suggested as the more correct form for ~Cr_2Al_{11} that is reported in the binary diagram), ~Cr_2Al_{11} (not included in the JCPDS database) or ~Cr_2Al_{13} (another JCPDS phase, reported in the binary diagram as ~$CrAl_7$). After eliminating most of the possibilities by superposing their XRD peaks onto the measured XRD pattern, it was a difficult choice between ~$CrAl_5$ and ~Cr_2Al_{13}. It was concluded that the dark phase was ~$CrAl_5$ since the $CrAl_5$ XRD peaks were the best fit to the measured pattern.

Taking into account the melting points of the phases and keeping in mind the positions of the phases relative to each other, the phases probably formed by:

$$L \rightarrow \sim PtAl_2$$

followed by a series of peritectic reactions:

$$L + \sim PtAl_2 \rightarrow \sim CrAl_5$$

(in which ~$PtAl_2$ was almost totally consumed)

$$L + \sim CrAl_5 \rightarrow (Al),$$

and finally the eutectic reaction

$$L \rightarrow (Al) + Pt_8Al_{21}.$$

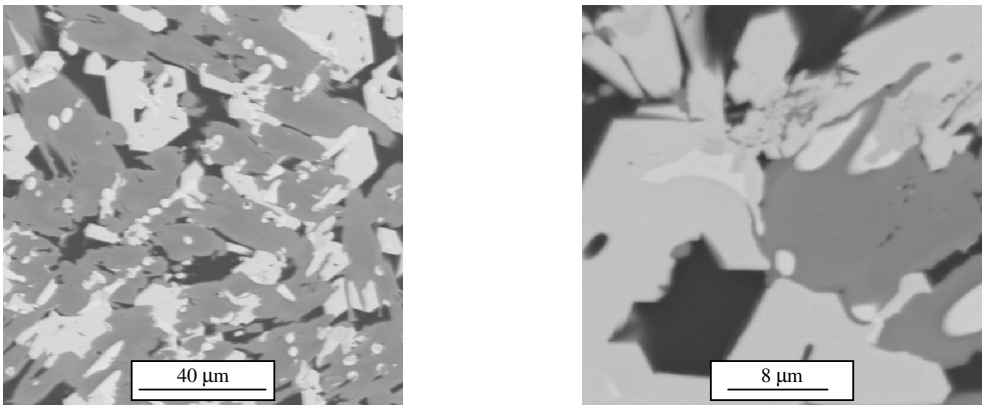

Figure 2.9. BSE-SEM image of nominal $Pt_{10}:Al_{80}:Cr_{10}$ in the as-cast condition: (Al) very dark; ~$CrAl_5$ dark; ~Pt_8Al_{21} light; ~$PtAl_2$ very light.

Table 2.4. Phase analyses for nominal $Pt_{10}:Al_{80}:Cr_{10}$ (at.%) in the as-cast condition.

Phase description	**Pt**	**Al**	**Cr**	**Phase**
Overall	8.4 ± 0.5	81.2 ± 0.7	10.3 ± 0.4	-
Dark	6.0 ± 0.5	78.9 ± 2.2	15.1 ± 2.7	~$CrAl_5$
Very dark	0.1 ± 0.0	99.5 ± 0.1	0.5 ± 0.1	(Al)
Light	21.2 ± 0.3	75.8 ± 0.1	3.0 ± 0.2	~Pt_8Al_{21}
Very light	27.5 ± 0.2	64.3 ± 0.8	8.2 ± 0.6	~$PtAl_2$

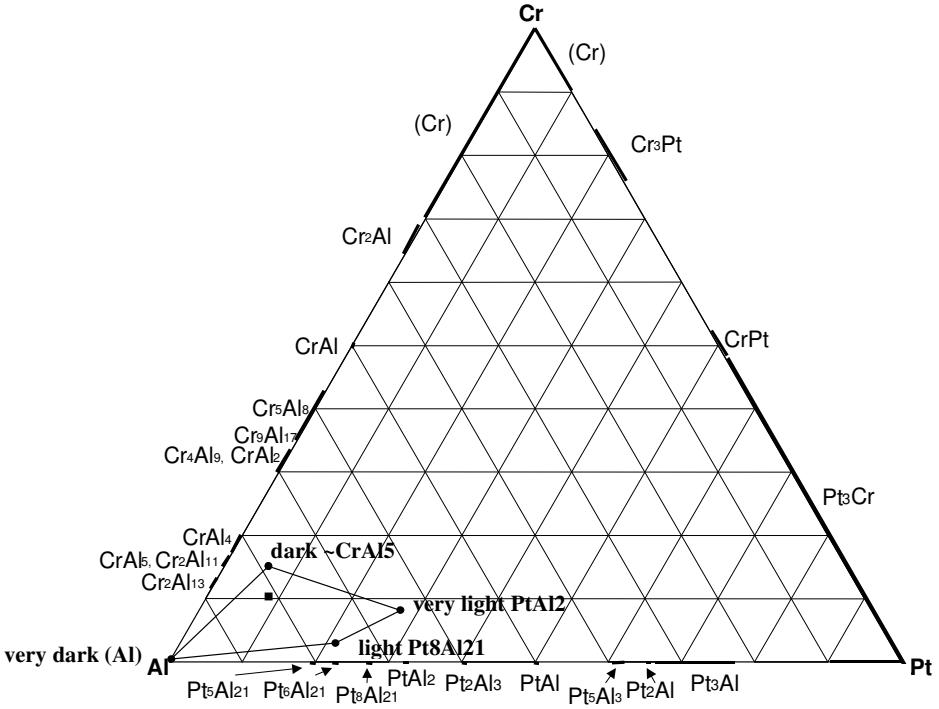

Figure 2.10. EDX analyses of nominal $Pt_{10}:Al_{80}:Cr_{10}$ (at.%) in the as-cast condition.

(■ overall composition; ● phases)

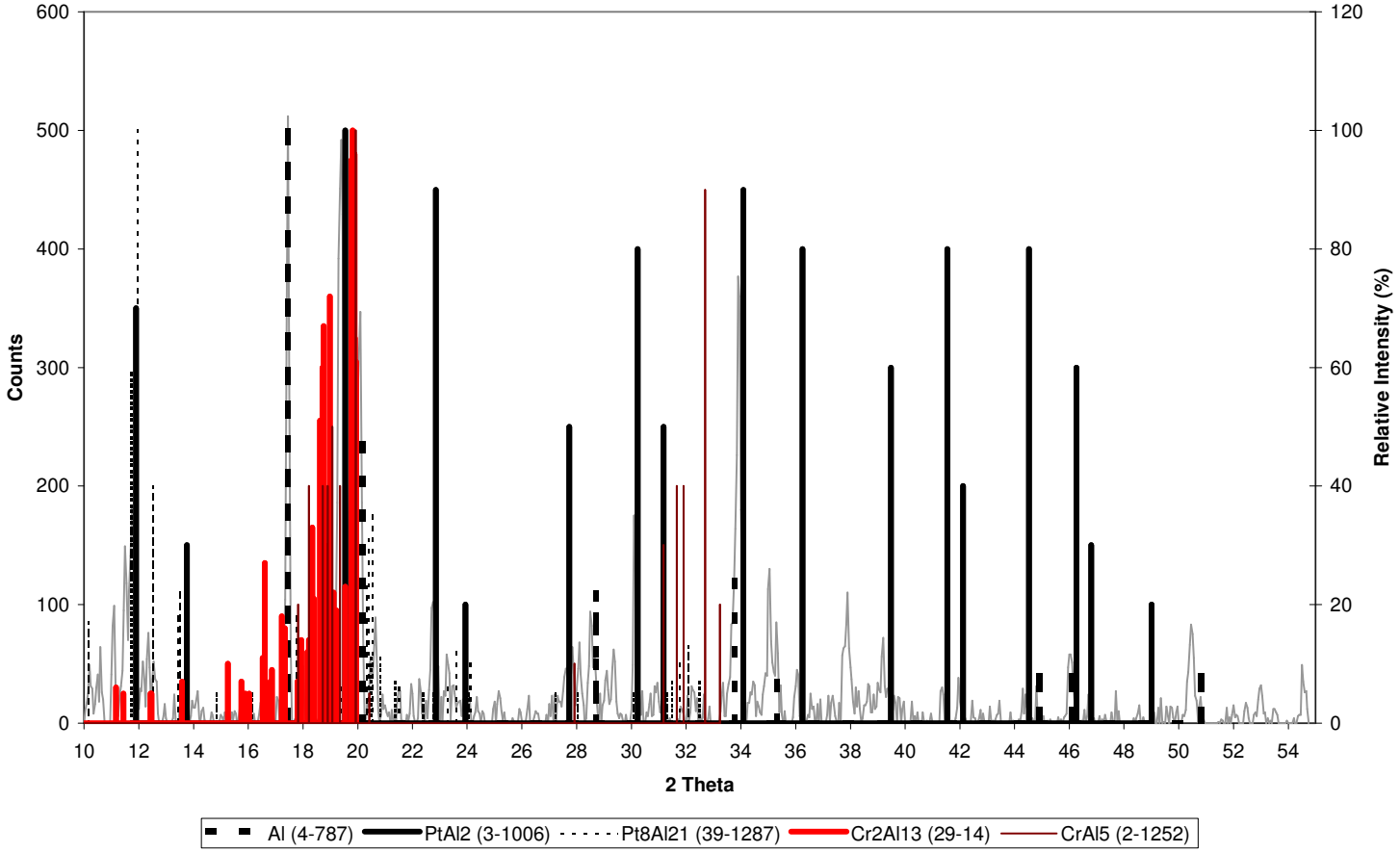

Figure 2.11. XRD pattern for nominal Pt_{10}:Al_{80}:Cr_{10} in the as-cast condition.

2.1.5. Nominal $Pt_{20}:Al_{20}:Cr_{60}$

Alloy $Pt_{20}:Al_{20}:Cr_{60}$ comprised dark dendrites with a mixture of light and dark located interdendritically (Figure 2.12), and was very similar in appearance to alloy $Pt_{10}:Al_{80}:Cr_{10}$ (Figure 2.1). The EDX analyses are given in Table 2.5 and shown graphically in Figure 2.13. From the XRD analysis (Figure 2.14) (an excellent fit) and the position of the phases on the ternary diagram (Figure 2.13) it would appear that the light phase was B20, and the dark phase (Cr). There was also the appearance of a sparse eutectic. The microstructure formed by:

$$L \rightarrow (Cr)$$

followed by an eutectic reaction

$$L \rightarrow (Cr) + \sim PtAl.$$

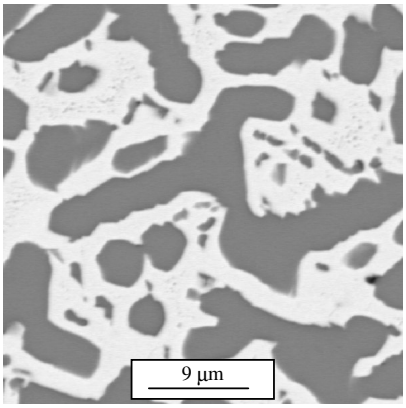

Figure 2.12. BSE-SEM image of nominal $Pt_{20}:Al_{20}:Cr_{60}$ in the as-cast condition: (Cr) dark; light ~PtAl.

Table 2.5. Phase analyses for nominal $Pt_{20}:Al_{20}:Cr_{60}$ (at.%) in the as-cast condition.

Phase description	**Pt**	**Al**	**Cr**	**Phase**
Overall	17.5 ± 0.4	18.3 ± 0.7	64.2 ± 1.1	-
Dark	4.3 ± 0.1	4.0 ± 0.2	91.7 ± 0.2	(Cr)
Light	41.3 ± 0.7	40.0 ± 0.6	18.7 ± 1.3	~PtAl

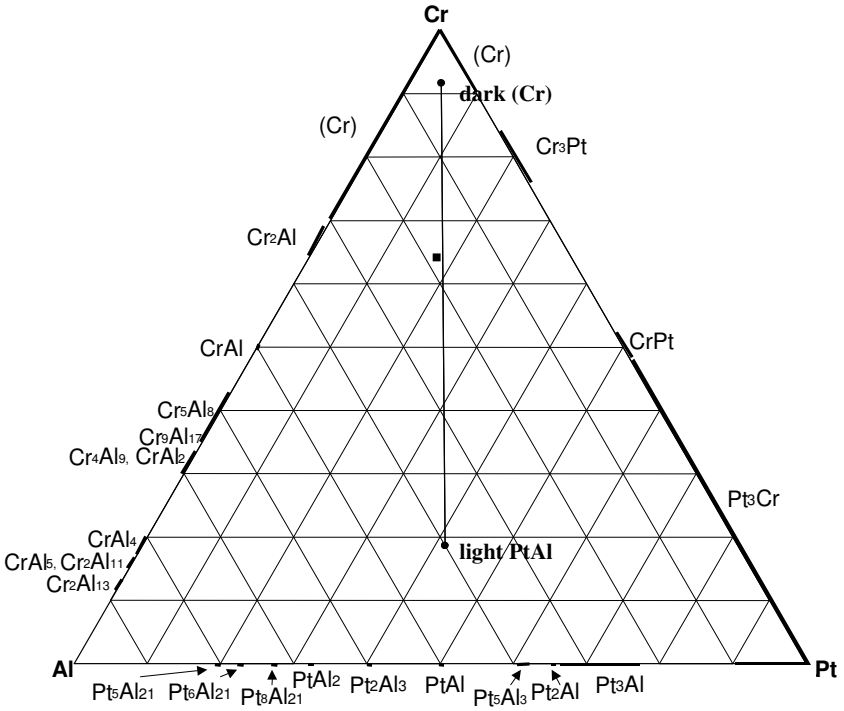

Figure 2.13. EDX analyses of nominal $Pt_{20}:Al_{20}:Cr_{60}$ (at.%) in the as-cast condition.

(■ overall composition; ● phases)

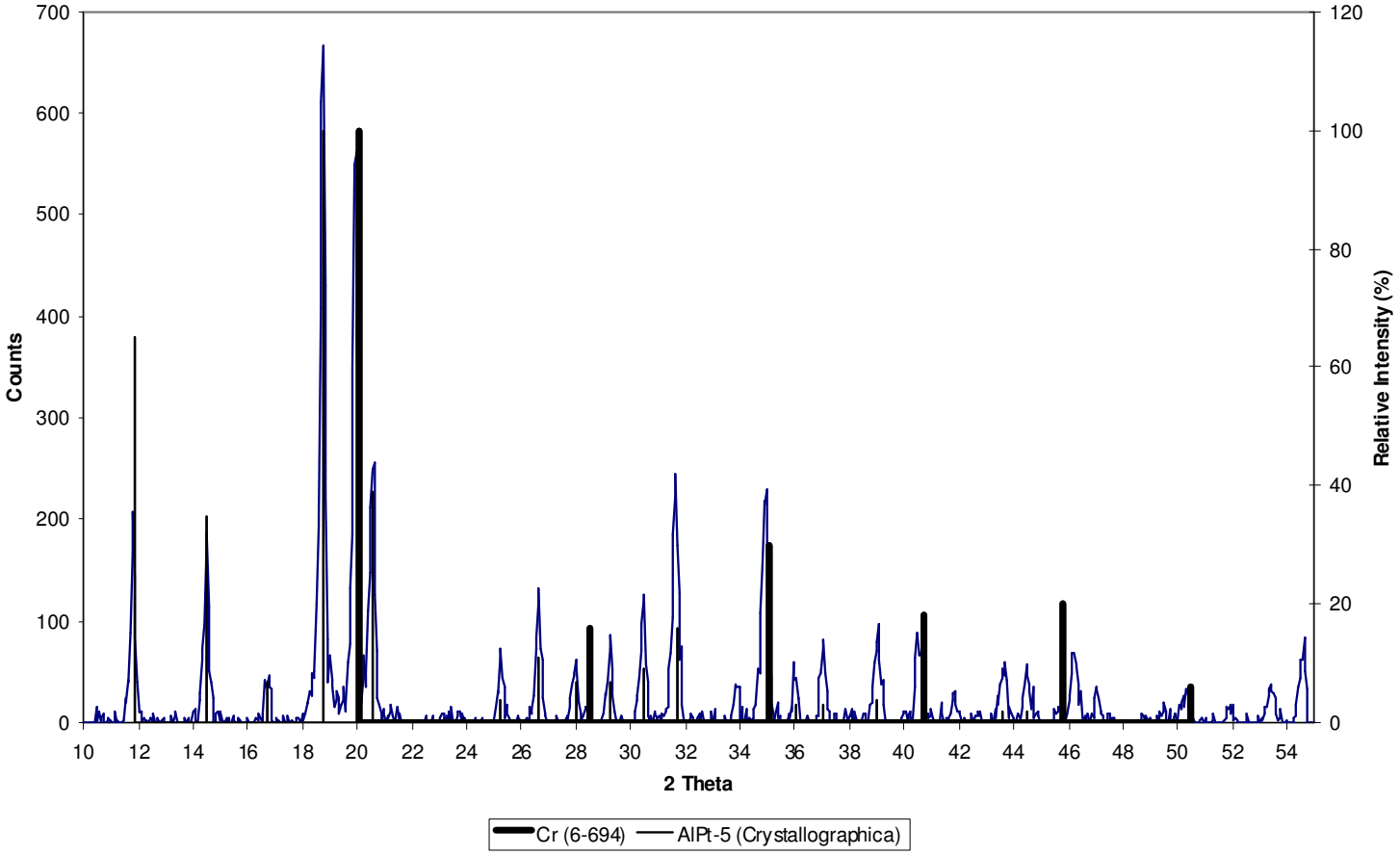

Figure 2.14. XRD pattern for nominal Pt_{20}:Al_{20}:Cr_{60} in the as-cast condition.

2.1.6. Nominal $Pt_{20}:Al_{40}:Cr_{40}$

At first glance, alloy $Pt_{20}:Al_{40}:Cr_{40}$ showed two phases: dark dendrites surrounded by a rim of light phase with interdendritic regions of a very fine eutectic mixture of dark and light (Figure 2.15). The EDX analyses are given in Table 2.6 and Figure 2.16. XRD analysis clearly detected (Cr) and B20 ~PtAl (Figure 2.17) (both phases' peaks being excellent fits to the measured pattern). However, some peaks also suggested the presence of ~$PtAl_2$ (Figure 2.17). The XRD analysis would suggest that the dark phase was (Cr) and the light phase was ~PtAl. However, the latter could not be the case when considering the results of alloys $Pt_{10}:Al_{30}:Cr_{60}$ (§2.1.2), $Pt_{30}:Al_{50}:Cr_{20}$ (§2.1.7) and $Pt_{75}:Al_{10}:Cr_{15}$ (§2.1.30). The light phase had to be ~$PtAl_2$, which implied that the third phase, ~PtAl, could not be distinguished from the other phases in Figure 2.15, because of too similar contrast. Based specifically on the results of alloy $Pt_{30}:Al_{50}:Cr_{20}$ (§2.1.7), an amended ternary diagram is suggested (Figure 2.18). With the suggested composition of the ~PtAl phase, its average atomic number would be so close to that of the measured light phase that they would be difficult to separate on grounds of contrast. It is also suggested that both a binary and ternary eutectic can be seen here, and that the phases formed by:

$$L \rightarrow (Cr)$$

$$L \rightarrow (Cr) + \sim PtAl_2$$

$$L \rightarrow (Cr) + \sim PtAl_2 + \sim PtAl.$$

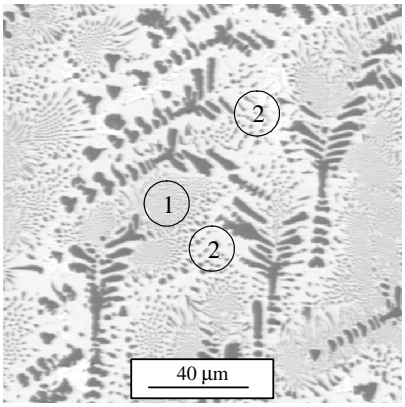

Figure 2.15. BSE-SEM image of nominal $Pt_{20}:Al_{40}:Cr_{40}$ in the as-cast condition: (Cr) dark; ~$PtAl_2$ light + ~PtAl light; different eutectics indicated by "1" and "2".

Table 2.6. Phase analyses for nominal $Pt_{20}:Al_{40}:Cr_{40}$ (at.%) in the as-cast condition.

Phase description	**Pt**	**Al**	**Cr**	**Phase**
Overall	18.9 ± 0.7	38.8 ± 0.1	42.3 ± 1.7	-
Dark	2.5 ± 0.8	12.8 ± 1.0	84.6 ± 0.2	~(Cr)
Light	29.7 ± 0.6	53.2 ± 1.1	17.1 ± 0.7	~$PtAl_2$
Ternary eutectic dark+light	21.4 ± 0.4	42.3 ± 0.3	35.3 ± 0.1	(Cr) + ~PtAl + ~$PtAl_2$

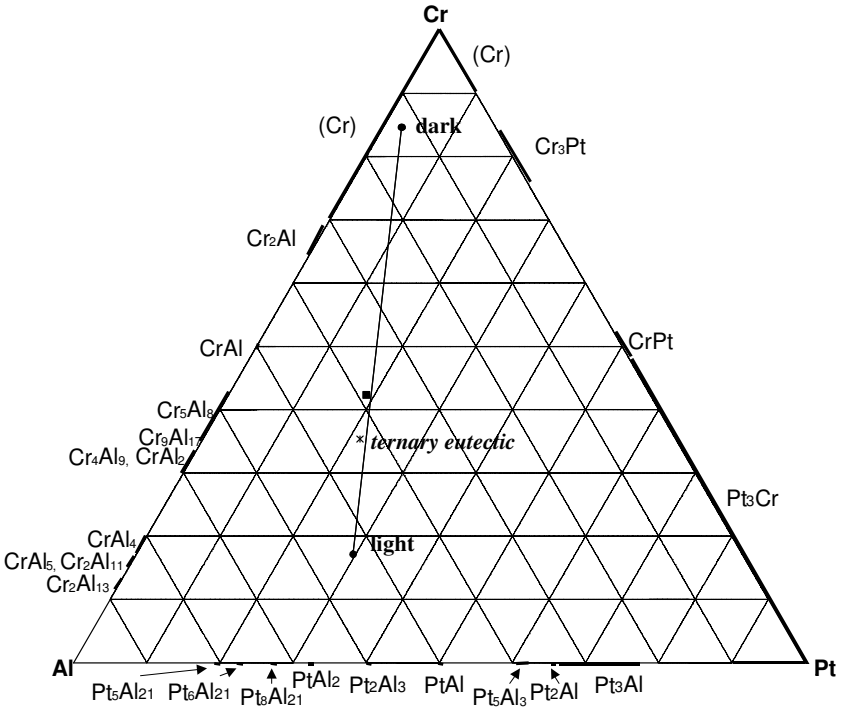

Figure 2.16. EDX analyses of nominal $Pt_{20}:Al_{40}:Cr_{40}$ (at.%) in the as-cast condition.

(■ overall composition; ● phases; ✶ eutectic)

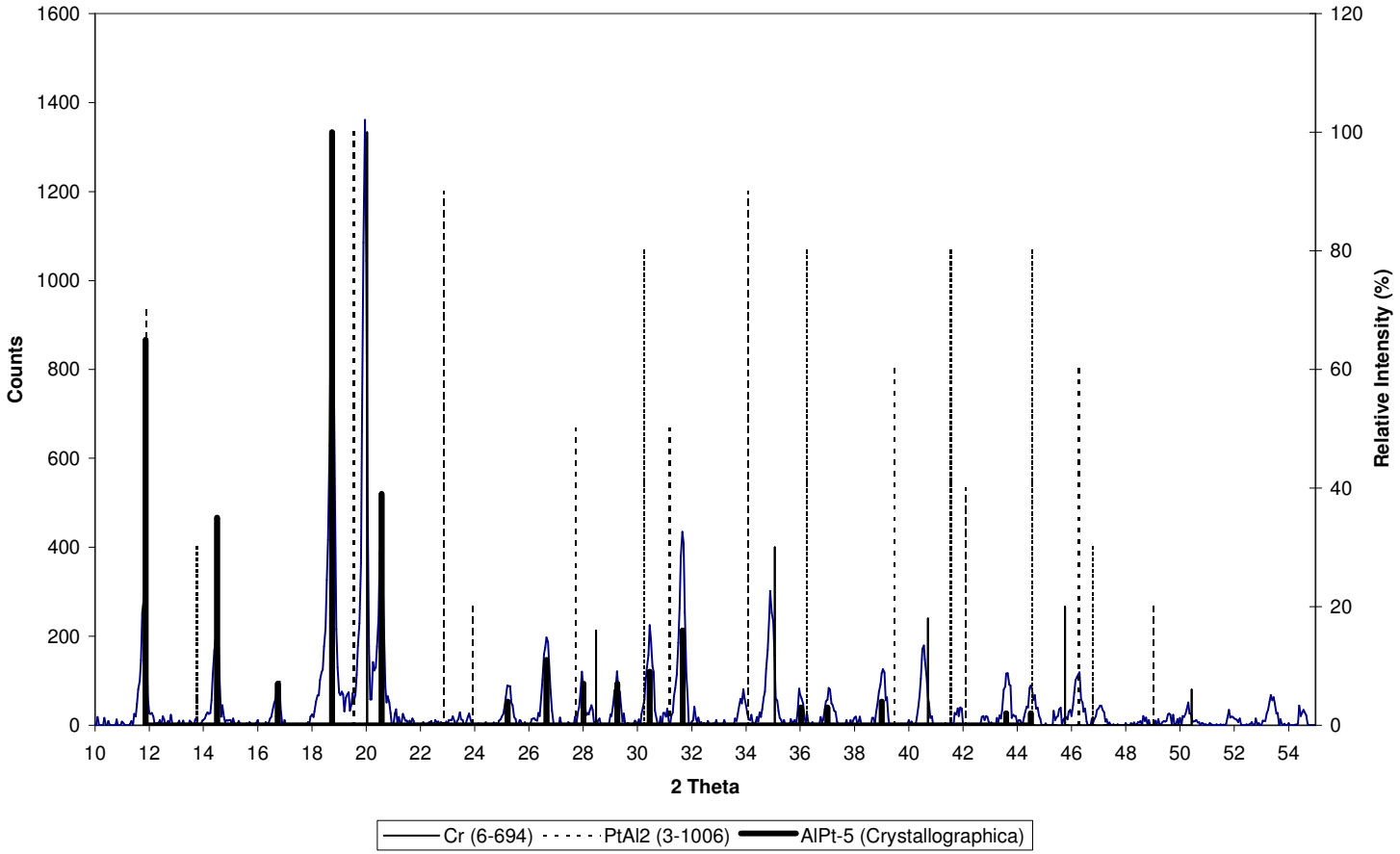

Figure 2.17. XRD pattern for nominal $Pt_{20}:Al_{40}:Cr_{40}$ in the as-cast condition.

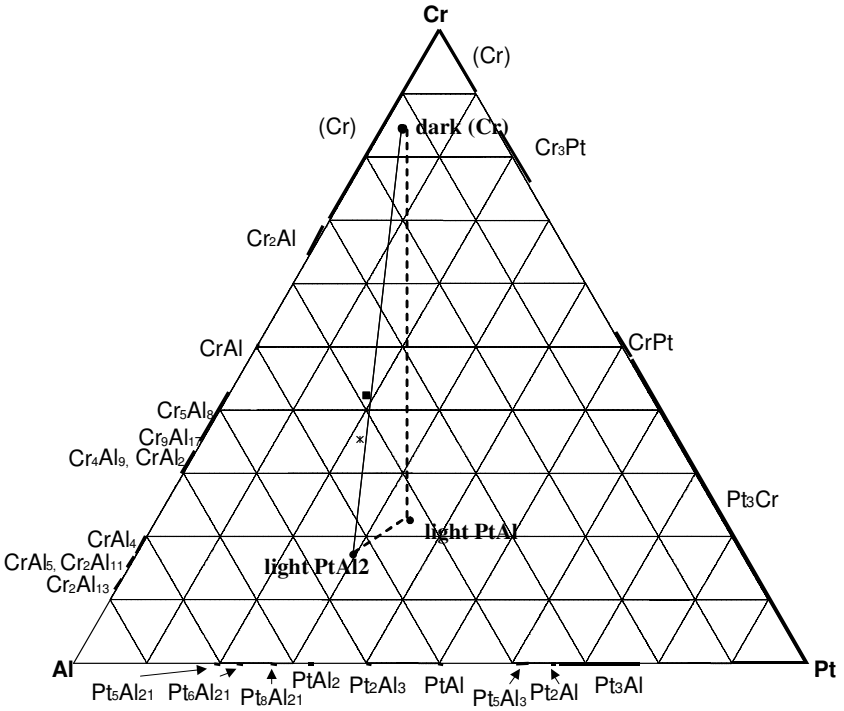

Figure 2.18. EDX analyses of nominal Pt_{20}:Al_{40}:Cr_{40} (at.%) in the as-cast condition with suggested extrapolations.

(■ overall composition; ● phases; ✶ eutectic)

2.1.7. Nominal Pt_{30}:Al_{50}:Cr_{20}

Alloy Pt_{30}:Al_{50}:Cr_{20} had a more complicated structure than that observed at first glance. It comprised primarily grey dendrites with interdendritic regions that comprised two different eutectic mixtures: binary grey + white, and ternary black + white + grey (Figure 2.19). There was also evidence of black precipitates within the grey phase (Figure 2.19). The EDX analyses of the alloy and its three phases are shown in Table 2.7 and Figure 2.20. Note the huge standard deviations in composition of all phases (except the grey phase) because they were too small to analyse accurately. The diffraction peaks of ~$PtAl_2$ (grey) and ~PtAl (white) [slightly shifted] matched the measured pattern well (Figure 2.21). This would agree with alloy Pt_{12}:Al_{18}:Cr_{70} where a white phase with similar composition to this one was identified as B20 ~PtAl. The black phase was very small to analyse well and its analyses were affected by the surrounding phases and it is highly likely that it was much more rich in (Cr) (confirmed by the variation of up to ~6 at.% Cr in composition (Table 2.7)). The black phase was most probably (Cr), and the dashed lines in Figure 2.20 shows the extrapolation in composition from the measured value to the ~90 at.%Cr level one would expect (Cr) to have.

The XRD fit for (Cr) was not good, probably due to the fact that the alloy did not contain a large amount of it. There was a slight suggestion that there are two phases (layers) within the dendrites, but the standard deviation in EDX analyses of the grey phase and the results of the XRD analyses, did not support it.

The phases formed by:

$$L \rightarrow \sim PtAl_2$$

$$L \rightarrow \sim PtAl_2 + \sim PtAl$$

$$L \rightarrow (Cr) + \sim PtAl + \sim PtAl_2.$$

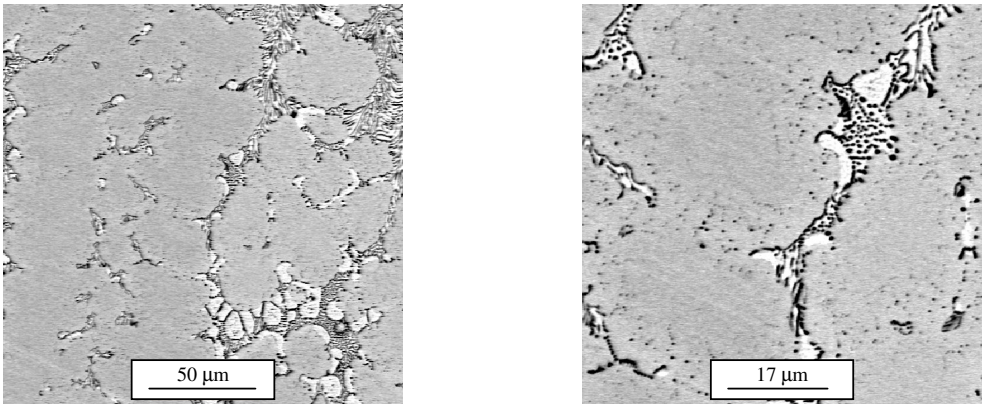

Figure 2.19. BSE-SEM image of nominal Pt_{30}:Al_{50}:Cr_{20} in the as-cast condition: (Cr) black; ~$PtAl_2$ grey; ~PtAl white.

Table 2.7. Phase analyses for nominal Pt_{30}:Al_{50}:Cr_{20} (at.%) in the as-cast condition.

Phase description	**Pt**	**Al**	**Cr**	**Phase**
Overall	29.9 ± 0.2	49.4 ± 0.5	20.7 ± 0.5	-
Black	18.8 ± 2.9	28.7 ± 3.6	51.5 ± 5.8	(Cr)
Grey	30.0 ± 0.4	53.2 ± 1.5	16.8 ± 1.0	~$PtAl_2$
White	38.4 ± 2.1	43.9 ± 1.2	17.7 ± 2.8	~PtAl
Ternary eutectic black+white+grey	31.6 ± 5.4	40.7 ± 5.0	27.7 ± 10.3	(Cr)+ ~PtAl + ~$PtAl_2$
Eutectic grey+white*	34.7	45.5	19.8	~$PtAl_2$ + ~PtAl

* Only one measurement taken due to small size.

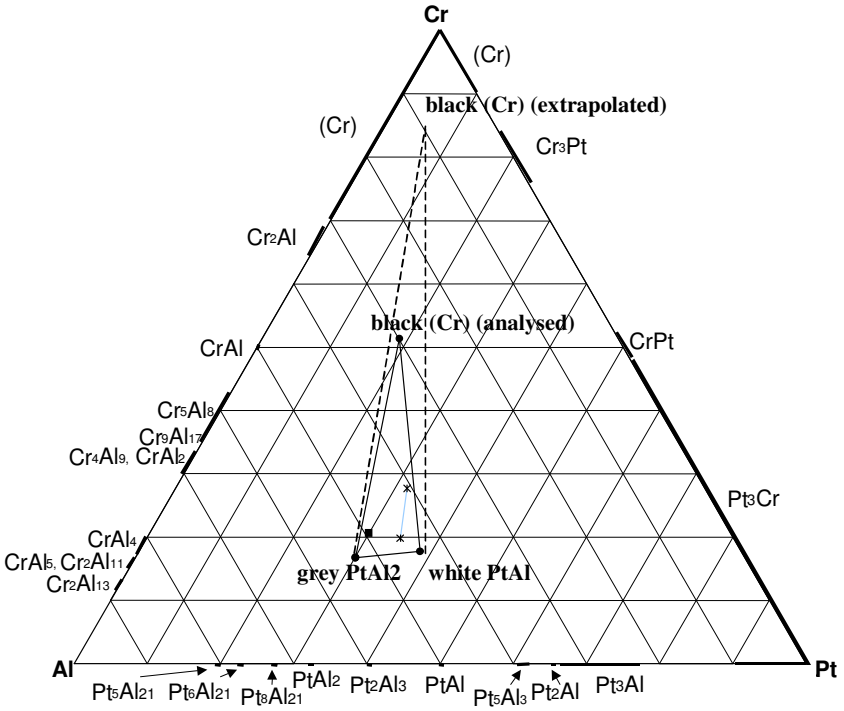

Figure 2.20. EDX analyses of nominal $Pt_{30}:Al_{50}:Cr_{20}$ (at.%) in the as-cast condition. (■ overall composition; ● phases; ✶ eutectic)

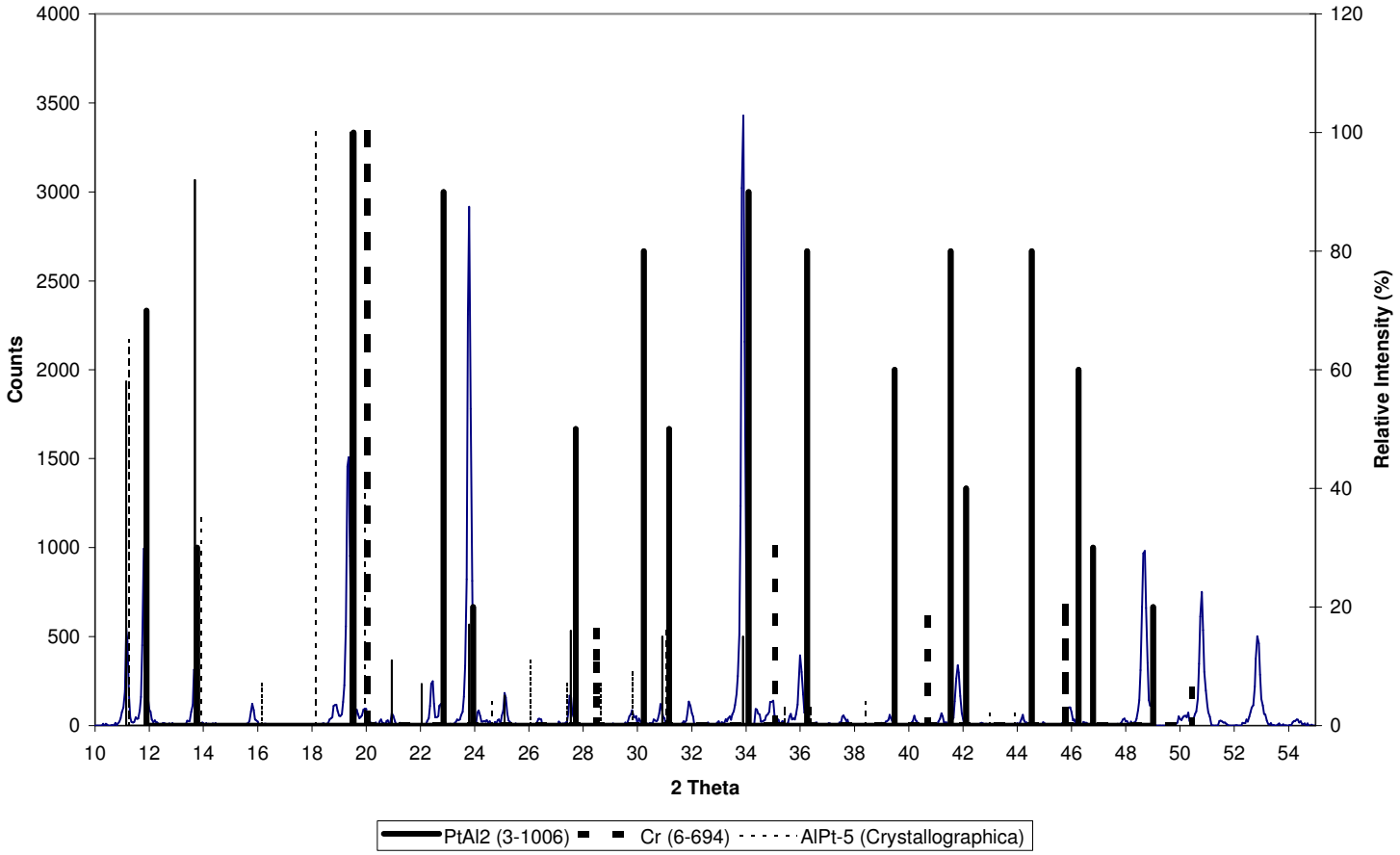

Figure 2.21. XRD pattern for nominal Pt_{30}:Al_{50}:Cr_{20} in the as-cast condition.

2.1.8. Nominal Pt_{40}:Al_{10}:Cr_{50}

Alloy Pt_{40}:Al_{10}:Cr_{50} comprised dark $L1_0$ ~CrPt dendrites with a small amount of an interdendritic eutectic mixture of dark ~CrPt and a light phase (Figure 2.22) plus some minor porosity. The EDX analyses are given in Table 2.8 and Figure 2.23. The presence of $L1_0$ ~CrPt was easily confirmed by XRD analysis, but it was not possible to identify the light phase from the XRD measurements (Figure 2.24). The measured XRD pattern was very complicated with a multitude of peaks of varying intensities. Taking into account the position of the light phase on the ternary diagram, ~Pt_5Al_3, ~Pt_2Al and ~Pt_3Al were chosen as candidates for its identity. Superposing the XRD peaks of $L1_0$ ~CrPt in combination with those of the different candidates onto the measured XRD pattern, both ~Pt_5Al_3 and ~Pt_3Al were eliminated as candidates. However, shifted XRD peaks for C23 ~Pt_2Al (low temperature variant) was a good match for the as yet unidentified phase, especially up to $2\theta \approx 35$ (Figure 2.24). In many instances, the JCPDS database does not give values beyond $2\theta=40$ and this could be the reason why the peaks beyond 40 degrees were not identified. ~Pt_2Al was the only candidate with a suitable amount of possible matches due to its own complicated (i.e. showing many peaks) XRD pattern (Figure 2.25). Considering the results of other alloys (Pt_{50}:Al_{10}:Cr_{40} (§2.1.11), Pt_{55}:Al_{25}:Cr_{20} (§2.1.39), Pt_{55}:Al_{20}:Cr_{25} (§2.1.40)), it was decided that the light phase was indeed ~Pt_2Al. Figure 2.25 shows the XRD patterns of these alloys and one can see how similar in structure they were. It was found that when plotting these alloys' XRD patterns together and identifying the peaks not matched by ~CrPt (where relevant), the unidentified peaks correspond very closely to that of C23 ~Pt_2Al.

This structure could have formed by the following reactions:

$$L \rightarrow (Pt)$$

$$L \rightarrow (Pt) + \sim Pt_3Al$$

$$\sim Pt_3Al \rightarrow \sim Pt_2Al$$

$$(Pt) \rightarrow \sim CrPt_3 \rightarrow \sim CrPt \text{ (ordering)}$$

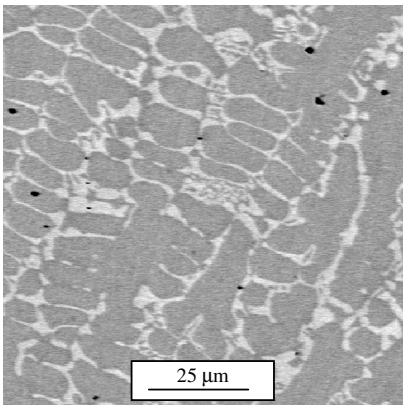

Figure 2.22. BSE-SEM image of nominal $Pt_{40}:Al_{10}:Cr_{50}$ in the as-cast condition: ~CrPt dark; ~Pt_2Al light.

Table 2.8. Phase analyses for nominal $Pt_{40}:Al_{10}:Cr_{50}$ (at.%) in the as-cast condition.

Phase description	**Pt**	**Al**	**Cr**	**Phase**
Overall	41.2 ± 0.6	8.5 ± 0.3	50.3 ± 0.4	-
Dark	41.5 ± 0.6	6.7 ± 0.5	51.9 ± 0.3	~CrPt
Light	46.8 ± 0.6	23.5 ± 0.1	29.7 ± 0.5	~Pt_2Al
Eutectic-like dark + light*	44.8	17.7	37.5	~CrPt + ~Pt_2Al

* Only one measurement taken because of difficulty selecting an appropriate region.

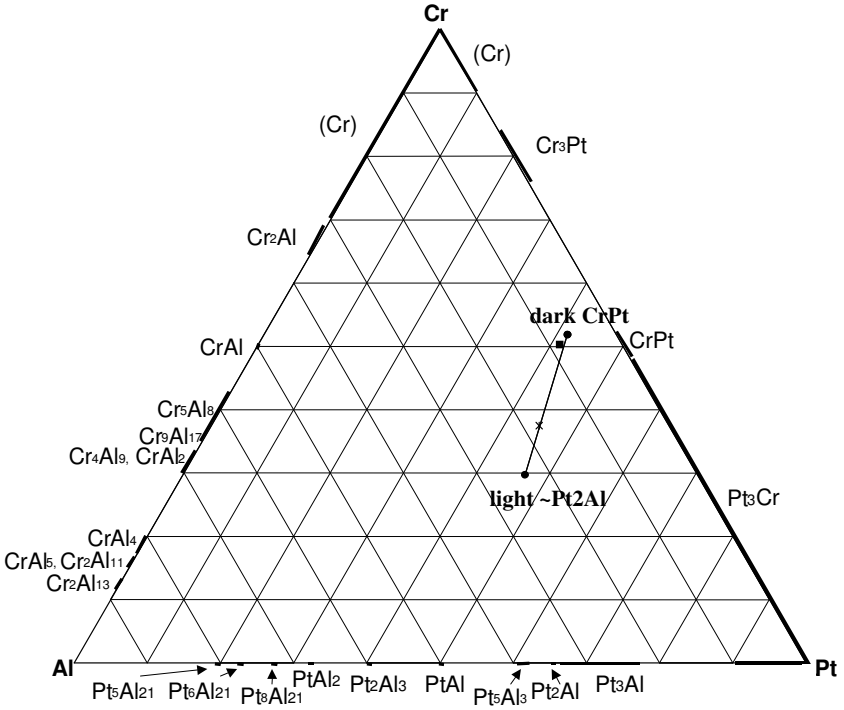

Figure 2.23. EDX analyses of nominal $Pt_{40}:Al_{10}:Cr_{50}$ (at.%) in the as-cast condition.(■ overall composition; ● phases; ✶ eutectic-like)

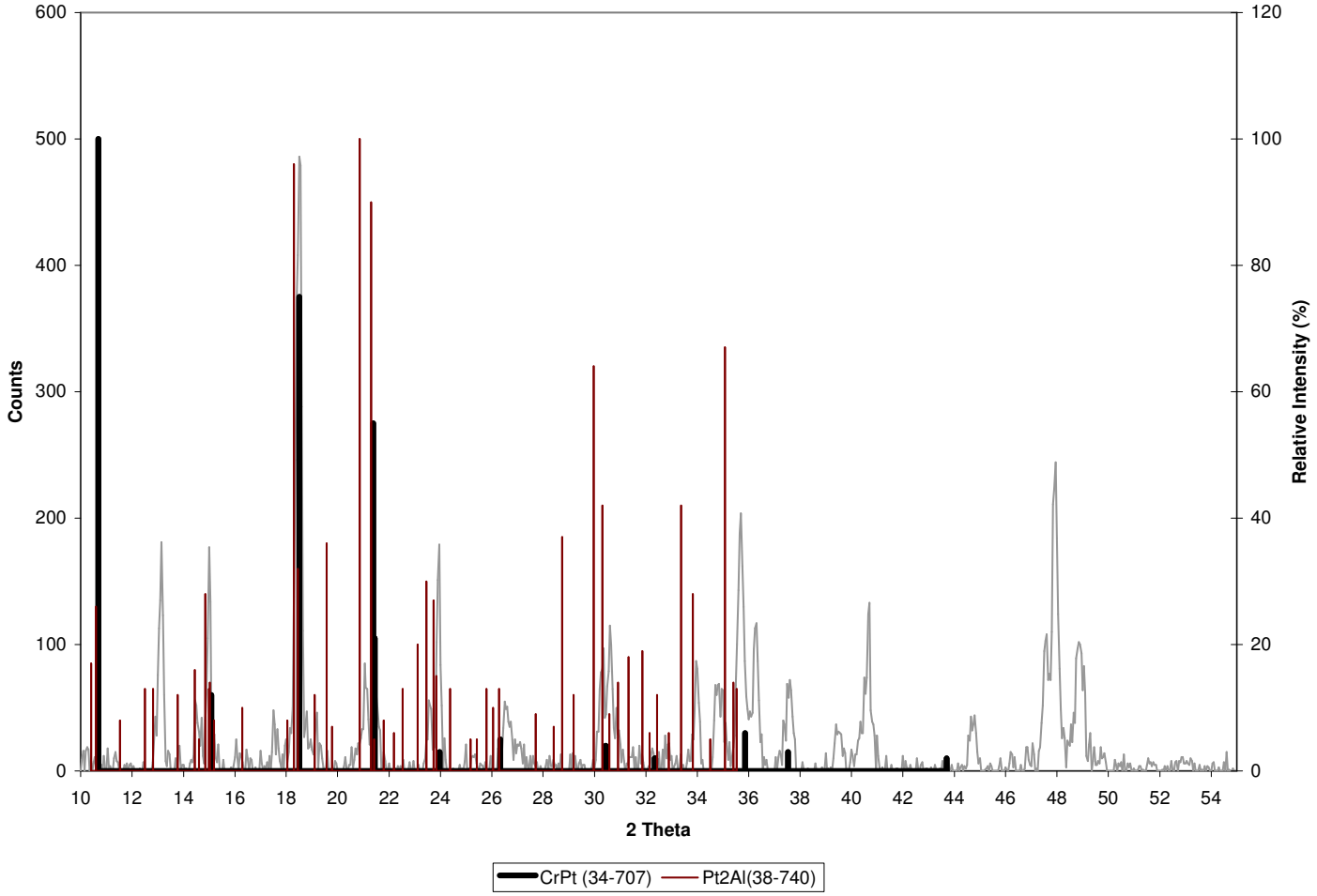

Figure 2.24. XRD pattern for nominal Pt_{40}:Al_{10}:Cr_{50} in the as-cast condition.

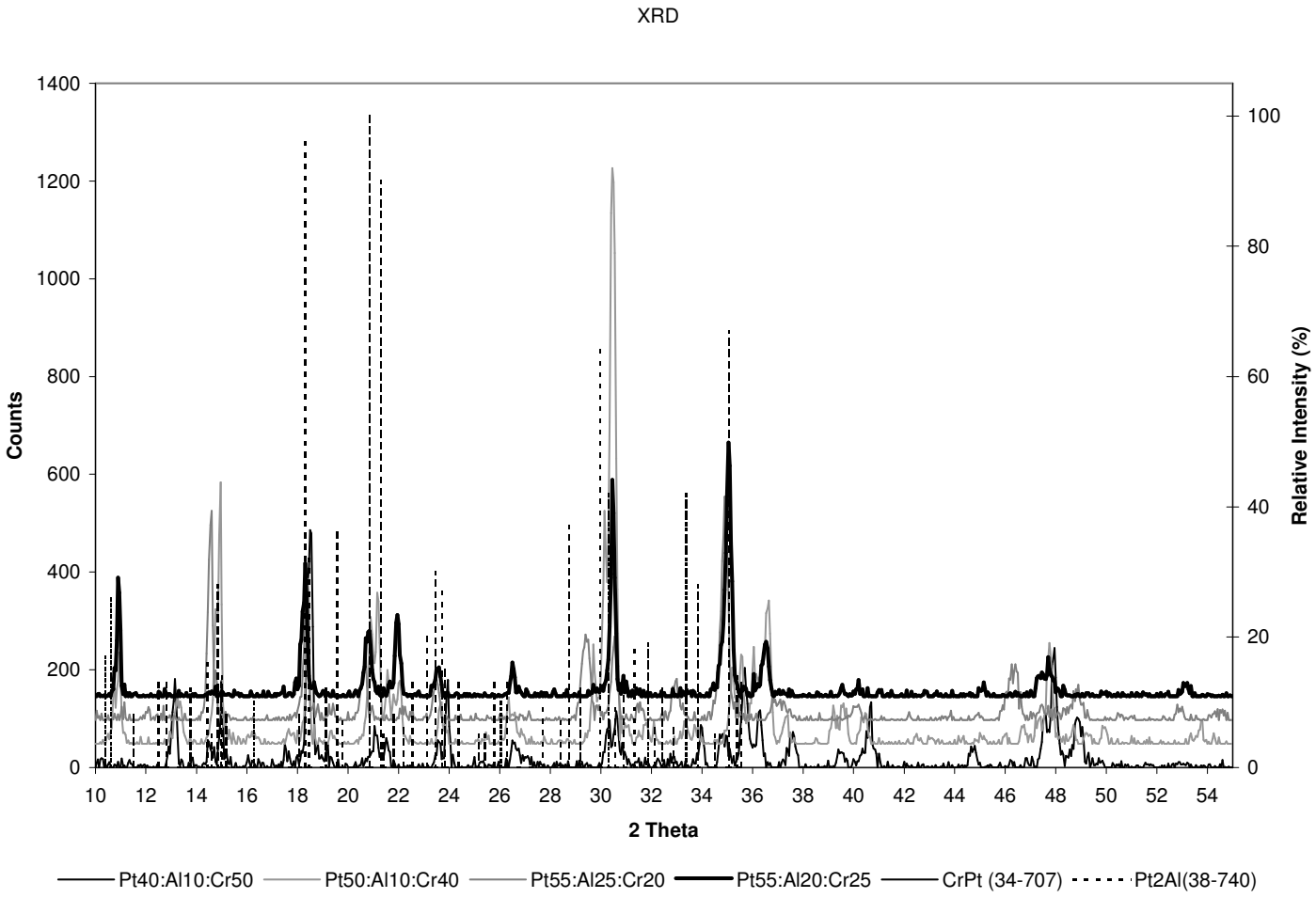

Figure 2.25. XRD pattern for nominal Pt_{40}:Al_{10}:Cr_{50}, Pt_{50}:Al_{10}:Cr_{40}, Pt_{55}:Al_{25}:Cr_{20}, Pt_{55}:Al_{20}:Cr_{25}, in the as-cast condition.

2.1.9. Nominal $Pt_{40}:Al_{30}:Cr_{30}$

Alloy $Pt_{40}:Al_{30}:Cr_{30}$ appeared to be cored single phase with black porosity (Figure 2.26). The alloy's EDX analyses are given in Table 2.9, and Figure 2.27, the graphic representation thereof, shows that the dark and lighter areas' compositions are close together, indicating a possible single phase, albeit cored. The measured XRD pattern was very complex (Figure 2.28). Out of the three possible candidates, ~PtAl, Pt_5Al_3 and ~Pt_2Al, the closest match to the measured XRD pattern was orthorhombic Co_2Si type ~Pt_2Al (Figure 2.28), but it was not totally satisfactory. Three other samples showed similar results: $Pt_{50}:Al_{35}:Cr_{15}$ (§2.1.24), $Pt_{45}:Al_{35}:Cr_{20}$ (§2.1.37) and $Pt_{52}:Al_{43}:Cr_5$ (§2.1.38). All of these were single phase alloys, and the XRD peaks for ~Pt_2Al (in itself complex) was the closest match to their measured XRD patterns. Figure 2.29 shows the similarity between the XRD patterns of these four alloys and it was concluded that these four alloys comprised the same phase. Figure 2.30 compares their XRD patterns with that of ~Pt_2Al as modelled by *Crystallographica*, and it can be seen that although the similarities are there, it is not a good match, especially at $2\theta>24$, i.e. for more than half of the measured angles. Considering the compositions of these alloys and the fact that they were far away from the binary Pt_2Al composition (Figure 2.27), it was concluded that these four alloys comprised a ternary phase, T1, suggested by the complex nature of the measured XRD pattern very similar to that of ~Pt_2Al. The four mentioned alloys' measured XRD patterns were plotted together and an approximate XRD pattern (peak positions only) was derived for T1 by identifying the obvious peaks these alloys had in common (Figure 2.31). This derived pattern for T1 was superposed on the measured pattern for $Pt_{40}:Al_{30}:Cr_{30}$. This is shown in Figure 2.32, and the match, although far from perfect, is quite good, especially considering that the peaks would shift with different compositions. This ternary phase must have solidified congruently:

$$L \rightarrow T1.$$

The coring shows that the slope of the T1 liquidus surface is downwards towards Cr.

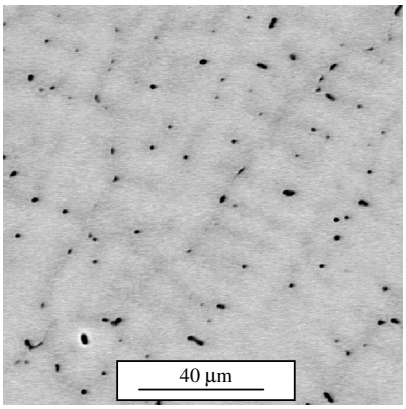

Figure 2.26. BSE-SEM image of nominal $Pt_{40}:Al_{30}:Cr_{30}$ in the as-cast condition: Cored T1.

Table 2.9. Phase analyses for nominal $Pt_{40}:Al_{30}:Cr_{30}$ (at.%) in the as-cast condition.

Phase description	**Pt**	**Al**	**Cr**	**Phase**
Overall	42.3 ± 0.2	31.2 ± 0.3	26.5 ± 0.1	-
Dark	41.8 ± 0.9	29.8 ± 0.5	28.4 ± 1.4	Cored T1
Light	43.7 ± 0.4	31.8 ± 0.6	24.5 ± 1.0	Cored T1

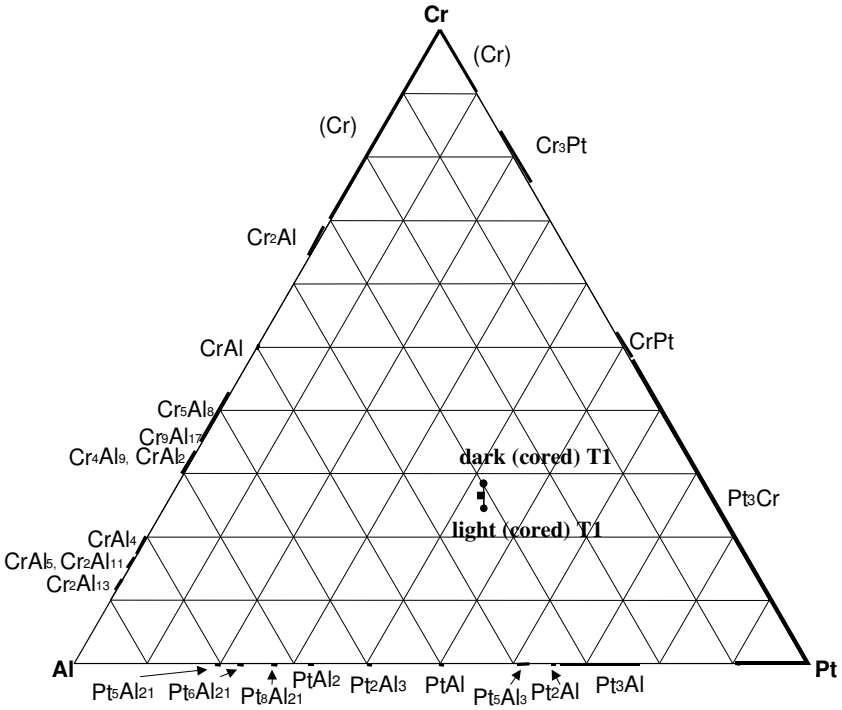

Figure 2.27. EDX analyses of nominal $Pt_{40}:Al_{30}:Cr_{30}$ (at.%) in the as-cast condition.

(■ overall composition; ● phases)

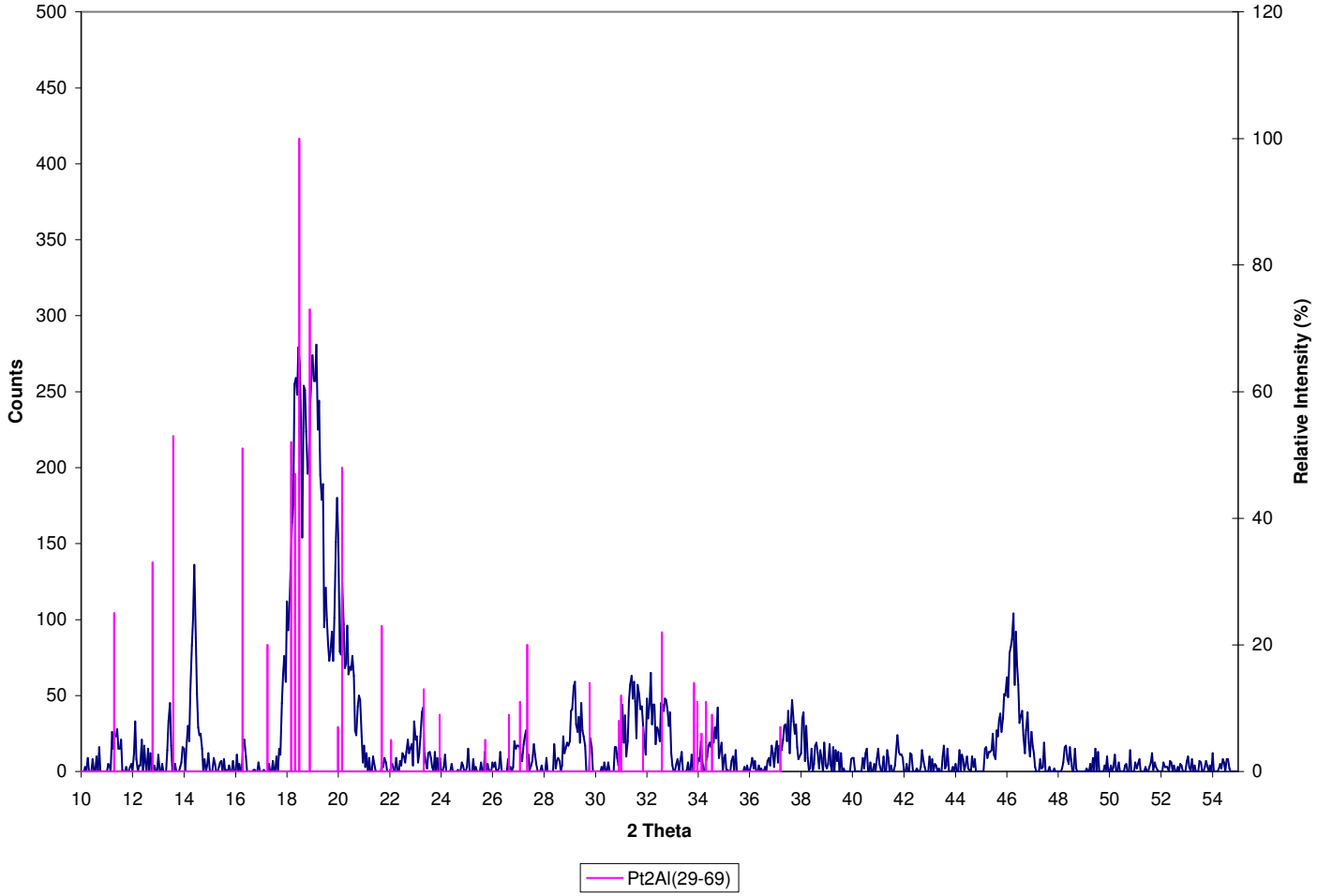

Figure 2.28. XRD pattern for nominal Pt_{40}:Al_{30}:Cr_{30} in the as-cast condition.

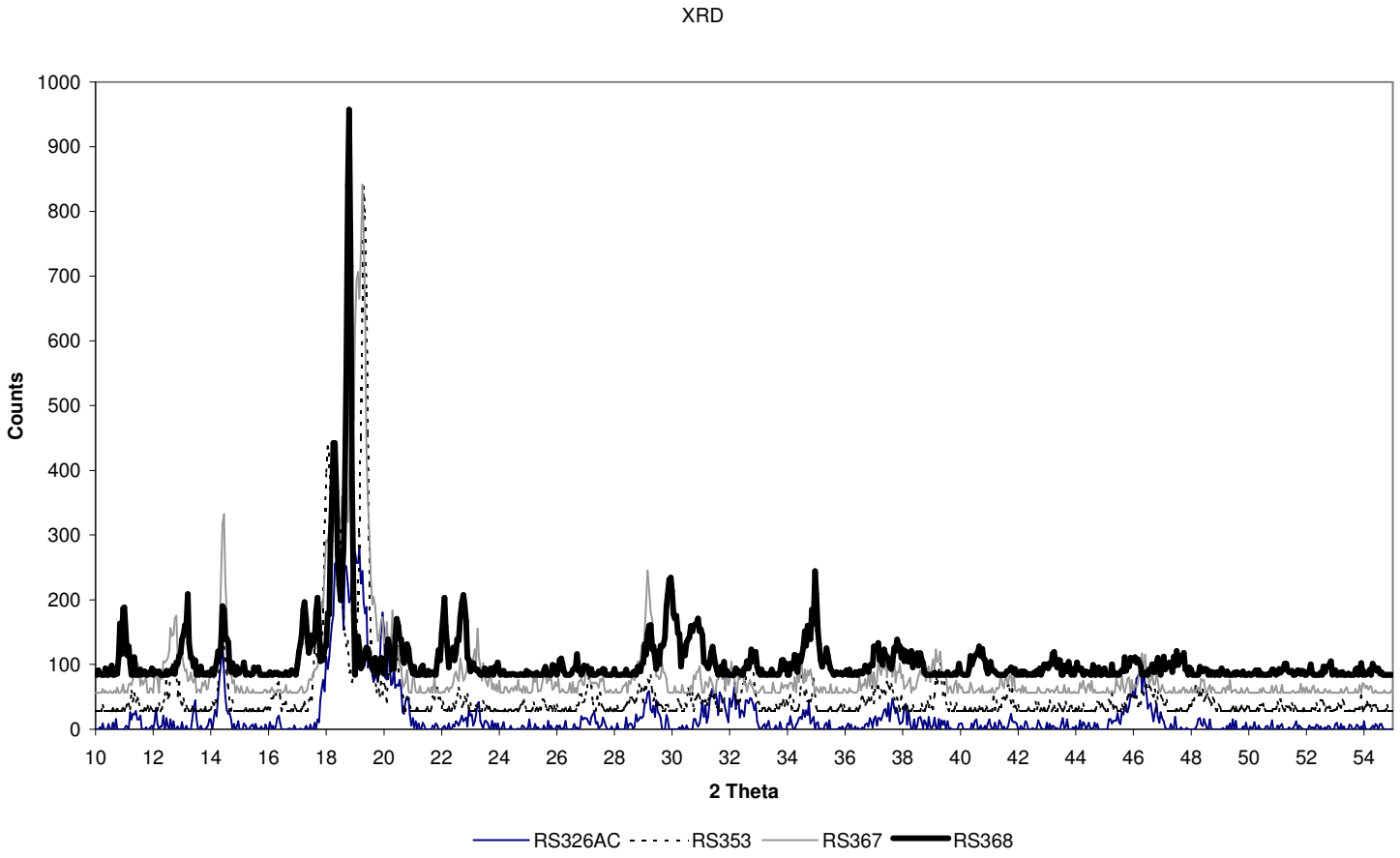

Figure 2.29. XRD pattern for nominal $Pt_{40}:Al_{30}:Cr_{30}$, $Pt_{50}:Al_{35}:Cr_{15}$, $Pt_{45}:Al_{35}:Cr_{20}$ and $Pt_{52}:Al_{43}:Cr_{5}$ (bottom to top) in the as-cast condition.

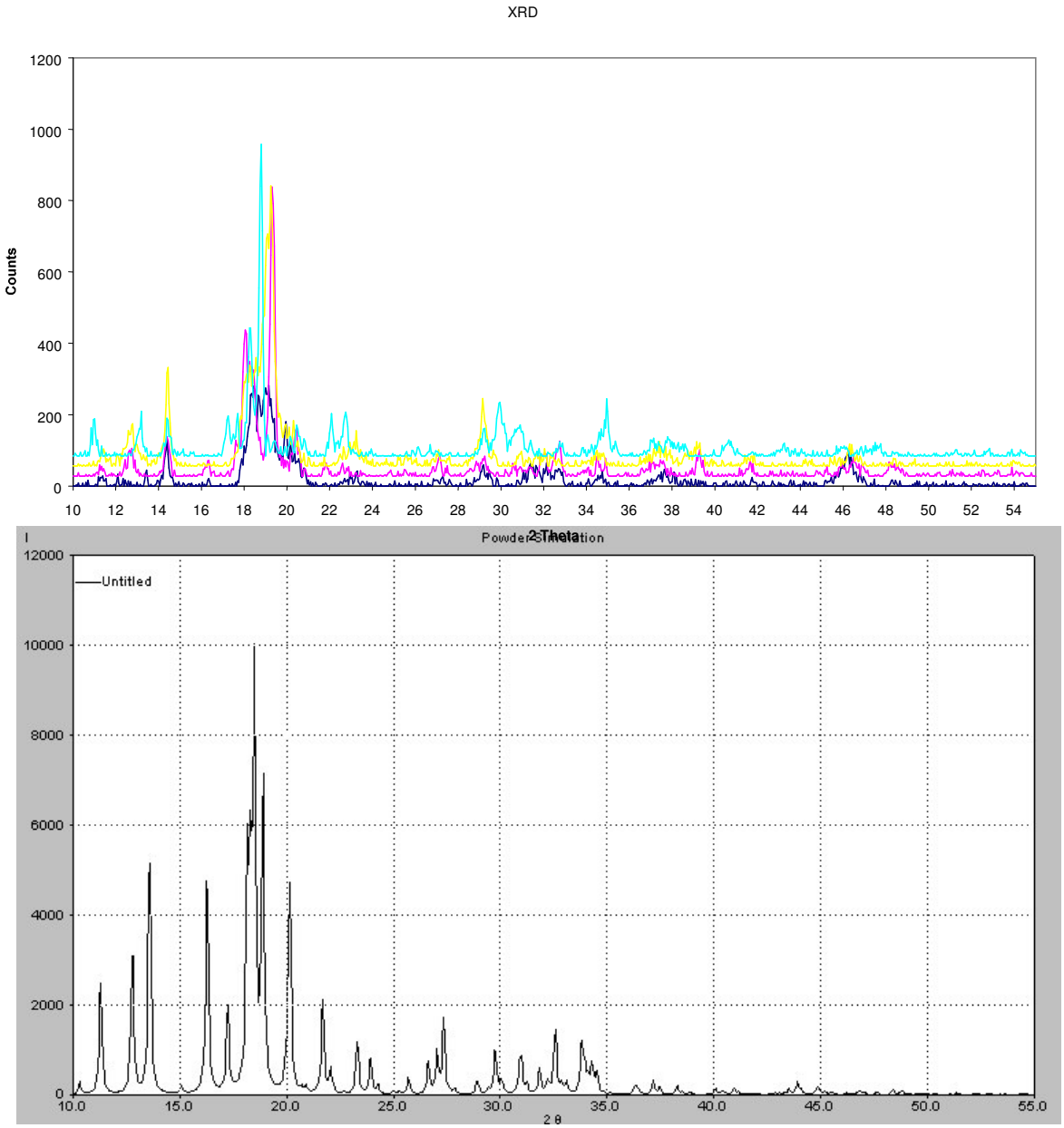

Figure 2.30. XRD pattern for nominal $Pt_{40}:Al_{30}:Cr_{30}$, $Pt_{50}:Al_{35}:Cr_{15}$, $Pt_{45}:Al_{35}:Cr_{20}$ and $Pt_{52}:Al_{43}:Cr_5$ in the as-cast condition compared to that of Pt_2Al as modelled by Crystallographica.

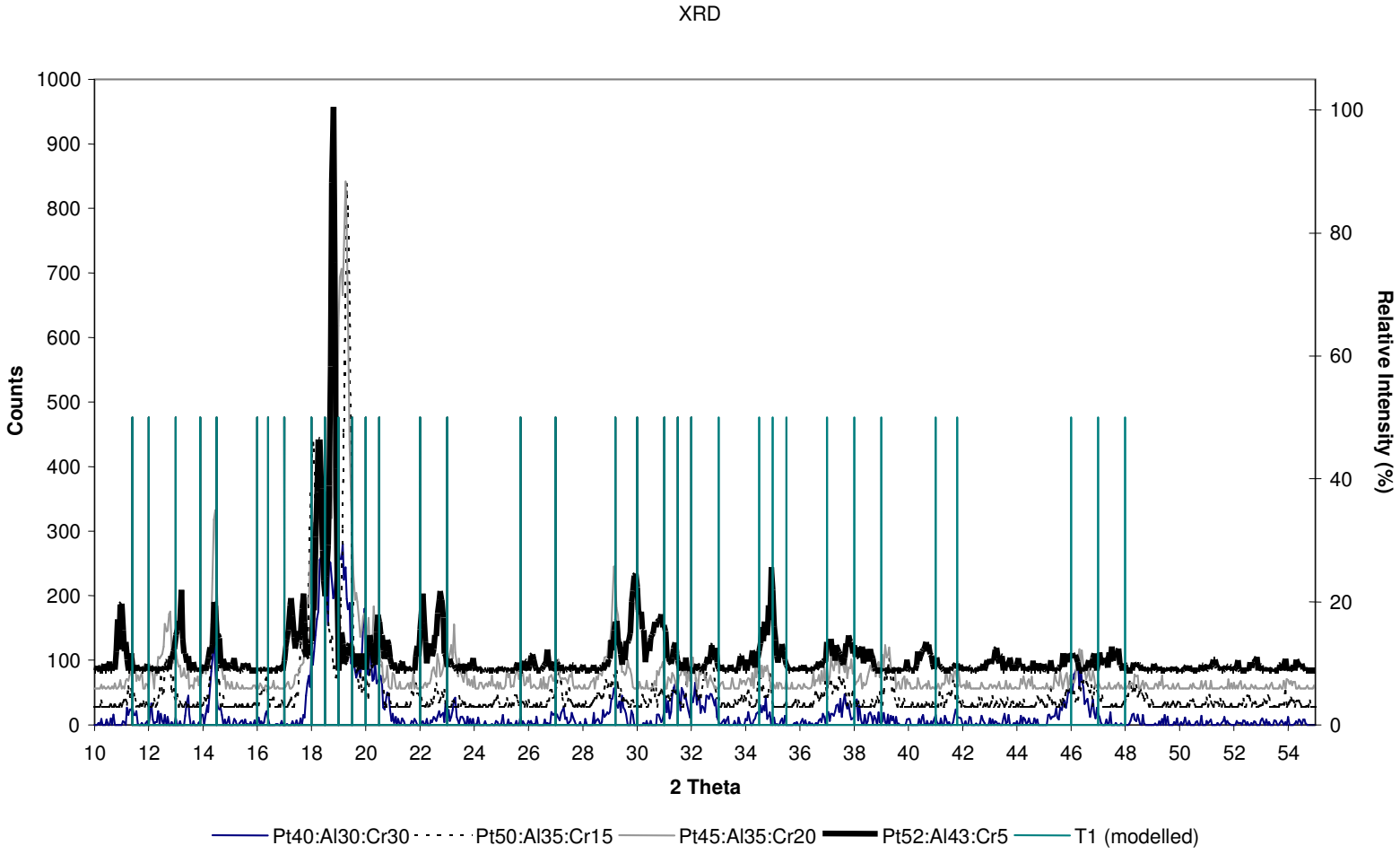

Figure 2.31. The average peak positions of ternary T1 as inferred from the shown measured XRD patterns for nominal $Pt_{40}:Al_{30}:Cr_{30}$, $Pt_{50}:Al_{35}:Cr_{15}$, $Pt_{45}:Al_{35}:Cr_{20}$ and $Pt_{52}:Al_{43}:Cr_5$ in the as-cast condition.

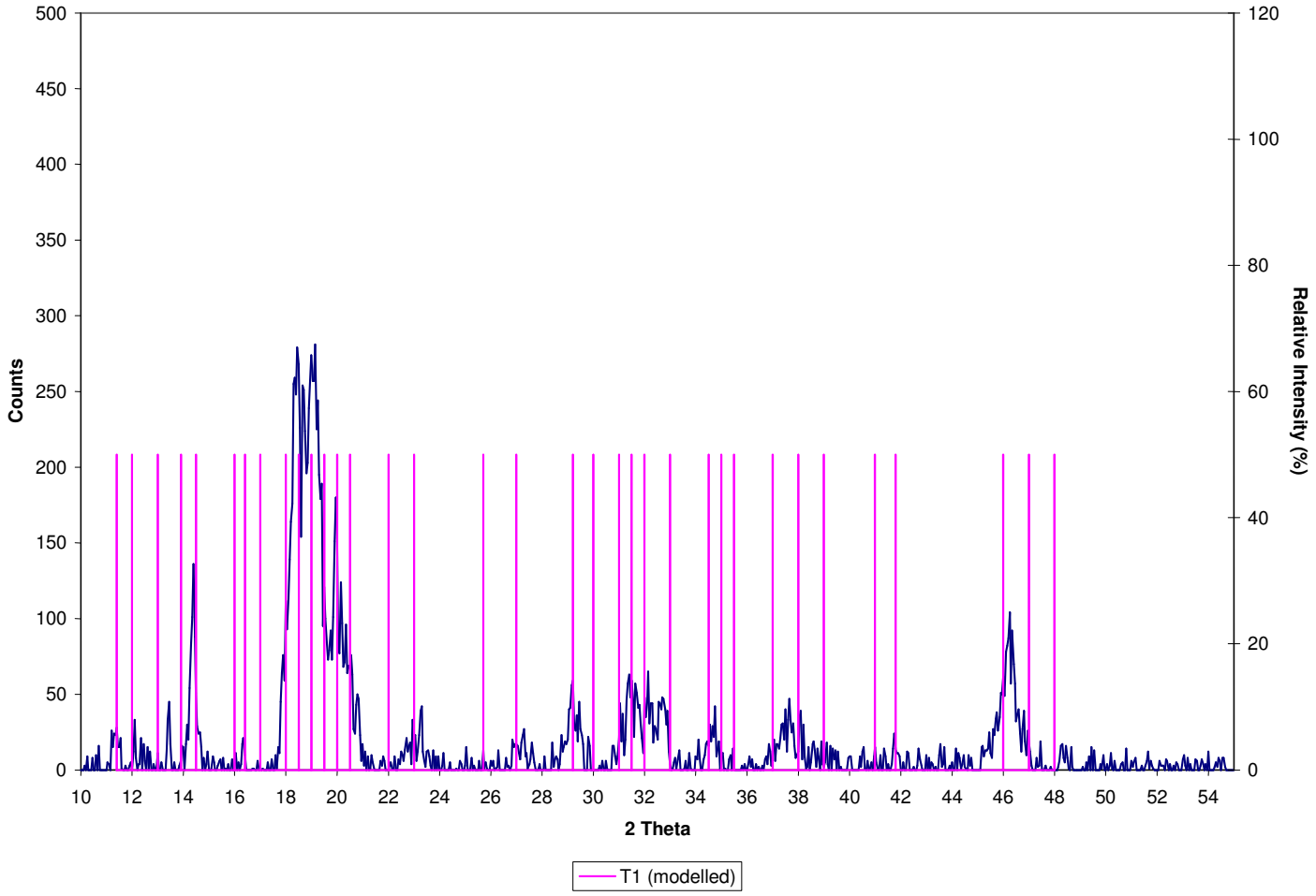

Figure 2.32. The average peak positions of ternary T1 superposed on the measured XRD patterns for nominal Pt_{40}:Al_{30}:Cr_{30} in the as-cast condition.

2.1.10. Nominal $Pt_{40}:Al_{50}:Cr_{10}$

Alloy $Pt_{40}:Al_{50}:Cr_{10}$ appeared to be cored single phase (Figure 2.33), but XRD analysis (Figure 2.34) clearly showed that it comprised two phases, namely a dark ~Pt_2Al_3 and lighter ~PtAl. Using *Crystallographica*, the XRD pattern for ~Pt_2Al_3 was modelled as Al_3Ni_2 type (*hP*5, spacegroup *P*3*ml*) as given by Massalski [1990Mas]. Looking at Figure 2.35 one can see that the peaks for ~Pt_2Al_3 and ~PtAl are an excellent fit to the pattern only up to $2\theta \approx 36$. This could suggest a ternary phase, or it could be because the JCPDS database often does not give information at higher angles. However, some angles ($2\theta \approx 23$, 26.3, 33) were not identified, and taking into account the results of alloys $Pt_{35}:Al_{55}:Cr_{10}$ (§2.1.21), $Pt_{43}:Al_{52}:Cr_5$ (§2.1.23) and $Pt_{75}:Al_{10}:Cr_{15}$ (§2.1.30), it looked possible that the dark phase was not ~Pt_2Al_3 but a ternary phase with a crystal structure very similar to that of Pt_2Al_3, especially considering the extension into the ternary. However, alloy $Pt_{37}:Al_{59}:Cr_4$ showed a single phase with composition very close to that of Pt_2Al_3 (i.e. stable at low Cr content). It was therefore decided to consider the phase present in these alloys as a binary phase Pt_2Al_3 stabilised by Cr into the ternary, and not a ternary phase as such. Therefore, what is seen in Figure 2.33, was cored dendrites of ~PtAl and an interdendritic ternary phase of darker contrast. These would have formed by:

$$L \rightarrow \sim PtAl$$

$$L \rightarrow \sim PtAl + \sim Pt_2Al_3.$$

The "dark" phase was probably a very fine eutectic which could not clearly be resolved.

The EDX analyses are given in Table 2.10 and Figure 2.34. If the dark phase was a combination of two phases actually (an eutectic), it might explain the fact that the overall composition of the alloy did lie away from the tie-line between the apparent phases, even more so than the standard deviations of the values would allow, because the dark phase was not measured accurately. There is much uncertainty about both analyses, but all lie close together.

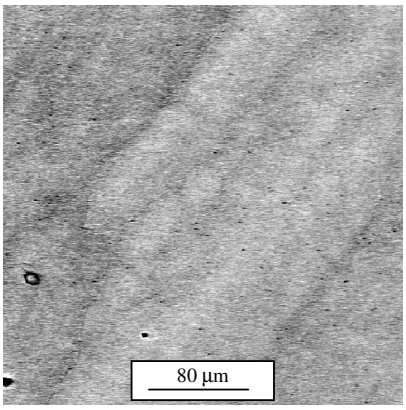

Figure 2.33. BSE-SEM image of nominal $Pt_{40}:Al_{50}:Cr_{10}$ in the as-cast condition: ~Pt_2Al_3 dark; ~PtAl lighter.

Table 2.10. Phase analyses for nominal $Pt_{40}:Al_{50}:Cr_{10}$ (at.%) in the as-cast condition.

Phase description	**Pt**	**Al**	**Cr**	**Phase**
Overall	40.7 ± 0.1	49.5 ± 0.1	9.8 ± 0.1	-
Dark	40.3 ± 0.1	47.9 ± 0.3	11.8 ± 0.4	~Pt_2Al_3
Light	41.6 ± 0.4	48.2 ± 0.8	10.2 ± 0.4	~PtAl

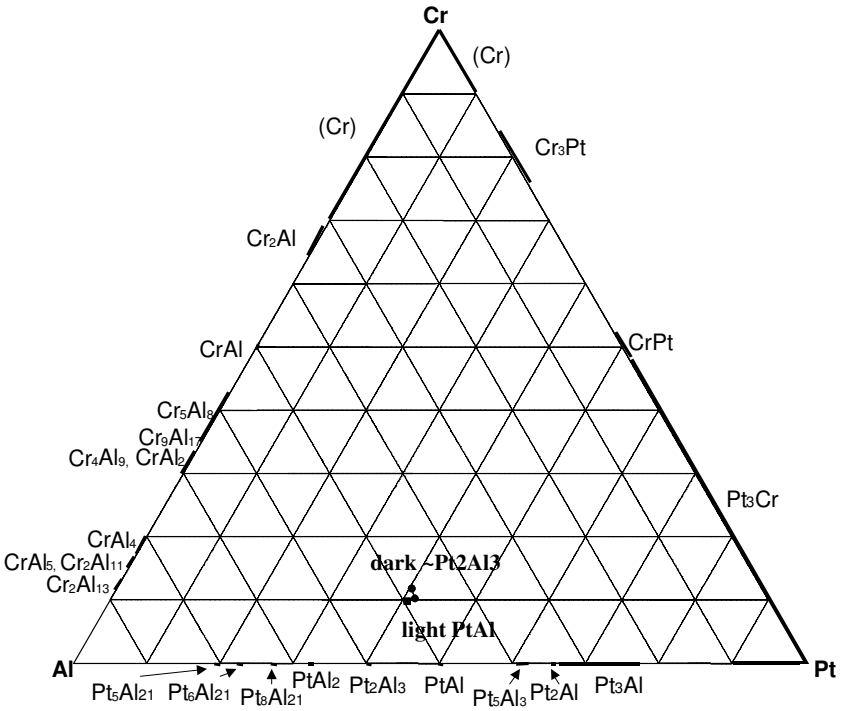

Figure 2.34. EDX analyses of nominal $Pt_{40}:Al_{50}:Cr_{10}$ (at.%) in the as-cast condition.

(■ overall composition; ● phases)

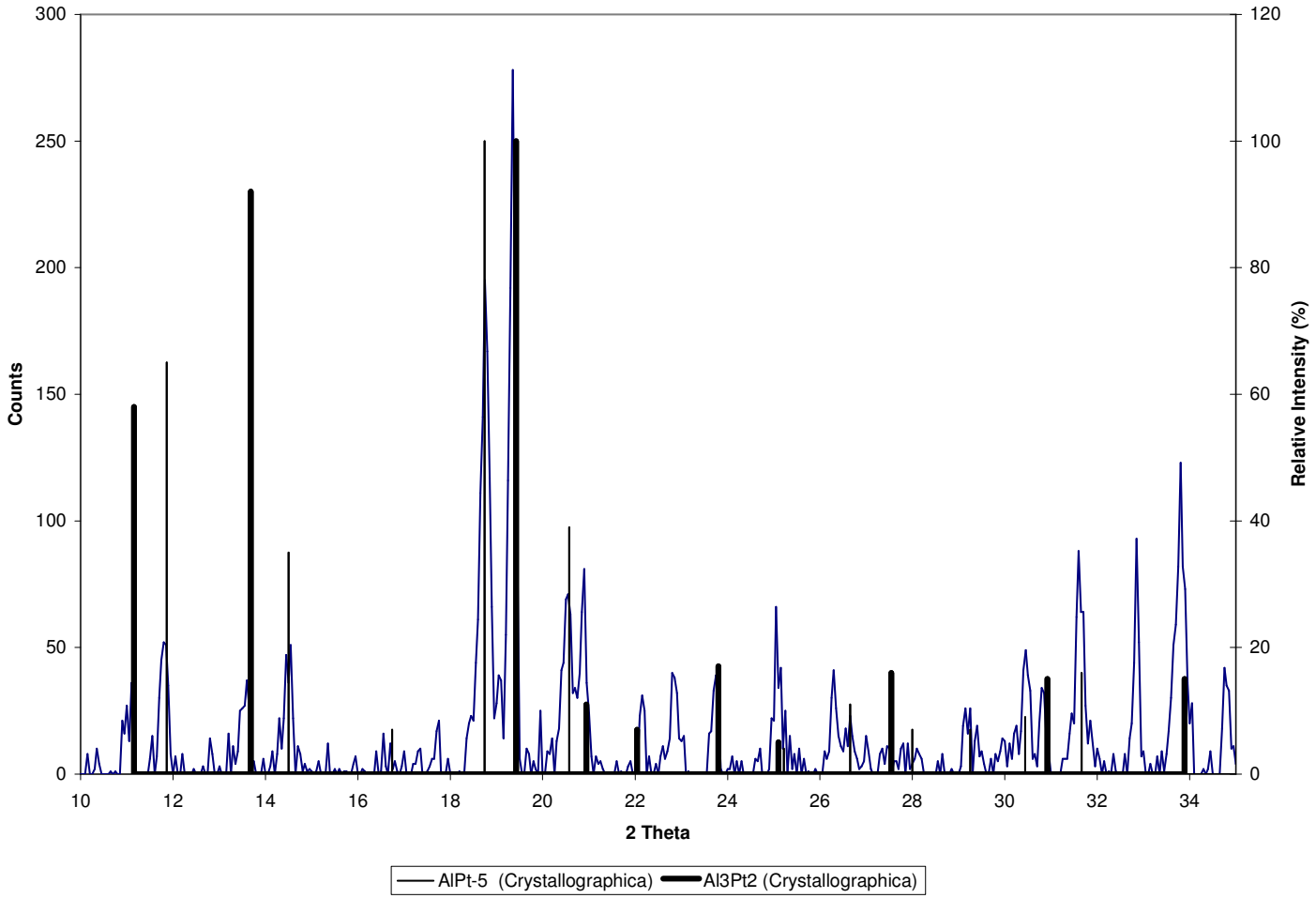

Figure 2.35. XRD pattern for nominal Pt_{40}:Al_{50}:Cr_{10} in the as-cast condition.

2.1.11. Nominal $Pt_{50}:Al_{10}:Cr_{40}$

Alloy $Pt_{50}:Al_{10}:Cr_{40}$ comprised dark $L1_0$ ~CrPt dendrites with a light interdendritic phase, probably a sparse eutectic (Figure 2.36). The EDX analyses are given in Table 2.11 and Figure 2.37. As was the case with alloy $Pt_{40}:Al_{10}:Cr_{50}$ (§8), the presence of $L1_0$ ~CrPt was easily confirmed by XRD analysis, but it was difficult to identify the light phase from the XRD measurements. The measured XRD pattern was very complicated with a multitude of peaks of varying intensities. Figure 2.38 shows that the amount of similarities in measured XRD patterns for alloys $Pt_{40}:Al_{10}:Cr_{50}$ and $Pt_{50}:Al_{10}:Cr_{40}$ outweighed the few differences ($2\theta \approx 11, 45$). It was thought that, because the two alloys were similar, the unknown phase was most probably C23 ~Pt_2Al as well. Figure 2.39 shows ~CrPt and the XRD pattern for ~Pt_2Al superposed on the measured pattern for alloy $Pt_{50}:Al_{10}:Cr_{40}$. The match seemed to be quite good up to $2\theta \approx 35$. The JCPDS database did not give information for higher angles.

This structure could have formed by the following reactions:

$$L \rightarrow (Pt)$$

$$L \rightarrow (Pt) + \sim Pt_3Al$$

$$\sim Pt_3Al \rightarrow \sim Pt_2Al$$

$$(Pt) \rightarrow \sim CrPt_3 \rightarrow \sim CrPt \text{ (ordering)}$$

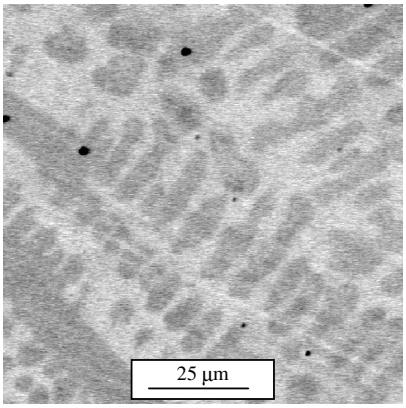

Figure 2.36. BSE-SEM image of nominal $Pt_{50}:Al_{10}:Cr_{40}$ in the as-cast condition: ~CrPt dark; ~Pt_2Al light.

Table 2.11. Phase analyses for nominal $Pt_{50}:Al_{10}:Cr_{40}$ (at.%) in the as-cast condition.

Phase description	**Pt**	**Al**	**Cr**	**Phase**
Overall	50.5 ± 0.3	9.7 ± 0.4	39.7 ± 0.1	-
Dark	50.1 ± 0.2	5.4 ± 0.2	44.5 ± 0.0	~CrPt
Light	51.1 ± 0.3	14.4 ± 0.3	34.5 ± 0.5	~Pt_2Al

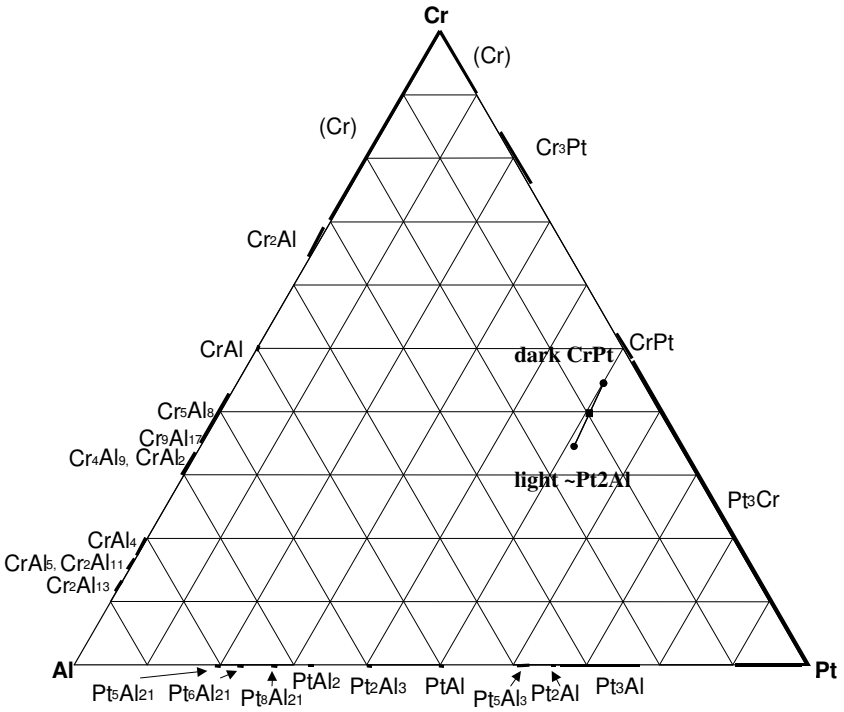

Figure 2.37. EDX analyses of nominal $Pt_{50}:Al_{10}:Cr_{40}$ (at.%) in the as-cast condition.

(■ overall composition; ● phases)

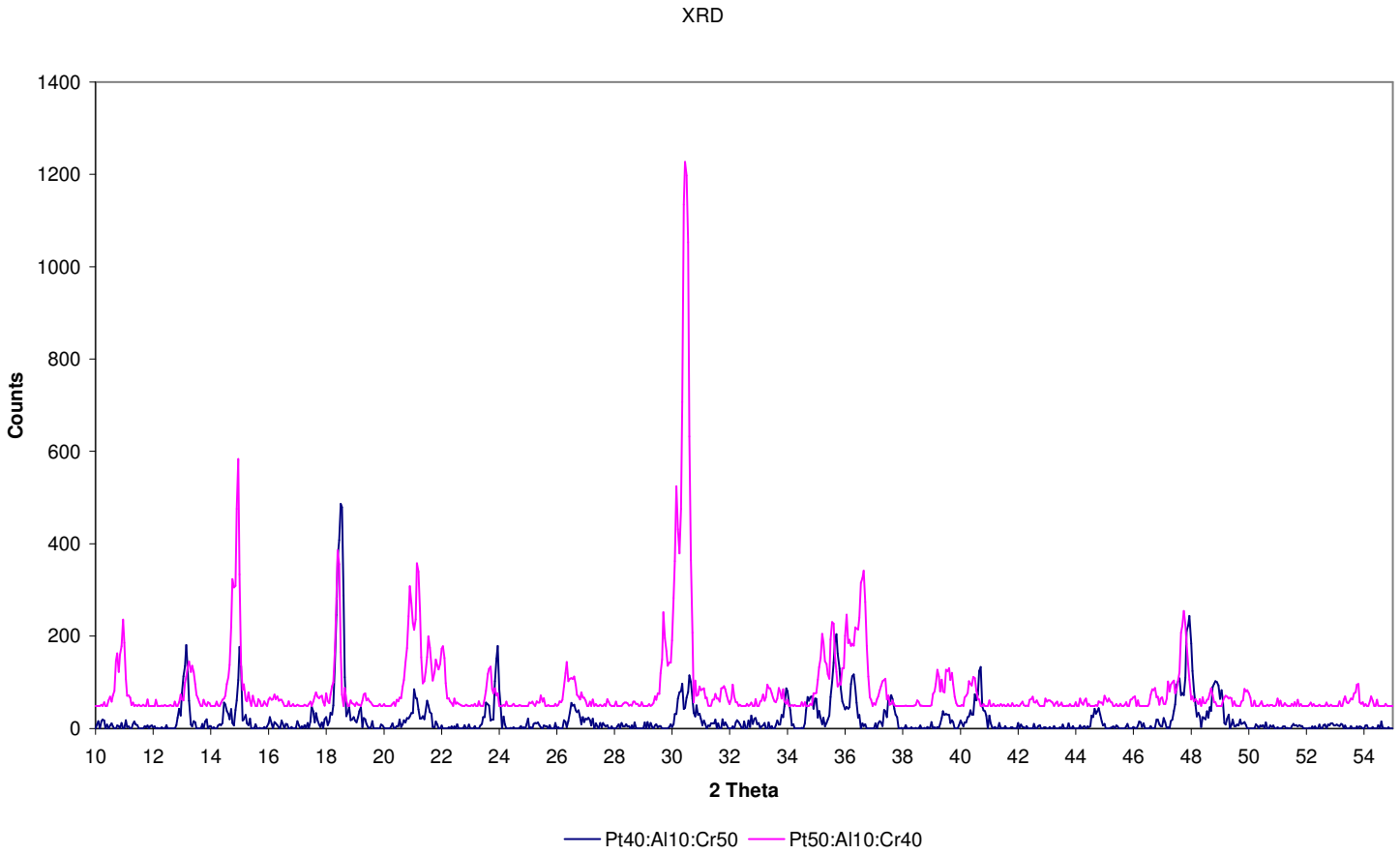

Figure 2.38. XRD patterns for nominal Pt_{50}:Al_{10}:Cr_{40} and Pt_{40}:Al_{10}:Cr_{50} in the as-cast condition.

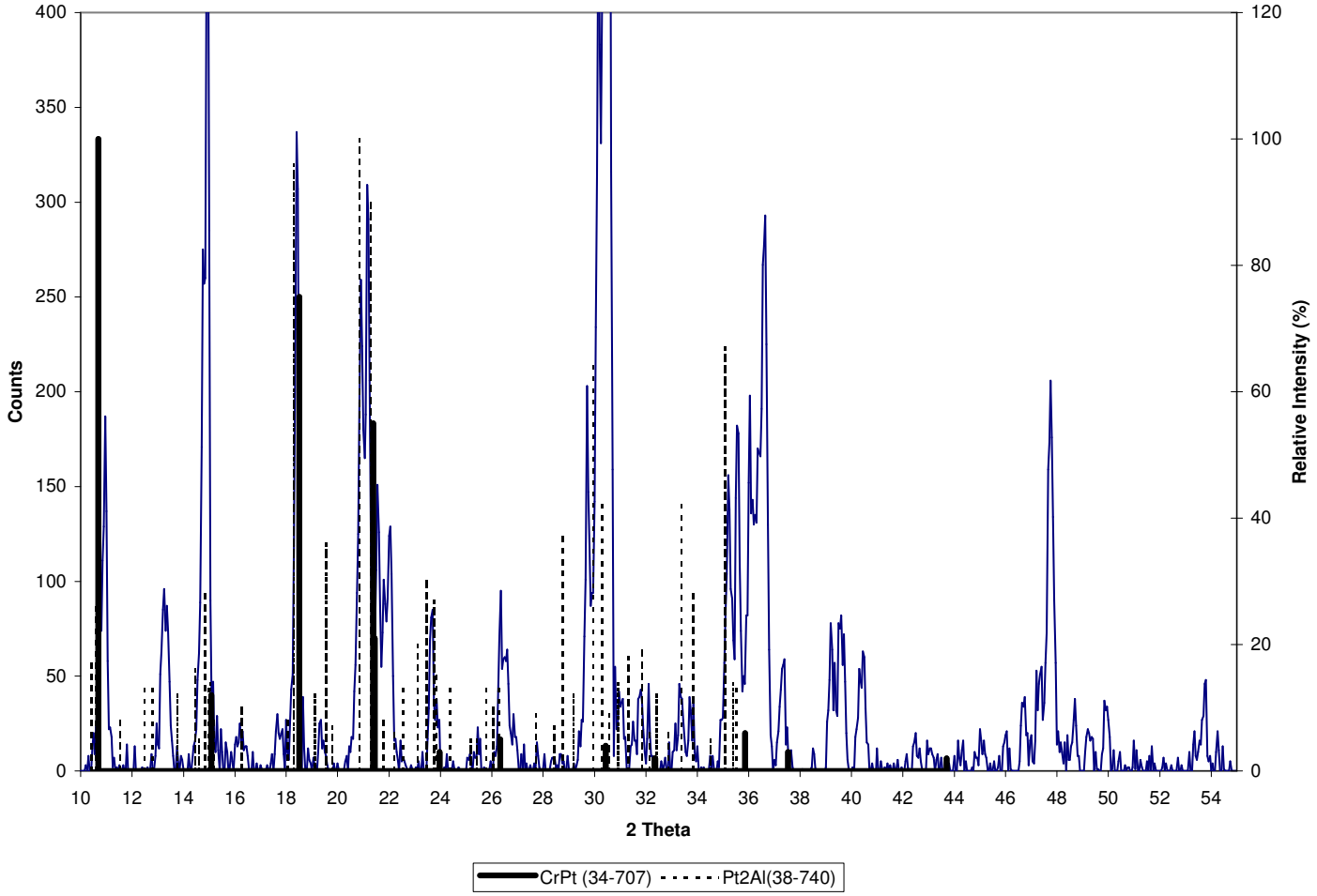

Figure 2.39. XRD pattern for nominal Pt_{50}:Al_{10}:Cr_{40} in the as-cast condition.

2.1.12. Nominal $Pt_{65}:Al_5:Cr_{30}$

Alloy $Pt_{65}:Al_5:Cr_{30}$ appeared cored single phase (medium and light) with a very small amount of dark second phase particles visible (Figure 2.40). XRD analysis did detect two phases (Figure 2.41), and one can assume that the two phases detected were the medium ~Pt_3Cr dendrites and dark ~Pt_3Al particles. These phases were a very good fit for the measured pattern. It was not possible to discern whether the ~Pt_3Al was of the ~$GaPt_3$ (tetragonal, $D0'_C$, low temperature) or $AuCu_3$ (cubic, $L1_2$, high temperature) type. The microstructure could have formed by:

$$L \rightarrow (Pt)$$

$$L \rightarrow (Pt) + \sim Pt_3Al$$

$$(Pt) \rightarrow \sim Pt_3Cr \text{ (ordering)}$$

The EDX analyses are shown in Table 2.12 and Figure 2.42.

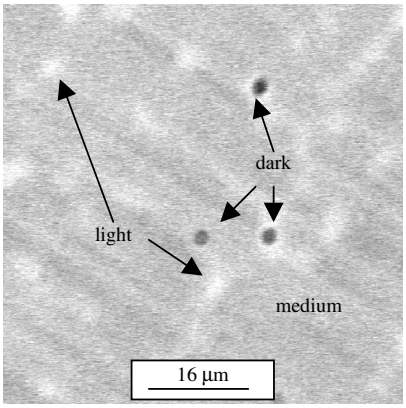

Figure 2.40. BSE-SEM image of nominal $Pt_{65}:Al_5:Cr_{30}$ in the as-cast condition: ~Pt_3Cr medium and light; ~Pt_3Al dark.

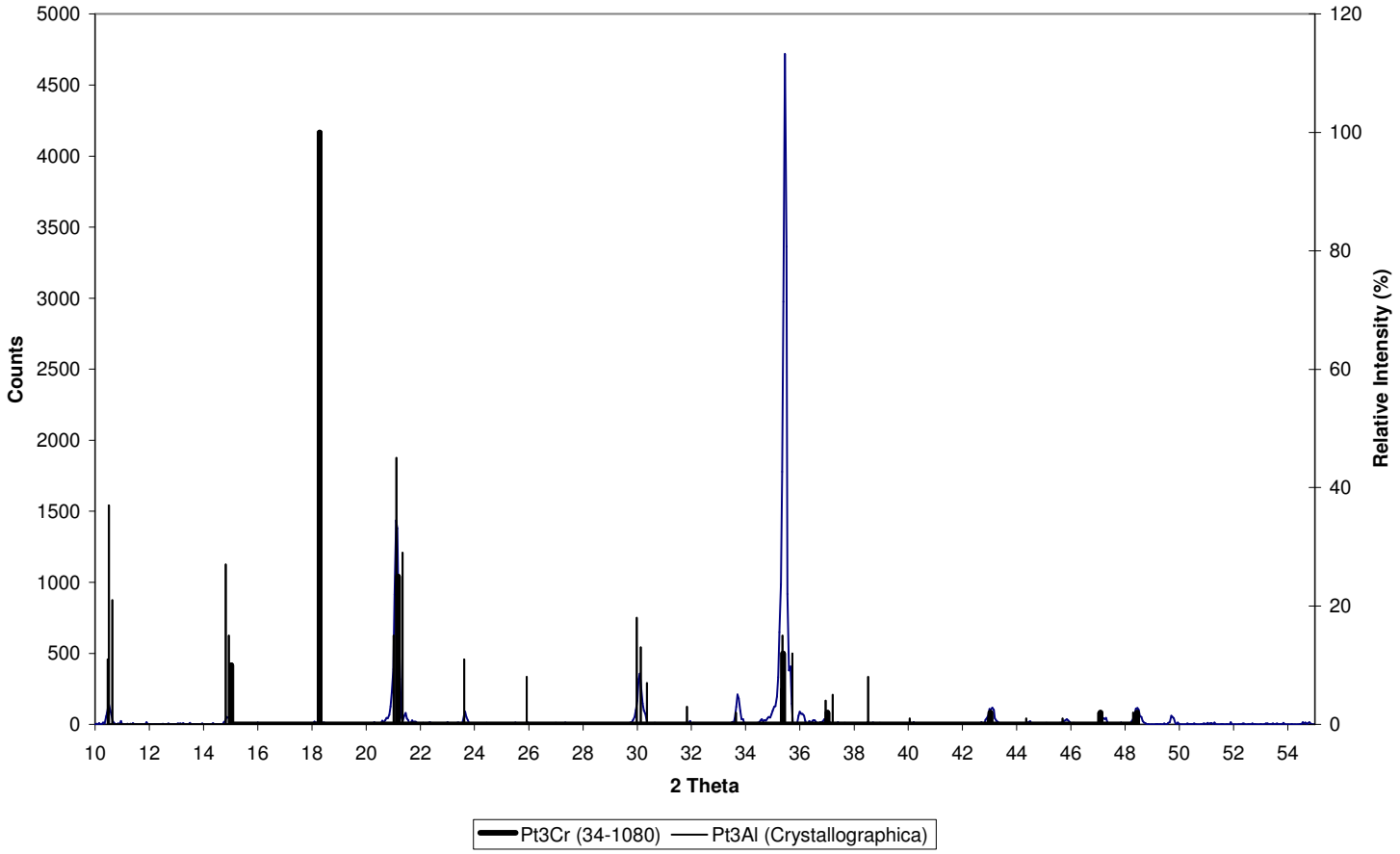

Figure 2.41. XRD pattern for nominal $Pt_{65}:Al_5:Cr_{30}$ in the as-cast condition.

Table 2.12. Phase analyses for nominal $Pt_{65}:Al_5:Cr_{30}$ (at.%) in the as-cast condition.

Phase description	**Pt**	**Al**	**Cr**	**Phase**
Overall	64.6 ± 0.2	5.2 ± 0.2	30.2 ± 0.2	-
Dark particles	63.5 ± 4.3	12.9 ± 0.3	23.6 ± 0.4	~Pt_3Al
Medium	64.4 ± 0.2	3.9 ± 0.3	31.7 ± 0.1	Cored ~Pt_3Cr
Light*	64.3	3.2	32.5	Cored ~Pt_3Cr

*Only one measurement taken due to small size.

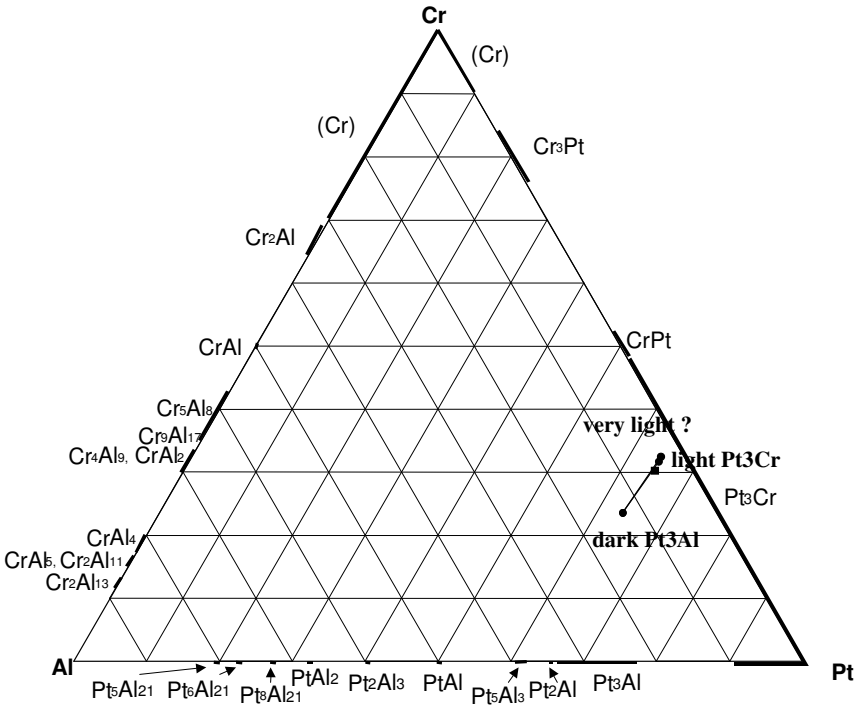

Figure 2.42. EDX analyses of nominal $Pt_{65}:Al_5:Cr_{30}$ (at.%) in the as-cast condition.
(■ overall composition; ● phases)

2.1.13. Nominal $Pt_3:Al_{65}:Cr_{32}$

Alloy $Pt_3:Al_{65}:Cr_{32}$ was similar in appearance to alloy $Pt_{10}:Al_{60}:Cr_{30}$ (§2.1.3), comprising dark dendrites with a light interdendritic phase in some areas, while in other areas the interdendritic areas comprised an eutectic mixture of dark and light (Figure 2.43). The EDX analyses are given in Table 2.13 and Figure 2.44. XRD analysis clearly confirmed that the one phase – the light one – was ~$PtAl_2$ (Figure 2.45). Taking into account the position of the dark phase on the ternary diagram (Figure 2.44), one would expect that it could be ~Cr_5Al_8, ~Cr_9Al_{17} (a JCPDS intermetallic compound) or ~Cr_4Al_9, but the XRD analysis showed that the remaining experimental peaks (not matching with those of ~$PtAl_2$) coincided with a

combination of that of ~Cr_4Al_9 and ~Cr_9Al_{17}. The compositions and diffraction patterns of these intermetallics are so similar, making it difficult to decide on the most correct one. Since ~Cr_9Al_{17} is not observed in the Cr-Al binary phase diagram, it was assumed that the dark phase was probably ~Cr_4Al_9.

The structure could have formed by the following reaction sequence:

$$L \rightarrow \sim Cr_4Al_9$$

$$L \rightarrow \sim Cr_4Al_9 + \sim PtAl_2$$

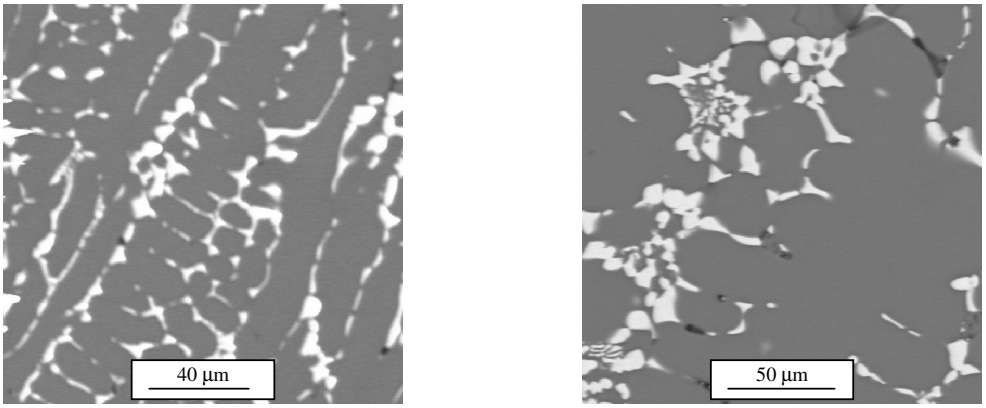

Figure 2.43. BSE-SEM image of nominal Pt_3:Al_{65}:Cr_{32} in the as-cast condition: ~Cr_4Al_9 dark; ~$PtAl_2$ light.

Table 2.13. Phase analyses for nominal Pt_3:Al_{65}:Cr_{32} (at.%) in the as-cast condition.

Phase description	**Pt**	**Al**	**Cr**	**Phase**
Overall	3.0 ± 0.7	64.5 ± 0.2	32.5 ± 0.5	-
Dark	0.8 ± 0.1	65.2 ± 0.3	34.0 ± 0.3	~Cr_4Al_9
Light	25.2 ± 1.5	61.1 ± 0.8	13.7 ± 2.1	~$PtAl_2$
Eutectic dark + light	Too small to be measured	Too small to be measured	Too small to be measured	~Cr_4Al_9 + ~$PtAl_2$

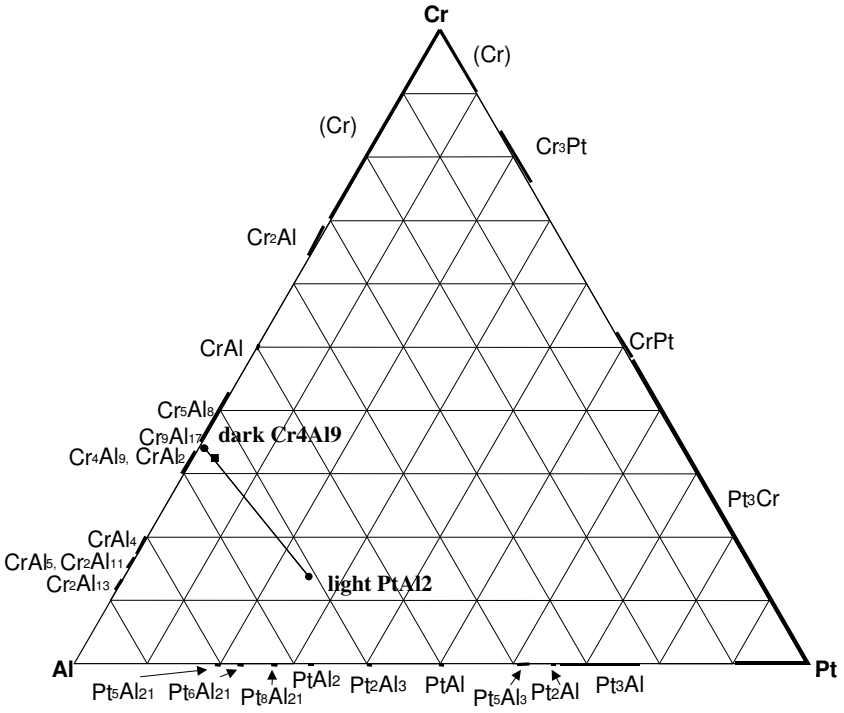

Figure 2.44. EDX analyses of nominal $Pt_3:Al_{65}:Cr_{32}$ (at.%) in the as-cast condition. (■ overall composition; ● phases)

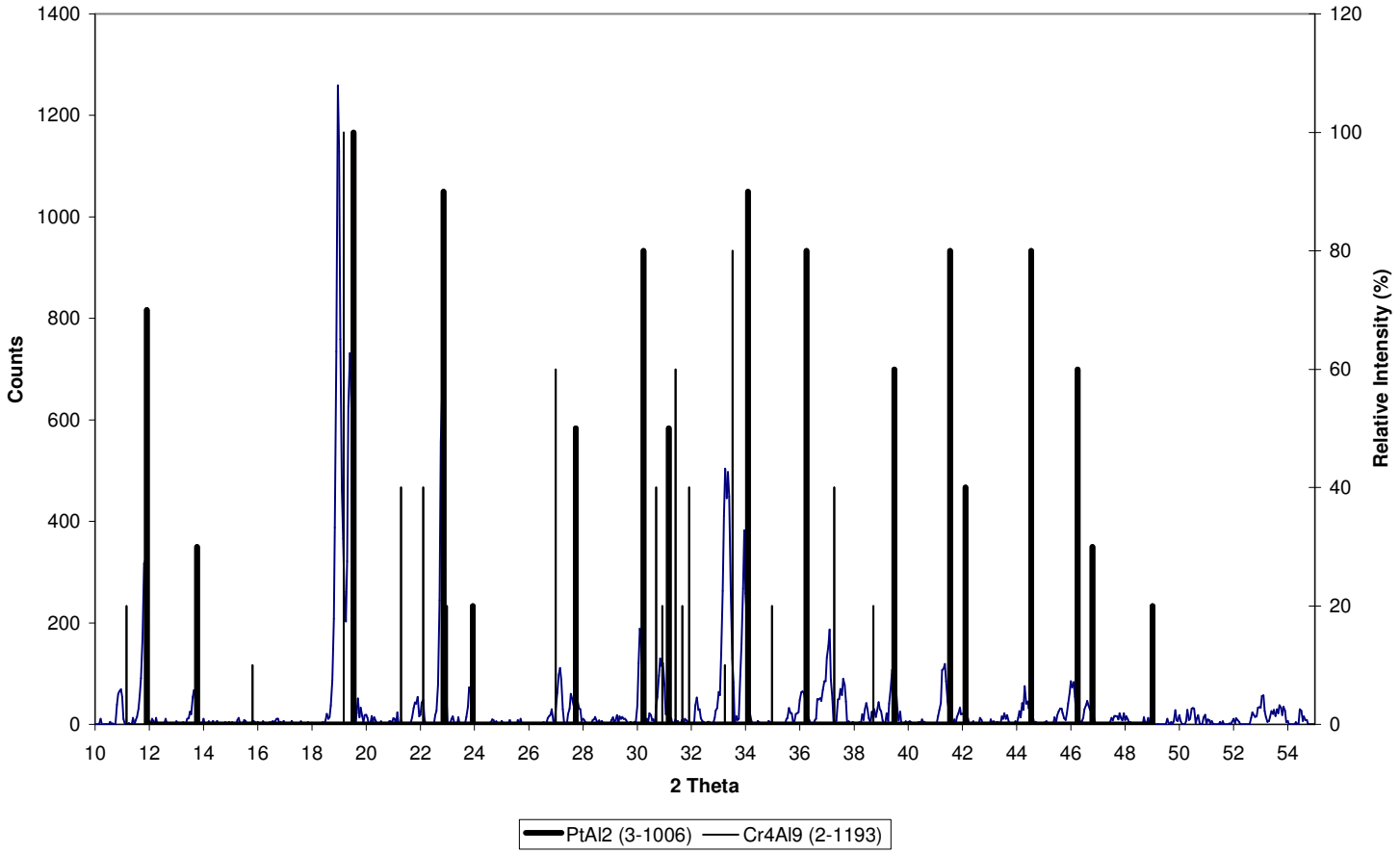

Figure 2.45. XRD pattern for nominal Pt_3:Al_{65}:Cr_{32} in the as-cast condition.

2.1.14. Nominal $Pt_3:Al_{35}:Cr_{62}$

Alloy $Pt_3:Al_{35}:Cr_{62}$ had a very peculiar microstructure. It showed a black phase with tiny grey particles inside; a white phase; and a eutectic mixture of black and white with a web-like appearance (Figure 2.46). The white phase was analysed in the centre of the "big" white areas (i.e. not in the "web" areas). No attempt was made to analyse either the grey particles or black phase due to their extremely small sizes. The compositions "as-is" (Table 2.14) can be seen graphically in Figure 2.47. Even the white phase was too small to yield any accurate results. The only compositions that would be accurate in Table 2.14 are the two-phase compositions, i.e. that of the black + light combination (area analysis of webs) and that of the black + grey combination (area analysis of dendrite interiors).

Figure 2.48 shows an adjusted version of Figure 2.47, where a number of extrapolations had been made to fit the situation best. These can be explained as follows:

- Since the measured analyses of the white phase were in fact "diluted" values, and since the black + light composition still had to lie on the tie-line between the black and light phases, one can extrapolate the composition of the white phase along a tie-line to much lower levels of Cr, and one can also extrapolate the composition of the dark phase along a tie-line to lower levels of Pt.
- The composition of the grey phase was totally unknown. However, since there is a grey + black composition, a tie-line between grey and black exists. Furthermore, the distinction of phases in BSE mode is dependent on the average atomic number of a phase, where the darkest phase would have the lowest average atomic number and the lightest phase the highest atomic number. The composition of the grey phase therefore had to be such that its average atomic number is in-between that of the black and white phases.
- The last point that had to be kept in mind is the fact that the overall composition of the alloy had to lie inside the composition triangle.

The extrapolated triangle in Figure 2.48 is probably the only configuration that satisfied all the above-mentioned criteria.

From Figure 2.48 one would expect that the dark phase was ~Cr_2Al and the light phase probably ~$PtAl_2$. These two phases were confirmed by XRD analysis (Figure 2.49). Using *Crystallographica*, Cr_2Al was modelled as A2 $MoSi_2$ type. The identity of ~Cr_2Al was also confirmed by the results of alloy Pt_{13}:Al_{45}:Cr_{42} (§2.1.33). The grey phase was less easy to identify, because the presence of either Cr_3Al_2 (a JCPDS compound) or CrAl (listed in Pearson's Handbook) was suggested. Since the diffraction peaks of CrAl overlap with the other phases' and are therefore not visible, an insert is given in Figure 2.49 to clearly show how the peaks of W-type CrAl (also modelled using *Crystallographica*) is a clear fit to some of the measured peaks. Having said that, Cr_3Al_2 was detected in both alloys Pt_{10}:Al_{50}:Cr_{40} (§2.1.15) and Pt_5:Al_{52}:Cr_{43} (§2.1.32). Furthermore, the latter alloy had ~Cr_3Al_2 and ~Cr_5Al_8 in equilibrium, and not ~CrAl which lies between these phases in composition. It can therefore be concluded that the dark phase in alloy Pt_3:Al_{35}:Cr_{62} was most probably a ternary phase T2 based on the structure of Cr_3Al_2. The microstructure formed by the following reactions:

$$L \rightarrow (Cr)$$

$$L \rightarrow (Cr) + \sim PtAl_2$$

$$(Cr) \rightarrow \sim Cr_2Al \text{ (ordering)}$$

$$\sim Cr_2Al \rightarrow T2 \text{ (solid state precipitation)}$$

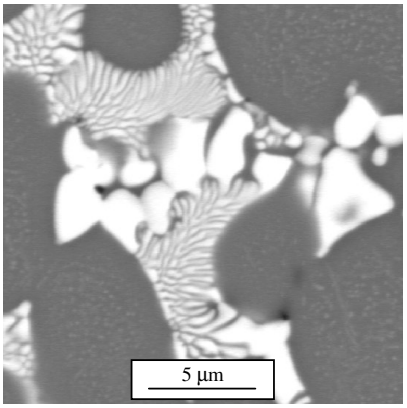

Figure 2.46. BSE-SEM image of nominal Pt_3:Al_{35}:Cr_{62} in the as-cast condition: ~Cr_2Al black; ~$PtAl_2$ white; T2≈Cr_3Al_2 grey.

Table 2.14. Phase analyses for nominal $Pt_3:Al_{35}:Cr_{62}$ (at.%) in the as-cast condition.

Phase description	**Pt**	**Al**	**Cr**	**Phase**
Overall	2.5 ± 0.1	34.1 ± 1.0	63.3 ± 1.0	-
Black	Too small to measure	Too small to measure	Too small to measure	~Cr_2Al
White	23.7 ± 2.6	54.6 ± 2.6	21.8 ± 5.2	~$PtAl_2$
Grey	Too small to measure	Too small to measure	Too small to measure	T2≈Cr_3Al_2
Eutectic black + white	14.5 ± 0.3	45.7 ± 0.1	39.9 ± 0.4	~Cr_2Al + ~$PtAl_2$
Two-phase black + grey*	4.2	37.7	58.1	~Cr_2Al + T2≈Cr_3Al_2

* Only one measurement taken.

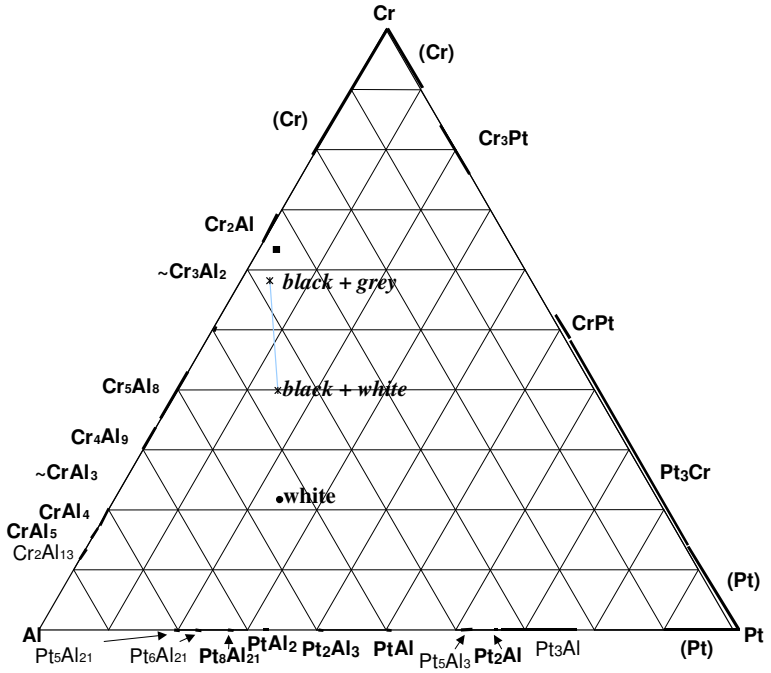

Figure 2.47. EDX analyses of nominal $Pt_3:Al_{35}:Cr_{62}$ (at.%) in the as-cast condition. (■ overall composition; ● phases; ✶ eutectic/two-phase)

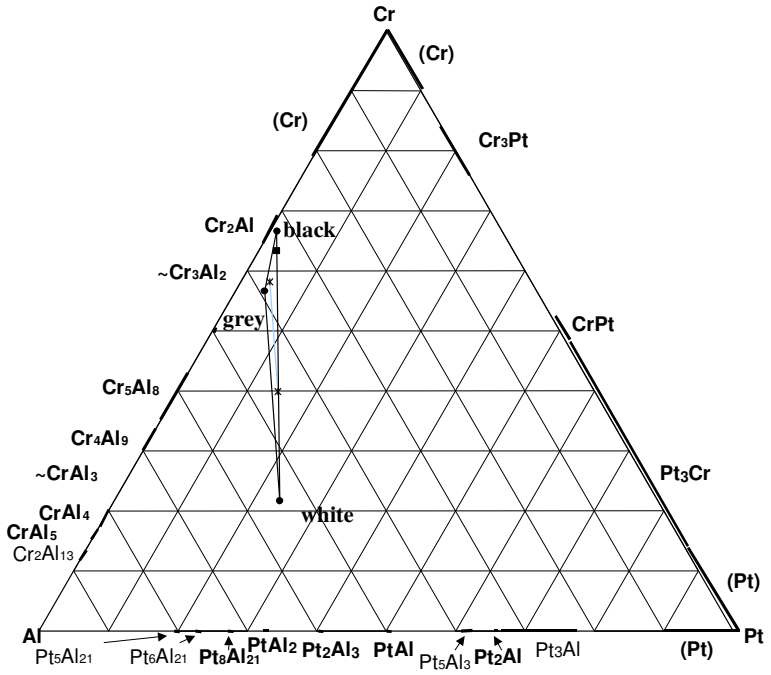

Figure 2.48. EDX analyses of nominal Pt_3:Al_{35}:Cr_{62} (at.%) in the as-cast condition.

(■ overall composition; ● phases; ✶ eutectic/ two-phase)

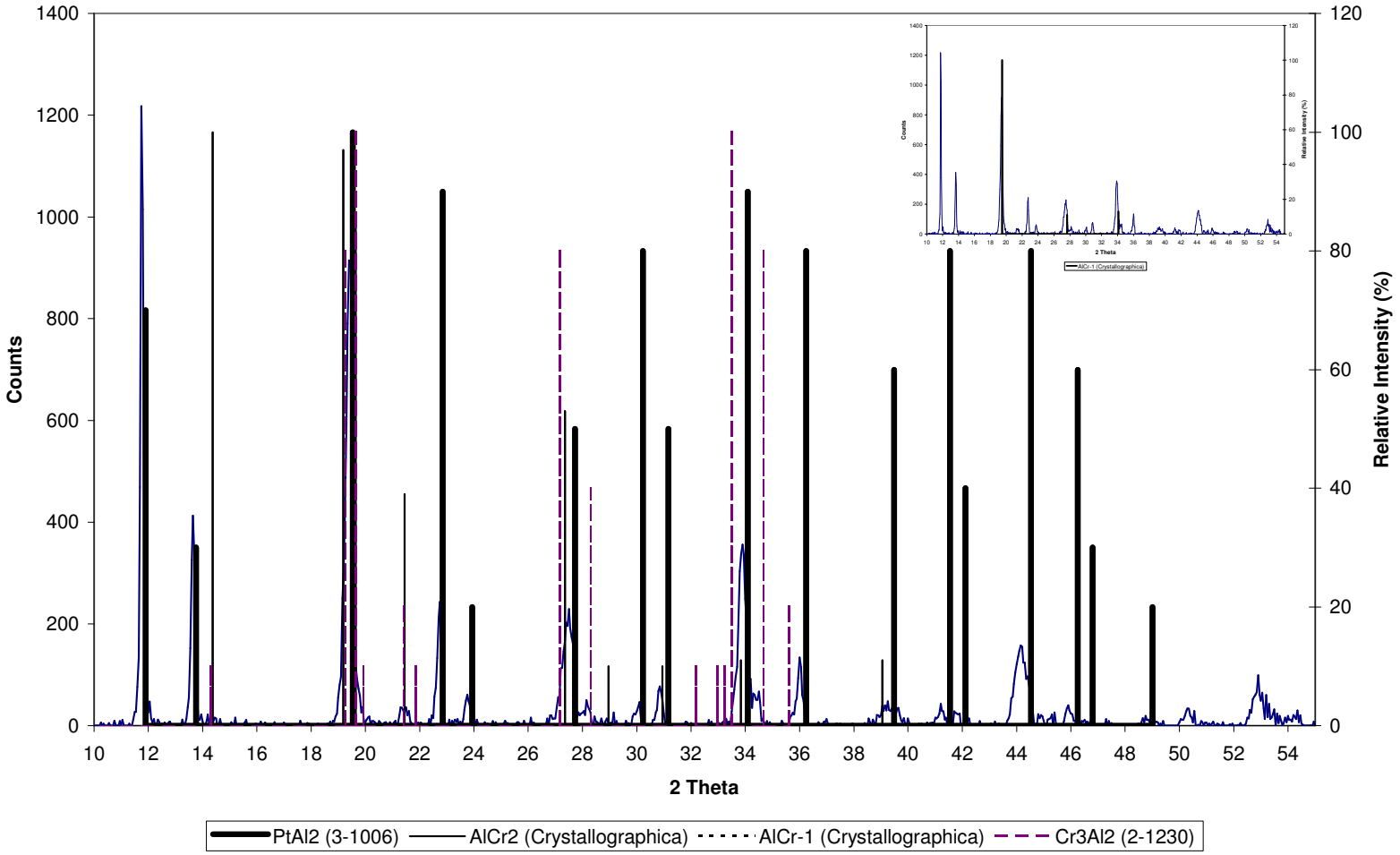

Figure 2.49. XRD pattern for nominal Pt_3:Al_{35}:Cr_{62} in the as-cast condition.

2.1.15. Nominal $Pt_{10}:Al_{50}:Cr_{40}$

Alloy $Pt_{10}:Al_{50}:Cr_{40}$ also had an extraordinary microstructure. Apart from some out-of-focus areas due to a sectioning effect, there were dark dendrites, with areas of coarse dark and light mixture as well as fine web-like dark/light mixture (Figure 2.50). There was an obvious similarity between alloys $Pt_{10}:Al_{50}:Cr_{40}$ and $Pt_3:Al_{35}:Cr_{62}$ (§2.1.14), but no precipitates were observed in the dark phase. The EDX analyses are given in Table 2.15 and Figure 2.51. XRD analysis detected ~$PtAl_2$ (dark phase), while ~Cr_3Al_2 (a compound listed in the JCPDS database) and/or ~Cr_2Al seemed to be the best fit to other measured peaks (Figure 2.52). As said before, ~Cr_3Al_2 does not feature in the Cr-Al binary phase diagram, and ~Cr_2Al would therefore be considered as the most probable phase to form. However, a phase similar to Cr_3Al_2 was in fact detected in alloys $Pt_3:Al_{35}:Cr_{62}$ (§2.1.14) and $Pt_5:Al_{52}:Cr_{43}$ (§2.1.32). That and the position of the dark phase composition on the ternary diagram (Figure 2.51) and the fact that the tie-line is located almost exactly the same as the ~Cr_3Al_2 tie-line in alloy $Pt_5:Al_{52}:Cr_{43}$, made ~Cr_3Al_2 (or more precise, a ternary phase T2 with a similar crystal structure) a better candidate. The fact that the overall analysis was lying off the tie-line could be explained by the standard deviation in its composition, however, the presence of a third phase is suggested. The possible extrapolation to a third phase is also shown in Figure 2.51. The third phase being ~Cr_5Al_8 would agree much with alloy $Pt_5:Al_{52}:Cr_{43}$ (Figure 2.105), although the two alloys microstructures differed (Figure 2.50 vs. Figure 2.104). The XRD peaks for ~Cr_5Al_8 seem to fit some of the measured peaks (Figure 2.52 insert). The identities of the phases are therefore clear. Similar to alloy $Pt_3:Al_{35}:Cr_{62}$, the microstructure probaby formed by the following reactions:

$$L \rightarrow (Cr)$$

$$L \rightarrow (Cr) + \sim PtAl_2$$

$$(Cr) \rightarrow T2 \text{ (ordering)},$$

although there is still uncertainty about the exact nature of the solid state reaction(s) that form T2 from (Cr).

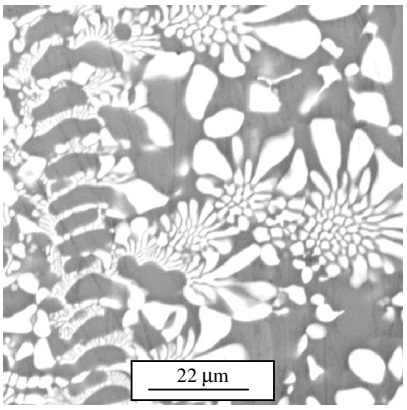

Figure 2.50. BSE-SEM image of nominal $Pt_{10}:Al_{50}:Cr_{40}$ in the as-cast condition: T2≈Cr_3Al_2 dark; ~$PtAl_2$ light.

Table 2.15. Phase analyses for nominal $Pt_{10}:Al_{50}:Cr_{40}$ (at.%) in the as-cast condition.

Phase description	**Pt**	**Al**	**Cr**	**Phase**
Overall	9.2 ± 0.5	50.3 ± 1.5	40.5 ± 1.3	-
Dark	0.5 ± 0.1	41.7 ± 0.6	57.8 ± 0.7	T2≈Cr_3Al_2
Light	27.7 ± 0.3	58.5 ± 0.4	13.8 ± 0.2	~$PtAl_2$
Eutectic Dark + light	14.0 ± 1.1	50.9 ± 1.5	35.1 ± 2.6	T2≈Cr_3Al_2 + ~$PtAl_2$

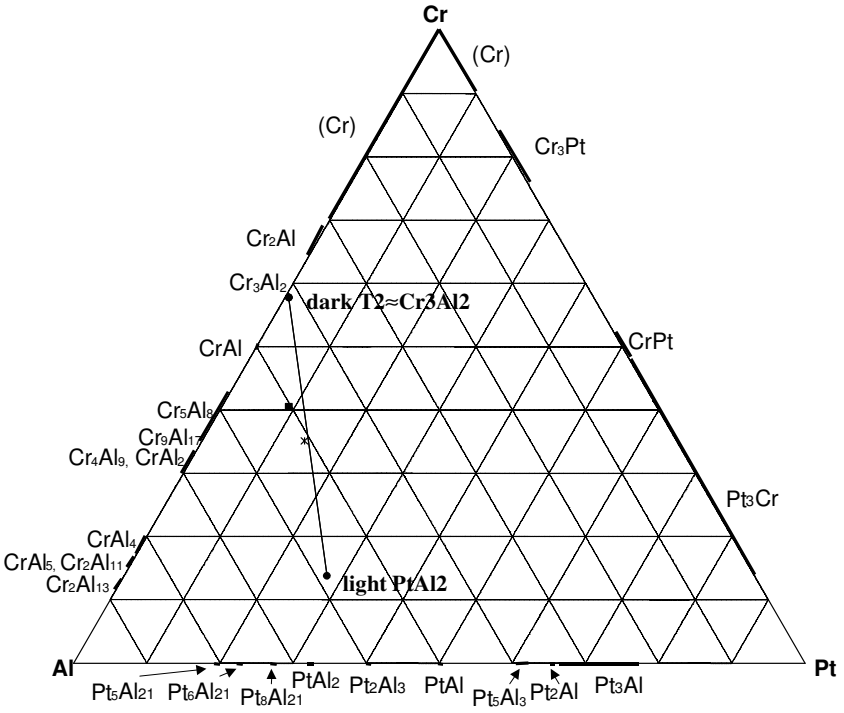

Figure 2.51. EDX analyses of nominal Pt_{10}:Al_{50}:Cr_{40} (at.%) in the as-cast condition.

(■ overall composition; ● phases; ✶ eutectic-like)

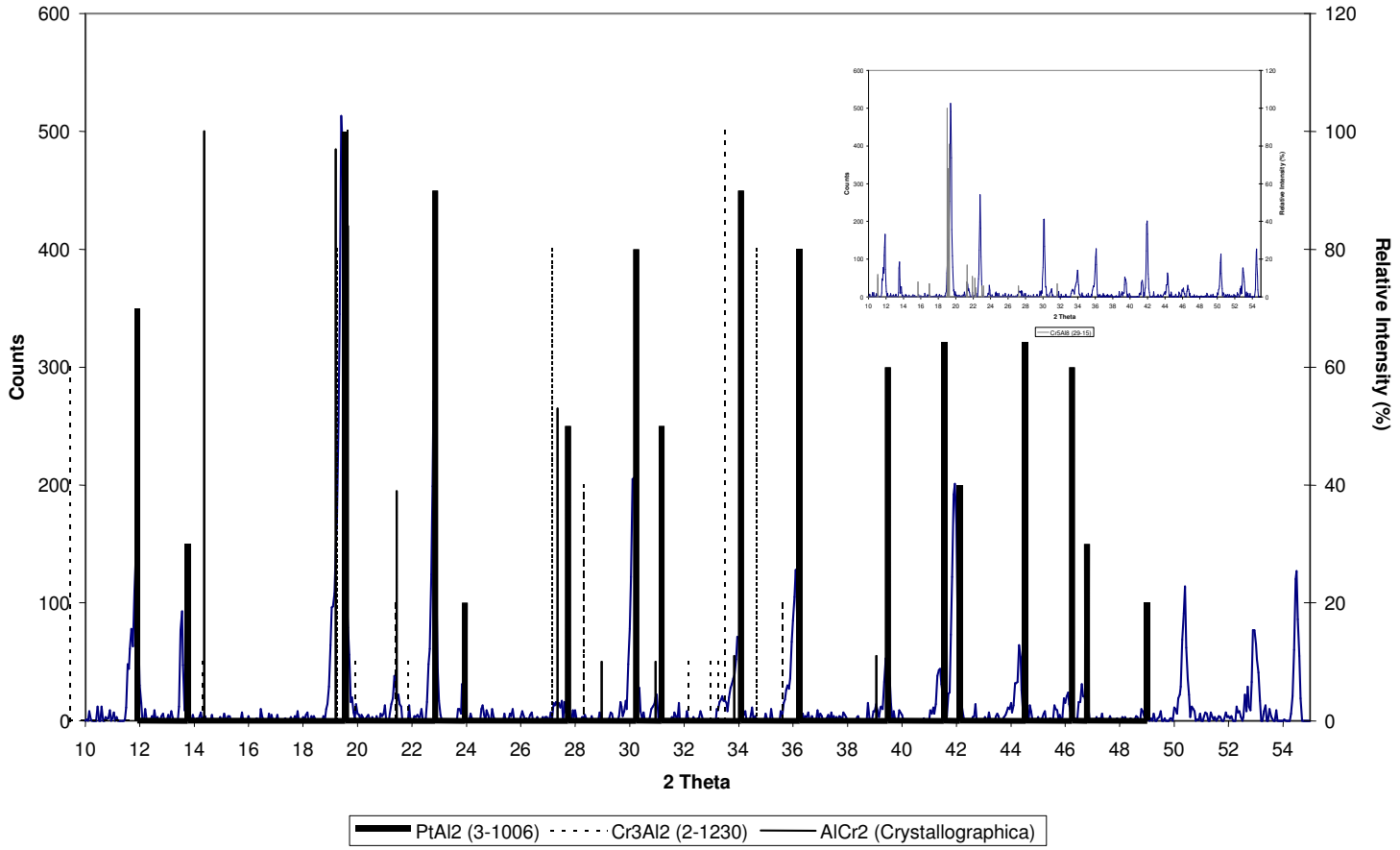

Figure 2.52. XRD pattern for nominal Pt_{10}:Al_{50}:Cr_{40} in the as-cast condition.

2.1.16. Nominal $Pt_{12}:Al_{18}:Cr_{70}$

At first glance, alloy $Pt_{12}:Al_{18}:Cr_{70}$ comprised black dendrites with a light interdendritic phase. At higher magnification, the interdendritic region actually comprised a eutectic-like mixture of light and grey and the interfaces on the dendrites were "stepped" (Figure 2.53). The EDX analyses are given in Table 2.16 and Figure 2.54. Although the light phase and grey particles were analysed, it must be noted that they were both in fact too small to yield accurate values. The area analysis of combined grey and light should however be accurate because there were big enough areas to be analysed without the risk of being affected by the black phase, but considering the huge standard deviation in measurements, that was not the case. This meant that the compositions of the grey, light and two-phase areas as shown in Figure 2.54 were compromised and could therefore be extrapolated. Figure 2.55 shows an adjusted version of Figure 2.54, where the compositions of the light and grey phases and the two-phase area were extrapolated to show their possible actual values without influence of surrounding phases. These changes would make the plot true within the given standard deviations. It also made the identification of the phases easier. Superposing the diffraction peaks of (Cr), ~$PtAl_2$ (with shift) and ~PtAl onto the measured diffraction pattern, yielded a good match (Figure 2.56). This was self-consistent with the results of alloy $Pt_{30}:Al_{50}:Cr_{20}$ (§2.1.7). The phases formed by

$$L \rightarrow (Cr)$$

$$L + (Cr) \rightarrow \sim PtAl$$

$$L \rightarrow \sim PtAl + \sim PtAl_2 + (Cr)$$

with the stepped interfaces evidence of the sparse ternary eutectic caused by rapid cooling. This was identical to alloy $Pt_{30}:Al_{50}:Cr_{20}$ where a ternary eutectic of (Cr), ~$PtAl_2$ and ~PtAl was observed.

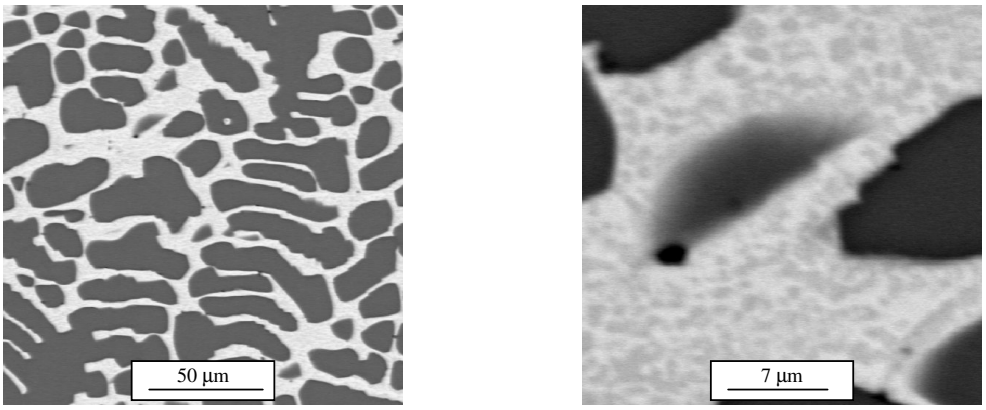

Figure 2.53. BSE-SEM image of nominal Pt_{12}:Al_{18}:Cr_{70} in the as-cast condition: (Cr) black; $PtAl_2$ grey; ~PtAl light.

Table 2.16. Phase analyses for nominal Pt_{12}:Al_{18}:$Cr7_{70}$ (at.%) in the as-cast condition.

Phase description	**Pt**	**Al**	**Cr**	**Phase**
Overall	11.7 ± 2.4	18.6 ± 2.9	69.7 ± 5.4	-
Black	2.9 ± 0.1	7.1 ± 0.3	90.0 ± 0.2	(Cr)
Grey	28.0 ± 4.3	41.3 ± 4.9	30.7 ± 9.2	~$PtAl_2$
Light	37.2 ± 0.3	44.3 ± 0.6	18.5 ± 0.9	~PtAl
Two-phase grey + light	28.0 ± 4.3	41.3 ± 4.9	30.7 ± 9.2	~$PtAl_2$ + ~PtAl

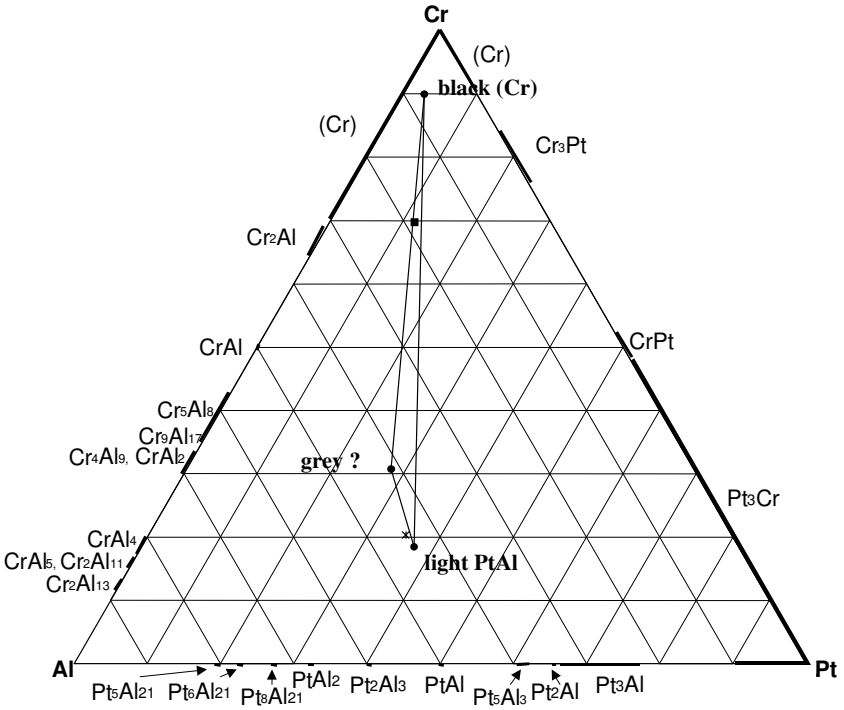

Figure 2.54. EDX analyses of nominal $Pt_{12}:Al_{18}:Cr_{70}$ (at.%) in the as-cast condition.

(■ overall composition; ● phases; ✶ two-phase)

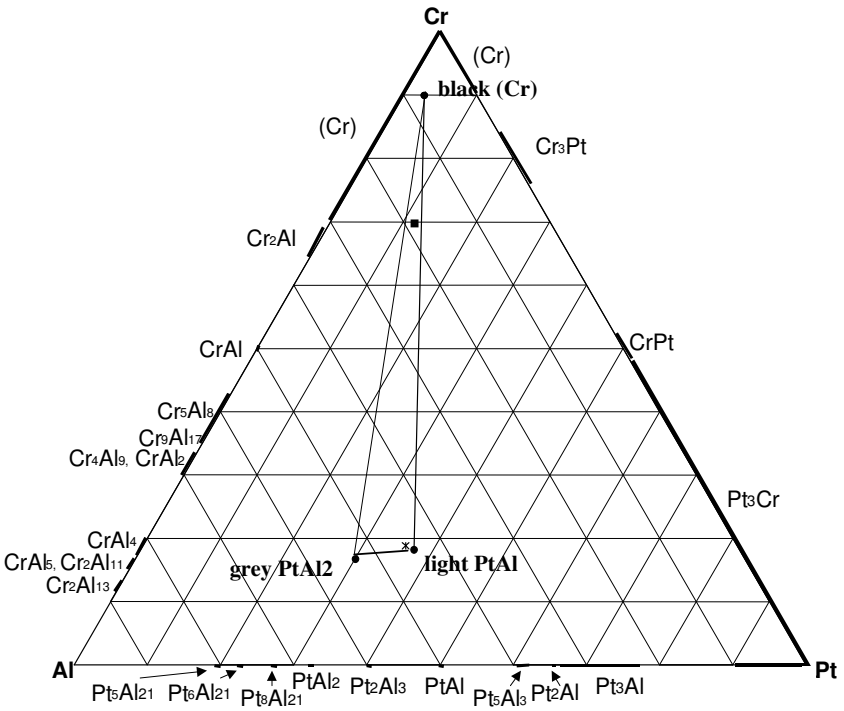

Figure 2.55. Extrapolation of inaccurate phase compositions of nominal $Pt_{12}:Al_{18}:Cr_{70}$ (at.%) in the as-cast condition to more probable compositions.

(■ overall composition; ● phases; ✶ two-phase)

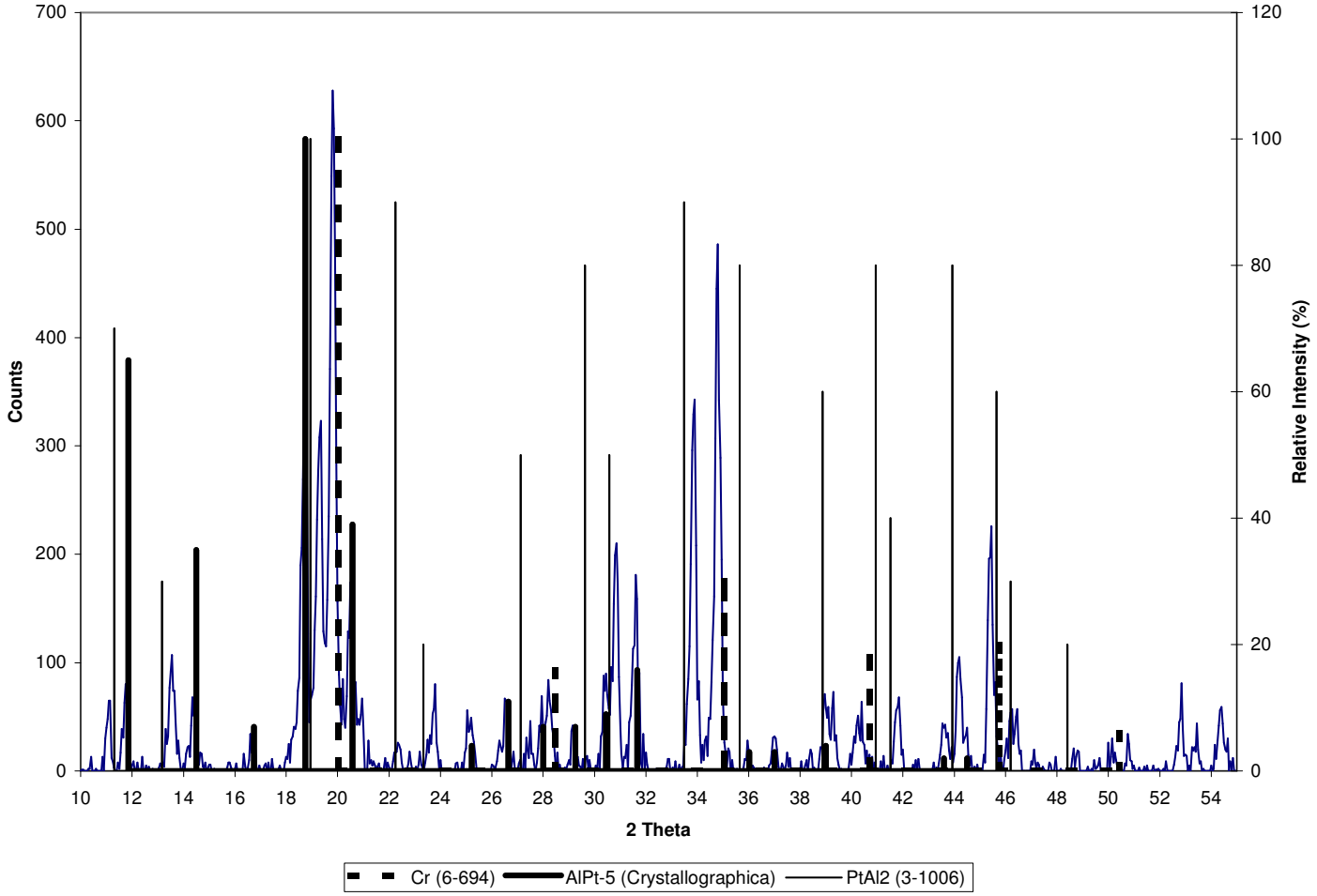

Figure 2.56. XRD pattern for nominal Pt_{12}:Al_{18}:Cr_{70} in the as-cast condition.

2.1.17. Nominal $Pt_{17}:Al_{68}:Cr_{15}$

Alloy $Pt_{17}:Al_{68}:Cr_{15}$ comprised white dendrites with a grey interdendritic phase which also contained a black phase (Figure 2.57). The EDX analyses are given in Table 2.17 and Figure 2.58. The intensities of the XRD peaks were low, and only the diffraction peaks of ~$PtAl_2$ (the white phase) were easy to identify (Figure 2.59). The second and third phases were more difficult to identify, although the diffraction peaks of ~$CrAl_4$ (grey) and ~Cr_4Al_9 (black) did seem to fit the tiny measured peaks best, compared to other possibilities like $CrAl_3$ (taken from Pearson's Handbook [1985Vil]) and ~$CrAl_2$ (from the JCPDS database), which are both not included in the binary Cr-Al diagram. The preference of ~$CrAl_4$ above ~$CrAl_3$ was confirmed by the results of alloy $Pt_3:Al_{79}:Cr_{18}$ (§2.1.31) where ~$CrAl_3$ (or more precisely, a ternary phase with similar crystal structure to $CrAl_3$) as well as ~$CrAl_4$ were observed.

The phase probably formed by:

$$L \rightarrow \sim PtAl_2$$

$$L + \sim PtAl_2 \rightarrow \sim Cr_4Al_9$$

$$L + \sim Cr_4Al_9 \rightarrow \sim CrAl_4$$

although the microstructure was not a clear example of a succession of peritectic reactions that have occurred.

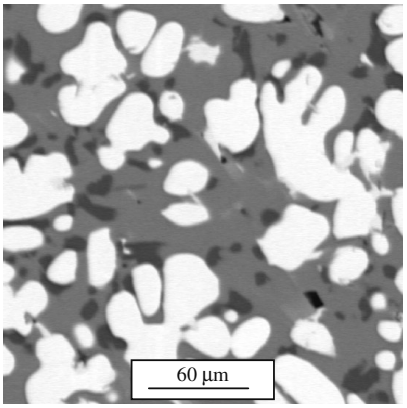

Figure 2.57. BSE-SEM image of nominal $Pt_{17}:Al_{68}:Cr_{15}$ in the as-cast condition: ~Cr_4Al_9 black; ~$CrAl_4$ grey; ~$PtAl_2$ white.

Table 2.17. Phase analyses for nominal $Pt_{17}:Al_{68}:Cr_{15}$ (at.%) in the as-cast condition.

Phase description	**Pt**	**Al**	**Cr**	**Phase**
Overall	14.4 ± 3.5	69.0 ± 1.9	16.6 ± 2.1	-
Black	0.8 ± 0.1	69.2 ± 0.3	30.0 ± 0.4	~Cr_4Al_9
Grey	4.3 ± 0.2	75.2 ± 0.6	20.5 ± 0.8	~$CrAl_4$
White	28.9 ± 0.3	60.5 ± 0.1	10.6 ± 0.2	~$PtAl_2$

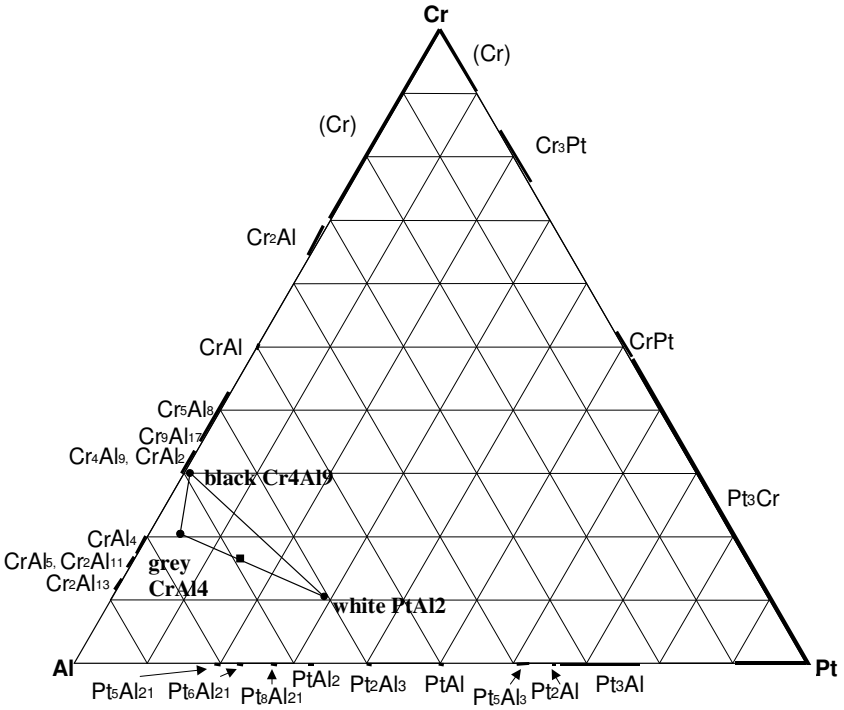

Figure 2.58. EDX analyses of nominal $Pt_{17}:Al_{68}:Cr_{15}$ (at.%) in the as-cast condition.

(■ overall composition; ● phases)

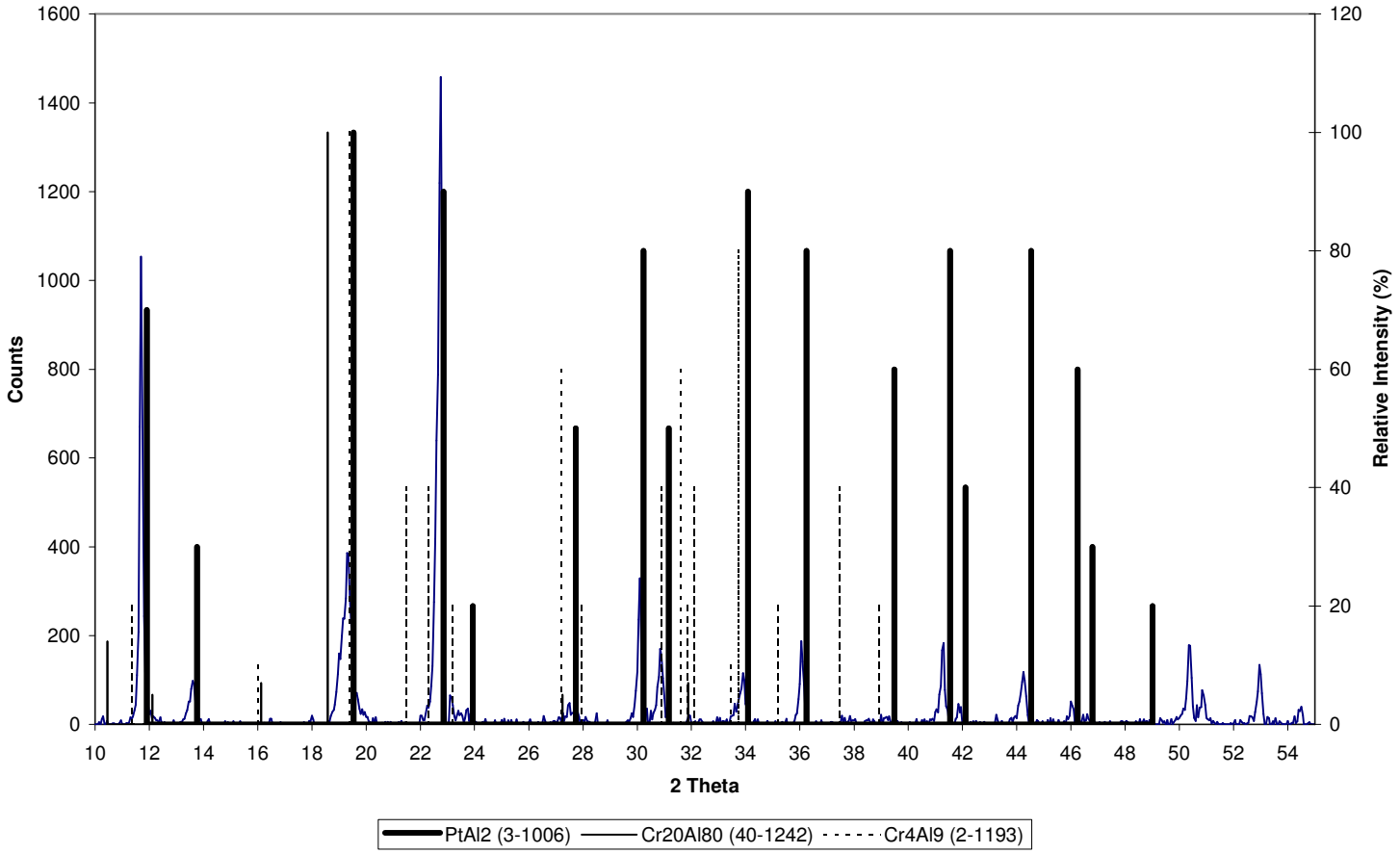

Figure 2.59. XRD pattern for nominal Pt_{17}:Al_{68}:Cr_{15} in the as-cast condition.

2.1.18. Nominal $Pt_{18}:Al_2:Cr_{80}$

Alloy $Pt_{18}:Al_2:Cr_{80}$ comprised three phases: dark (Cr), medium ~Cr_3Pt and light $L1_0$ ~CrPt (Figure 2.60). The identities of the phases were confirmed by XRD analysis (Figure 2.61). The EDX analyses are shown in Table 2.18 and Figure 2.62. The layer (medium) around the dark (Cr), and especially the irregular shape of the (Cr) showed a succession of peritectic reactions. The structure formed by:

$$L \rightarrow (Cr)$$

$$L + (Cr) \rightarrow \sim Cr_3Pt$$

$$L + \sim Cr_3Pt \rightarrow (Pt)$$

$$(Pt) \rightarrow \sim Pt_3Cr \rightarrow \sim CrPt \text{ (ordering)}$$

It was interesting to see that the size of the ~CrPt phase field (or in fact, of (Pt), its origin) are even bigger (~27 at.%Cr) than the binary Cr-Pt diagram would suggest. This is very similar to the Pt-Cr-Ru system where as much as 80 at.% Cr could dissolve in ~CrPt [2004Süs1, 2006Süs1]. It is also interesting to see that the $L \rightarrow (Cr) + \sim Cr_3Pt$ and $L \rightarrow \sim Cr_3Pt + (Pt)$ eutectics in the binary Cr-Pt system, acted peritectically in the Pt-Al-Cr ternary.

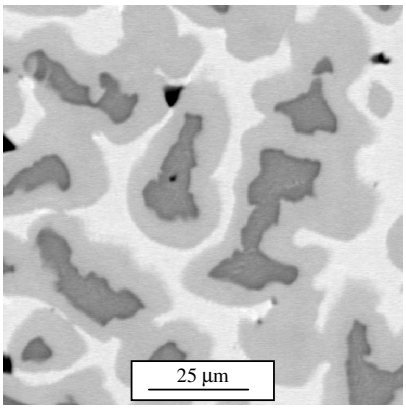

Figure 2.60. BSE-SEM image of nominal $Pt_{18}:Al_2:Cr_{80}$ in the as-cast condition: (Cr) dark; ~Cr_3Pt medium; ~CrPt light.

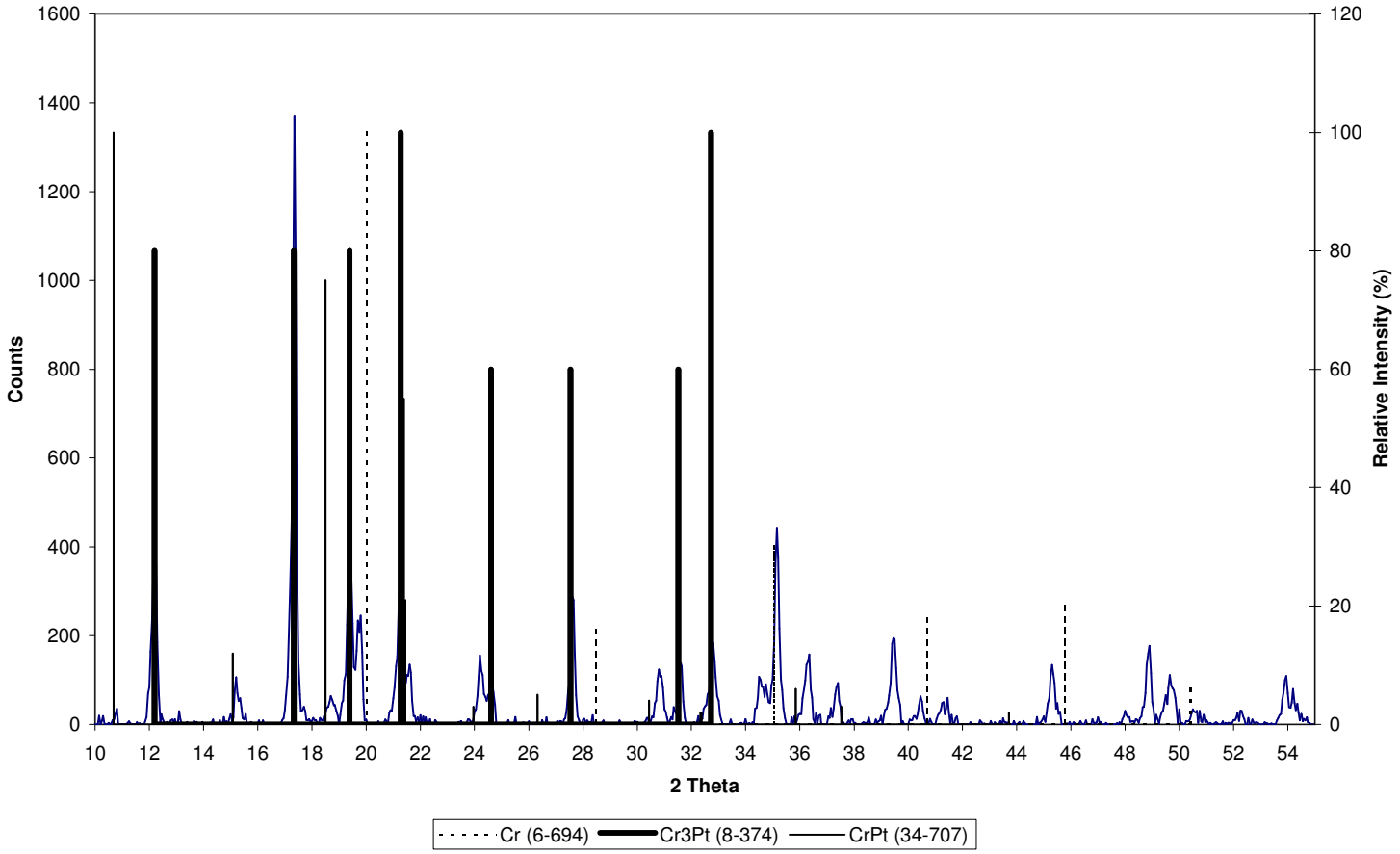

Figure 2.61. XRD pattern for nominal $Pt_{18}:Al_2:Cr_{80}$ in the as-cast condition.

Table 2.18. Phase analyses for nominal $Pt_{18}:Al_2:Cr_{80}$ (at.%) in the as-cast condition.

Phase description	**Pt**	**Al**	**Cr**	**Phase**
Overall	18.1 ± 0.4	2.3 ± 0.2	79.6 ± 0.2	-
Dark	10.7 ± 0.4	1.1 ± 0.1	88.2 ± 0.4	(Cr)
Medium	18.4 ± 0.4	1.1 ± 0.4	80.5 ± 0.0	~Cr_3Pt
Light	26.9 ± 0.1	4.0 ± 0.4	69.1 ± 0.4	~CrPt

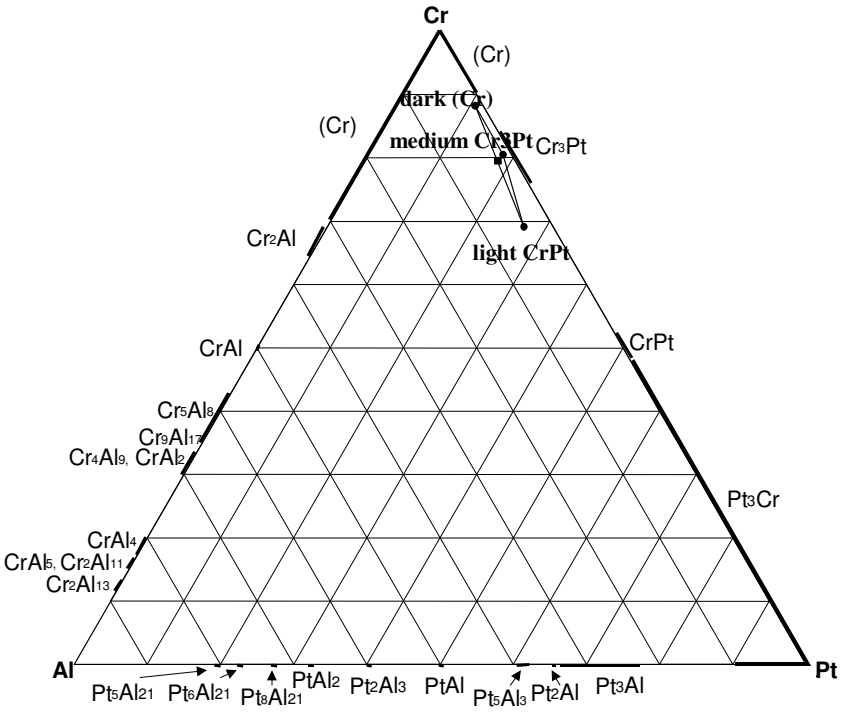

Figure 2.62. EDX analyses of nominal $Pt_{18}:Al_2:Cr_{80}$ (at.%) in the as-cast condition.
(■ overall composition; ● phases)

2.1.19. Nominal $Pt_{28}:Al_{12}:Cr_{60}$

Alloy $Pt_{28}:Al_{12}:Cr_{60}$ comprised grey dendrites with an interdendritic ternary eutectic mixture of black, white and grey (Figure 2.63). The EDX analyses are given in Table 2.19 and Figure 2.64. The grey phase, $L1_0$ ~CrPt, was easily identified by XRD analyses (Figure 2.65). Taking into account their positions on the ternary plot (Figure 2.64), the white phase was probably ternary T1 and the black phase (Cr), although it was difficult to say from the XRD analyses (Figure 2.65). The peaks for $L1_0$ ~CrPt, (Cr) and T1 showed some shift. Considering that the dark (Cr) phase and light T1 phases were extremely small, their analyses would have

been affected by the surrounding phase(s). This can be seen from the significant variation in their compositions (Table 2.19).

The structure formed by:

$$L \rightarrow (Pt)$$

$$L \rightarrow (Pt) + (Cr) + T1$$

$$(Pt) \rightarrow \sim Pt_3Cr \rightarrow \sim CrPt \text{ (ordering in both the dendrites and the eutectic).}$$

It is unusual to form a ternary eutectic immediately after the primary phase without an intermediate binary eutectic. The apparent grey could be an edge effect, however, the ternary eutectic was confirmed in alloy Pt_{15}:Al_5:Cr_{80} (§2.1.34).

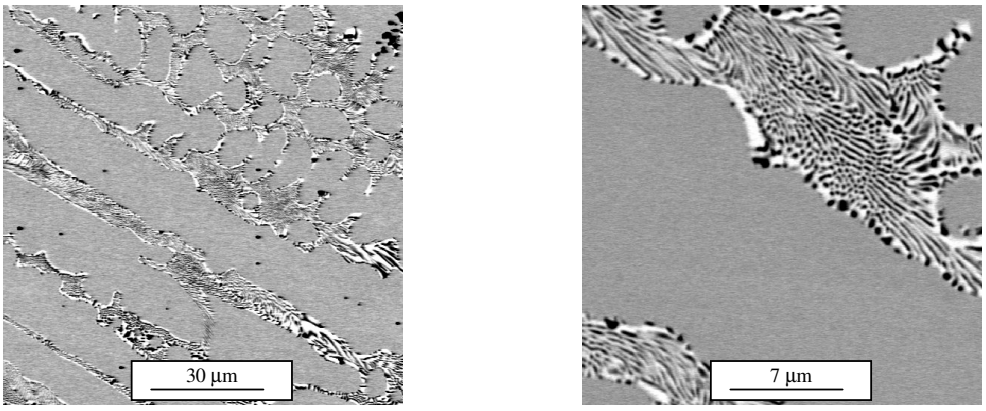

Figure 2.63. BSE-SEM image of nominal Pt_{28}:Al_{12}:Cr_{60} in the as-cast condition: (Cr) black; ~CrPt grey; T1 white.

Table 2.19. Phase analyses for nominal Pt_{28}:Al_{12}:Cr_{60} (at.%) in the as-cast condition.

Phase description	**Pt**	**Al**	**Cr**	**Phase**
Overall	28.4 ± 0.2	11.3 ± 0.7	60.3 ± 0.6	-
Black*	14.6 ± 1.5	5.2 ± 1.0	80.2 ± 2.4	(Cr)
Grey	28.4 ± 0.2	9.2 ± 0.6	62.4 ± 0.4	~CrPt
White*	40.9 ± 3.1	26.5 ± 1.6	32.6 ± 4.7	T1
Eutectic black + white + grey	29.6 ± 0.6	18.5 ± 0.2	51.9 ± 0.8	(Cr) + T1 + ~CrPt

* Too small for accurate analyses.

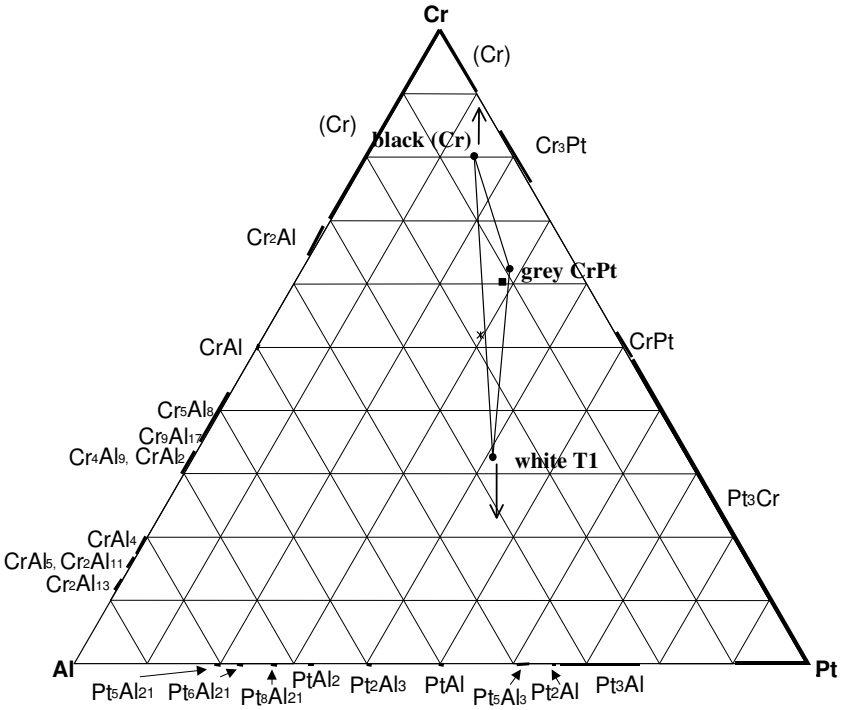

Figure 2.64. EDX analyses of nominal $Pt_{28}:Al_{12}:Cr_{60}$ (at.%) in the as-cast condition with directions of possible extrapolation indicated.

(■ overall composition; ● phases; ✶ ternary eutectic)

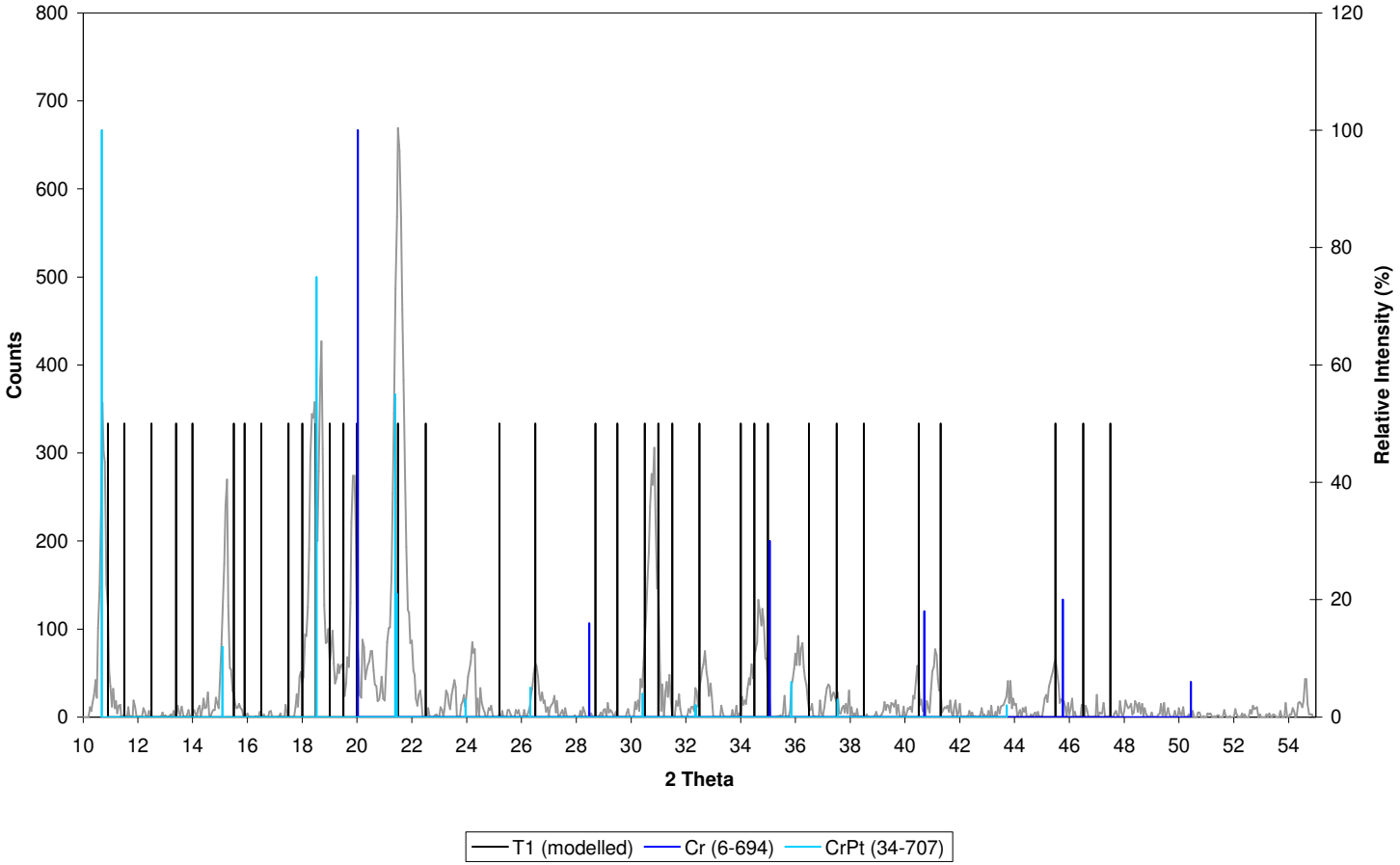

Figure 2.65. XRD pattern for nominal $Pt_{28}:Al_{12}:Cr_{60}$ in the as-cast condition.

2.1.20. Nominal $Pt_{28}:Al_{70}:Cr_2$

Alloy $Pt_{28}:Al_{70}:Cr_2$ showed a dark and light phase (Figure 2.66), with compositions given in Table 2.20 and shown graphically in Figure 2.67. There was also some porosity present in the dark phase, indicating that it was the last phase to solidify. The XRD analysis (Figure 2.68) clearly identified ~$PtAl_2$ as the light phase, while it was difficult to decide whether the dark phase was ~Pt_6Al_{21} (a JCPDS compound) or ~Pt_8Al_{21} (found in the binary Pt-Al phase diagram). Therefore it was more likely that the dark phase was ~Pt_8Al_{21}, which formed by the following reactions:

$$L \rightarrow \sim PtAl_2$$

$$L + \sim PtAl_2 \rightarrow \sim Pt_8Al_{21}.$$

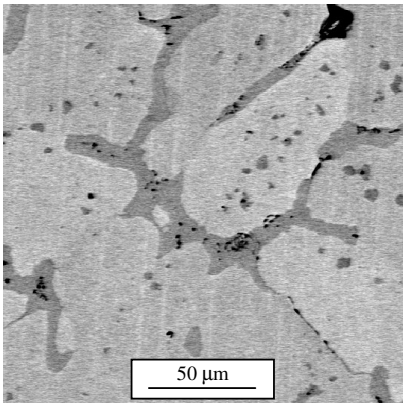

Figure 2.66. BSE-SEM image of nominal $Pt_{28}:Al_{70}:Cr_2$ in the as-cast condition: ~$PtAl_2$ light; ~Pt_8Al_{21} dark; porosity black.

Table 2.20. Phase analyses for nominal $Pt_{28}:Al_{70}:Cr_2$ (at.%) in the as-cast condition.

Phase description	**Pt**	**Al**	**Cr**	**Phase**
Overall	27.5 ± 2.2	70.4 ± 2.7	2.1 ± 0.5	-
Dark	24.9 ± 0.2	74.8 ± 0.1	0.3 ± 0.1	~Pt_8Al_{21}
Light	31.0 ± 0.2	66.2 ± 0.9	2.8 ± 1.1	~$PtAl_2$

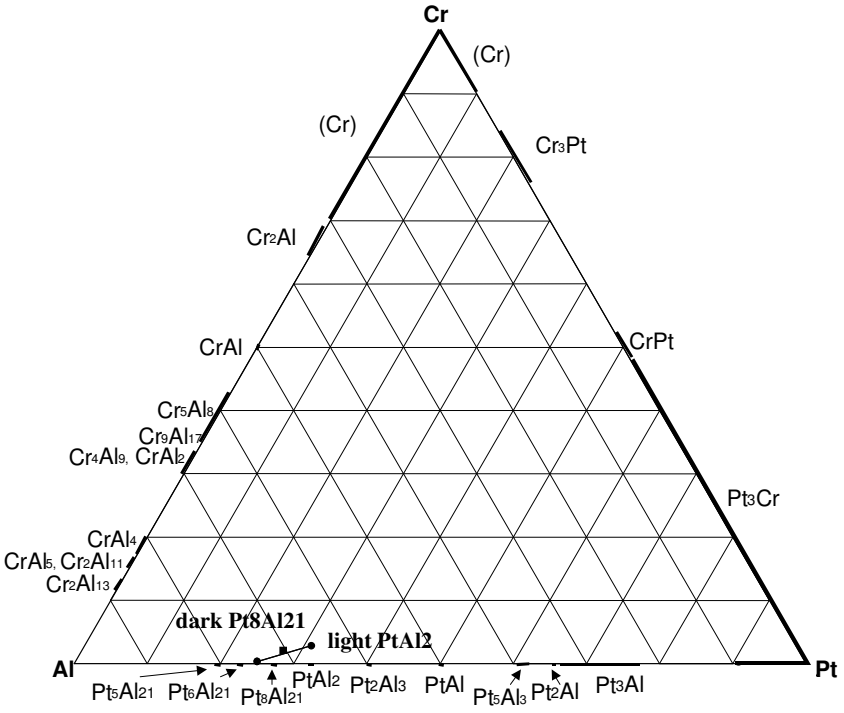

Figure 2.67. EDX analyses of nominal $Pt_{28}:Al_{70}:Cr_2$ (at.%) in the as-cast condition. (■ overall composition; ● phases)

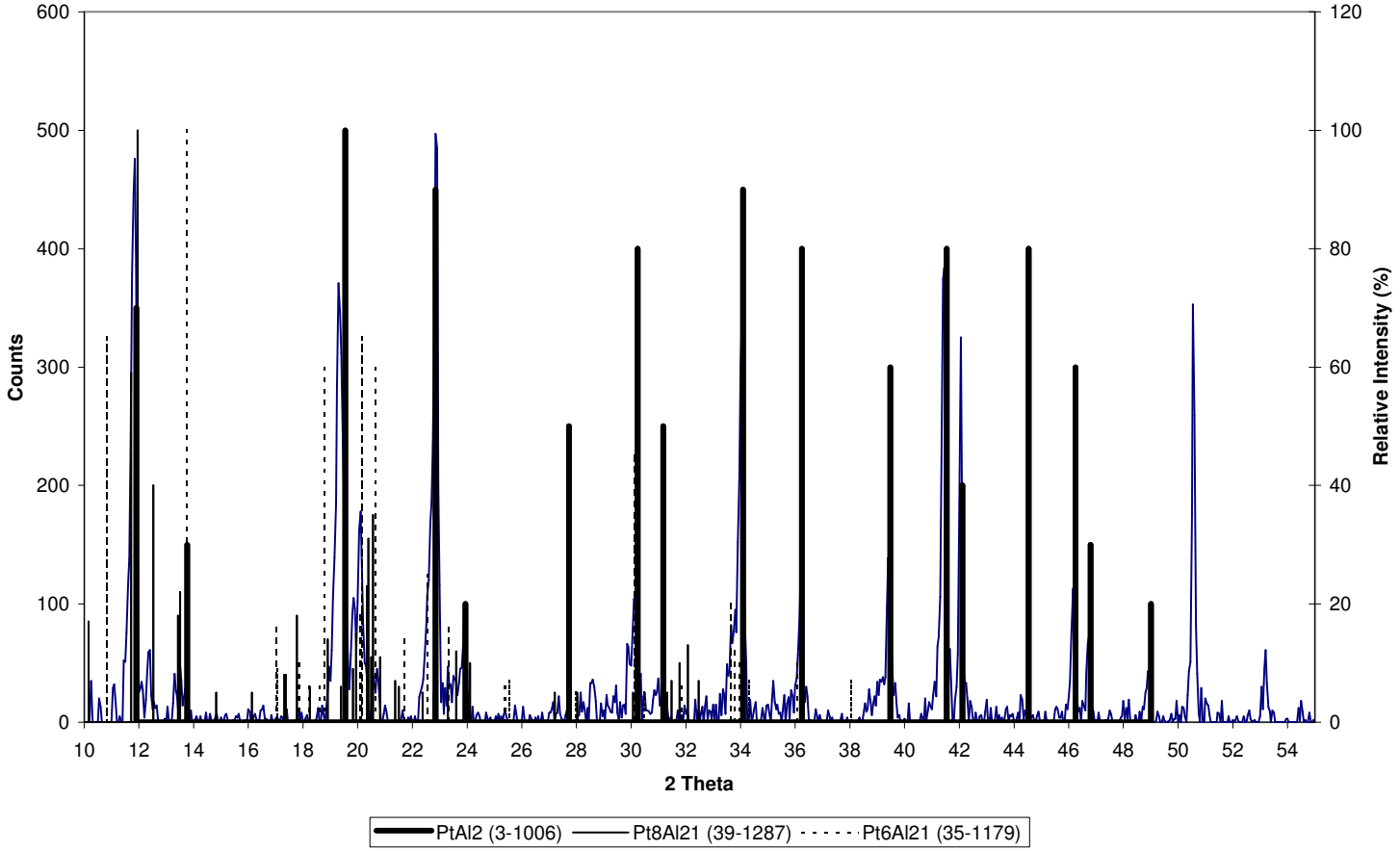

Figure 2.68. XRD pattern for nominal Pt_{28}:Al_{70}:Cr_2 in the as-cast condition.

2.1.21. Nominal $Pt_{35}:Al_{55}:Cr_{10}$

Alloy $Pt_{35}:Al_{55}:Cr_{10}$ comprised dark dendrites with a light interdendritic phase (Figure 2.69). The EDX analyses of the phases and the alloy are given in Table 2.21 and Figure 2.70. The overall composition of the alloy did not lie on the tie-line between the two phases, but the standard deviation in composition of the light phase was very big, suggesting that the light contrast phase as seen in Figure 2.69 is actually a mixture of phases. However, higher magnification microscopy did not offer any more detail. As in the case of alloy $Pt_{40}:Al_{50}:Cr_{10}$, some of the measured peaks ($2\theta \approx 20$, 26.3, 33) are unaccounted for, and it could imply the presence of a ternary phase. Alloy $Pt_{37}:Al_{59}:Cr_4$ (§2.1.36) was single phase, probably ~Pt_2Al_3 (it would agree with the results of alloy $Pt_{43}:Al_{52}:Cr_5$ (§2.1.23), but unfortunately no XRD could be done on that badly cracked/porous sample to confirm. Taking into account the results of alloys $Pt_{40}:Al_{50}:Cr_{10}$ (§2.1.10) and $Pt_{75}:Al_{10}:Cr_{15}$ (§2.1.30), it was mooted that the dark dendrites were indeed ~$PtAl_2$, while the light area was a ternary eutectic of ~$PtAl_2$, PtAl and Pt_2Al_3 . The XRD analysis (Figure 2.72) confirmed the identity of ~$PtAl_2$ and ~PtAl, but not really that of ~Pt_2Al_3. It is suggested that ~$PtAl_2$ melted congruently

$$L \rightarrow \sim PtAl_2$$

followed by a binary eutectic reaction

$$L \rightarrow \sim PtAl_2 + \sim PtAl \text{ (ternary plot is given in Figure 2.70),}$$

or a ternary eutectic reaction

$$L \rightarrow \sim PtAl_2 + \sim PtAl + \sim Pt_2Al_3 \text{ (ternary plot is given in Figure 2.71).}$$

In the XRD pattern, only one small peak for Pt_2Al_3 was missing (at $2\theta=22$). The micrograph could therefore have a ternary eutectic, but is of insufficient quality to show it. The first scenario was favoured.

There was an obvious similarity between alloys $Pt_{35}:Al_{55}:Cr_{10}$ and $Pt_{75}:Al_{10}:Cr_{15}$, as is evident when comparing Figure 2.69 to Figure 2.97(a).

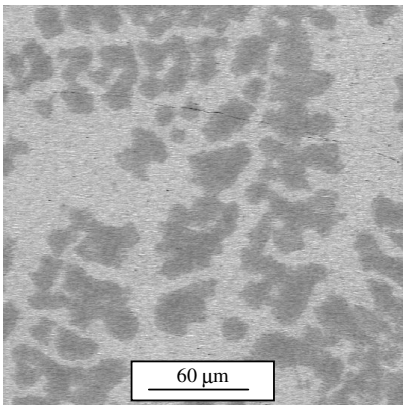

Figure 2.69. BSE-SEM image of nominal $Pt_{35}:Al_{55}:Cr_{10}$ in the as-cast condition: ~$PtAl_2$ + ~PtAl light; ~$PtAl_2$ dark.

Table 2.21. Phase analyses for nominal $Pt_{35}:Al_{55}:Cr_{10}$ at.%) in the as-cast condition.

Phase description	**Pt**	**Al**	**Cr**	**Phase**
Overall	36.3 ± 0.4	53.4 ± 0.1	10.3 ± 0.4	-
Dark	31.9 ± 0.4	56.5 ± 0.6	11.5 ± 0.5	~$PtAl_2$
Light eutectic	37.8 ± 1.4	49.8 ± 4.9	12.4 ± 6.2	~$PtAl_2$ + ~PtAl

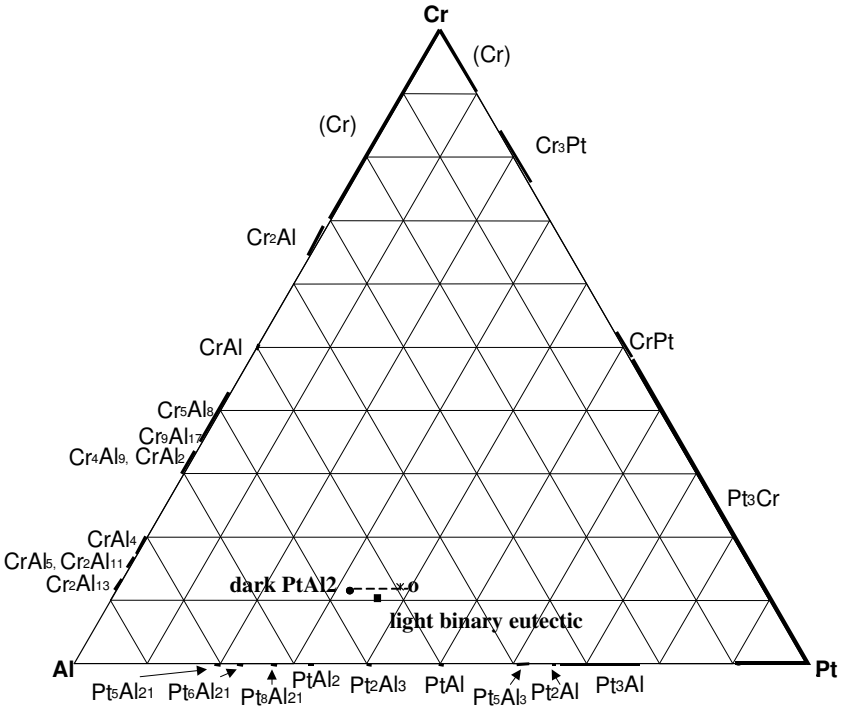

Figure 2.70. EDX analyses of nominal $Pt_{35}:Al_{55}:Cr_{10}$ (at.%) in the as-cast condition.

(■ overall composition; ● phase; ✶ eutectic; o extrapolated phase)

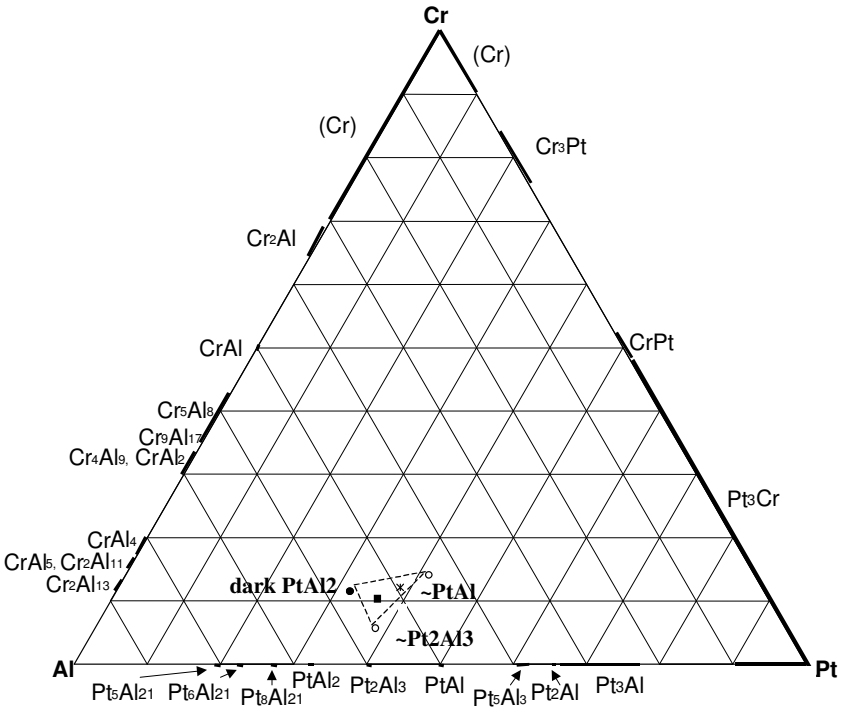

Figure 2.71. EDX analyses of nominal $Pt_{35}:Al_{55}:Cr_{10}$ (at.%) in the as-cast condition. (■ overall composition; ● phases; o suggested phases; ✶ ternary eutectic)

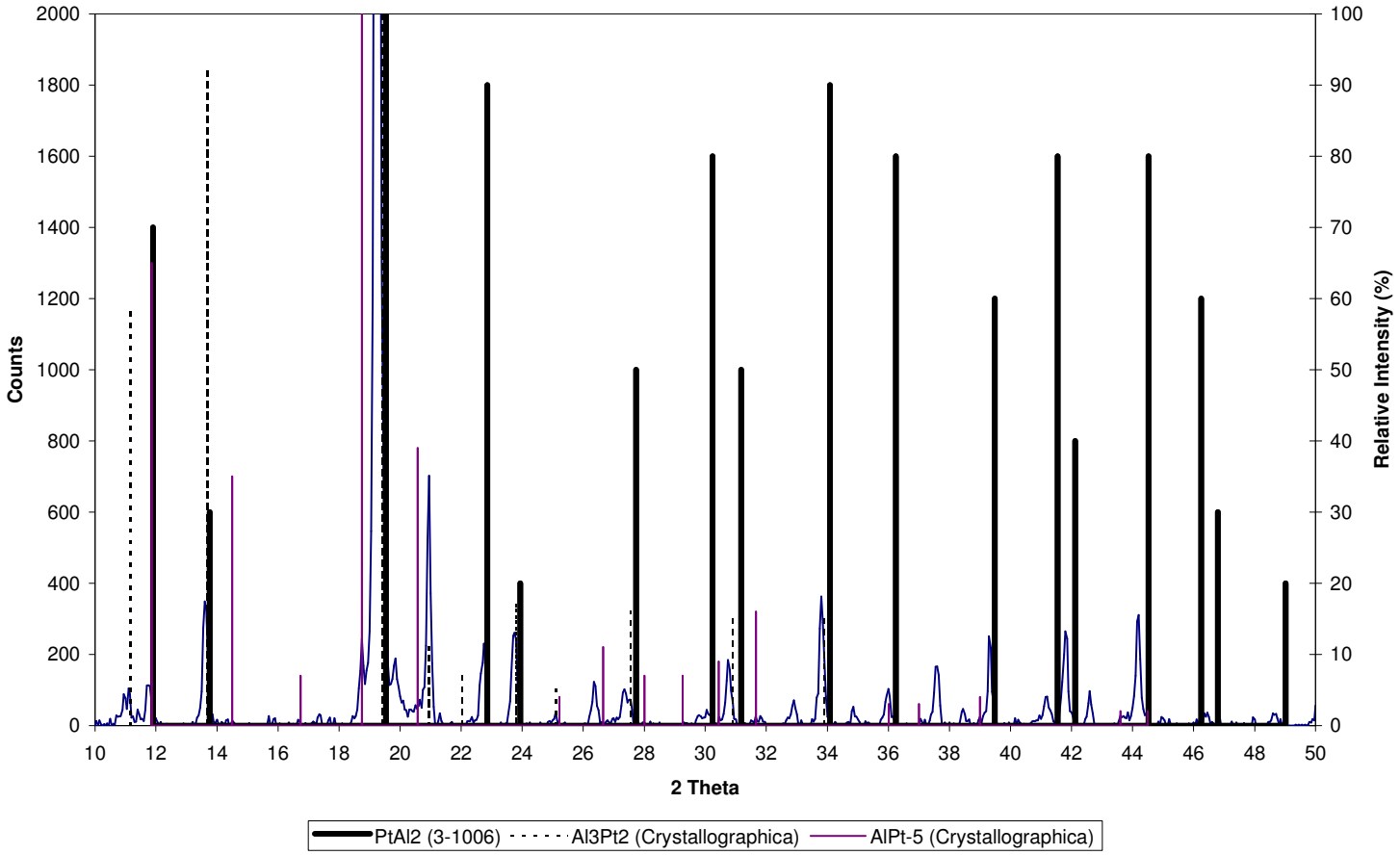

Figure 2.72. XRD pattern for nominal Pt_{35}:Al_{55}:Cr_{10} in the as-cast condition.

2.1.22. Nominal $Pt_{38}:Al_{22}:Cr_{40}$

Alloy $Pt_{38}:Al_{22}:Cr_{40}$ comprised light dendrites with interdendritic regions comprising a very sparse eutectic of light and dark (Figure 2.73). Close examination of the light phase suggested that it could have actually comprised two phases, but the EDX analyses (Table 2.22 and Figure 2.74) showed that it was probably only one phase, since the standard deviation was low and area analysis of the phase was the same as the average of spot analyses of the phase. XRD analysis detected ~CrPt (dark phase) (Figure 2.75). Considering the position of the light phase on the ternary diagram, and its proximity to that of the white phase of alloy $Pt_{28}:Al_{12}:Cr_{60}$ (Figure 2.19), it was most probably ternary T1. Superposing the derived XRD pattern onto the measured pattern of alloy $Pt_{38}:Al_{22}:Cr_{40}$ seemed to confirm that (Figure 2.75). These phases formed by:

$$L \rightarrow T1$$

$$L \rightarrow T1 + (Pt)$$

$$(Pt) \rightarrow \sim CrPt_3 \rightarrow \sim CrPt \text{ (ordering)}$$

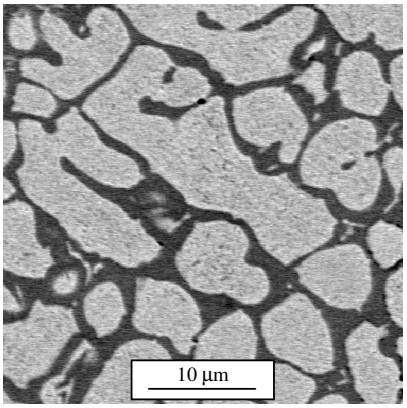

Figure 2.73. BSE-SEM image of nominal $Pt_{38}:Al_{22}:Cr_{40}$ in the as-cast condition: ~CrPt dark; T1 light.

Table 2.22. Phase analyses for nominal $Pt_{38}:Al_{22}:Cr_{40}$ (at.%) in the as-cast condition.

Phase description	**Pt**	**Al**	**Cr**	**Phase**
Overall	39.2 ± 0.4	22.7 ± 0.7	38.1 ± 1.0	-
Dark	32.7 ± 0.7	9.7 ± 0.6	57.6 ± 1.3	~CrPt
Light (spot analyses)	42.6 ± 0.7	27.7 ± 1.0	29.7 ± 0.8	T1
Light (area analyses) *	41.2	27.1	31.7	T1

* Only one measurement taken.

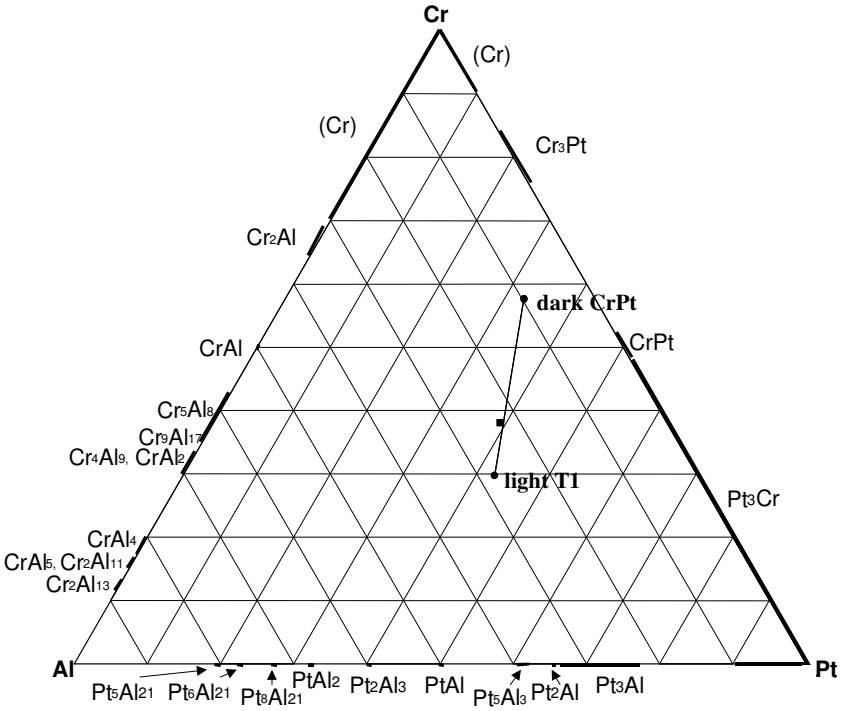

Figure 2.74. EDX analyses of nominal $Pt_{38}:Al_{22}:Cr_{40}$ (at.%) in the as-cast condition.

(■ overall composition; ● phases)

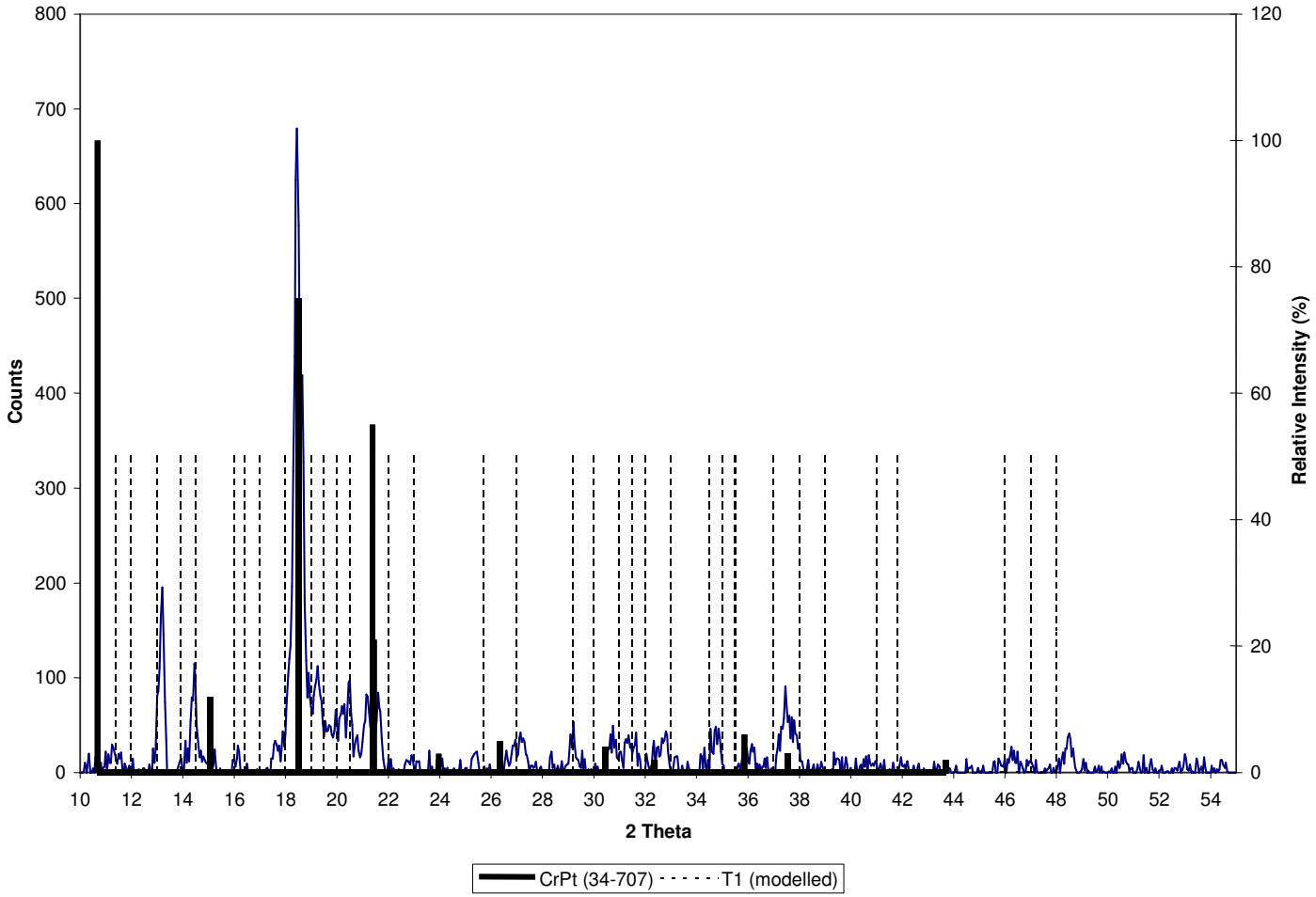

Figure 2.75. XRD pattern for nominal $Pt_{38}:Al_{22}:Cr_{40}$ in the as-cast condition.

2.1.23. Nominal $Pt_{43}:Al_{52}:Cr_5$

Alloy $Pt_{43}:Al_{52}:Cr_5$ comprised a very fine mixture of dark ~Pt_2Al_3 and light ~PtAl (Figure 2.76). Only a high magnification micrograph is shown because low magnification showed hardly any detail. These phases (EDX analyses given in Table 2.23 and Figure 2.77) were confirmed by XRD analysis (Figure 2.78), where one can see a very good fit to the measured pattern, although peaks at $2\theta \approx 26.3$ and 33 could not be identified (like alloys $Pt_{40}:Al_{50}:Cr_{10}$ (§2.1.10) and $Pt_{35}:Al_{55}:Cr_{10}$ (§2.1.21)), and it was again decided that the dark phase was ~Pt_2Al_3 (with slightly distorted crystal structure due to substititutional solid solution). The solidification sequence was:

$$L \rightarrow \sim Pt_2Al_3$$

$$L \rightarrow \sim PtAl + \sim Pt_2Al_3$$

It must however be noted that these phases were too small to yield accurate analyses, being much smaller than the potential ~3μm size of beam spread on interaction. The overall composition did lie perfectly on the tie-line though.

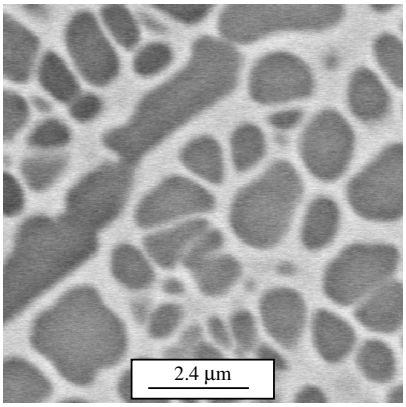

Figure 2.76. BSE-SEM image of nominal $Pt_{43}:Al_{52}:Cr_5$ in the as-cast condition: ~Pt_2Al_3 dark; ~PtAl light.

Table 2.23. Phase analyses for nominal $Pt_{43}:Al_{52}:Cr_5$ (at.%) in the as-cast condition.

Phase description	**Pt**	**Al**	**Cr**	**Phase**
Overall	43.1 ± 0.2	51.8 ± 0.6	5.1 ± 0.4	-
Dark	40.7 ± 0.8	56.8 ± 1.2	2.5 ± 0.4	~Pt_2Al_3
Light	45.3 ± 1.2	46.8 ± 0.4	7.9 ± 0.8	~PtAl

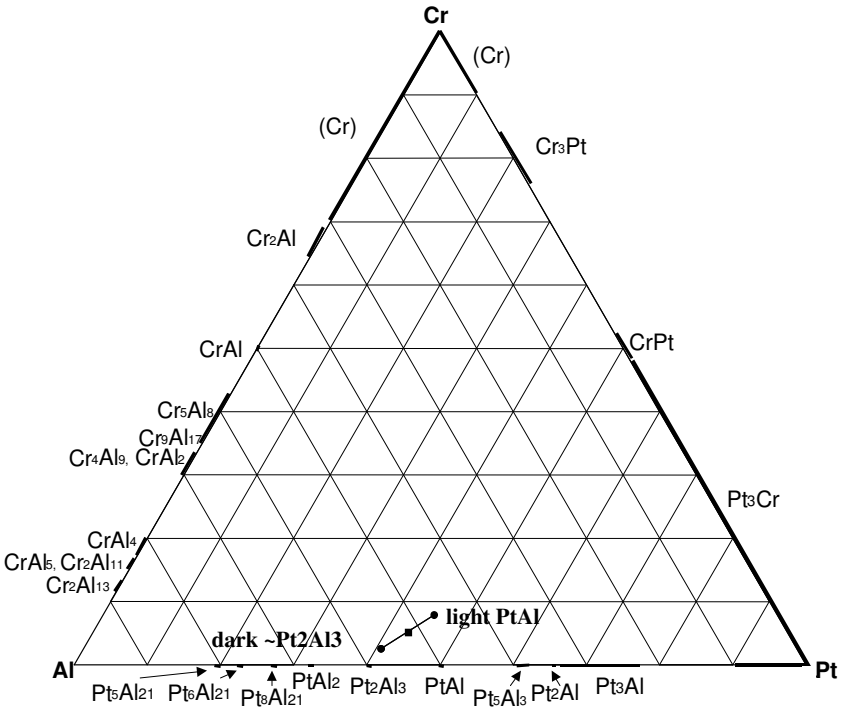

Figure 2.77. EDX analyses of nominal $Pt_{43}:Al_{52}:Cr_5$ (at.%) in the as-cast condition.

(■ overall composition; ● phases)

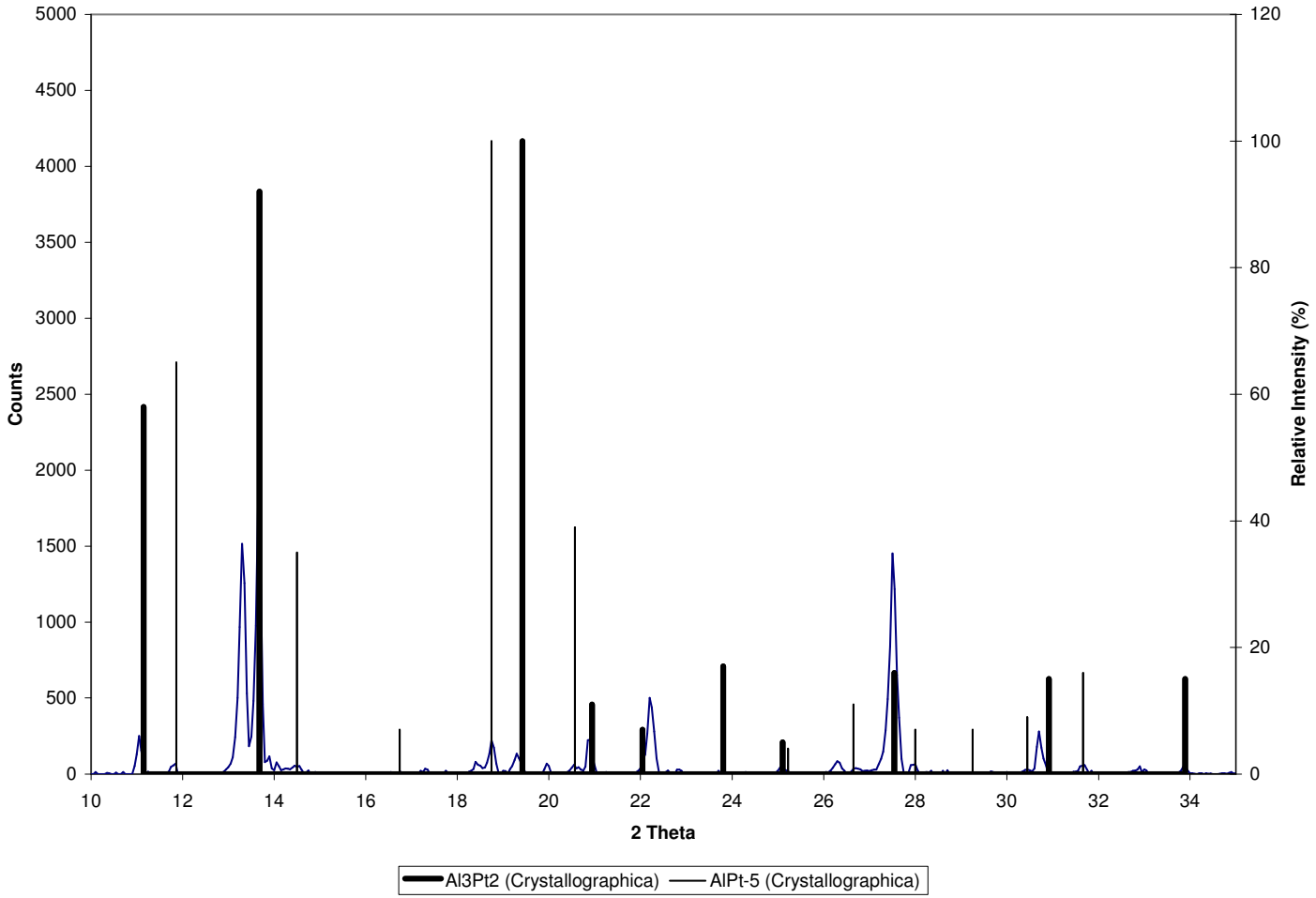

Figure 2.78. XRD pattern for nominal Pt_{43}:Al_{52}:Cr_5 in the as-cast condition.

2.1.24. Nominal $Pt_{50}:Al_{35}:Cr_{15}$

Alloy $Pt_{50}:Al_{35}:Cr_{15}$ seemed to comprise only one phase (Figure 2.79). The EDX analyses confirmed this (Table 2.24 and Figure 2.80). Taking into consideration other alloys' results, the alloy probably comprised ternary phase T1. See §2.1.9 for a full discussion of ternary T1. The derived XRD peaks for T1 superposed on the measured XRD pattern for $Pt_{50}:Al_{35}:Cr_{15}$ are shown in Figure 2.81, and is shown to be a good match. Although some peaks seem to be unidentified, it must be remembered that the derived pattern for T1 does not include all its peaks but only the most obvious higher intensity ones. The peaks of other candidates like ~Pt_5Al_3 and Pt_2Al are shown in an insert in Figure 2.81, but it is obvious that those of T1 were a better match. The ternary phase must have solidified congruently:

$$L \rightarrow T1.$$

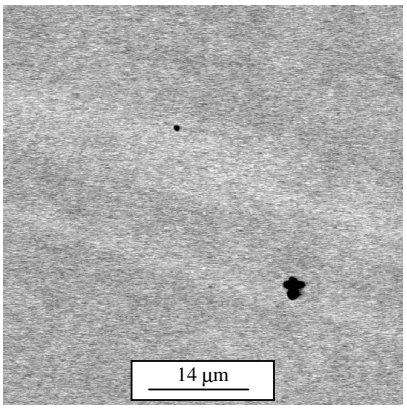

Figure 2.79. BSE-SEM image of nominal $Pt_{50}:Al_{35}:Cr_{15}$ in the as-cast condition: cored T1.

Table 2.24. Phase analyses for nominal $Pt_{50}:Al_{35}:Cr_{15}$ (at.%) in the as-cast condition.

Phase description	**Pt**	**Al**	**Cr**	**Phase**
Overall	50.8 ± 0.3	35.0 ± 0.4	14.2 ± 0.4	-
Dark	51.2 ± 0.6	35.1 ± 0.2	13.7 ± 1.4	cored T1
Light	51.2 ± 0.5	35.1 ± 0.2	13.7 ± 0.6	cored T1

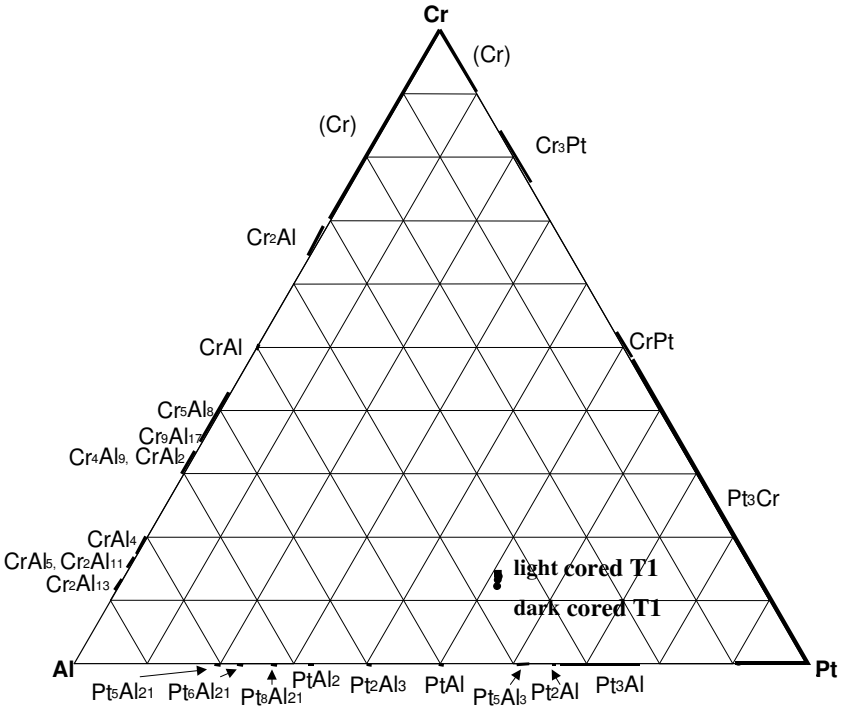

Figure 2.80. EDX analyses of nominal Pt_{50}:Al_{35}:Cr_{15} (at.%) in the as-cast condition. (■ overall composition; ● phases)

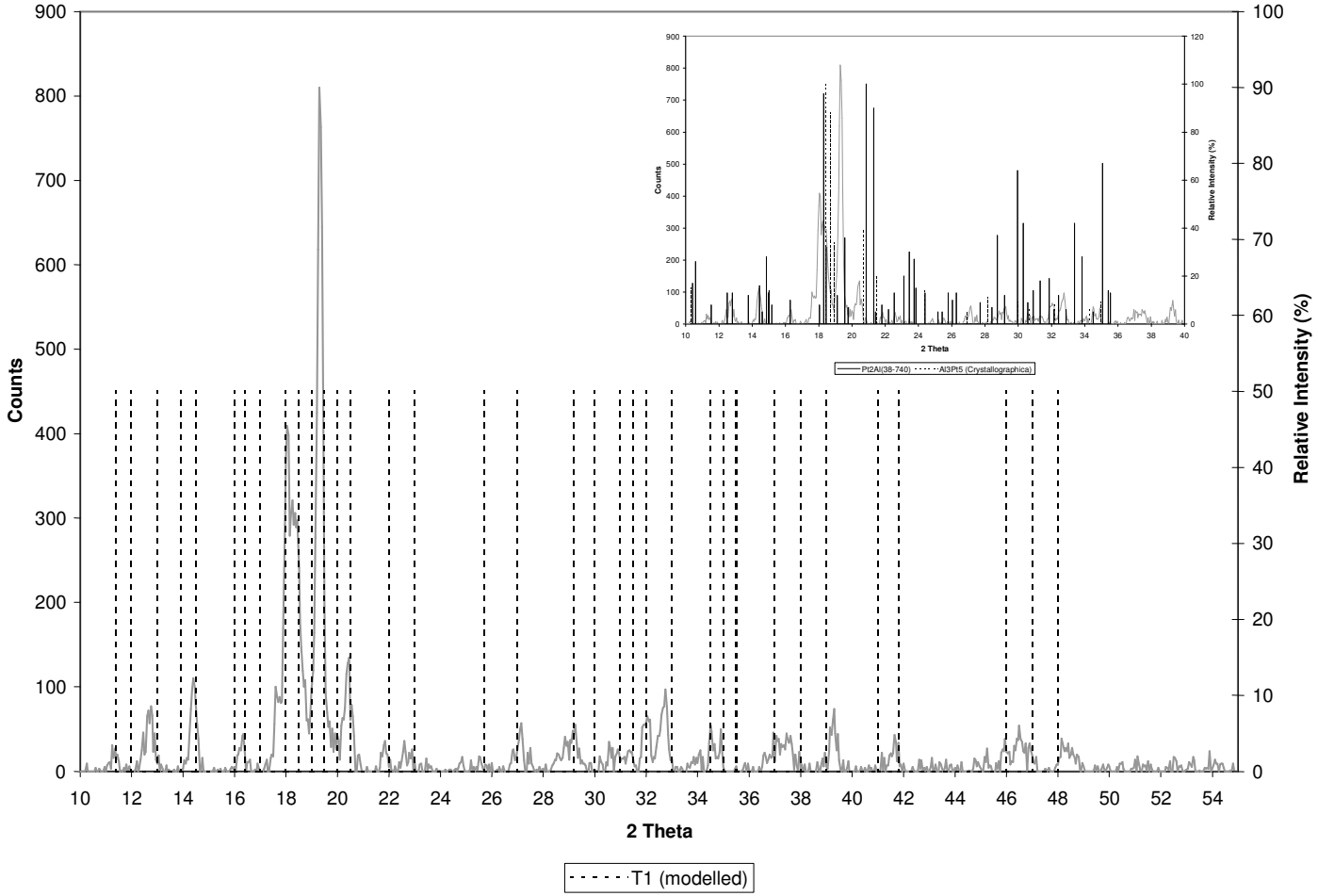

Figure 2.81. XRD pattern for nominal Pt_{50}:Al_{35}:Cr_{15} in the as-cast condition.

2.1.25. Nominal $Pt_{58}:Al_{10}:Cr_{32}$

Alloy $Pt_{58}:Al_{10}:Cr_{32}$ looked like a cored single phase alloy (Figure 2.82), but EDX analyses (Table 2.25, Figure 2.82) showed that there was a difference between the darker dendrites and the lighter interdendritic regions. There were also dark particles located in the light phase, but EDX analyses (although they were actually too small to be accurately analysed) showed that they were oxides (the combined at.% of Pt, Al and Cr only adding up to ~60%). It was rather odd to see that the overall analysis was lying outside the tie-line between the two phases, and although it is possible that it could have badly affected by the oxides, the latter was so little in volume, which suggested that an unseen third phase is present, although the XRD results did not support this. The phase identities were confirmed as ~CrPt ($L1_0$) and ~Pt_3Al (cubic $L1_2$, high temperature form) by XRD analysis (Figure 2.84), both phases' peaks fitting well to the measured pattern. Considering the position of the phases on the ternary plot, the third phase is probably ~Pt_2Al. The phases could have formed by:

$$L \rightarrow (Pt)$$

$$L \rightarrow (Pt) + \sim Pt_3Al$$

$$\sim Pt_3Al \rightarrow \sim Pt_2Al$$

$$(Pt) \rightarrow \sim Pt_3Cr \rightarrow \sim CrPt \text{ (ordering)}$$

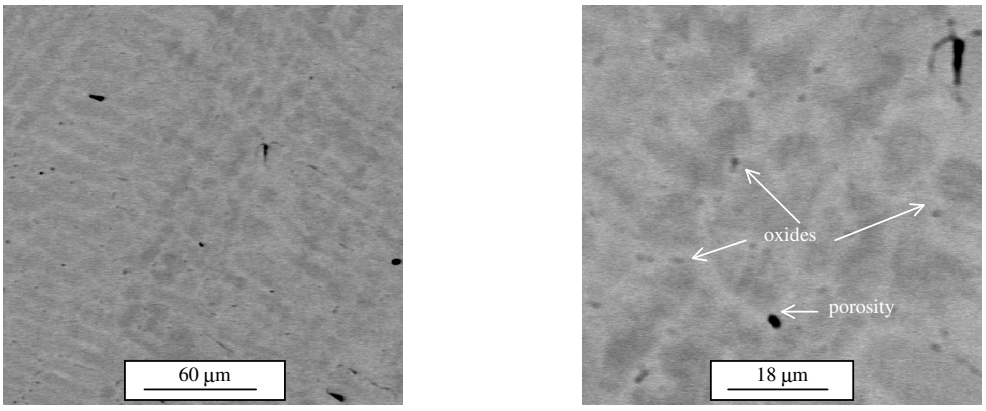

Figure 2.82. BSE-SEM image of nominal $Pt_{58}:Al_{10}:Cr_{32}$ in the as-cast condition: ~CrPt dark; ~Pt_3Al light; very dark oxides.

Table 2.25. Phase analyses for nominal $Pt_{58}:Al_{10}:Cr_{32}$ (at.%) in the as-cast condition.

Phase description	**Pt**	**Al**	**Cr**	**Phase**
Overall	57.9 ± 0.4	9.9 ± 0.9	32.2 ± 1.0	-
Dark	57.8 ± 0.6	4.9 ± 0.5	37.3 ± 0.3	~CrPt
Light	58.1 ± 0.0	7.6 ± 0.3	34.3 ± 0.3	~Pt_3Al
Dark particles	-	-	-	oxide

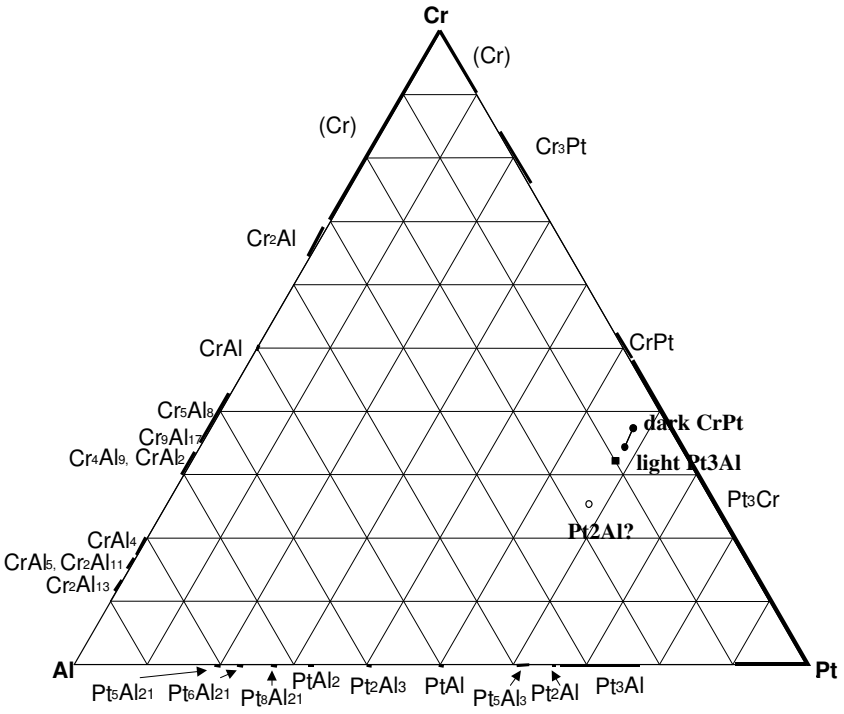

Figure 2.83. EDX analyses of nominal $Pt_{58}:Al_{10}:Cr_{32}$ at.%) in the as-cast condition.

(■ overall composition; ● phases; o possible phase)

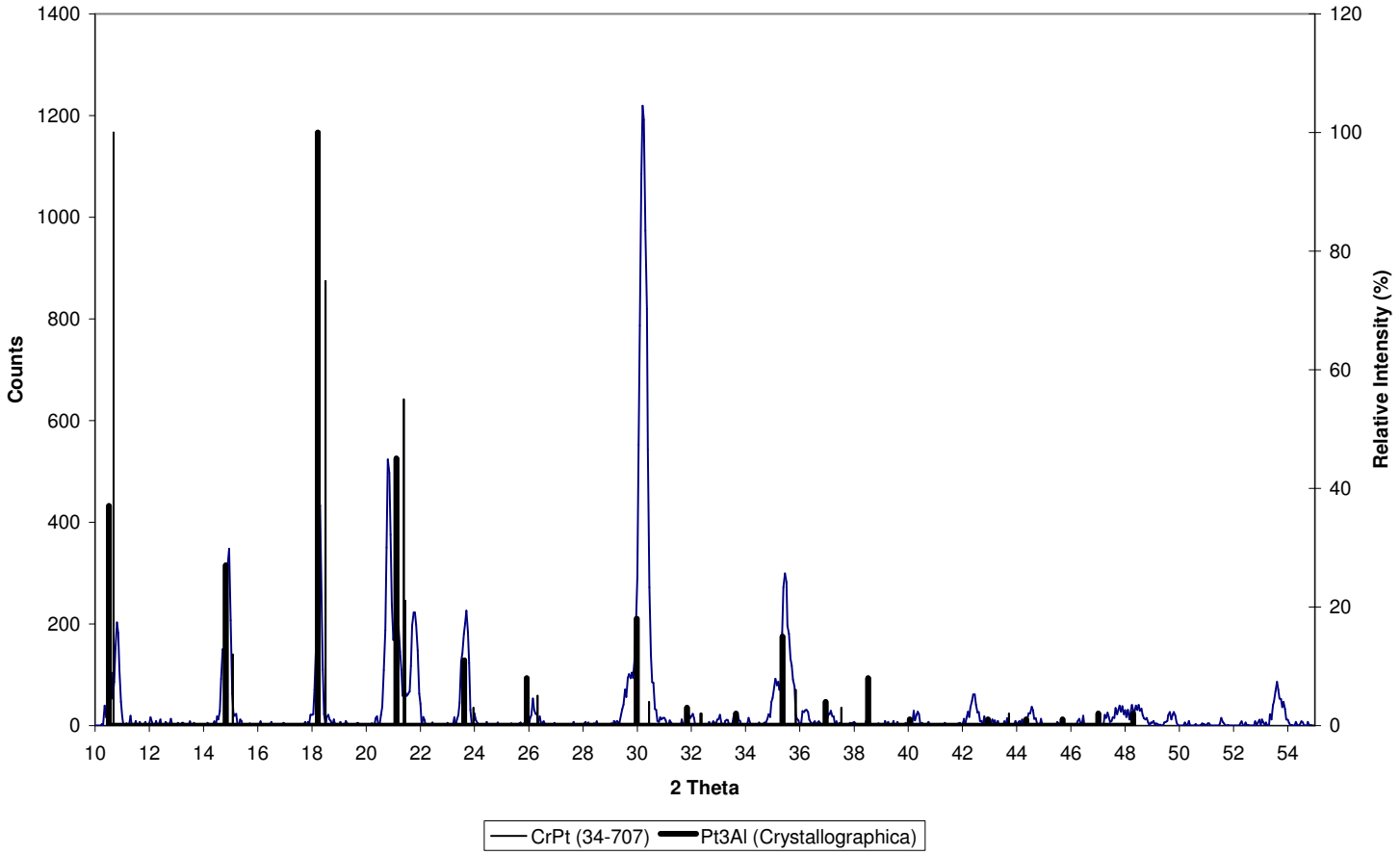

Figure 2.84. XRD pattern for nominal Pt_{58}:Al_{10}:Cr_{32} in the as-cast condition.

2.1.26. Nominal $Pt_{60}:Al_2:Cr_{38}$

Alloy $Pt_{60}:Al_2:Cr_{38}$ did not show many features, and at high magnification it appeared to comprise a cored single phase (Figure 2.85). The EDX analyses are given in Table 2.26 and Figure 2.86, showing the insignificant difference in composition for the two phases. XRD analysis confirmed this assessment by detecting both A1 (modelled by *Crystallographica*) and $L1_0$ ~CrPt (Figure 2.87) (with only one peak at $2\theta \approx 34$ not identified), although some measured peaks suggested the presence of some ~Pt_3Cr.

The microstructure formed by:

$$L \rightarrow (Pt)$$

$$(Pt) \rightarrow \sim Pt_3Cr \rightarrow \sim CrPt \text{ (ordering)}$$

If ~Pt_3Cr is present, it is merely the remnants of an incomplete ordering reaction.

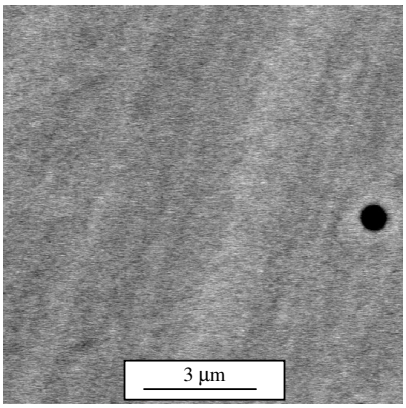

Figure 2.85. BSE-SEM image of nominal $Pt_{60}:Al_2:Cr_{38}$ in the as-cast condition: cored ~CrPt.

Table 2.26. Phase analyses for nominal $Pt_{60}:Al_2:Cr_{38}$ (at.%) in the as-cast condition.

Phase description	**Pt**	**Al**	**Cr**	**Phase**
Overall	59.7 ± 0.3	2.2 ± 0.3	38.1 ± 0.5	-
Dark	59.1 ± 0.9	2.7 ± 0.8	38.2 ± 0.1	Cored ~CrPt
Light	59.7 ± 0.1	2.4 ± 0.3	37.9 ± 0.2	Cored ~CrPt

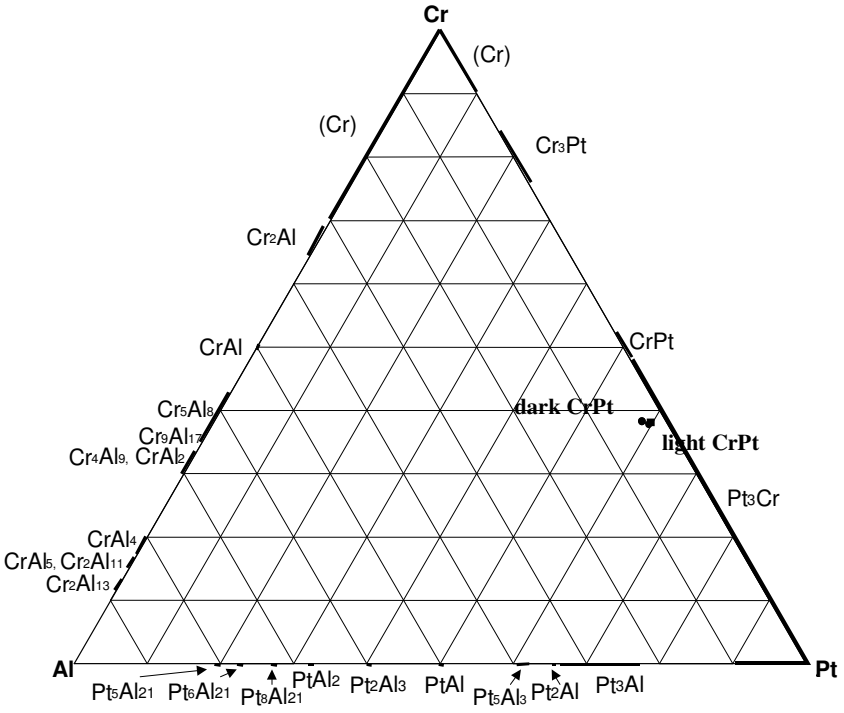

Figure 2.86. EDX analyses of nominal $Pt_{60}:Al_2:Cr_{38}$ (at.%) in the as-cast condition. (■ overall composition; ● phases)

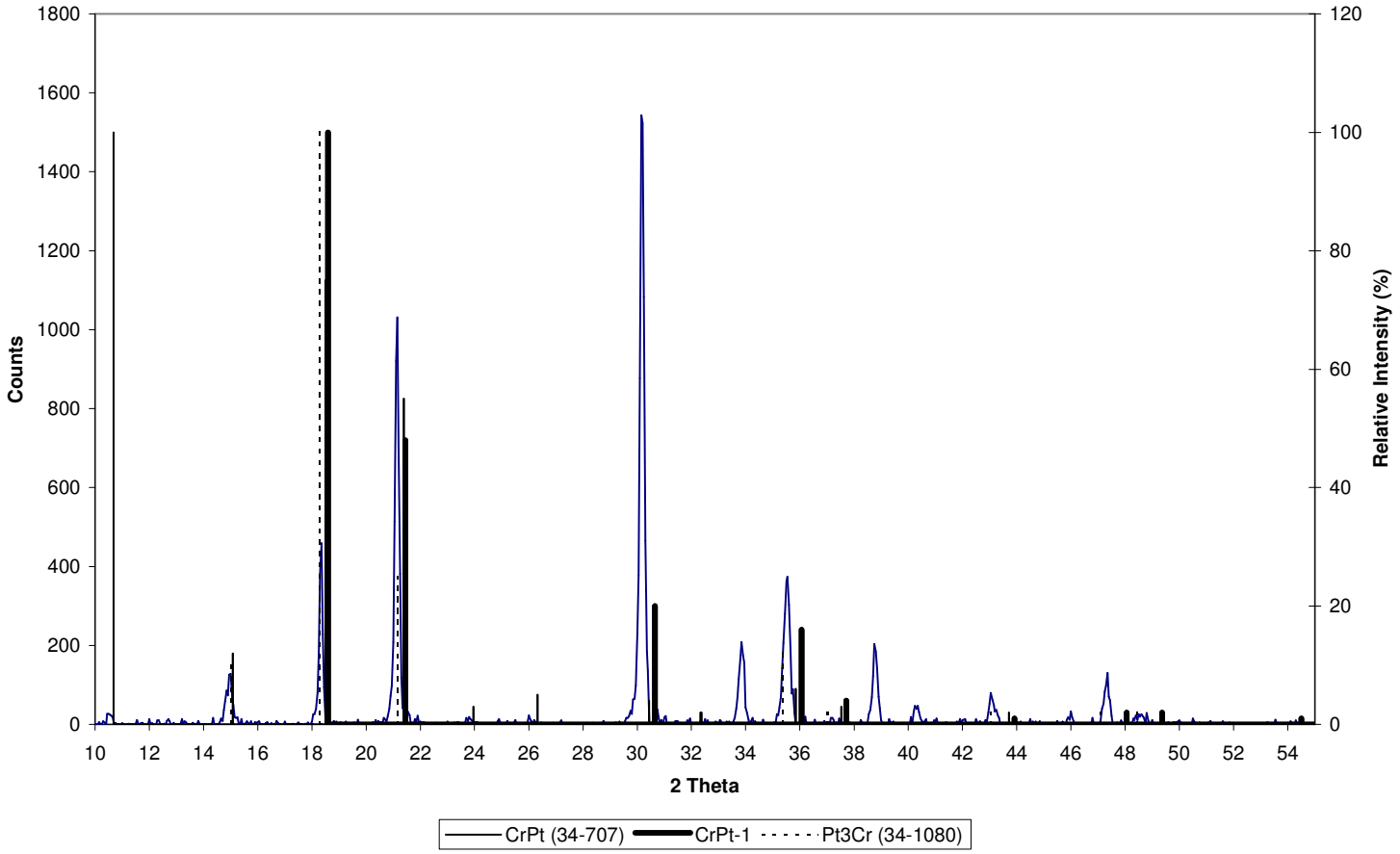

Figure 2.87. XRD pattern for nominal $Pt_{60}:Al_2:Cr_{38}$ in the as-cast condition.

2.1.27. Nominal $Pt_{63}:Al_{32}:Cr_5$

Alloy $Pt_{63}:Al_{32}:Cr_5$ appeared single phase but with image manipulation it was obvious that more than one phase was present. Figure 2.88 shows a very dark, dark and lighter phase, as well as some porosity. The EDX analyses showed that the dark and light phases were very similar in composition, either a single cored phase (Table 2.27, Figure 2.89), or possibly the result of some ordering. The very light phase, although small, and its measurement affected by the surrounding phase, was different in composition. The XRD intensities were very low, and the analyses were difficult to interpret due to the complex nature of the XRD peaks of the phases involved, but it detected what was probably T1 (very dark) and (high temperature, *oP24*) ~Pt_2Al (dark and light) (Figure 2.90). The shift was considerable for both phases (it has already been incorporated in the plot in Figure 2.90 and therefore not that obvious). Considering that the third phase in alloy $Pt_{63}:Al_{22}:Cr_{15}$ (§2.1.28) with composition not too far from that of the cored phase here had been shown to possibly be ~Pt_2Al , made it more likely that the phase here was ~Pt_2Al as well. The structure probably formed by:

$$L \rightarrow \sim Pt_3Al$$

$$L + \sim Pt_3Al \rightarrow T1$$

$$\sim Pt_3Al \rightarrow \sim Pt_2Al$$

possibly followed by

$$\sim Pt_2Al\ (HT) \rightarrow \sim Pt_2Al\ (LT).$$

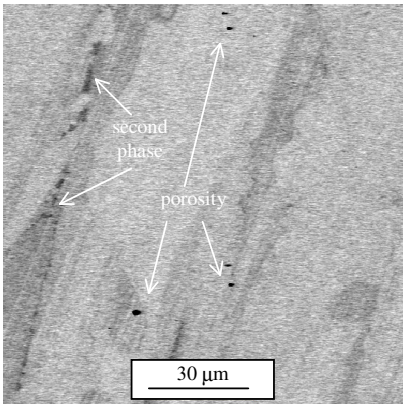

Figure 2.88. BSE-SEM image of nominal $Pt_{63}:Al_{32}:Cr_5$ in the as-cast condition: ~T1 very dark; ~Pt_2Al dark and light.

Table 2.27. Phase analyses for nominal $Pt_{63}:Al_{32}:Cr_5$ (at.%) in the as-cast condition.

Phase description	**Pt**	**Al**	**Cr**	**Phase**
Overall	63.6 ± 0.3	31.9 ± 0.4	4.5 ± 0.3	-
Very dark	56.0 ± 1.0	29.8 ± 1.1	14.3 ± 1.7	~T1
Dark	63.2 ± 0.3	31.6 ± 1.1	5.2 ± 1.4	~Pt_2Al
Light	63.9 ± 0.4	31.8 ± 0.4	4.3 ± 0.3	~Pt_2Al

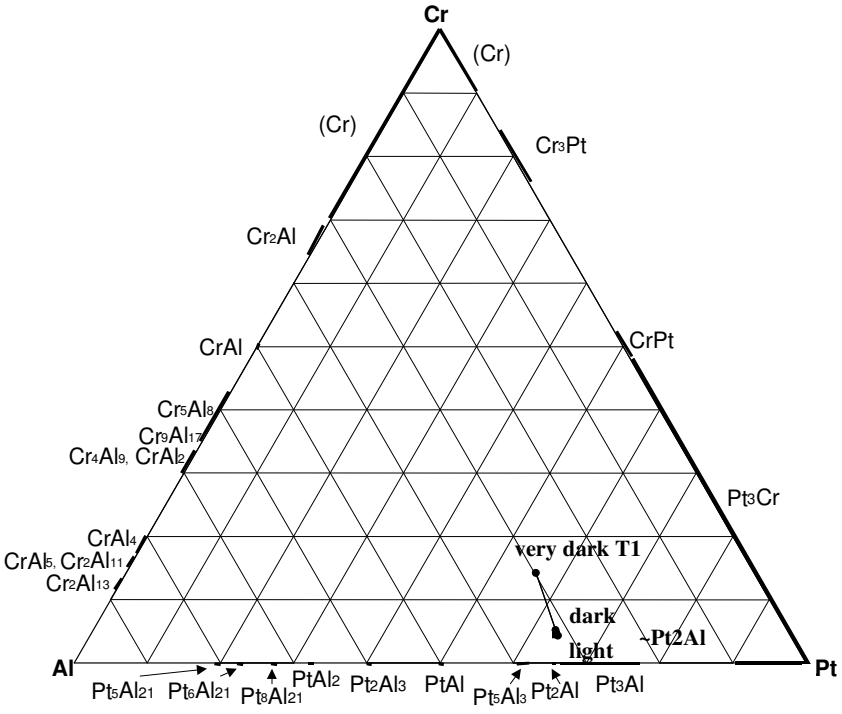

Figure 2.89. EDX analyses of nominal $Pt_{63}:Al_{32}:Cr_5$ (at.%) in the as-cast condition.
(■ overall composition; ● phases)

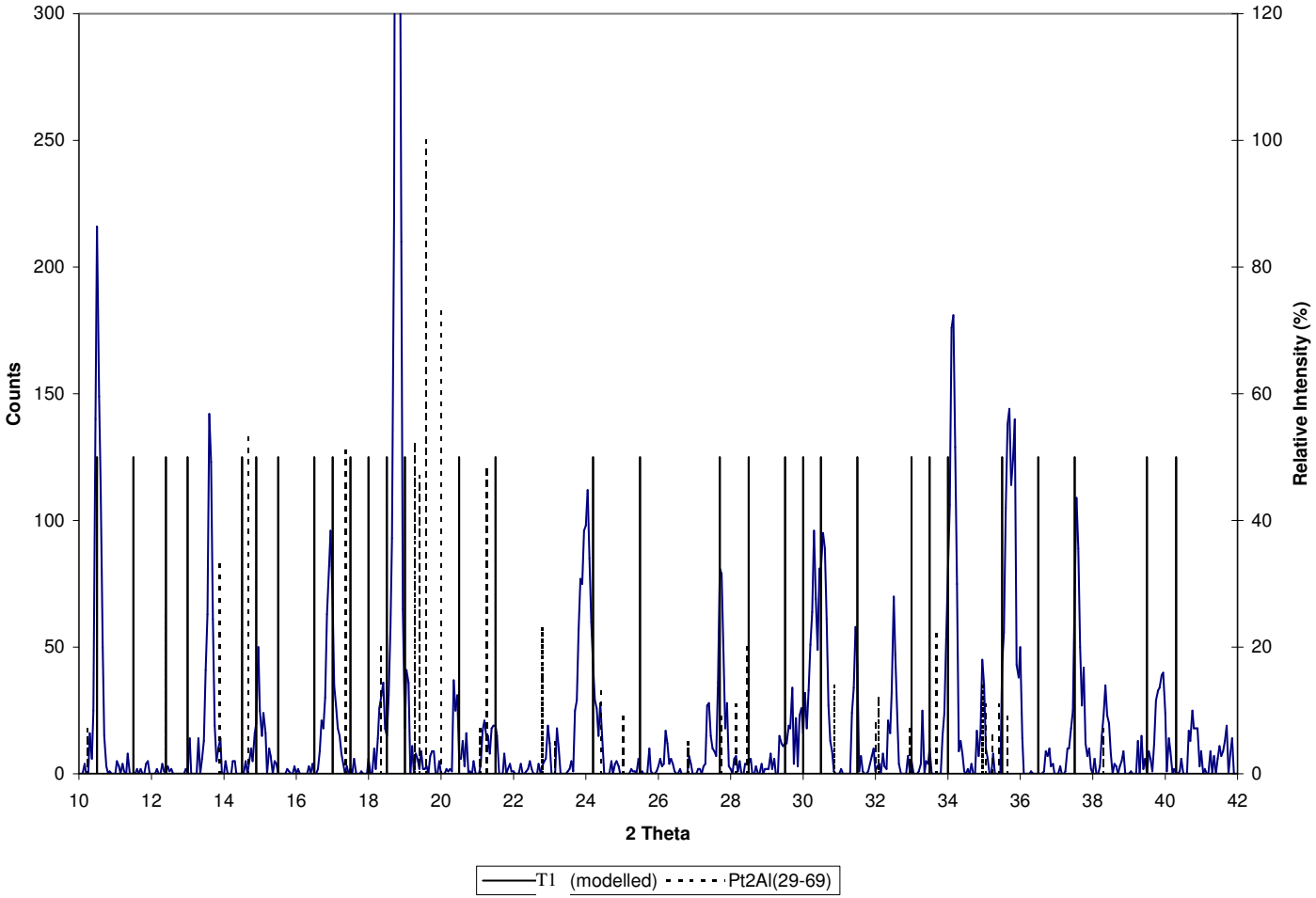

Figure 2.90. XRD pattern for nominal Pt_{63}:Al_{32}:Cr_5 in the as-cast condition.

2.1.28. Nominal $Pt_{63}:Al_{22}:Cr_{15}$

Alloy $Pt_{63}:Al_{22}:Cr_{15}$ looked like a single phase alloy but with a lot of digital image manipulation a contrast was obtained between dark dendrites and lighter regions (Figure 2.91). A tiny amount of white phase was also noticed. The results of the EDX analyses showed that the compositions of the two regions were similar (Table 2.28, Figure 2.92), and XRD analysis detected $L1_2$ ~Pt_3Al (Figure 2.93). There were many measured peaks of very low intensity that were not identified. The white phase seen in Figure 2.91 was present in such a small mount it is doubtful that XRD analysis would have detected it, being less than 5%. The phase was also so small that its analyses were affected by the surrounding phase, and would probably be much richer in Pt than the measured figure indicates. It was concluded that alloy $Pt_{63}:Al_{22}:Cr_{15}$ was cored single phase ~Pt_3Al with minute amounts of contamination of high average atomic number. The microstructure formed by:

$$L \rightarrow \sim Pt_3Al.$$

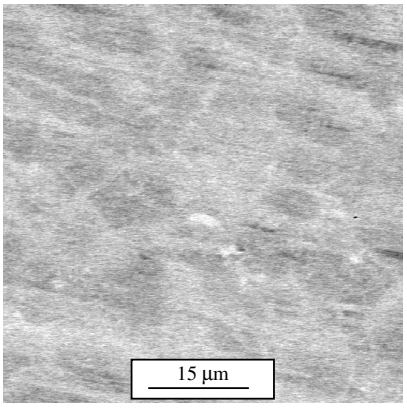

Figure 2.91. BSE-SEM image of nominal $Pt_{63}:Al_{22}:Cr_{15}$ in the as-cast condition: cored ~Pt_3Al grey; contamination white.

Table 2.28. Phase analyses for nominal $Pt_{63}:Al_{22}:Cr_{15}$ (at.%) in the as-cast condition.

Phase description	**Pt**	**Al**	**Cr**	**Phase**
Overall	63.7 ± 0.7	21.1 ± 0.7	15.2 ± 0.3	-
Dark	65.0 ± 0.5	17.4 ± 1.5	17.6 ± 1.4	Cored ~Pt_3Al
Light	64.1 ± 1.6	22.1 ± 3.0	13.8 ± 1.4	Cored ~Pt_3Al
White*	62.3	28.9	8.8	Contamination

* Only one measurement taken due to small size.

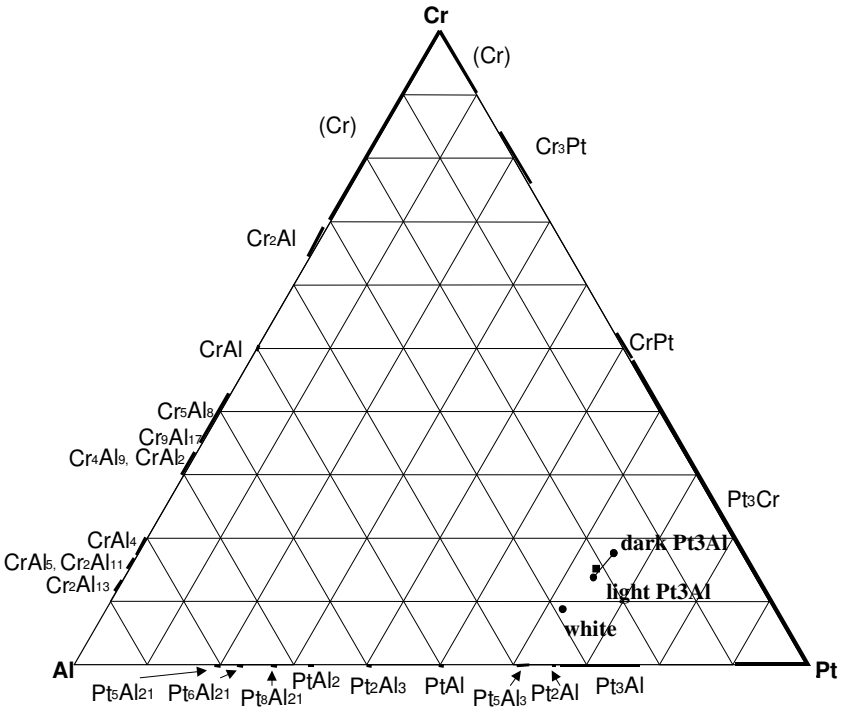

Figure 2.92. EDX analyses of nominal $Pt_{63}:Al_{22}:Cr_{15}$ (at.%) in the as-cast condition.

(■ overall composition; ● phases)

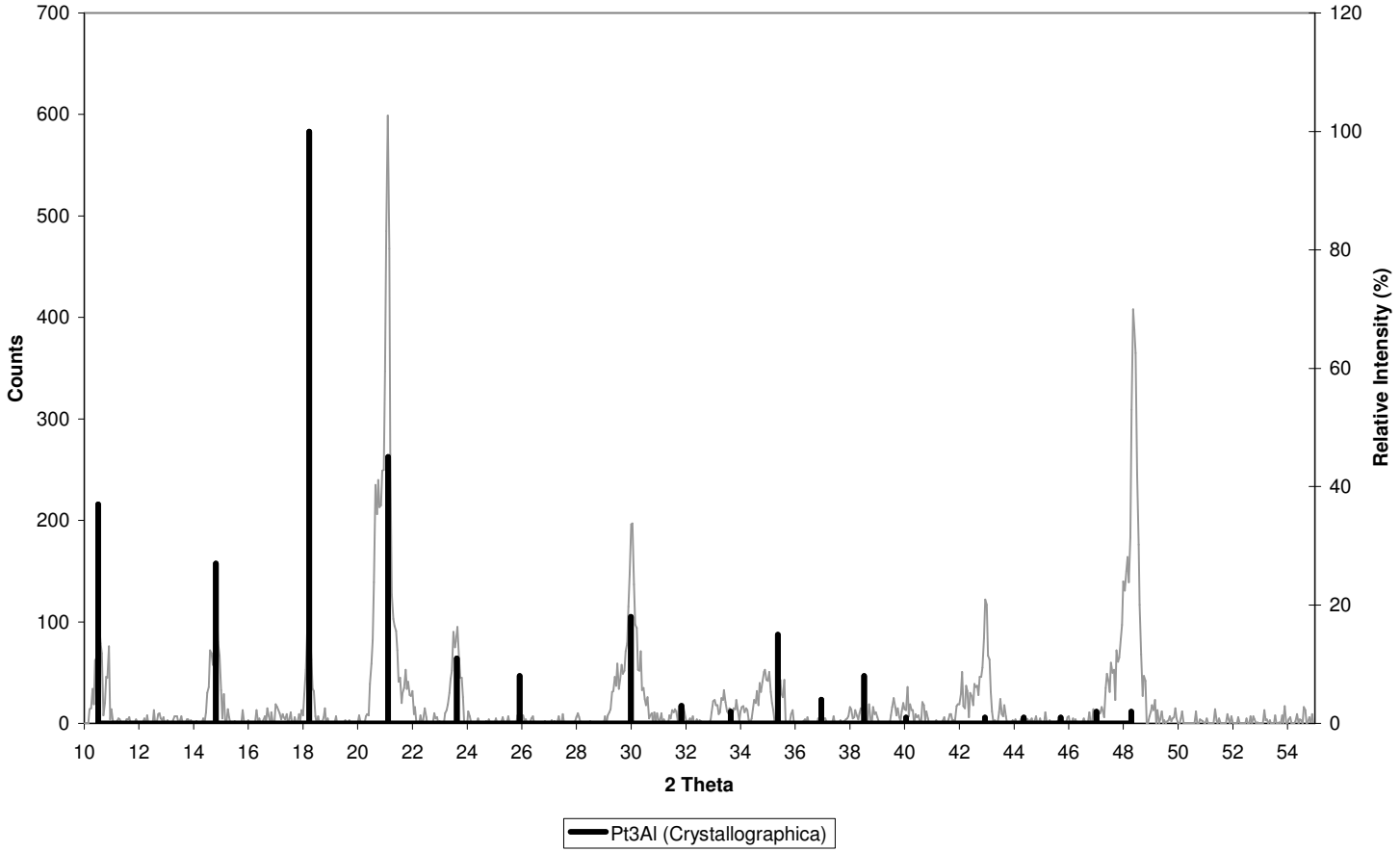

Figure 2.93. XRD pattern for nominal $Pt_{63}:Al_{22}:Cr_{15}$ in the as-cast condition.

2.1.29. Nominal $Pt_{78}:Al_{17}:Cr_5$

Alloy $Pt_{78}:Al_{17}:Cr_5$ comprised light (Pt) dendrites with cubic $L1_2$ ~Pt_3Al as interdendritic phase (Figure 2.94). The EDX analyses are shown in Table 2.29 and Figure 2.95. The identities of the phases were confirmed by XRD analysis (Figure 2.96), because there was a good fit between the phases' peaks and the measured pattern.

The structure formed by:

$$L \rightarrow (Pt)$$

followed by a eutectic reaction

$$L \rightarrow (Pt) + \sim Pt_3Al$$

in agreement with the binary Pt-Al system. This means that the dark contrast regions are in fact unresolved two-phase mixtures.

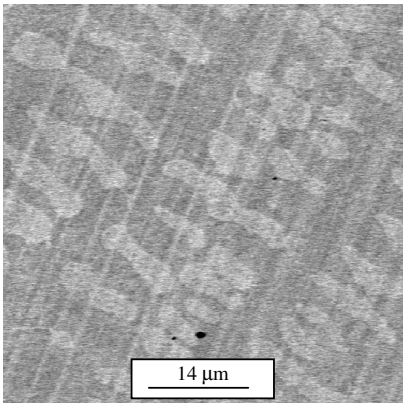

Figure 2.94. BSE-SEM image of nominal $Pt_{78}:Al_{17}:Cr_5$ in the as-cast condition: (Pt) light; ~Pt_3A l + (Pt) dark.

Table 2.29. Phase analyses for nominal $Pt_{78}:Al_{17}:Cr_5$ (at.%) in the as-cast condition.

Phase description	**Pt**	**Al**	**Cr**	**Phase**
Overall	78.6 ± 1.2	16.5 ± 1.3	4.9 ± 0.4	
Dark	77.9 ± 0.9	17.5 ± 0.2	4.6 ± 0.8	~Pt_3Al + (Pt)
Light	81.8 ± 1.7	10.4 ± 1.6	7.8 ± 0.6	(Pt)

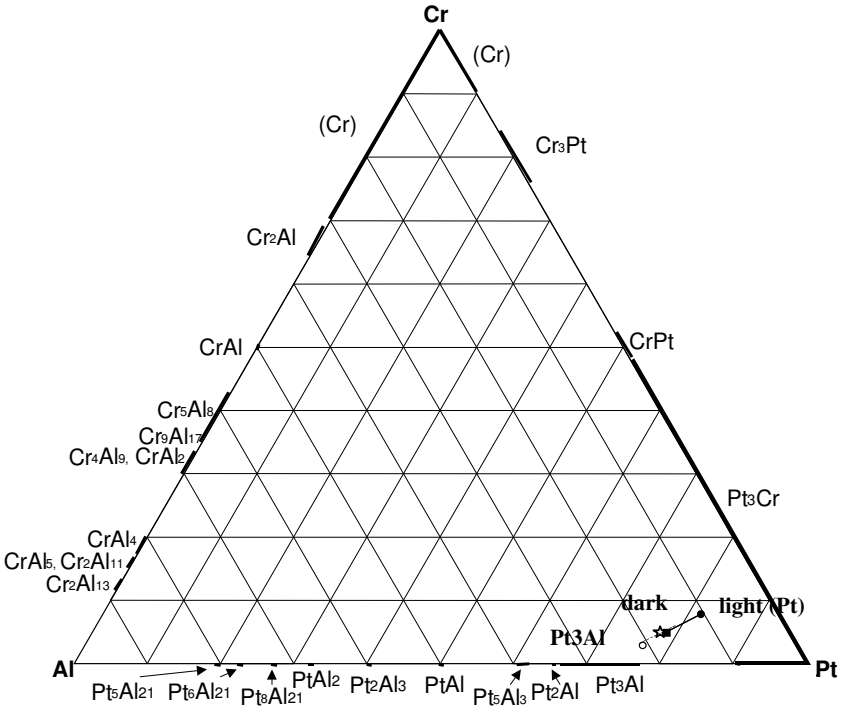

Figure 2.95. EDX analyses of nominal Pt_{78}:Al_{17}:Cr_5 (at.%) in the as-cast condition.

(■ overall composition; ● phase; o proposed phase; ★ eutectic)

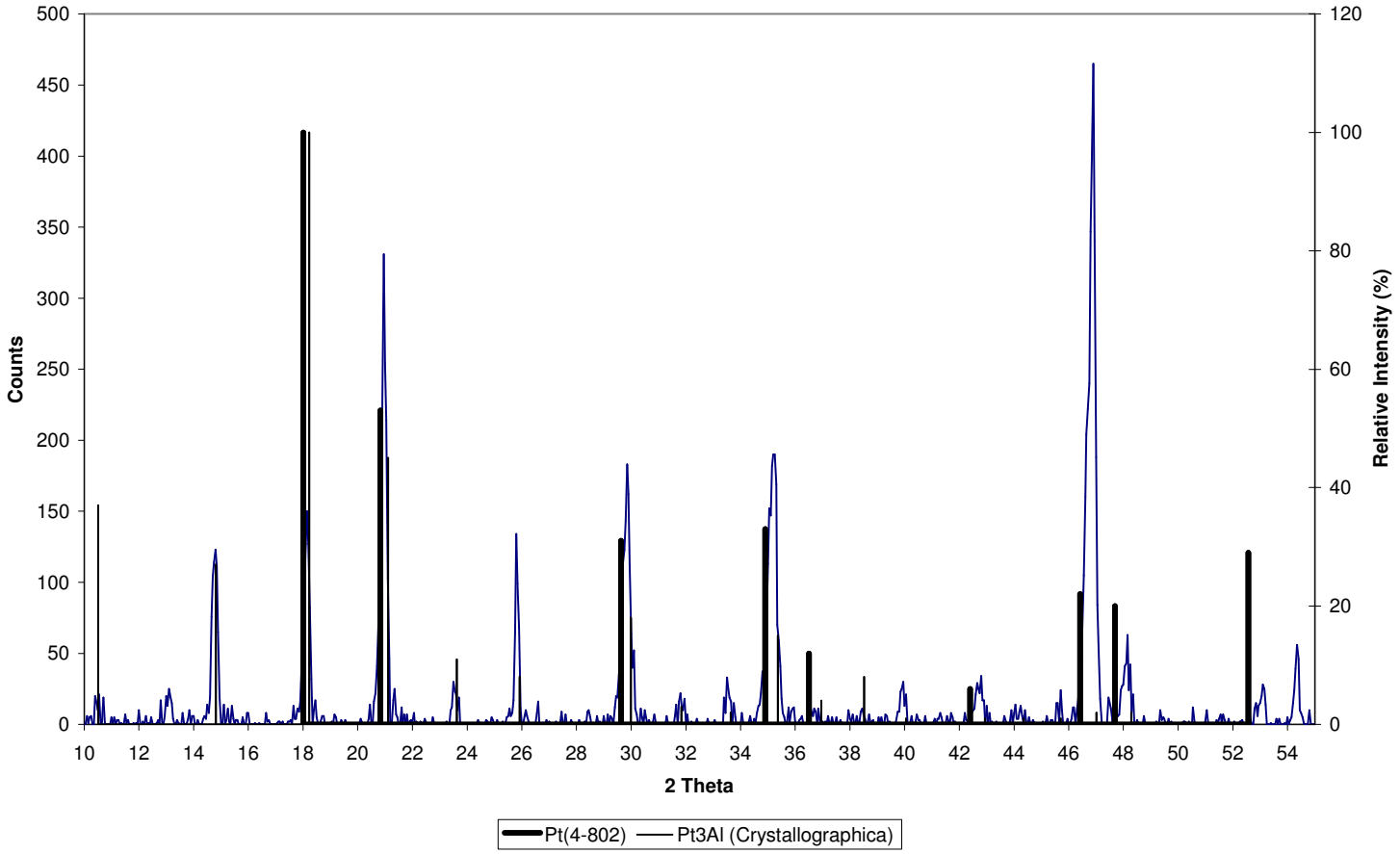

Figure 2.96. XRD pattern for nominal Pt_{78}:Al_{17}:Cr_5 in the as-cast condition.

2.1.30. Nominal Pt_{75}:Al_{10}:Cr_{15}

EDX analyses (Table 2.30) showed that alloy Pt_{75}:Al_{10}:Cr_{15} must have lost Pt due to sputtering during melting, because its actual composition was Pt_{34}:Al_{49}:Cr_{17}. At first glance, nominal alloy Pt_{75}:Al_{10}:Cr_{15} comprised a dark and a light phase (similar to alloy Pt_{35}:Al_{55}:Cr_{10}) with a considerable amount of porosity, but closer inspection revealed that it comprised a primary dark phase (dendrites) with a three-phase mixture of black, 'small dark' and light (Figure 2.97). The reason for the initial distinction between dark and 'small dark' is because the EDX analyses showed that their compositions differed (Table 2.30, Figure 2.98). However, the 'small dark' particles and the light phase were much smaller than the potential ~3μm size of beam spread on interaction and would be affected by the surrounding phase. The dark phases are therefore probably identical. The small black phase was not measured at all due to its small size. The only real accurate measurements would be those for the dark phase and the three-phase area, although some measurements for the latter might have been done in areas which was actually too small as well. The fact that the overall analysis was not on the dark-light tie-line, confirms that a third phase was present, namely the black phase. Figure 2.99 shows a slightly amended ternary plot of the dark (bulk) and light phases as well as the two-phase composition. From the XRD analysis it appeared as though the possible phases were ~$PtAl_2$ (with shift to the left), (Cr) and ~PtAl (Figure 2.100), which gave a good match to the measured pattern. Some peaks were not identified, and taking into account other alloys' results (Pt_{40}:Al_{50}:Cr_{10} (§2.1.10), Pt_{35}:Al_{55}:Cr_{10} (§2.1.21) and Pt_{12}:Al_{18}:Cr_{70} (§2.1.16)), the phases were probably ~$PtAl_2$ (dark), (Cr) (black) and ~PtAl (light). This alloy was probably not at equilibrium and annealing will hopefully shed more light on the assessment. The structure formed by:

$$L \rightarrow \sim PtAl_2$$

followed by a ternary eutectic reaction

$$L \rightarrow (Cr) + \sim PtAl + \sim PtAl_2.$$

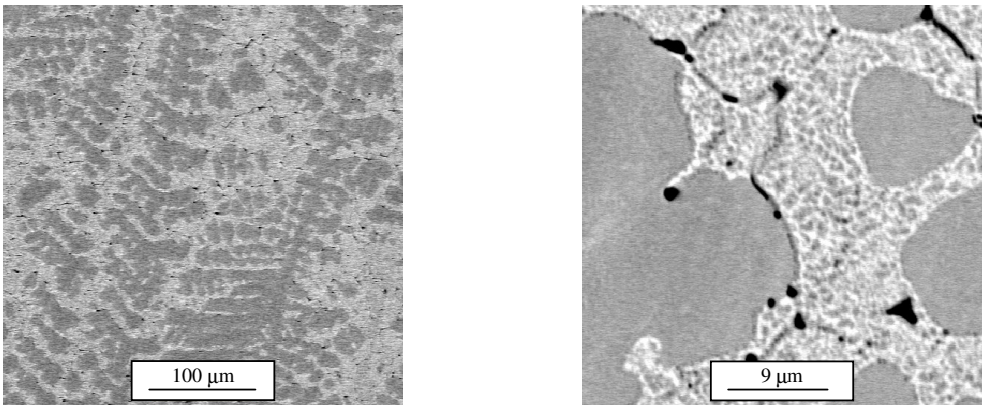

Figure 2.97. BSE-SEM image of nominal $Pt_{34}:Al_{49}Cr_{17}$ in the as-cast condition:~$PtAl_2$ dark; ~$PtAl_2$ grey; ~PtAl light; (Cr), porosity black.

Table 2.30. Phase analyses for nominal $Pt_{34}:Al_{49}Cr_{17}$ (at.%) in the as-cast condition.

Phase description	**Pt**	**Al**	**Cr**	**Phase**
Overall	34.0 ± 0.3	48.6 ± 0.6	17.4 ± 0.4	-
Dark	32.2 ± 0.4	52.0 ± 0.3	15.8 ± 0.3	~$PtAl_2$
Light	39.4 ± 0.7	44.4 ± 0.0	16.2 ± 0.7	~PtAl
Black	Not measured	Not measured	Not measured	(Cr) + porosity
Small dark	35.2 ± 1.5	46.9 ± 0.8	17.9 ± 0.7	~$PtAl_2$
Ternary eutectic	35.4 ± 0.2	45.7 ± 0.2	18.9 ± 0.0	(Cr) + ~PtAl + $PtAl_2$

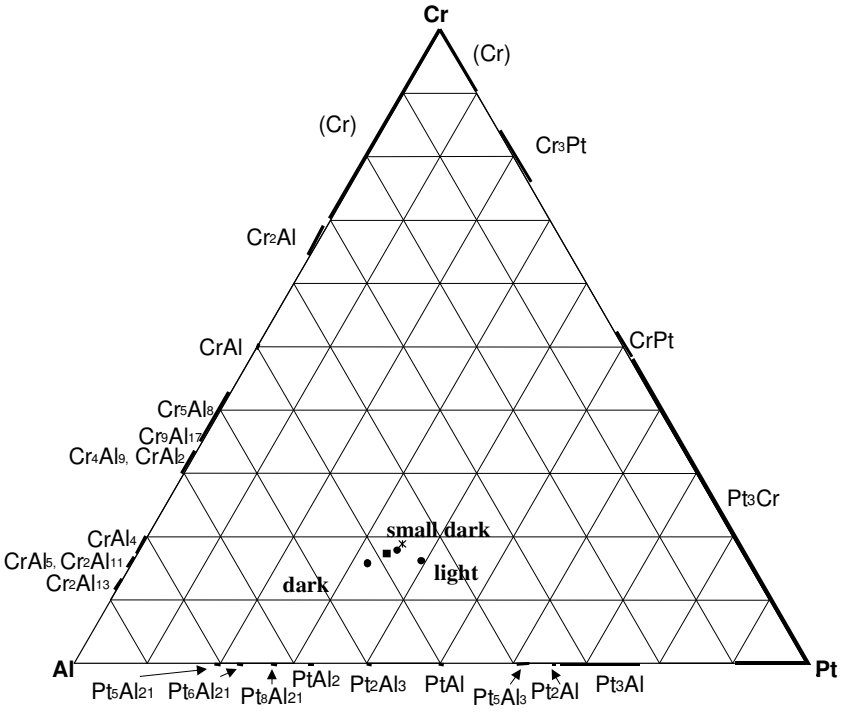

Figure 2.98. EDX analyses of nominal $Pt_{34}:Al_{49}Cr_{17}$ (at.%) in the as-cast condition. (■ overall composition; ● phases; ✶ three-phase)

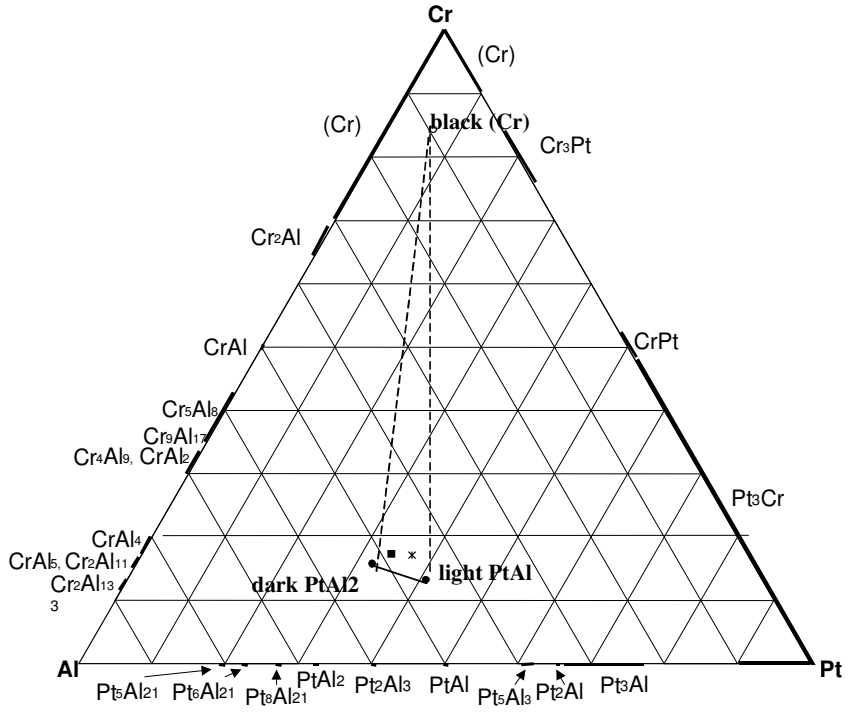

Figure 2.99. Extrapolation of phase compositions of nominal Pt_{34}:$Al_{49}Cr_{17}$ (at.%) in the as-cast condition.

(■ overall composition; ● phases; o suggested phase; ✶ three-phase)

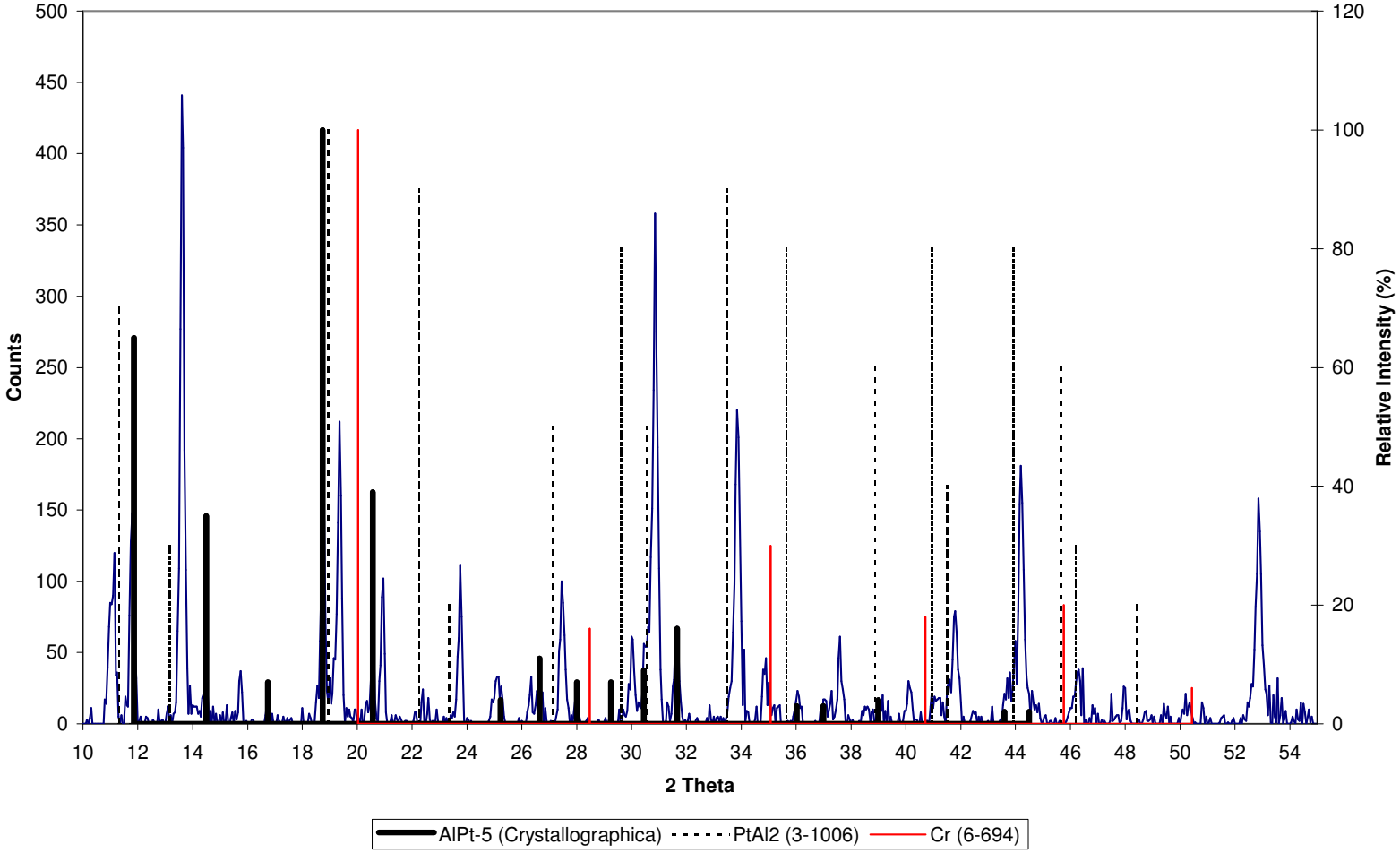

Figure 2.100. XRD pattern for nominal Pt_{34}:$Al_{49}Cr_{17}$ in the as-cast condition.

2.1.31. Nominal $Pt_3:Al_{79}:Cr_{18}$

Alloy $Pt_3:Al_{79}:Cr_{18}$ comprised dark, medium and light grey phases with black porosity always inside the light phase, indicating that it had solidified last. There were also white spots present, always associated with the porosity, but never surrounding it (Figure 2.101). The EDX analyses are shown in Table 2.31. The medium phase was very similar in composition to the grey phase in alloy $Pt_{17}:Al_{68}:Cr_{15}$ (§2.1.17), while the light phase was very similar in composition to what was a dark phase in alloy $Pt_{10}:Al_{80}:Cr_{10}$ (§2.1.4). This suggested that the medium phase was ~$CrAl_4$ and the light phase ~$CrAl_5$. From the position of the dark phase in Figure 2.102, it is likely that it was a ternary T3 with microstructure similar to $CrAl_3$, a phase that is not given in the Cr-Al binary diagram but listed in Pearson's Handbook. XRD analysis did not prove this assessment wrong. The peaks for $CrAl_3$, modelled with *Crystallographica*, were a much better fit to some of the peaks in the measured pattern than those of the nearest other possible phase ~Cr_4Al_9. There were many peaks, especially at $2\theta>34$, that were not identified (Figure 2.102). A lot of these unmatched peaks could be the result of the white phase, although it could also be because the relevant XRD lines (according to JCPDS) were only calculated up to a limit. The white phase extended to the composition of alloy $Pt_{10}:Al_{80}:Cr_{10}$ in which no phase with a similar composition was observed (§2.1.4). It has to be noted, however, that the white and especially the light phase was small and their measurements were affected by surrounding phases. The closest possible phases that it could be were ~Pt_8Al_{21} or ~Pt_6Al_{21} (a JCPDS compound), but neither of these seemed to fit the measured pattern, although it is difficult to judge because the JCPDS database often does not give information for values of $2\theta>40$.

Figure 2.103 shows the compositions of the phases on the ternary diagram. The overall analyses lie slightly outside the composition "triangle" shown. Since the standard deviation for the dark phase was particularly large, T3 is probably richer in Al which would make the overall lie inside the phase analyses.

The microstructure formed by:

$$L \rightarrow T3$$

$$L + T3 \rightarrow \sim CrAl_4$$

$$L + CrAl_4 \rightarrow \sim CrAl_5$$

$$L + \sim CrAl_5 \rightarrow \sim Pt_8Al_{21}$$

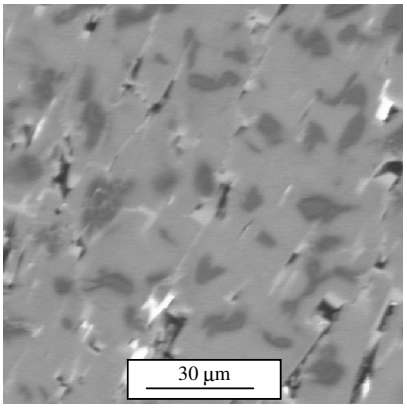

Figure 2.101. BSE-SEM image of nominal Pt_3:Al_{79}:Cr_{18} in the as-cast condition: T3≈$CrAl_3$ dark; ~$CrAl_4$ medium; ~$CrAl_5$ light; porosity black; white Pt_8Al_{21}.

Table 2.31. Phase analyses for nominal Pt_3:Al_{79}:Cr_{18} (at.%) in the as-cast condition.

Phase description	**Pt**	**Al**	**Cr**	**Phase**
Overall	3.5 ± 0.2	78.6 ± 0.5	17.9 ± 0.7	-
Dark	0.4 ± 0.1	74.5 ± 3.5	25.1 ± 3.6	T3≈$CrAl_3$
Medium	3.4 ± 0.2	76.5 ± 0.4	20.1 ± 0.5	~$CrAl_4$
Light	5.3 ± 1.1	79.3 ± 1.1	15.4 ± 1.9	~$CrAl_5$
White*	9.2	79.5	11.3	Pt_8Al_{21}

* Only one measurement taken due to small size.

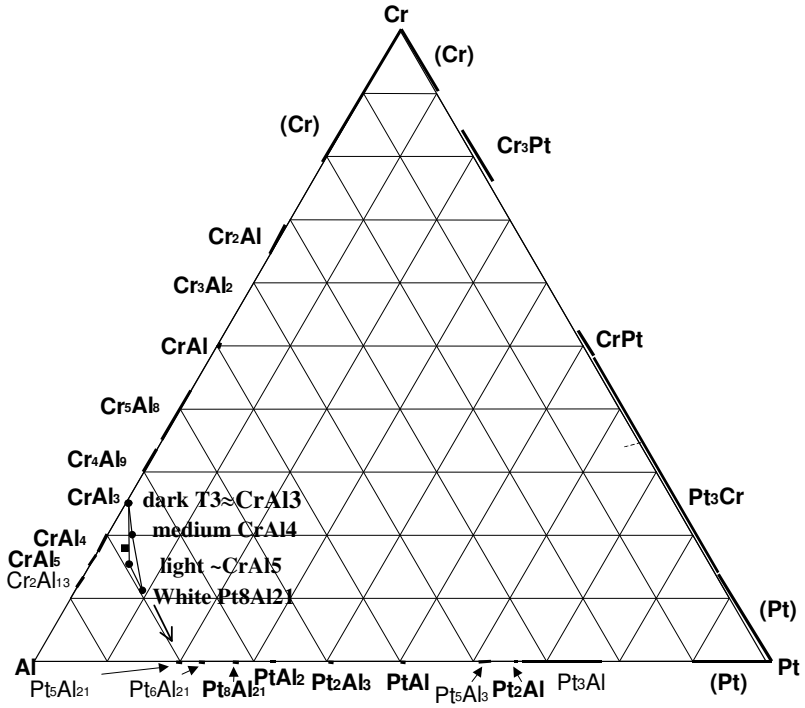

Figure 2.102. EDX analyses of nominal Pt_3:Al_{79}:Cr_{18} (at.%) in the as-cast condition.

(■ overall composition; ● phases; → probable extrapolation)

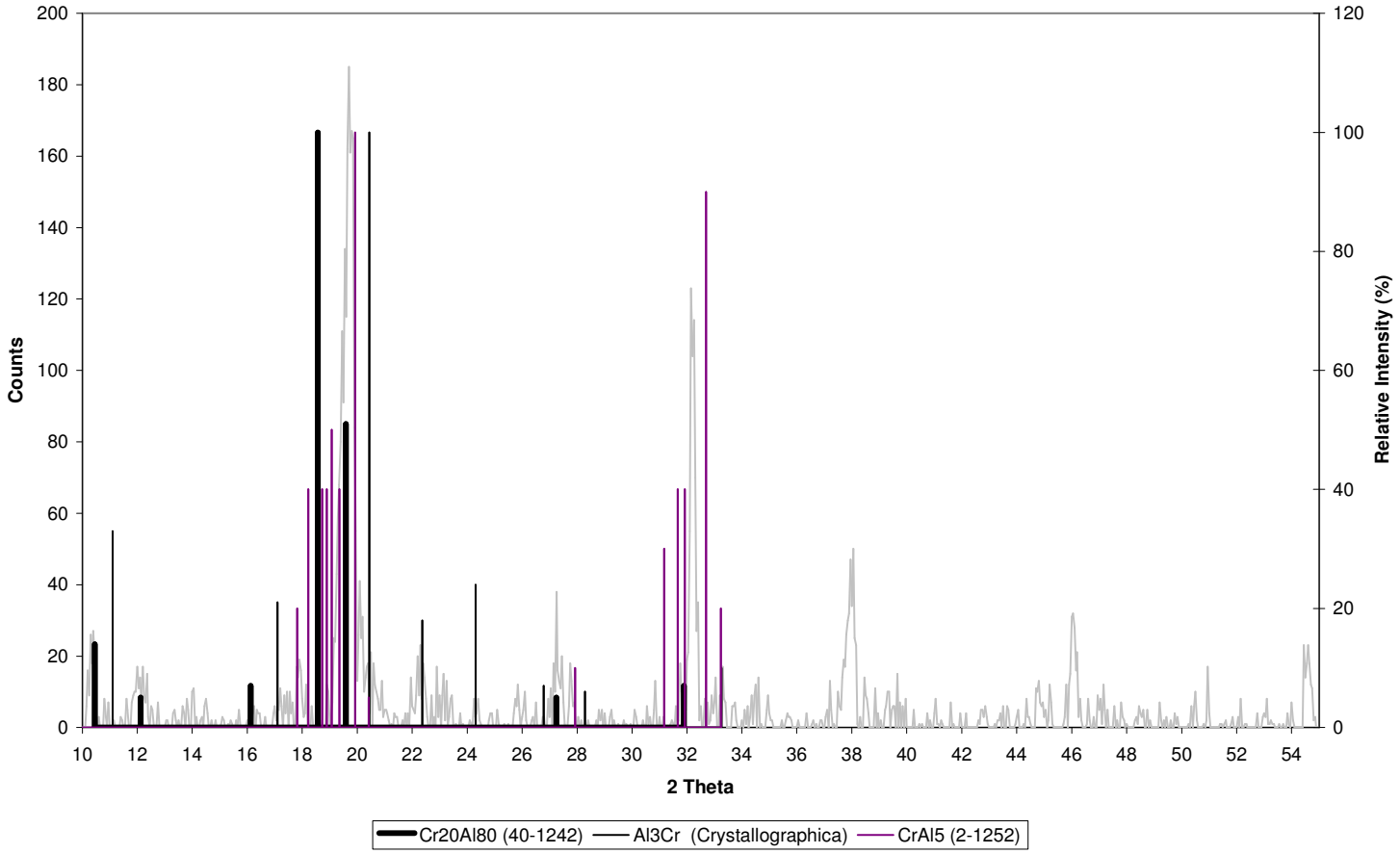

Figure 2.103. XRD pattern for nominal Pt_3:Al_{79}:Cr_{18} in the as-cast condition.

2.1.32. Nominal $Pt_5:Al_{52}:Cr_{43}$

Alloy $Pt_5:Al_{52}:Cr_{43}$ comprised a medium shaded phase with a darker rim with a mixture of light and a darker phase in-between (Figure 2.104). From the position of the phases on the ternary diagram that shows the alloy's EDX analyses (Figure 2.105), based on Table 2.32, the phases were probably ~Cr_5Al_8 (dark), a ternary based on the JCPDS compound Cr_3Al_2 or ~Cr_2Al (light) and ~$PtAl_2$ (white). The presence of ~Cr_5Al_8, ~$PtAl_2$, ~T2≈Cr_3Al_2 was confirmed by XRD analysis (~Cr_2Al was not a good fit) (Figure 2.106). The position of the multi-component composition, although lying off the tie-line, suggests that the mixture probably comprised medium T2≈Cr_3Al_2 and light ~$PtAl_2$. This is plausible considering the high standard deviation in the eutectic composition. The structure formed by:

$$L \rightarrow (Cr),$$

$$L + (Cr) \rightarrow \sim Cr_5Al_8$$

(a peritectic also found in the binary system), followed by an eutectic reaction

$$L \rightarrow \sim PtAl_2 + (Cr)$$

after which (Cr) transformed in the solid state

$$(Cr) \rightarrow T2 \approx Cr_3Al_2.$$

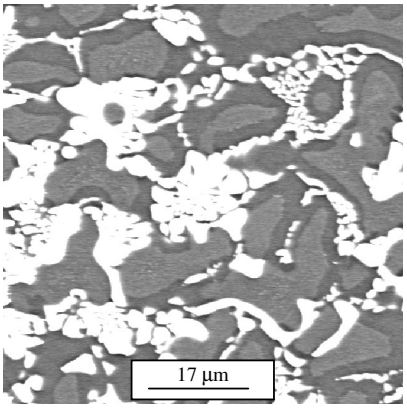

Figure 2.104. BSE-SEM image of nominal $Pt_5:Al_{52}:Cr_{43}$ in the as-cast condition: ~Cr_5Al_8 dark; T2≈Cr_3Al_2 medium; ~$PtAl_2$ light.

Table 2.32. Phase analyses for nominal Pt_5:Al_{52}:Cr_{43} (at.%) in the as-cast condition.

Phase description	**Pt**	**Al**	**Cr**	**Phase**
Overall	4.5 ± 0.7	51.7 ± 1.4	43.8 ± 1.2	-
Dark	1.1 ± 0.0	56.8 ± 0.4	42.1 ± 0.4	~Cr_5Al_8
Medium	0.6 ± 0.4	41.2 ± 0.6	58.2 ± 0.9	T2≈Cr_3Al_2
Light	27.5 ± 0.6	57.9 ± 0.4	14.6 ± 0.8	~$PtAl_2$
Medium + light eutectic	13.7 ± 1.4	52.1 ± 2.8	34.2 ± 4.2	T2≈Cr_3Al_2 + ~$PtAl_2$

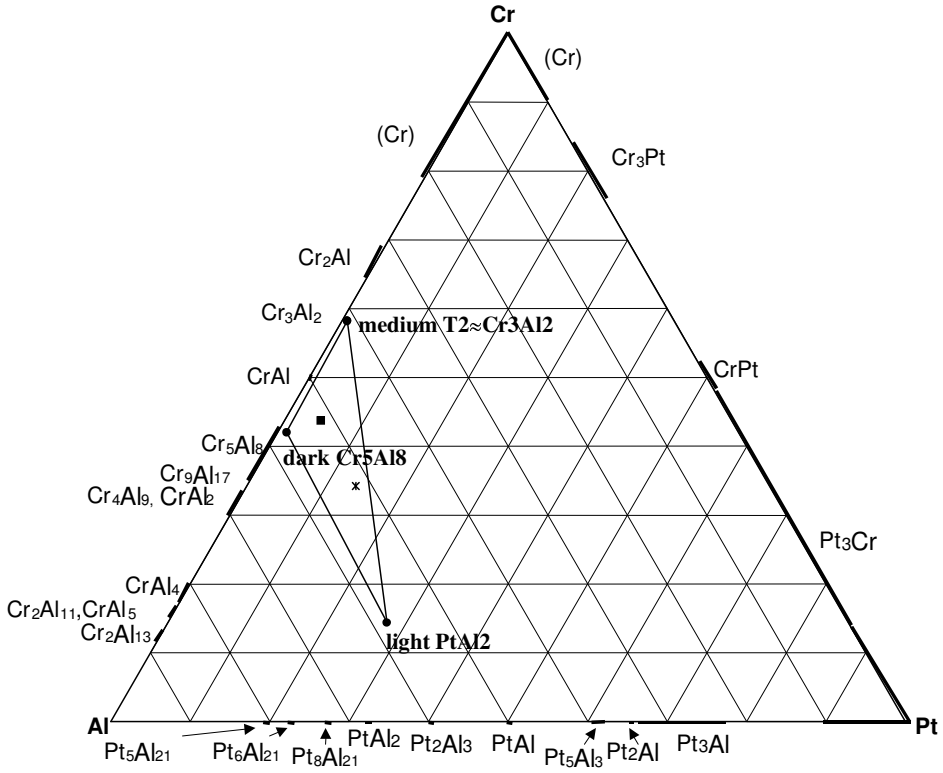

Figure 2.105. EDX analyses of nominal Pt_5:Al_{52}:Cr_{43} (at.%) in the as-cast condition.

(■ overall composition; ● phases; ✶ eutectic)

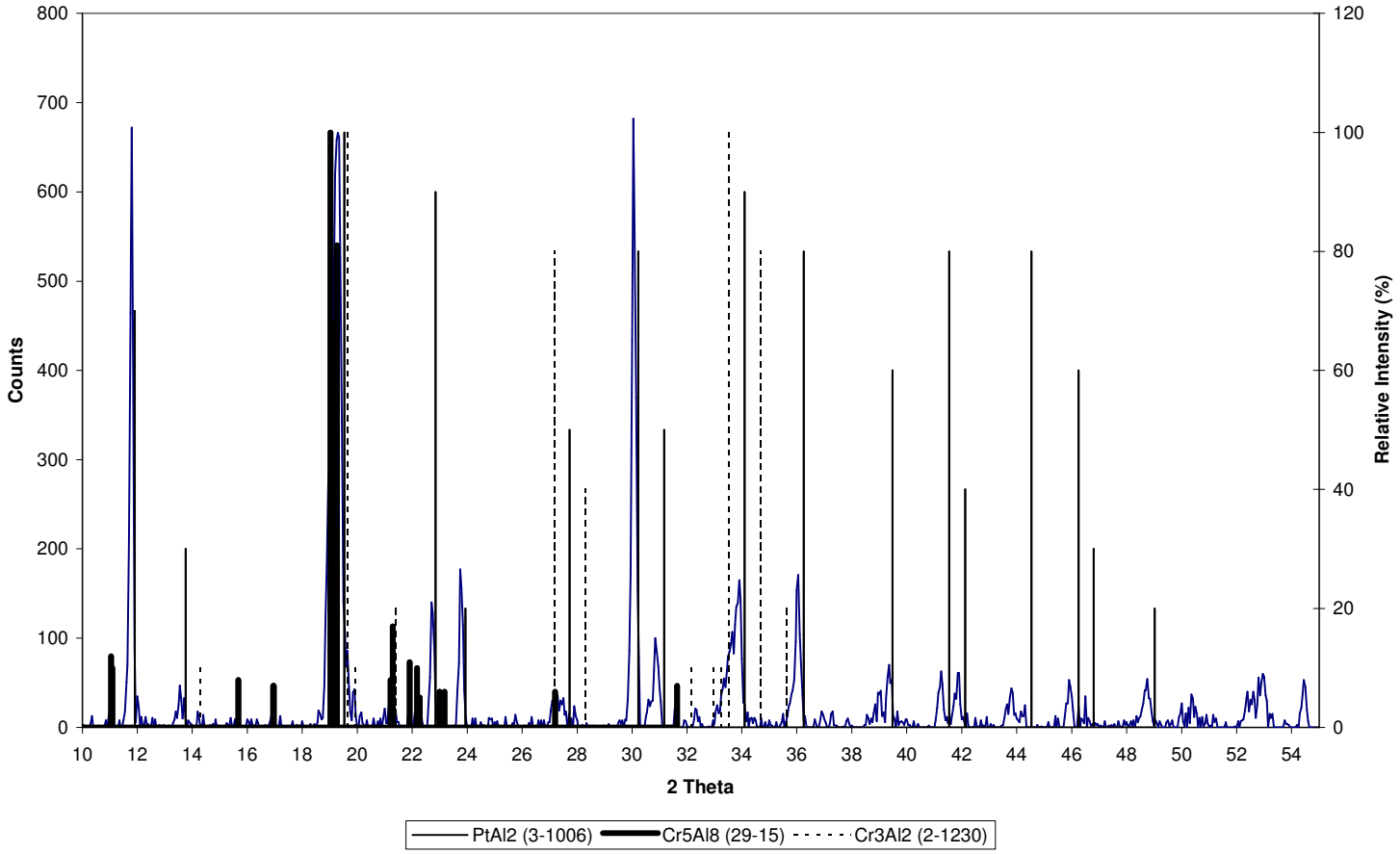

Figure 2.106. XRD pattern for nominal Pt_5:Al_{52}:Cr_{43} in the as-cast condition.

2.1.33. Nominal $Pt_{13}:Al_{45}:Cr_{42}$

Alloy $Pt_{13}:Al_{45}:Cr_{42}$ confirmed the results of alloy $Pt_3:Al_{35}:Cr_{62}$ (§2.1.14). They had very similar appearances, showing a dark phase, a light phase, and two eutectic mixtures, one very coarse close to the dendrites, the other very fine, of dark and light with a web-like appearance in-between (Figure 2.107). However, the EDX analyses showed that there was no difference in composition between the coarse and fine eutectic mixture, and the average is given in Table 2.33 and Figure 2.108. Analyses of the light phase were probably affected by the surrounding phase due to its small size, and its composition could be extrapolated along the tie-line to lower levels of Cr. The phases were confirmed by XRD analysis to be ~Cr_2Al (dark) and ~$PtAl_2$ (light). The latter peaks were shifted with $2\theta \approx 0.5$ due to alloying with Cr. The following reaction sequence is suggested:

$$L \rightarrow (Cr)$$

$$L \rightarrow (Cr) + \sim PtAl_2 \text{ (coarse and fine)}$$

$$(Cr) \rightarrow \sim Cr_2Al \text{ (solid state).}$$

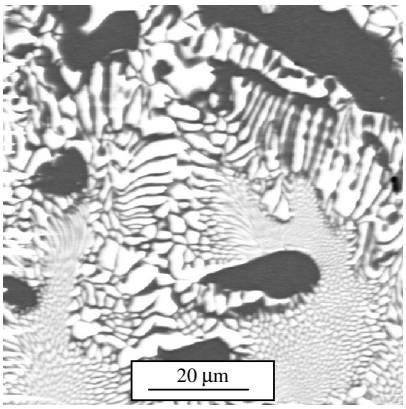

Figure 2.107. BSE-SEM image of nominal $Pt_{13}:Al_{45}:Cr_{42}$ in the as-cast condition: ~Cr_2Al dark; ~$PtAl_2$ light.

Table 2.33. Phase analyses for nominal $Pt_{13}:Al_{45}:Cr_{42}$ (at.%) in the as-cast condition.

Phase description	**Pt**	**Al**	**Cr**	**Phase**
Overall	13.1 ± 0.5	44.2 ± 0.4	42.7 ± 0.8	-
Dark	0.9 ± 0.2	32.5 ± 5.6	66.6 ± 5.4	~Cr_2Al
Light	25.9 ± 2.4	56.2 ± 1.4	17.9 ± 3.7	~$PtAl_2$
Dark + light eutectic	15.7 ± 0.0	45.5 ± 1.9	38.8 ± 1.9	~Cr_2Al + ~$PtAl_2$

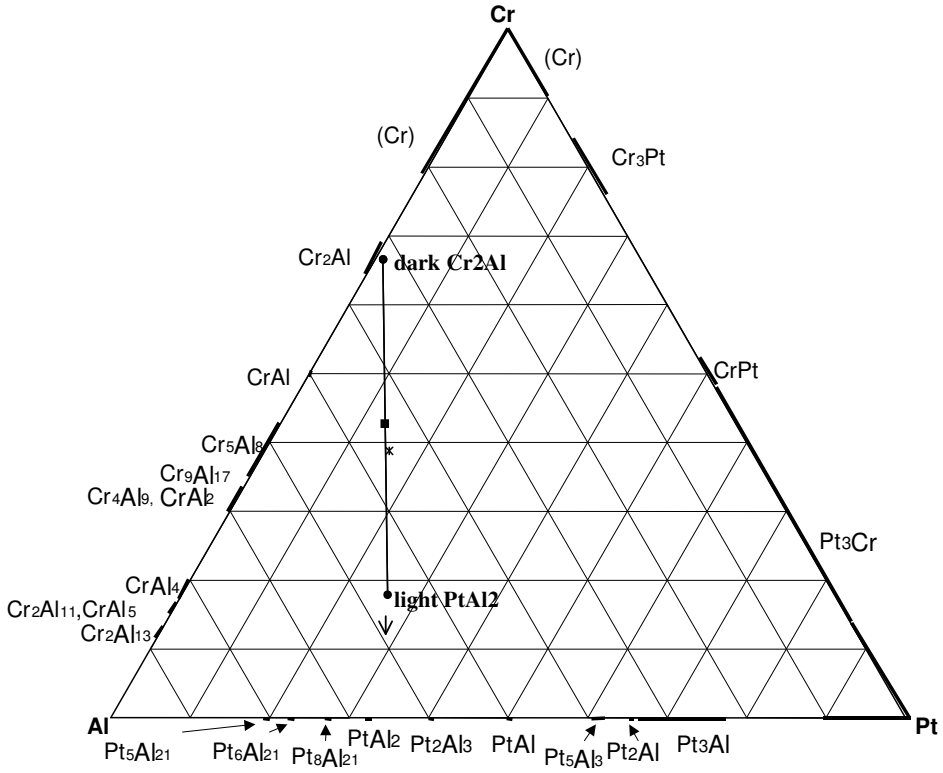

Figure 2.108. EDX analyses of nominal $Pt_{13}:Al_{45}:Cr_{42}$ (at.%) in the as-cast condition.

(■ overall composition; ● phases; ✶ eutectic)

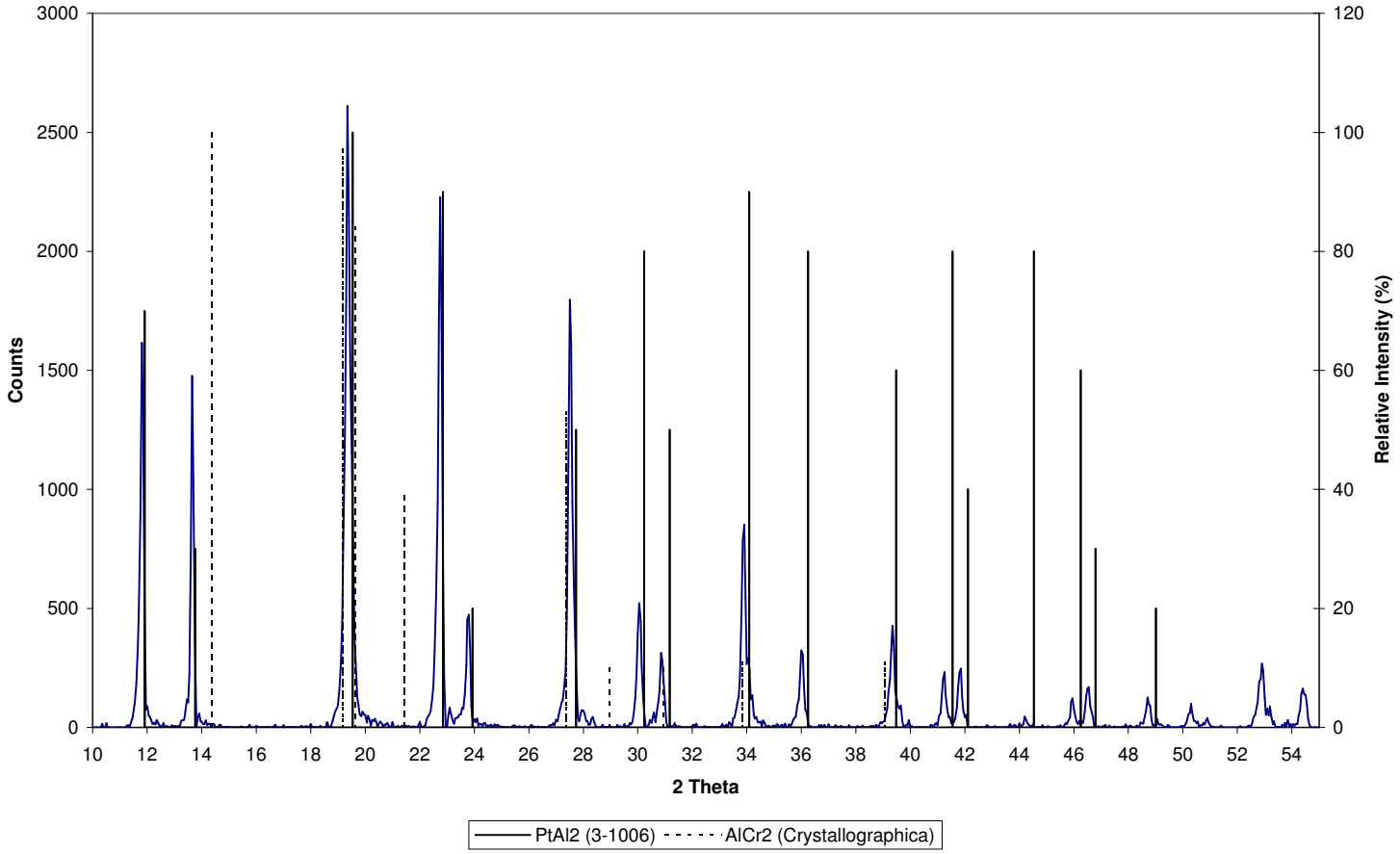

Figure 2.109. XRD pattern for nominal Pt_{13}:Al_{45}:Cr_{42} in the as-cast condition.

2.1.34. Nominal $Pt_{15}:Al_5:Cr_{80}$

Alloy $Pt_{15}:Al_5:Cr_{80}$ comprised three phases: black dendrites, with interdendritic regions that comprise mostly a phase of grey contrast, small white areas and a small amount of black phase (Figure 2.110). The EDX analyses are given in Table 2.34. The phases were very small, especially the white phase, and it is most likely that the white phase's analyses were affected by the surrounding phase. This is proven by two totally different measurements that were obtained for the phase (Table 2.34). One can assume that even the second measurement shown (which had to be the more accurate one in order to be self-consistent in terms of contrast obtained in BSE mode according to average atomic numbers) could possibly be even less rich in Cr. This is illustrated by Figure 2.111 which shows the measured values as well as a possible extrapolated value for the composition of the white phase. The extrapolation showed the white phase could possibly be ternary T1, while the black phase was (Cr) and the medium grey phase ~CrPt. Since the black, white and grey phases were not evenly distributed in the interdendritic areas, no multi-phase analyses were taken. It is proposed that the interdendritic area comprised a ternary eutectic. The phase identities were confirmed by XRD analyses (Figure 2.112), and the assessment would agree with the results of alloy $Pt_{28}:Al_{12}:Cr_{60}$ (§2.1.19). The structure formed by:

$$L \rightarrow (Cr)$$

$$L \rightarrow (Pt) + (Cr) + T1$$

$$(Pt) \rightarrow \sim Pt_3Cr \rightarrow \sim CrPt \text{ (ordering)}$$

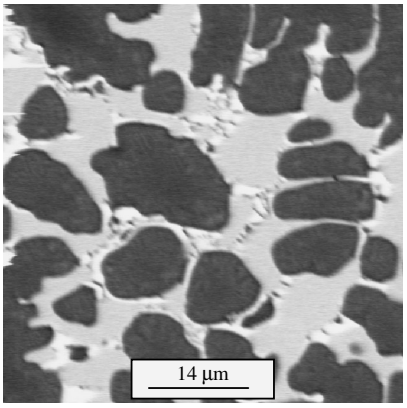

Figure 2.110. BSE-SEM image of nominal $Pt_{15}:Al_5:Cr_{80}$ in the as-cast condition: (Cr) black; ~CrPt grey; T1 white.

Table 2.34. Phase analyses for nominal $Pt_{15}:Al_5:Cr_{80}$ (at.%) in the as-cast condition.

Phase description	**Pt**	**Al**	**Cr**	**Phase**
Overall	12.9 ± 0.4	4.3 ± 0.2	82.8 ± 0.6	-
Black	8.3 ± 0.5	1.7 ± 0.3	90.0 ± 0.4	(Cr)
Grey	26.9 ± 0.4	9.2 ± 0.6	63.9 ± 0.4	~CrPt
White (#1)*	16.7	8.3	75.0	T1
White (#2)*	38.8	24.5	36.7	T1

*Only one measurement taken due to small size.

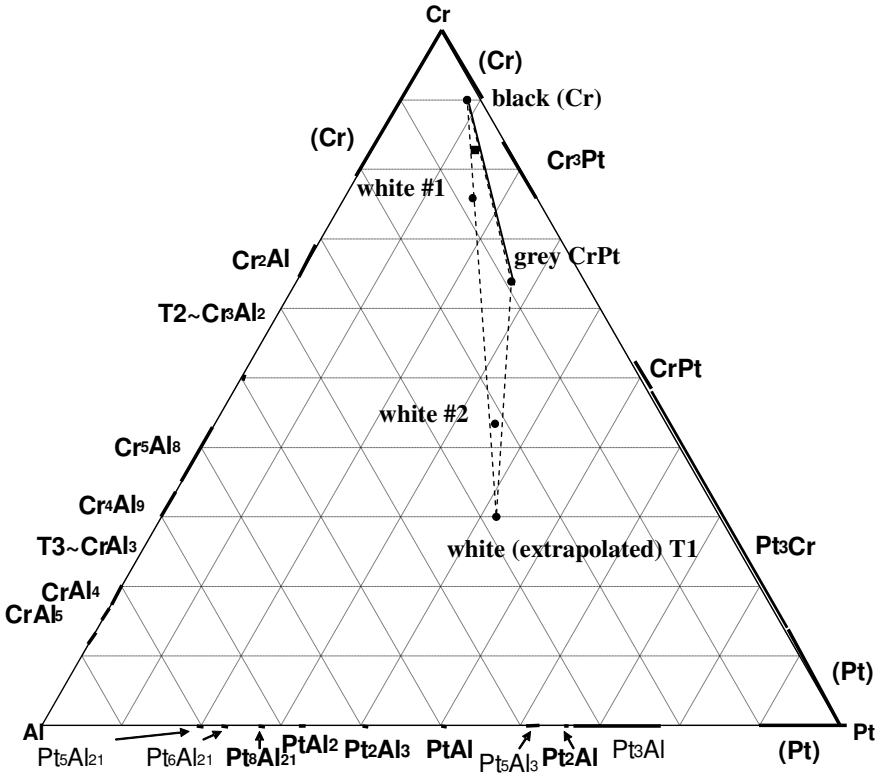

Figure 2.111. EDX analyses of nominal $Pt_{15}:Al_5:Cr_{80}$ (at.%) in the as-cast condition.

(■ overall composition; ● phases; o suggested phase composition)

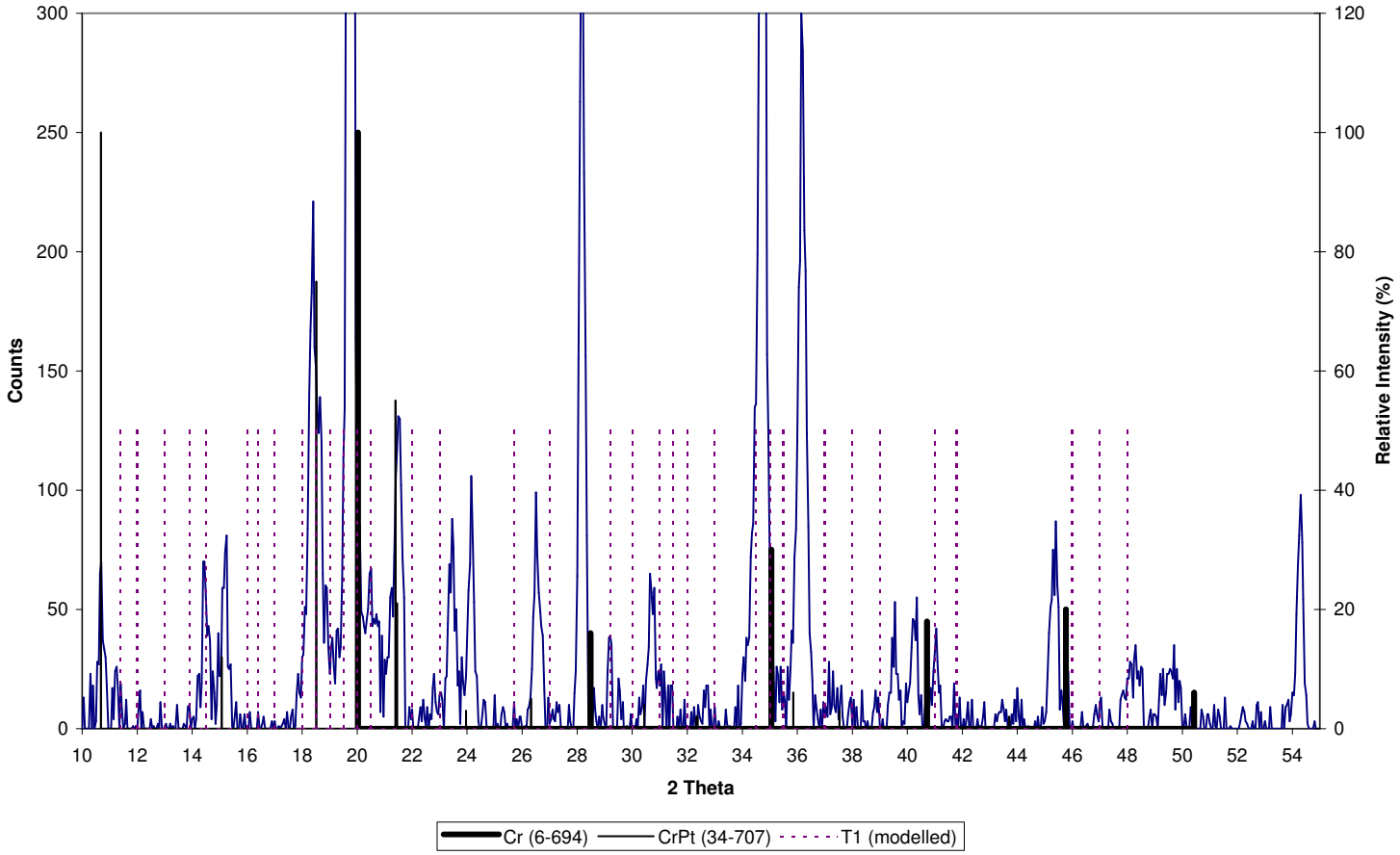

Figure 2.112. XRD pattern for nominal Pt_{15}:Al_5:Cr_{80} in the as-cast condition.

2.1.35. Nominal $Pt_{34}:Al_{27}:Cr_{39}$

Alloy $Pt_{34}:Al_{27}:Cr_{39}$ comprised light dendrites of white and grey phases, with a dark (grey) interdendritic phase which contained porosity (Figure 2.113). The EDX analyses are given in Table 2.35. The graphic representation thereof shows that the dendrites were a composite of the two phases (the two-phase composition lying on tie-line between the two phases) (Figure 2.114). XRD analyses showed that the two phases were probably dark (Cr) and ternary T1 (Figure 2.114). The presence of T1 would fit in with the results of other alloys. The (Cr) areas were quite small (< 3μm) and its analyses would have been affected by the surrounding dendrites. The (Cr) phase would be much richer in Cr than Figure 2.114 shows. An extrapolation arrow is shown to where the (Cr) phase's actual composition would probably lie.

As found before, the structure formed by the congruent solidification of T1

$$L \rightarrow T1$$

which was at first thought to be followed by a peritectic reaction

$$L + T1 \rightarrow (Cr)$$

and additional solid state precipitation of (Cr) in T1 to give the two-phased dendrites.

However, after drawing the liquidus surface (Figure 2.140), the latter is more self-consistent if the second reaction is

$$L \rightarrow T1 + (Cr)$$

forming a sparse eutectic instead, in order to allow the formation of the ternary eutectic T1 + (Cr) + (Pt) in other alloys ($Pt_{28}:Al_{12}:Cr_{60}$ and $Pt_{15}:Al_5:Cr_{80}$). Some small areas in the microstructure suggested this as well.

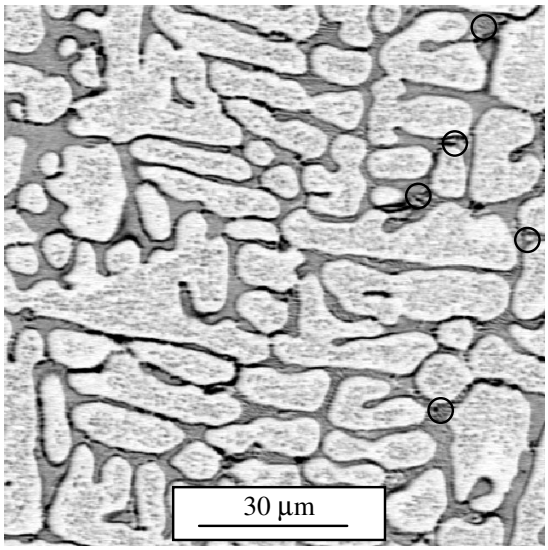

Figure 2.113. BSE-SEM image of nominal $Pt_{34}:Al_{27}:Cr_{39}$ in the as-cast condition: (Cr) dark; T1 light; porosity black; sparse eutectic shown by encircled areas.

Table 2.35. Phase analyses for nominal $Pt_{34}:Al_{27}:Cr_{39}$ (at.%) in the as-cast condition.

Phase description	**Pt**	**Al**	**Cr**	**Phase**
Overall	33.8 ± 1.5	26.9 ± 1.4	39.3 ± 2.8	-
Dark	26.8 ± 2.8	21.8 ± 2.3	51.4 ± 5.1	(Cr)
Light	42.5 ± 0.8	33.6 ± 0.4	23.9 ± 1.0	T1
Dark + light Two-phase*	38.1	30.4	31.5	(Cr) + T1

* Only one measurement taken.

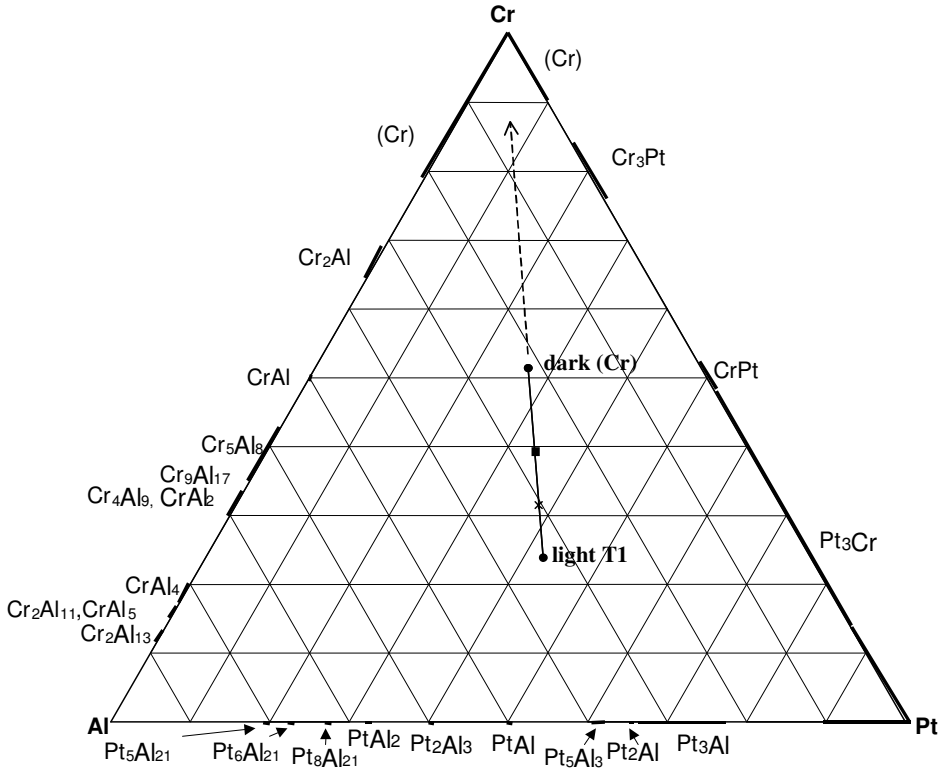

Figure 2.114. EDX analyses of nominal Pt_{34}:Al_{27}:Cr_{39} (at.%) in the as-cast condition. (■ overall composition; ● phases; ✶ two-phase; → direction of probable extrapolation)

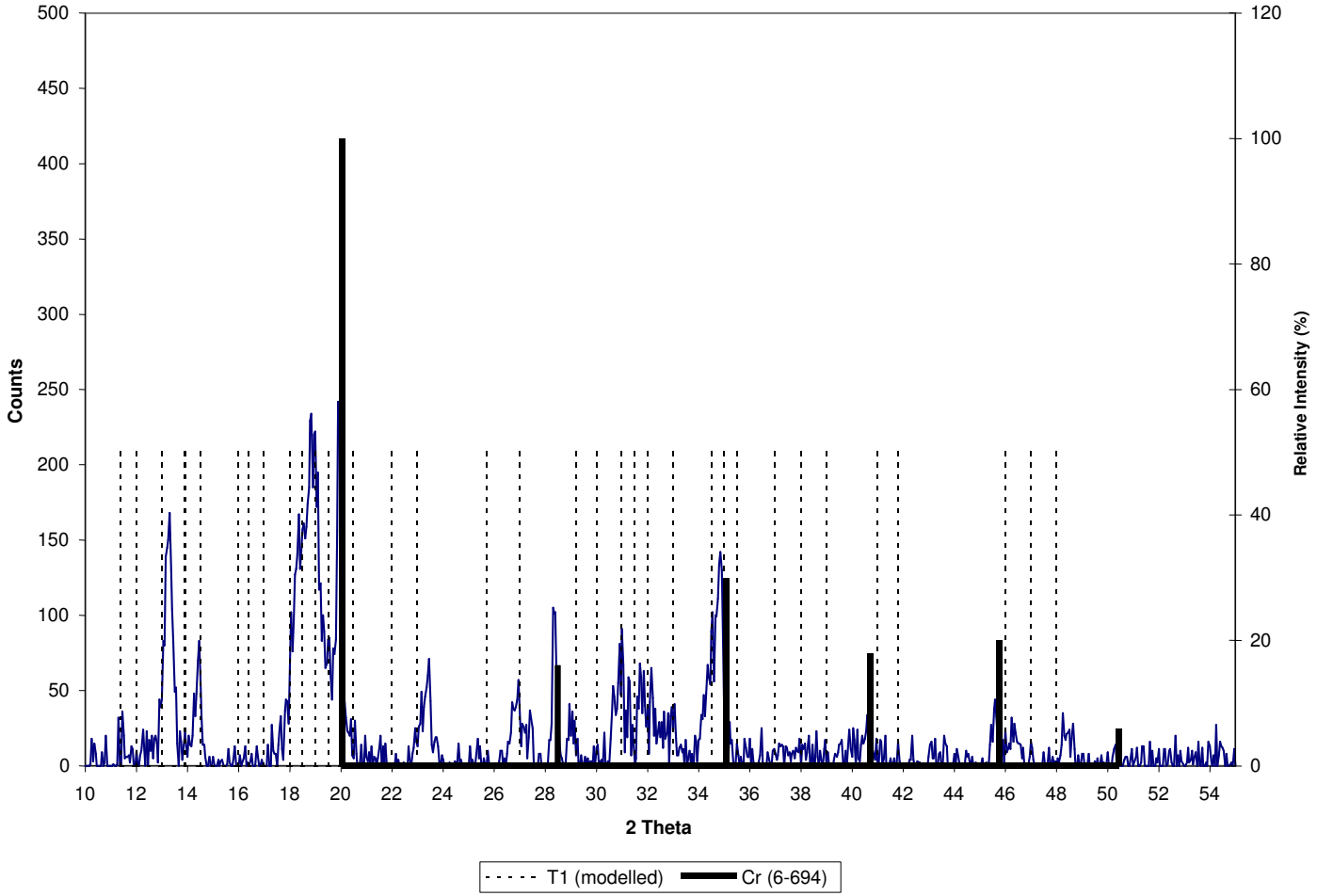

Figure 2.115. XRD pattern for nominal $Pt_{34}:Al_{27}:Cr_{39}$ in the as-cast condition.

2.1.36. Nominal $Pt_{37}:Al_{59}:Cr_4$

Alloy $Pt_{37}:Al_{59}:Cr_4$ was a badly cracked and porous sample (Figure 2.116). The EDX analysis (Table 2.36, Figure 2.117) suggested that it was probably single phase. From the results of alloys $Pt_{28}:Al_{70}:Cr_2$ (§2.1.20), $Pt_{35}:Al_{55}:Cr_{10}$ (§2.1.21) and $Pt_{43}:Al_{52}:Cr_5$ (§2.1.23), alloy $Pt_{37}:Al_{59}:Cr_4$ probably comprised ~Pt_2Al_3. Unfortunately no XRD could be done for confirmation because the surface was too irregular. This sample suggested that the ~Pt_2Al_3 solidified congruently:

$$L \rightarrow \sim Pt_2Al_3.$$

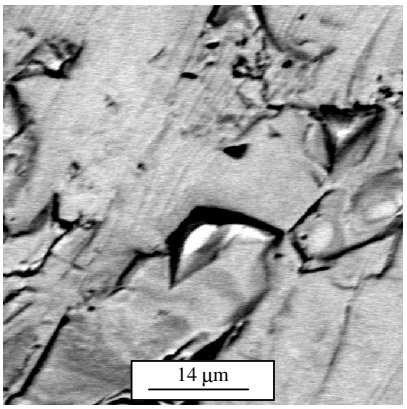

Figure 2.116. BSE-SEM image of nominal $Pt_{37}:Al_{59}:Cr_4$ in the as-cast condition: cored ~Pt_2Al_3.

Table 2.36. Phase analyses for nominal $Pt_{37}:Al_{59}:Cr_4$ (at.%) in the as-cast condition.

Phase description	**Pt**	**Al**	**Cr**	**Phase**
Overall	37.7 ± 0.8	58.1 ± 0.8	4.2 ± 0.4	-
Medium	38.9 ± 0.5	57.9 ± 0.2	3.2 ± 0.8	Cored ~Pt_2Al_3
Light	39.2 ± 0.5	58.1 ± 0.0	2.7 ± 0.5	Cored ~Pt_2Al_3

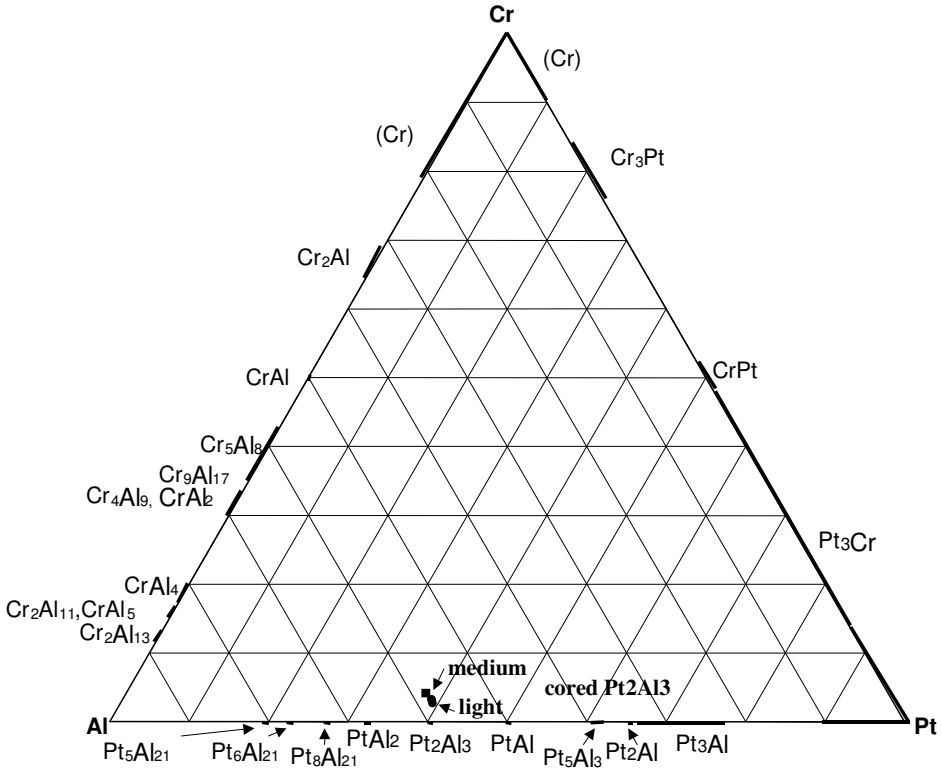

Figure 2.117. EDX analyses of nominal Pt_{37}:Al_{59}:Cr_4 (at.%) in the as-cast condition. (■ overall composition; ● phases)

2.1.37. Nominal $Pt_{45}:Al_{35}:Cr_{20}$

Alloy $Pt_{45}:Al_{35}:Cr_{20}$ seemed to comprise only one phase (Figure 2.118). By analysing areas, as well as doing random spot analyses, the EDX analyses confirmed that only one phase was present since the analyses were virtually identical (Table 2.37 and Figure 2.119). Since the XRD peaks of none of the possible phases from the binary diagrams matched the measured pattern well, the alloy probably comprised ternary phase T1. See §1.1.9 for a full discussion on ternary phase T1. Figure 2.120 shows the modelled peaks (averaged positions) of T1 superposed on the measured pattern. The measured pattern showed many peaks indicative of the ternary phase, and the match was reasonable. Once again T1 solidified congruently:

$$L \rightarrow T1.$$

This assessment was consistent with that of other results, especially alloy $Pt_{52}:Al_{43}:Cr_5$.

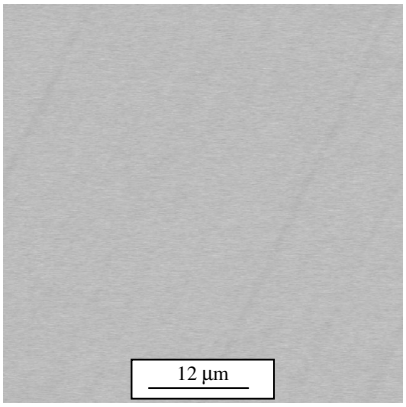

Figure 2.118. BSE-SEM image of nominal $Pt_{45}:Al_{35}:Cr_{20}$ in the as-cast condition: grey T1.

Table 2.37. Phase analyses for nominal $Pt_{45}:Al_{35}:Cr_{20}$ (at.%) in the as-cast condition.

Phase description	**Pt**	**Al**	**Cr**	**Phase**
Overall	47.9 ± 0.7	34.7 ± 0.2	17.4 ± 0.6	-
Grey*	47.8 ± 0.3	34.6 ± 0.3	17.6 ± 0.6	T1

* Random spot analyses.

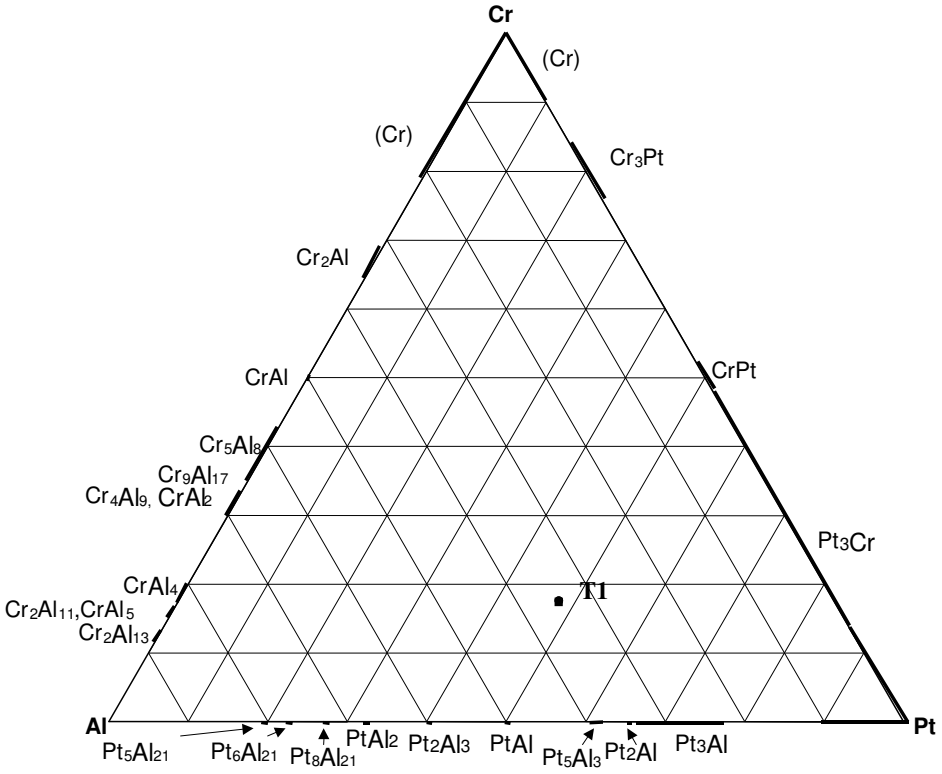

Figure 2.119. EDX analyses of nominal Pt_{45}:Al_{35}:Cr_{20} (at.%) in the as-cast condition. (■ overall composition; ● phases)

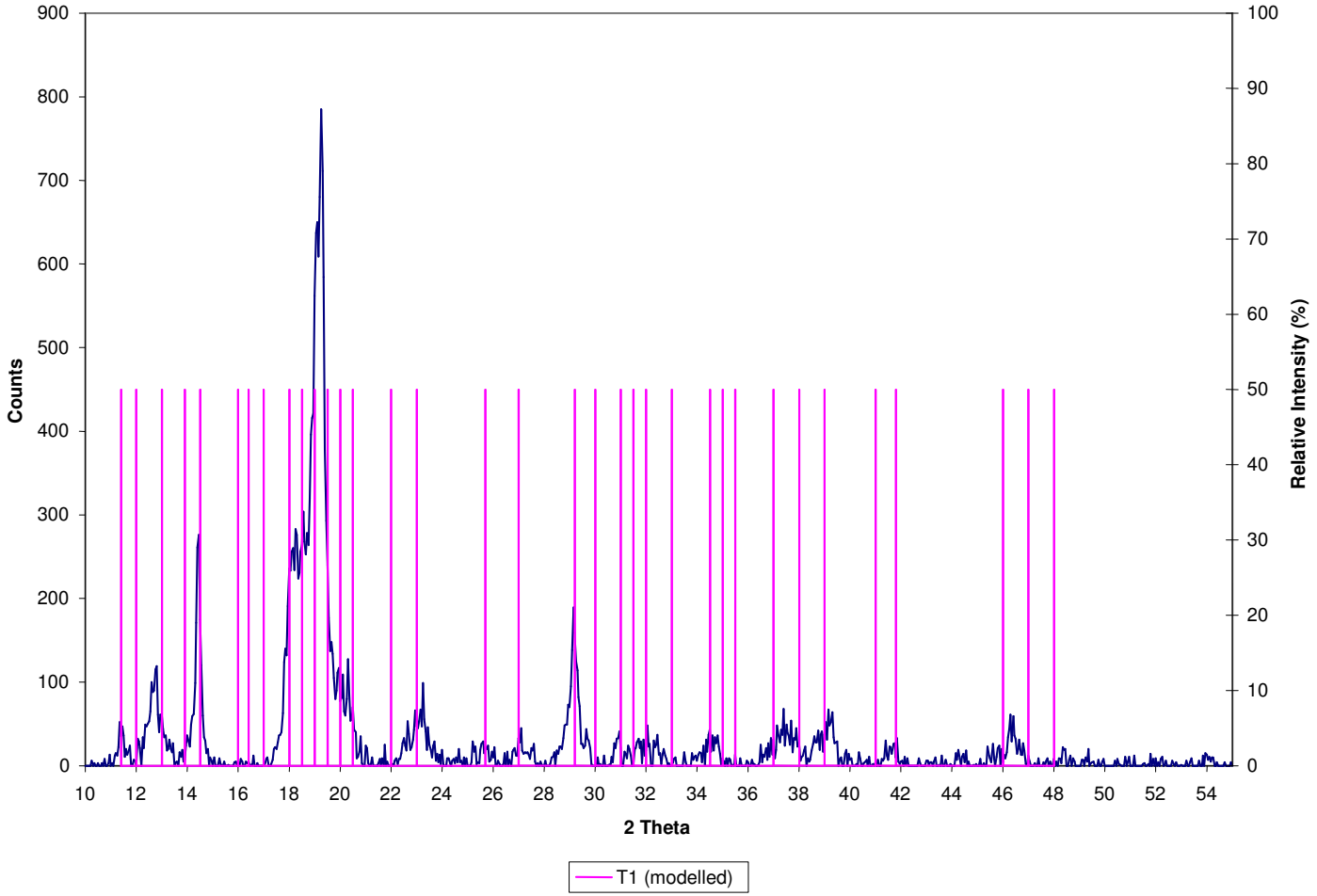

Figure 2.120. XRD pattern for nominal Pt_{45}:Al_{35}:Cr_{20} in the as-cast condition.

2.1.38. Nominal $Pt_{52}:Al_{43}:Cr_5$

Alloy $Pt_{52}:Al_{43}:Cr_5$ seemed to comprise only one phase (Figure 2.121). Some minor porosity was present. The EDX analyses confirmed this (Table 2. 38 and Figure 2.122). Taking into consideration other alloys' results (especially alloy $Pt_{45}:Al_{35}:Cr_{20}$ (§2.1.37)), the alloy probably comprised ternary phase T1. See §2.1.9 for a full discussion on T1. Figure 2.123 shows the modelled peaks (averaged positions) of T1 superposed on the measured pattern. The measured pattern showed a lot of peaks indicative of a ternary phase. The match was very good (even better than that of alloy $Pt_{45}:Al_{35}:Cr_{20}$). Like before, T1 solidified congruently:

$$L \rightarrow T1.$$

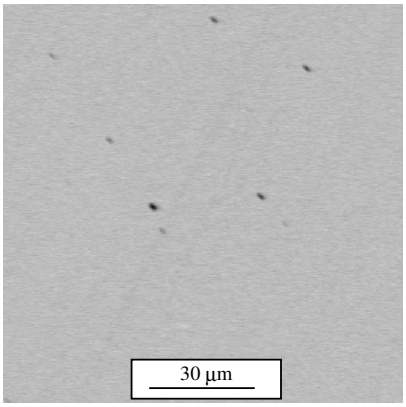

Figure 2.121. BSE-SEM image of nominal $Pt_{52}:Al_{43}:Cr_5$ in the as-cast condition: grey T1.

Table 2.38. Phase analyses for nominal $Pt_{52}:Al_{43}:Cr_5$ (at.%) in the as-cast condition.

Phase description	**Pt**	**Al**	**Cr**	**Phase**
Overall	53.3 ± 0.3	41.9 ± 0.2	4.8 ± 0.3	-
Grey	53.4 ± 0.5	41.4 ± 0.3	5.2 ± 0.3	T1

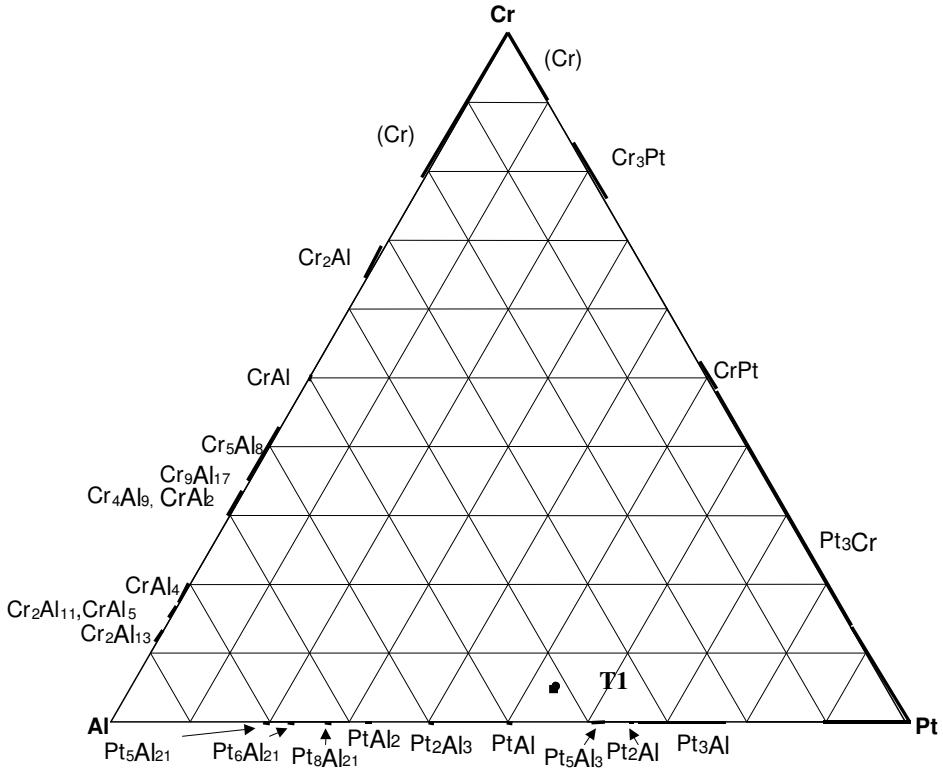

Figure 2.122. EDX analyses of nominal Pt_{52}:Al_{43}:Cr_5 (at.%) in the as-cast condition. (■ overall composition; ● phase)

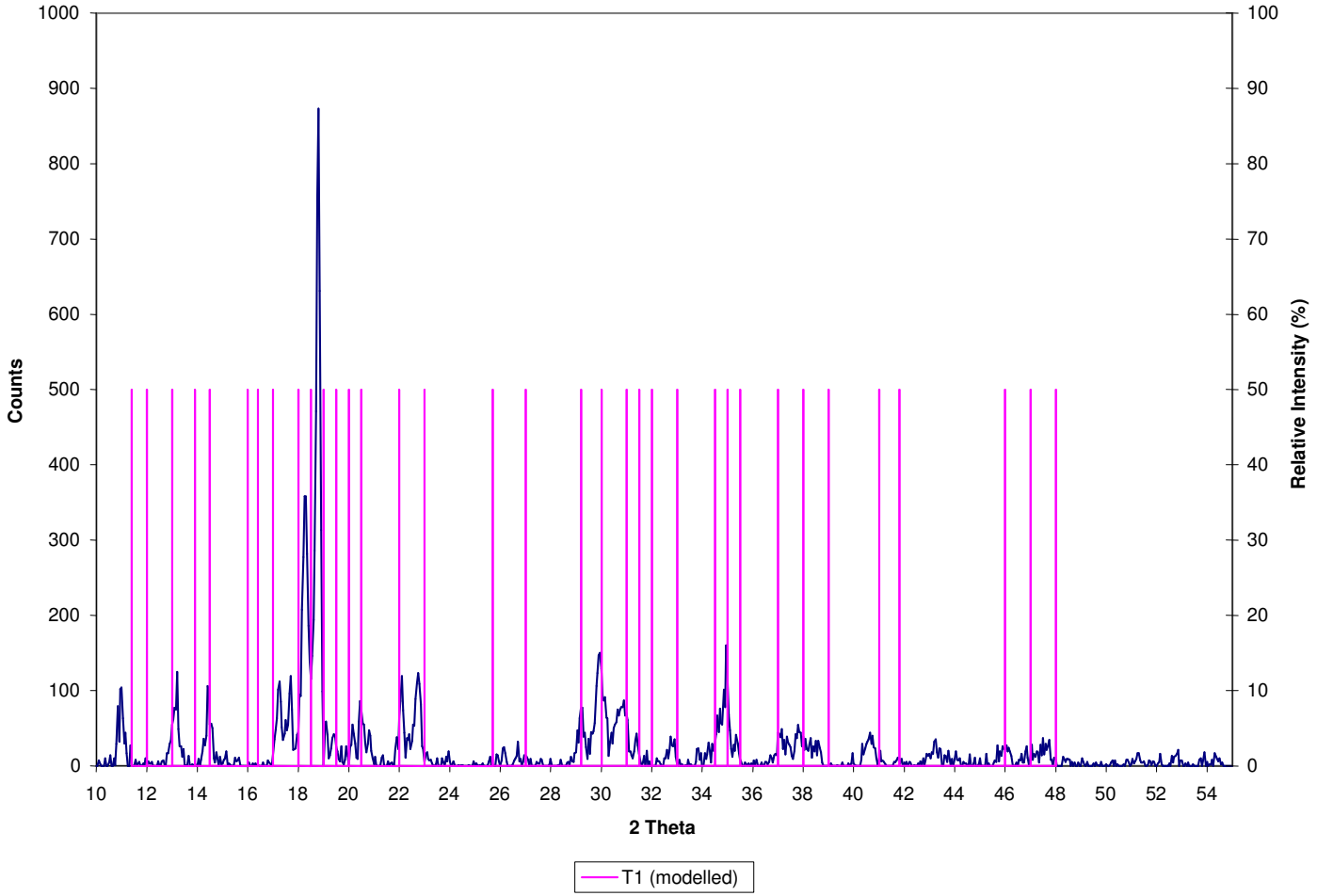

Figure 2.123. XRD pattern for nominal Pt_{52}:Al_{43}:Cr_5 in the as-cast condition.

2.1.39. Nominal $Pt_{55}:Al_{25}:Cr_{20}$

At high magnification, alloy $Pt_{55}:Al_{25}:Cr_{20}$ comprised a dark and a light phase (Figure 2.124) with black porosity. The EDX analyses are given in Table 2.39 and Figure 2.125. From the position of the phases on the ternary diagram, ~Pt_2Al and T1 were possibilities. XRD analysis confirmed the presence of C23 (space group *oP*12, low temperature) ~Pt_2Al, as well as T1 (Figure 2.126). This was in agreement with the results of alloys $Pt_{63}:Al_{32}:Cr_5$ (§2.1.27). The white phase was quite small, and its actual composition could possibly be extrapolated as indicated by the arrow in Figure 2.125, to coincide with the T1 composition of alloy $Pt_{63}:Al_{32}:Cr_5$. The direction of extrapolation appeared to be strange, but for the sake of self-consistency of the solidification projection (Figure 2.138), this seemed to be the best solution. The intensity of the peak at $2\theta \approx 14$ was high, probably due to a texture effect, which was likely to be the result of highly directional solid growth during of cooling on the copper hearth. The XRD peaks of ~Pt_3Al were also superposed on the measured pattern, but to no satisfaction. This structure formed by the following reactions:

$$L \rightarrow \sim Pt_3Al$$

$$L + \sim Pt_3Al \rightarrow T1$$

$$\sim Pt_3Al \rightarrow \sim Pt_2Al.$$

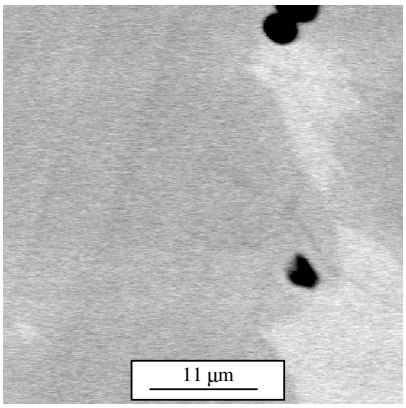

Figure 2.124. BSE-SEM image of nominal $Pt_{55}:Al_{25}:Cr_{20}$ in the as-cast condition: ~ Pt_2Al dark; T1 light.

Table 2.39. Phase analyses for nominal $Pt_{55}:Al_{25}:Cr_{20}$ (at.%) in the as-cast condition.

Phase description	**Pt**	**Al**	**Cr**	**Phase**
Overall	57.6 ± 0.2	24.6 ± 0.7	17.8 ± 0.7	-
Dark	56.1 ± 0.9	23.6 ± 1.4	20.3 ± 0.7	~Pt_2Al
Light	61.3 ± 0.5	29.8 ± 0.8	8.9 ± 0.7	T1

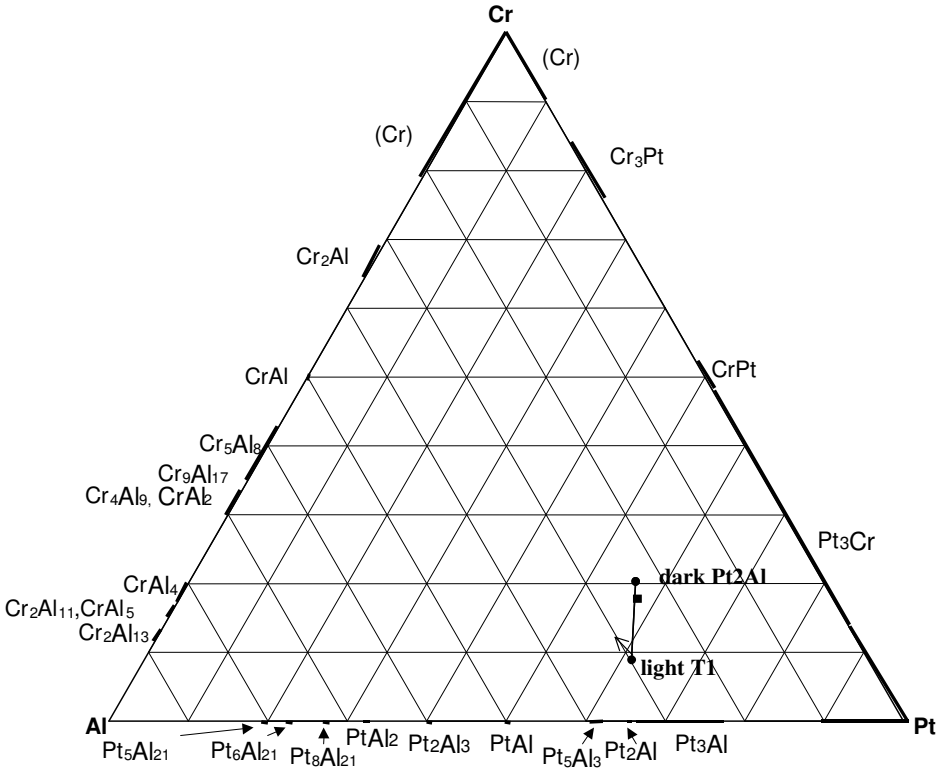

Figure 2.125. EDX analyses of nominal $Pt_{55}:Al_{25}:Cr_{20}$ (at.%) in the as-cast condition.

(■ overall composition; ● phases; → possible extrapolation)

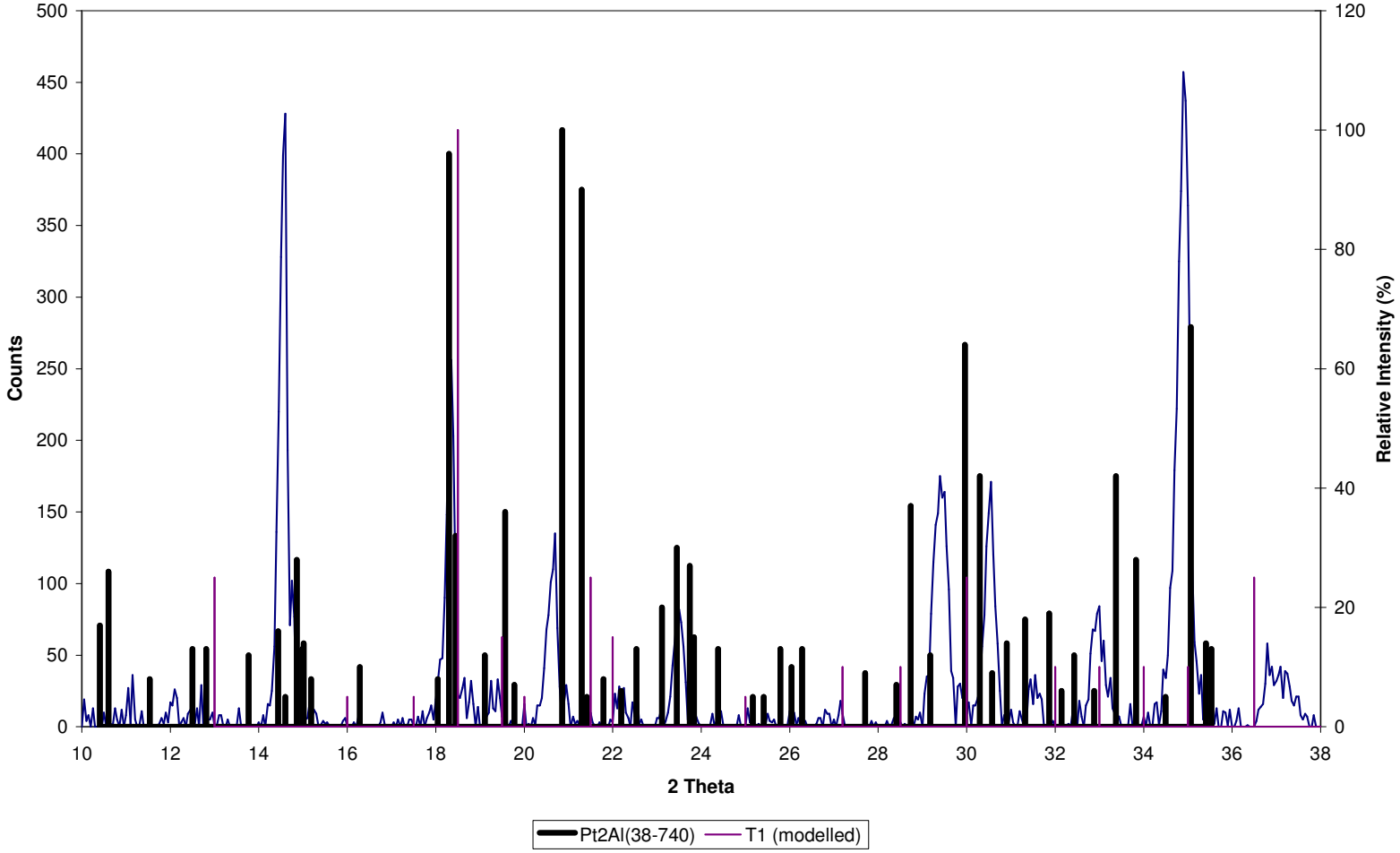

Figure 2.126. XRD pattern for nominal Pt_{55}:Al_{25}:Cr_{20} in the as-cast condition.

2.1.40. Nominal $Pt_{55}:Al_{20}:Cr_{25}$

At high magnification alloy $Pt_{55}:Al_{20}:Cr_{25}$ comprised a dark and a slightly light phase (Figure 2.127) with black porosity. The presence of two phases was confirmed by EDX analyses (given in Table 2.40 and Figure 2.128), which showed the clear difference in composition, contrary to the image which did not show it as clearly (Figure 2.127). The reason for the almost non-existent contrast between the two phases is due to the fact that their average atomic numbers are almost equal (~52.5). It was possible that the alloy was only single phase, but the position of the measurements on the ternary diagram suggested that alloys $Pt_{55}:Al_{20}:Cr_{25}$ (§2.1.40) and $Pt_{55}:Al_{25}:Cr_{20}$ (§2.1.39) could be similar. However, comparing their measured XRD patterns (peak positions) (Figure 2.129), shows that both were two-phase alloys with one phase common, but the other not, because the patterns did not totally match. XRD analysis confirmed the presence of C23 (space group *oP*12, low temperature) ~Pt_2Al (Figure 2.130), and the other phase (of darker contrast) was probably ~Pt_3Al. This structure formed by the following reactions:

$$L \rightarrow \sim Pt_3Al$$

$$\sim Pt_3Al \rightarrow \sim Pt_2Al.$$

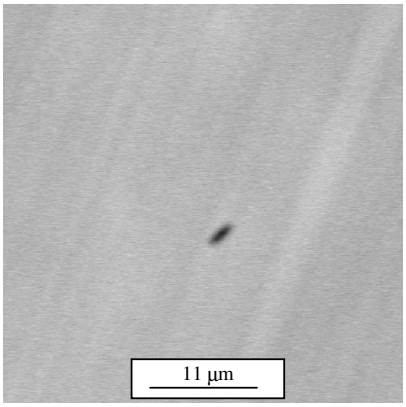

Figure 2.127. BSE-SEM image of nominal $Pt_{55}:Al_{20}:Cr_{25}$ in the as-cast condition: ~Pt_3Al dark; ~Pt_2Al; porosity black.

Table 2.40. Phase analyses for nominal $Pt_{55}:Al_{20}:Cr_{25}$ (at.%) in the as-cast condition.

Phase description	**Pt**	**Al**	**Cr**	**Phase**
Overall	56.6 ± 0.2	19.1 ± 0.7	24.3 ± 0.8	-
Dark	56.5 ± 1.1	17.3 ± 2.0	26.2 ± 3.0	~Pt_3Al
Light	58.3 ± 0.5	23.9 ± 1.2	17.8 ± 1.7	~Pt_2Al

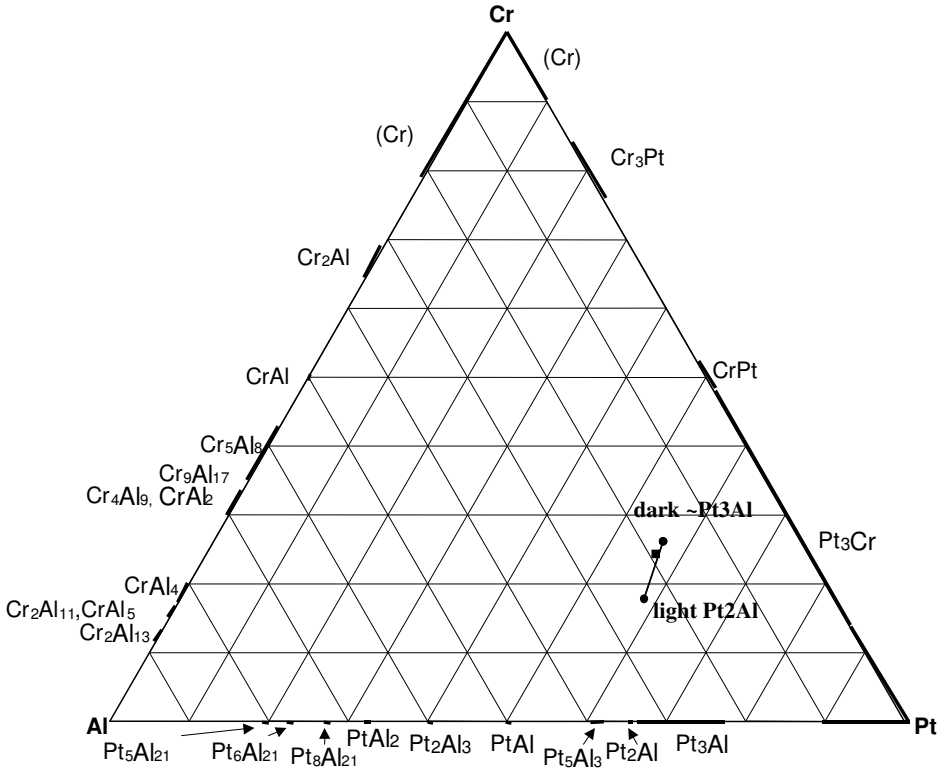

Figure 2.128. EDX analyses of nominal $Pt_{55}:Al_{20}:Cr_{25}$ (at.%) in the as-cast condition.

(■ overall composition; ● phases)

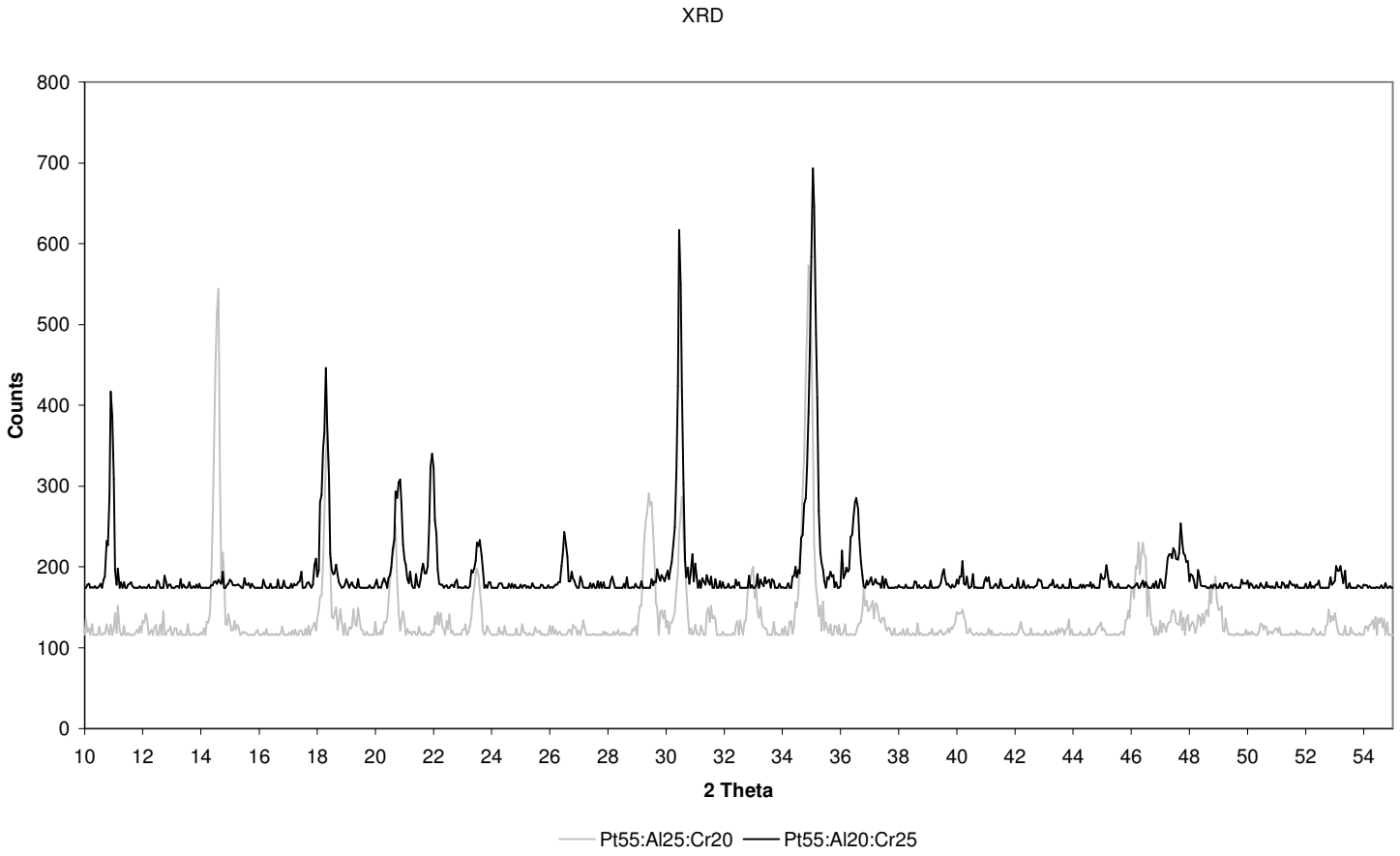

Figure 2.129. XRD patterns for nominal Pt_{55}:Al_{20}:Cr_{25} and Pt_{55}:Al_{25}:Cr_{20} in the as-cast condition.

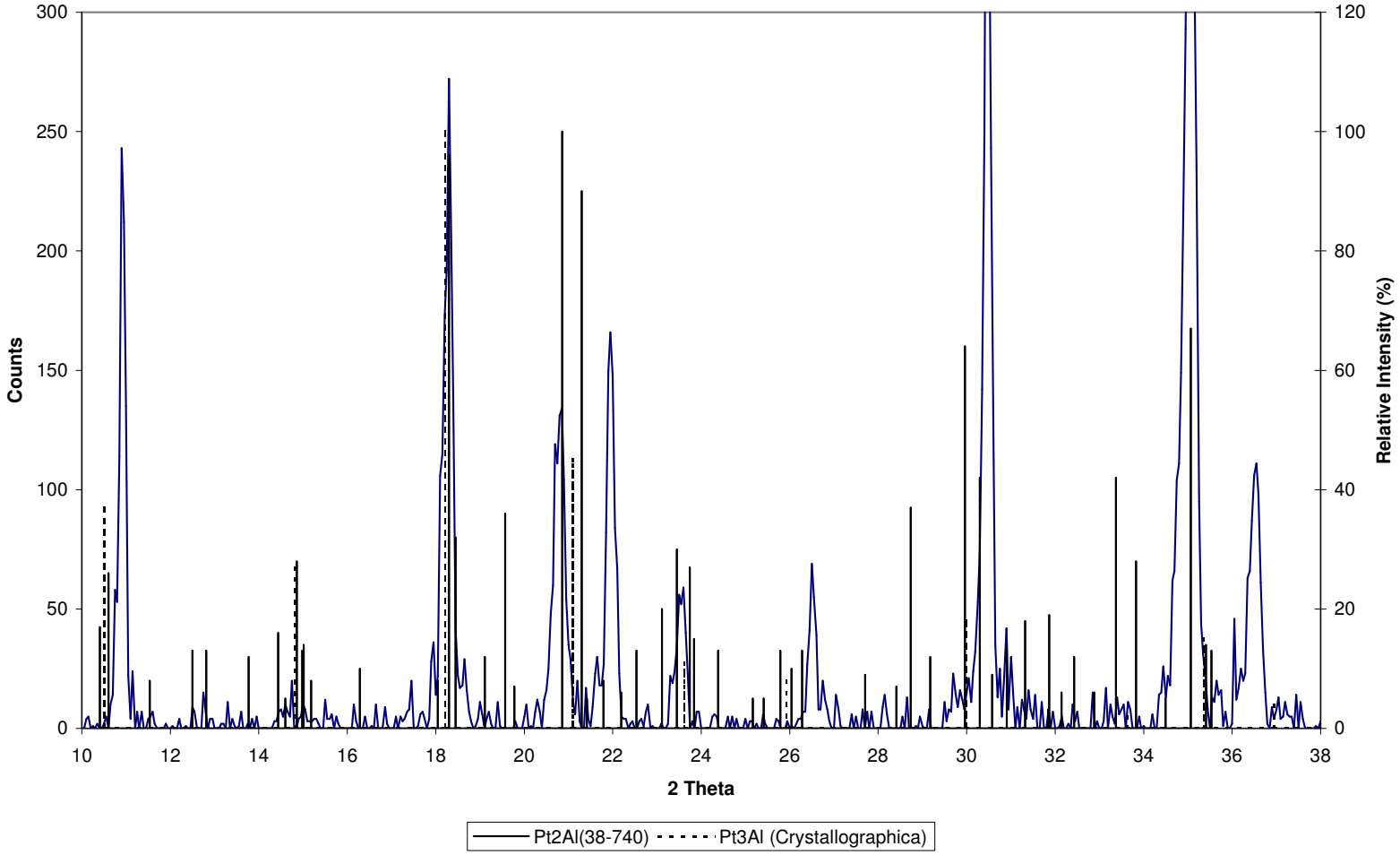

Figure 2.130. XRD patterns for nominal Pt_{55}:Al_{20}:Cr_{25} in the as-cast condition.

2.1.41. Nominal $Pt_{64}:Al_{16}:Cr_{20}$

Alloy $Pt_{64}:Al_{16}:Cr_{20}$ appeared cored single phase, but could also be two phases (Figure 2.131), especially considering the fact that the difference in composition of the differently contrasted regions was significant (see EDX analyses, Table 2. 41 and Figure 2.132). The overall composition of the alloy was not on the tie-line, probably because the phase analyses were not totally accurate due to the phases' small sizes. Taking into account the positions of the phases on the ternary plot (Figure 2.132), and the results of alloys $Pt_{65}:Al_5:Cr_{30}$ (§2.1.12) and $Pt_{78}:Al_{17}:Cr_5$ (§2.1.29), one could expect that the darker phase was ~Pt_3Cr and the lighter phase $L1_2$ ~Pt_3Al. These phases were confirmed by XRD (Figure 2.133). The image was unsatisfactory and no more detail could be resolved to clarify the solidification sequence, but by consulting the binary Pt-Al and Pt-Cr binary phase diagrams, the structure probably formed by:

$$L \rightarrow (Pt)$$

$$L \rightarrow \sim Pt_3Al + (Pt)$$

$$(Pt) \rightarrow \sim Pt_3Cr \text{ (ordering)}.$$

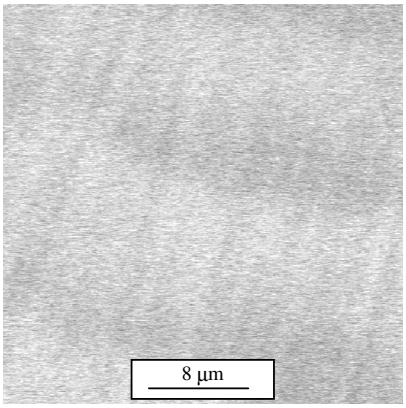

Figure 2.131. BSE-SEM image of nominal $Pt_{64}:Al_{16}:Cr_{20}$ in the as-cast condition: ~Pt_3Cr dark;~Pt_3Al light.

Table 2.41. Phase analyses for nominal $Pt_{64}:Al_{16}:Cr_{20}$ (at.%) in the as-cast condition.

Phase description	**Pt**	**Al**	**Cr**	**Phase**
Overall	64.5 ± 0.6	15.2 ± 0.7	20.3 ± 0.9	-
Dark	65.1 ± 0.7	8.2 ± 0.6	26.7 ± 0.3	~Pt_3Cr
Light	66.1 ± 0.7	15.2 ± 1.7	18.7 ± 1.8	~Pt_3Al

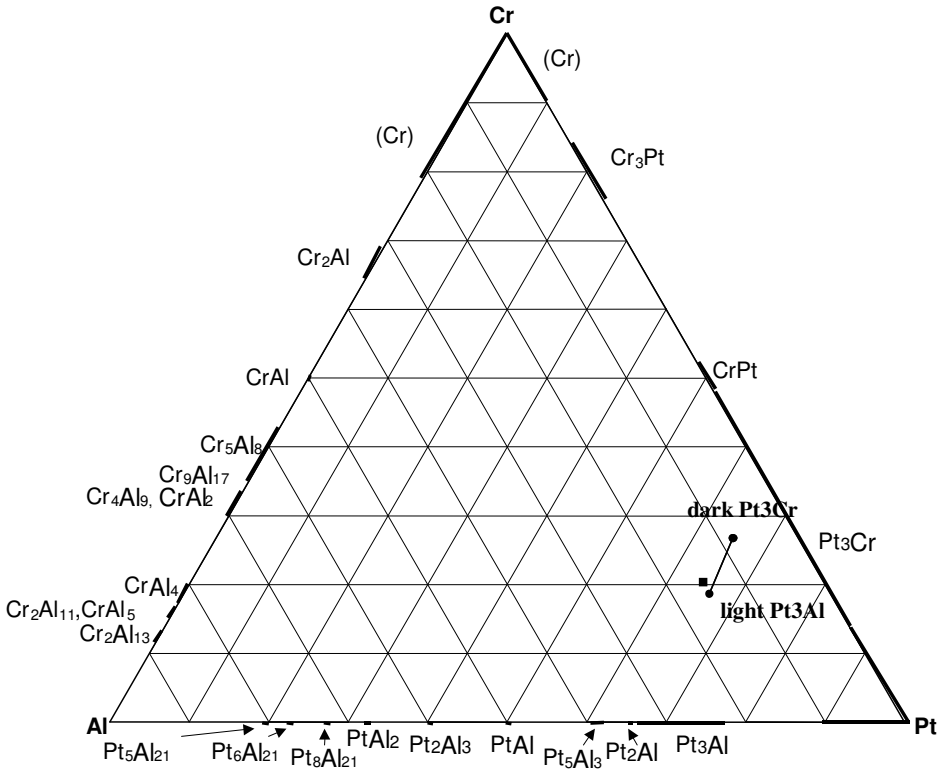

Figure 2.132. EDX analyses of nominal $Pt_{64}:Al_{16}:Cr_{20}$ (at.%) in the as-cast condition. (■ overall composition; ● phases)

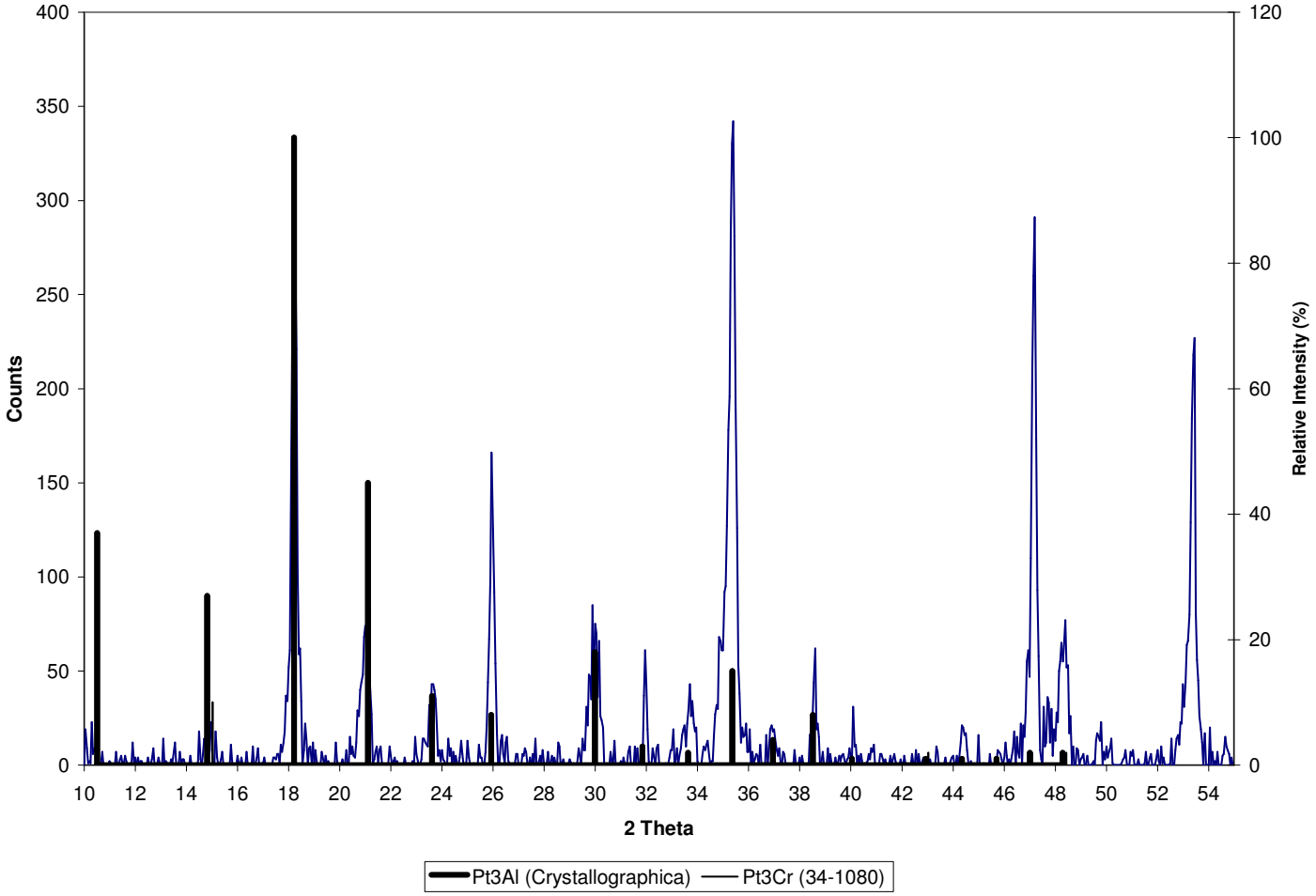

Figure 2.133. XRD patterns for nominal Pt_{64}:Al_{16}:Cr_{20} in the as-cast condition.

2.1.42. Nominal $Pt_8:Al_{89}:Cr_3$

Alloy $Pt_8:Al_{89}:Cr_3$ had a very complicated structure, similar to alloy $Pt_{10}:Al_{80}:Cr_{10}$ (§2.1.4), comprising three phases: black, medium and light, with what appeared to be a very sparse eutectic in the black phase (Figure 2.2.134). The EDX analyses of the alloy and all its phases are given in Table 2.42 and shown graphically in Figure 2.135. From Figure 2.135, the black phase was obviously (Al). The light phase was most probably either ~Pt_8Al_{21} or ~Pt_6Al_{21} (a metastable compound [1986McA] in the JCPDS database but not shown in the Pt-Al binary phase diagram), and therefore probably the former. The medium phase was more difficult to identify, the range of possible phases being quite large: ~$CrAl_4$, ~$CrAl_5$ (a JCPDS compound reported in the binary diagram as ~Cr_2Al_{11}), or ~Cr_2Al_{13} (another JCPDS compound reported in the published binary diagram as ~$CrAl_7$). Taking into consideration the results of alloys $Pt_{10}:Al_{80}:Cr_{10}$ (§2.1.4), $Pt_3:Al_{79}:Cr_{18}$ (§2.1.31) and $Pt_4:Al_{83}:Cr_{13}$ (§2.1.43), it looked highly plausible that the medium phase could be either ~Cr_2Al_{13} or ~$CrAl_5$. It should also be noted that, at close inspection, there was a suggestion of a very light phase (indicated by the arrows in Figure 2.134), which was probably ~$PtAl_2$ (similar to alloy $Pt_{10}:Al_{80}:Cr_{10}$ (§2.1.4)). This sample was very brittle and although enough material was available for SEM examination, XRD could not be performed. Because of the similarity in XRD patterns for many of these phases, XRD results would not have been that helpful.

Taking into account the morphology of the microstructure and the melting points of the phases and keeping in mind the positions of the phases relative to each other, the phases probably formed by:

$$L \rightarrow \sim PtAl_2$$

followed by a series of peritectic reactions:

$$L + \sim PtAl_2 \rightarrow \sim Cr_2Al_{13}$$

(in which ~$PtAl_2$ was almost totally consumed)

$$L + \sim Cr_2Al_{13} \rightarrow (Al),$$

and finally the eutectic reaction

$$L \rightarrow (Al) + Pt_8Al_{21}.$$

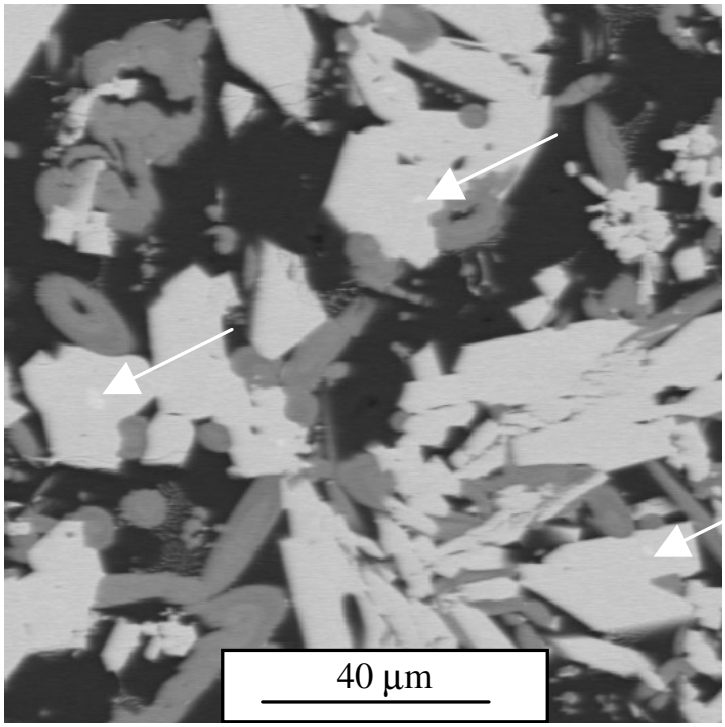

Figure 2.134. BSE-SEM image of nominal $Pt_8:Al_{89}:Cr_3$ in the as-cast condition: (Al) black; ~Cr_2Al_{13} medium; ~Pt_8Al_{21} light; ~$PtAl_2$ very light (arrows).

Table 2.42. Phase analyses for nominal $Pt_8:Al_{89}:Cr_3$ (at.%) in the as-cast condition.

Phase description	**Pt**	**Al**	**Cr**	**Phase**
Overall	8.3 ± 1.7	88.7 ± 2.2	3.0 ± 0.5	-
Black	0.1 ± 0.1	99.5 ± 0.1	0.4 ± 0.1	(Al)
Medium	6.3 ± 0.5	79.5 ± 0.2	14.2 ± 0.4	~Cr_2Al_{13}
Light	21.0 ± 0.1	76.5 ± 0.3	2.5 ± 0.4	~Pt_8Al_{21}
Very light*				~$PtAl_2$

* Not analysed due to small size.

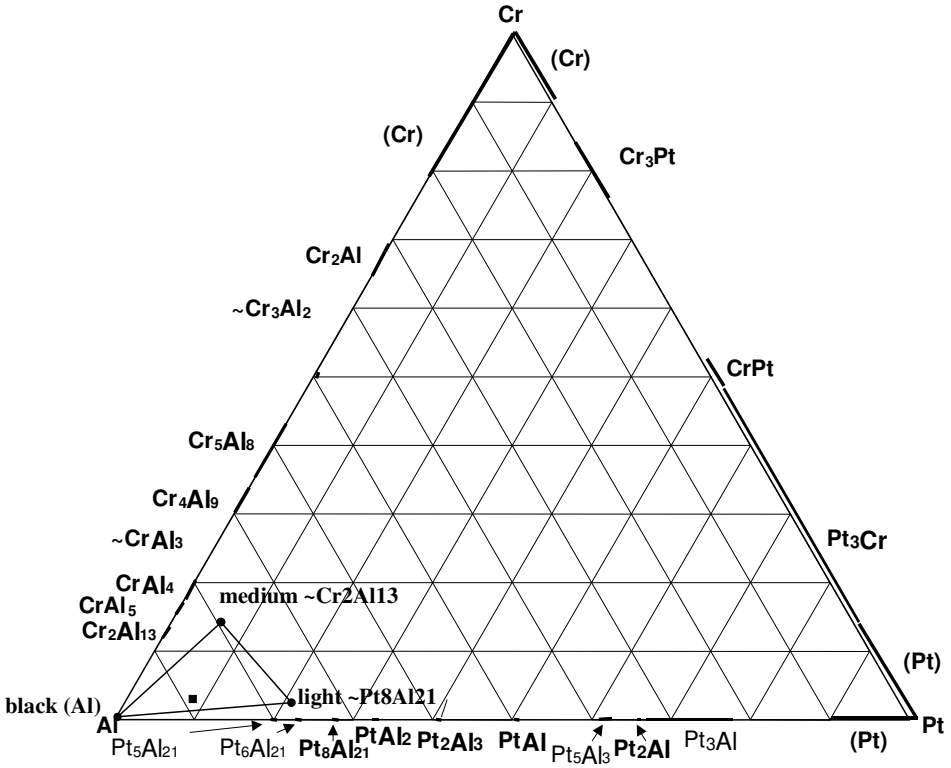

Figure 2.135. EDX analyses of nominal Pt_8:Al_{89}:Cr_3 (at.%) in the as-cast condition. (■ overall composition; ● phases)

2.1.43. Nominal $Pt_4:Al_{83}:Cr_{13}$

Alloy $Pt_4:Al_{83}:Cr_{13}$ had a very complicated structure, comprising five phases: black, very dark, dark, light and white (Figure 2.136). The EDX analyses of the alloy and all its phases are given in Table 2.43 and shown graphically in Figure 2.137. From Figure 2.136, the black phase was obviously (Al). The white phase was most probably either ~Pt_8Al_{21} or ~Pt_6Al_{21} (a metastable compound [1986Mca] in the JCPDS database but not shown in the Pt-Al binary phase diagram), and therefore probably the former. The very dark, dark and light phases were more difficult to identify, the range of possible phases being quite large: ~$CrAl_4$, ~$CrAl_5$ (a JCPDS compound reported in the binary diagram as ~Cr_2Al_{11}), or ~Cr_2Al_{13} (another JCPDS compound reported in the published binary diagram as ~$CrAl_7$). From the positions of the phase compositions on the ternary diagram, and taking into consideration the results of alloys $Pt_{10}:Al_{80}:Cr_{10}$ (§2.1.4), $Pt_3:Al_{79}:Cr_{18}$ (§2.1.31) and $Pt_8:Al_{89}:Cr_3$ (§2.1.42), it seemed like the very dark phase was ~$CrAl_4$, the dark phase ~$CrAl_5$ and the light phase ~Cr_2Al_{13}. There also appeared to be a eutectic in the micrograph. This sample was also very brittle and although enough material was available for SEM examination, XRD could not be performed. Because of the similarity in XRD patterns for many of these phases, XRD results would not have been helpful to distinguish between the different phases.

The dendrites, ~$CrAl_4$, formed first

$$L \rightarrow \sim CrAl_4$$

followed by peritectic reactions

$$L + \sim CrAl_4 \rightarrow \sim CrAl_5$$

$$L + \sim CrAl_5 \rightarrow \sim Cr_2Al_{13}$$

$$L + \sim Cr_2Al_{13} \rightarrow (Al)$$

and finally the eutectic reaction

$$L \rightarrow (Al) + Pt_8Al_{21}.$$

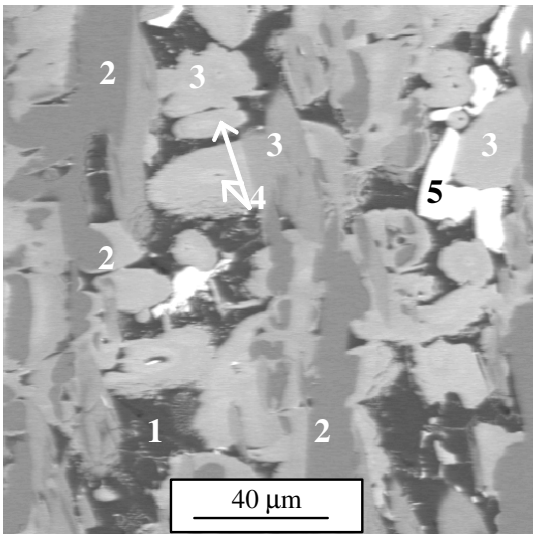

Figure 2.136. BSE-SEM image of nominal $Pt_4:Al_{83}:Cr_{13}$ in the as-cast condition: (Al) black (1); ~$CrAl_4$ very dark (2); ~$CrAl_5$ dark (3); ~Cr_2Al_{13} light (4); ~Pt_8Al_{21} white (5).

Table 2.43. Phase analyses for nominal $Pt_8:Al_{89}:Cr_3$ (at.%) in the as-cast condition.

Phase description	**Pt**	**Al**	**Cr**	**Phase**
Overall	3.6 ± 0.4	82.7 ± 0.6	13.7 ± 0.9	-
Black	0.2 ± 0.1	98.9 ± 0.5	0.9 ± 0.4	(Al)
Very dark	1.4 ± 0.2	77.4 ± 0.5	21.2 ± 0.6	~$CrAl_4$
Dark	3.5 ± 0.1	78.9 ± 0.1	17.6 ± 0.2	~$CrAl_5$
Light	6.1 ± 0.5	78.8 ± 0.3	15.1 ± 0.7	~Cr_2Al_{13}
White	20.1 ± 1.2	78.5 ± 2.2	1.4 ± 1.0	~Pt_8Al_{21}

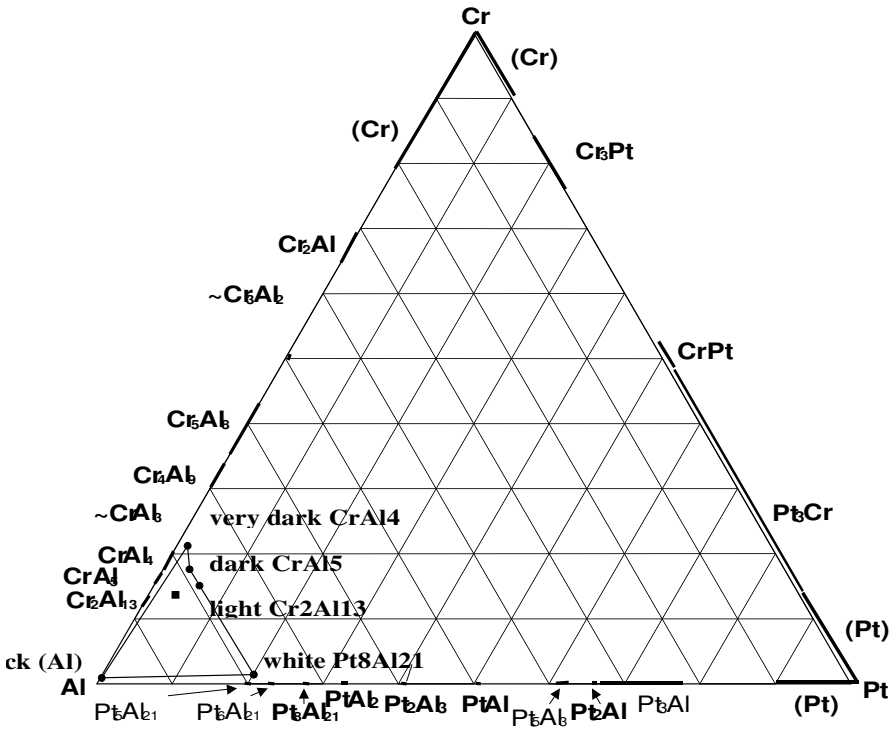

Figure 2.137. EDX analyses of nominal Pt_4:Al_{83}:Cr_{13} (at.%) in the as-cast condition. (■ overall composition; ● phases)

2.1.44. Solidification projection

Figure 2.134 shows the solidification projection for the Pt-Cr-Al system, based on the preferred interpretation of data, with reasons as discussed earlier. The data were self-consistent and the information gleaned from 43 samples seemed to be enough to complete the diagram. Note that some of the tie-lines cross, and that it is allowed because this is not an equilibrium diagram but merely a reflection of the most likely phase to form during solidification, and it is likely with so many peritectic reactions that samples solidified at different temperatures.

Three ternary phases were found:

- T1: ~Pt_3Al_2Cr with ~59-41 at.% Pt, 27-42 at.% Al; 5-30 at.% Cr; A true ternary phase for which none of the XRD patterns of the phases in the three binary phases was a good match to its measured pattern.
- T2: ≈Cr_3Al_2 with ~3-4 at.% Pt in solution; A phase with crystal structure similar to that of ~Cr_3Al_2 (a compound listed by the JCPDS database).

- T3: ≈$CrAl_3$ with 0.5 at.% Pt in solution; A phase with crystal structure similar to that of ~$CrAl_3$ (a compound listed in Pearson's Handbook [1985Vil] and modelled accordingly with *Crystallographica*).

The extensions of the binary phases were determined to be:

- (Cr): ~ 20 at.% Al max., ~11 at.% Pt max.;
- ~Cr_3Pt: ~ 1 at.% Al;
- ~CrPt [$L1_0$]: ~ 9 at.% Al;
- ~Pt_3Cr: ~ 9 at.% Al;
- (Pt): ~10 at.% Al max., ~ 12 at.% Cr max.;
- ~Pt_3Al [$L1_2$]: ~35 at.% Cr;
- ~Pt_2Al [HT & LT]: ~35 at.% Cr;
- ~PtAl [B20]: ~ 19 at.% Cr;
- ~Pt_2Al_3: ~6 at.% Cr (estimated by extrapolation);
- ~$PtAl_2$: ~17 at.% Cr;
- ~Pt_8Al_{21}: ~ 5 at.% Cr;
- (Al): <1 at.% Cr and Pt;
- ~$CrAl_5$: ~ 6 at.% Pt;
- ~$CrAl_4$: ~ 4 at.% Pt;
- ~Cr_4Al_9: ~ 1 at.% Pt;
- ~Cr_5Al_8: ~ 1 at.% Pt;
- ~Cr_2Al: ~ 1 at.% Pt;

The extension of the Pt-Al intermetallic compounds (~$PtAl_2$, ~PtAl and especially ~Pt_2Al and ~Pt_3Al) were surprisingly significant, compared to those of the Cr-Al system, and is probably due to the relative atomic sizes and substitution sites.

The ~CrPt/~Pt_3Cr and ~Pt_3Cr/(Pt) boundaries are shown as a dashed lines. Around the former boundary it will be difficult to predict whether the solidified (Pt) will order to form ~Pt_3Cr or not, and around the latter it will be difficult to say and whether the ~Pt_3Cr will order to form $L1_0$ ~CrPt at lower temperatures (below ~700°C) or not. This was different to the Pt-Cr-Ru

system where the ordered $L1_2$ ~Pt_3Cr was not observed at all [2004Süs1, 2006Süs1]. This is based on the still generally accepted diagram given by Massalski [1990Mas]. If the diagram of Zhao et al. is correct, the dashed lines in Figure 2.138 would not denote actual phase boundaries, but the estimated positions of the ~CrPt/~Pt_3Cr and ~Pt_3Cr/(Pt) two-phase regions shown in Figure 1.2.

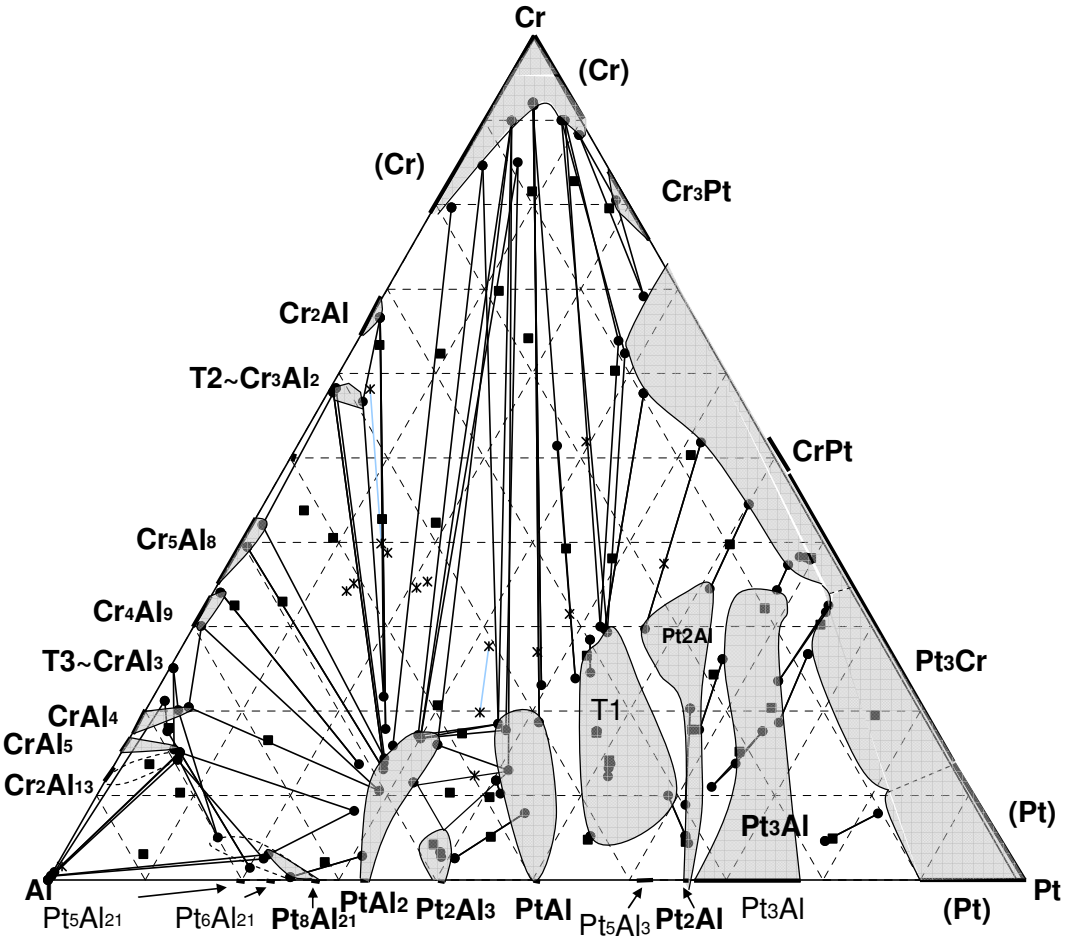

Figure 2.138. Solidification projection diagram for Pt-Cr-Al.

2.1.45 Liquidus projection

Figure 2.139 shows all the alloy compositions numbered from Alloy 1 to 43 and each alloy's corresponding solidification sequence is given in Table 2.44.

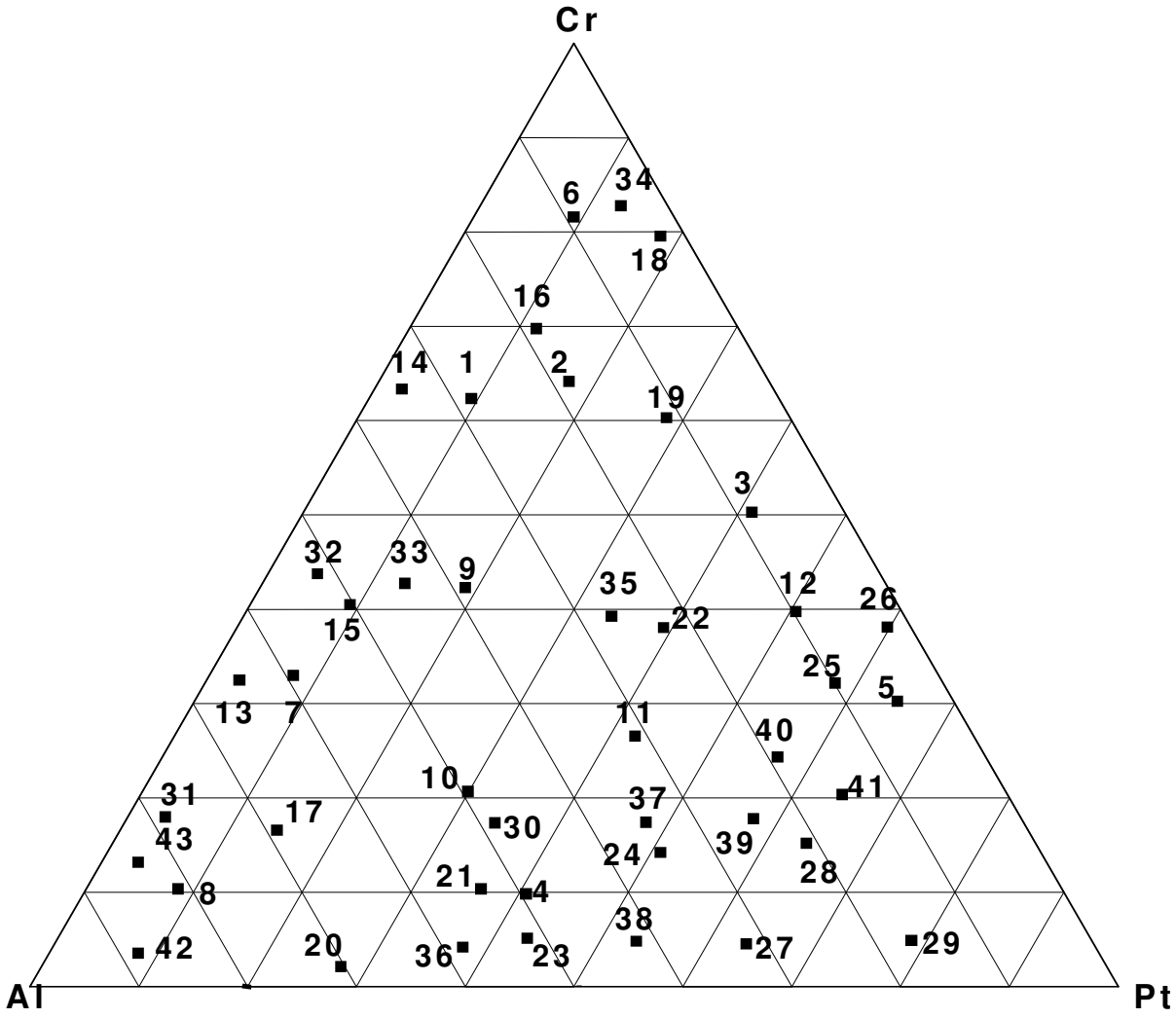

Figure 2.139. Alloy Numbers of samples characterised in the Pt-Al-Cr system.

Table 2.44. Solidification reactions in the Pt-Al-Cr system.

Alloy no.	**Nominal Composition**	**Solidification reactions**
1	Pt_{10}:Al_{30}:Cr_{60}	L → (Cr) L → (Cr) + ~$PtAl_2$
2	Pt_{20}:Al_{20}:Cr_{60}	L → (Cr) L → (Cr) + ~PtAl.
3	Pt_{40}:Al_{10}:Cr_{50}	L → (Pt) L → (Pt) + ~Pt_3Al ~Pt_3Al→~Pt_2Al (Pt) → ~$CrPt_3$ → ~CrPt (ordering)
4	Pt_{40}:Al_{50}:Cr_{10}	L → ~PtAl L → ~PtAl + ~Pt_2Al_3
5	Pt_{65}:Al_5:Cr_{30}	L → (Pt) L → (Pt) + ~Pt_3Al (Pt) → ~Pt_3Cr (ordering)
6	Pt_{10}:Al_{10}:Cr_{80}	L → (Cr) L → (Cr) + ~PtAl
7	Pt_{10}:Al_{60}:Cr_{30}	L → ~$PtAl_2$ L → ~$PtAl_2$ + ~Cr_5Al_8
8	Pt_{10}:Al_{80}:Cr_{10}	L → ~$PtAl_2$ L + ~$PtAl_2$ → ~Pt_8Al_{21} L + ~Pt_8Al_{21} → ~$CrAl_5$ L + ~$CrAl_5$ → (Al)
9	Pt_{20}:Al_{40}:Cr_{40}	L → (Cr) L + (Cr) → ~$PtAl_2$ L → ~PtAl + (Cr) + ~$PtAl_2$
10	Pt_{30}:Al_{50}:Cr_{20}	L → ~$PtAl_2$ L → ~$PtAl_2$ + ~PtAl L → (Cr) + ~PtAl + ~$PtAl_2$.
11	Pt_{40}:Al_{30}:Cr_{30}	L → T1
12	Pt_{50}:Al_{10}:Cr_{40}	L → (Pt) L → (Pt) + ~Pt_3Al ~Pt_3Al → ~Pt_2Al (Pt) → ~$CrPt_3$ → ~CrPt (ordering)
13	Pt_3:Al_{65}:Cr_{32}	L → ~Cr_4Al_9 L → ~Cr_4Al_9 + ~$PtAl_2$
14	Pt_3:Al_{35}:Cr_{62}	L → (Cr) L → (Cr) + ~$PtAl_2$ (Cr) → ~Cr_2Al (ordering) ~Cr_2Al → T4 (solid state precipitation)
15	Pt_{10}:Al_{50}:Cr_{40}	L → (Cr) L → (Cr) + ~$PtAl_2$ (Cr) → T2

Table 3.1. Solidification reactions in the Pt-Al-Cr system (cont.)

16	Pt_{12}:Al_{18}:Cr_{70}	L → (Cr) L + (Cr) → ~PtAl L + (Cr) → ~PtAl + ~$PtAl_2$
17	Pt_{17}:Al_{68}:Cr_{15}	L → ~$PtAl_2$ L + ~$PtAl_2$ → ~Cr_4Al_9 L + ~Cr_4Al_9 → ~$CrAl_4$
18	Pt_{18}:Al_2:Cr_{80}	L → (Cr) L + (Cr) → ~Cr_3Pt L + ~Cr_3Pt → (Pt) (Pt) → ~Pt_3Cr → ~CrPt (ordering)
19	Pt_{28}:Al_{12}:Cr_{60}	L → (Pt) L → (Pt) + (Cr) + T1 (Pt) → ~Pt_3Cr → ~CrPt
20	Pt_{28}:Al_{70}:Cr_2	L → ~$PtAl_2$ L + ~$PtAl_2$ → ~Pt_8Al_{21}
21	Pt_{35}:Al_{55}:Cr_{10}	L → ~$PtAl_2$ L → ~$PtAl_2$ + ~PtAl
22	Pt_{38}:Al_{22}:Cr_{40}	L → T1 L → T1 + (Pt) (Pt) → ~$CrPt_3$ → ~CrPt (ordering)
23	Pt_{43}:Al_{52}:Cr_5	L → ~Pt_2Al_3 L → ~PtAl + ~Pt_2Al_3
24	Pt_{50}:Al_{35}:Cr_{15}	L → T1
25	Pt_{58}:Al_{10}:Cr_{32}	L → (Pt) L → (Pt) + ~Pt_3Al ~Pt_3Al → ~Pt_2Al (Pt) → ~Pt_3Cr → ~CrPt (ordering)
26	Pt_{60}:Al_2:Cr_{38}	L → (Pt) (Pt) → ~Pt_3Cr → ~CrPt (ordering)
27	Pt_{63}:Al_{32}:Cr_5	L → ~Pt_3Al L + ~ Pt_3Al → T1 ~Pt_3Al → ~Pt_2Al
28	Pt_{63}:Al_{22}:Cr_{15}	L → ~Pt_3Al
29	Pt_{78}:Al_{17}:Cr_5	L → (Pt) L → (Pt) + ~Pt_3Al
30	Pt_{75}:Al_{10}:Cr_{15}	L → ~$PtAl_2$ L → (Cr) + ~PtAl + ~$PtAl_2$
31	Pt_3:Al_{79}:Cr_{18}	L → T3 L + T3 → ~$CrAl_4$ L + $CrAl_4$ → ~$CrAl_5$ L + ~$CrAl_5$ → ~Pt_8Al_{21}
32	Pt_5:Al_{52}:Cr_{43}	L → (Cr), L + (Cr) → ~Cr_5Al_8 L → ~$PtAl_2$ + (Cr) Cr) → T2≈Cr_3Al_2

Table 3.1. Solidification reactions in the Pt-Al-Cr system (cont.)

33	Pt_{13}:Al_{45}:Cr_{42}	L → (Cr) L → (Cr) + ~$PtAl_2$ (Cr) → ~Cr_2Al (ordering)
34	Pt_{15}:Al_5:Cr_{80}	L → (Cr) L → (Pt) + (Cr) + T1 (Pt) → ~Pt_3Cr → ~CrPt (ordering)
35	Pt_{34}:Al_{27}:Cr_{39}	L → T1 L → (Cr) + T1
36	Pt_{37}:Al_{59}:Cr_4	L → ~Pt_2Al_3
37	Pt_{45}:Al_{35}:Cr_{20}	L → T1
38	Pt_{52}:Al_{43}:Cr_5	L → T1
39	Pt_{55}:Al_{25}:Cr_{20}	L → ~Pt_3Al L + ~ Pt_3Al → T1 ~Pt_3Al → ~Pt_2Al
40	Pt_{55}:Al_{20}:Cr_{25}	L → ~Pt_3Al ~Pt_3Al → ~Pt_2Al
41	Pt_{64}:Al_{16}:Cr_{20}	L → (Pt) L → ~Pt_3Al + (Pt) (Pt) → ~Pt_3Cr (ordering)
42	Pt_8:Al_{89}:Cr_3	L → ~$PtAl_2$ L + ~Pt_8Al_{21} → ~Cr_2Al_{13} L + ~Cr_2Al_{13} → (Al)
43	Pt_4:Al_{83}:Cr_{13}	L → ~$CrAl_4$ L + ~$CrAl_4$→ ~$CrAl_5$ L + ~$CrAl_5$ → ~Cr_2Al_{13} L + ~Cr_2Al_{13} → (Al) L → (Al) + Pt_8Al_{21}

From the above information it was possible to derive a liquidus surface for the Pt-Cr-Al system. The surface was drawn to be consistent with the as-reported binary reactions and the reactions of the ternary samples. Where inconsistencies were found, the reaction sequences were checked again. The experimental liquidus surface projection is given in Figure 2.140, with the alloy compositions marked. The insert is a magnified view of the Al-rich corner. Alloys in each labelled field solidify with that phase as the primary component. Each solid line represents a reaction involving the liquid phase. At the triple points, there is an invariant reaction (Table 2.45). The arrows show the direction of the reactions with decreasing temperature.

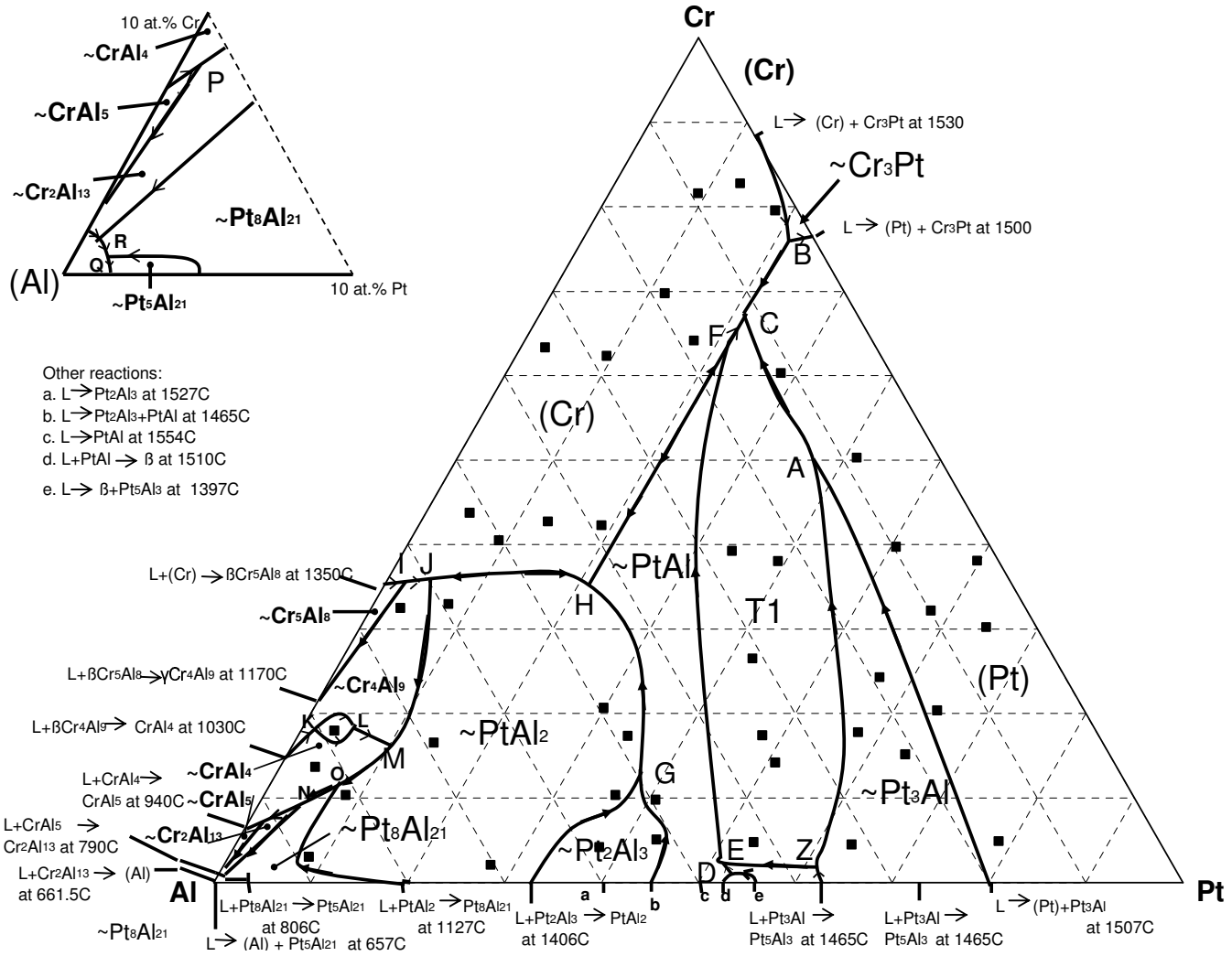

Figure 2.140. Experimental liquidus surface projection for the Pt-Al-Cr system.

Table 2.45. Ternary invariant reactions in the Pt-Al-Cr system.

Reaction no.	Composition	Reaction
A	~Pt_{37}:Al_{13}:Cr_{50}	L + ~Pt_3Al → (Pt) + T1
B	~Pt_{22}:Al_4:Cr_{74}	L + (Cr) + ~Cr_3Pt → (Pt)
C	~Pt_{21}:Al_{12}:Cr_{67}	L → (Pt) + (Cr) + T1
D	~Pt_{53}:Al_{46}:Cr_1	L + β → ~Pt_5Al_3 + ~PtAl
E	~Pt_{52}:Al_{45}:Cr_3	L + ~Pt_5Al_3 → T1 + ~PtAl
F	~Pt_{21}:Al_{14}:Cr_{65}	L + ~PtAl → (Cr) + T1
	~Pt_{21}:Al_{16}:Cr_{63}	Maximum in L → (Cr) + T1
G	~Pt_{37}:Al_{50}:Cr_{13}	L + ~Pt_2Al_3 → ~PtAl + ~$PtAl_2$
H	~Pt_{20}:Al_{44}:Cr_{36}	L → (Cr) + ~PtAl + ~$PtAl_2$
	~Pt_{12}:Al_{52}:Cr_{36}	Maximum in L → (Cr) + ~$PtAl_2$
I	~Pt_2:Al_{62}:Cr_{36}	L + (Cr) + ~Cr_5Al_8 → ~Cr_4Al_9
J	~Pt_5:Al_{60}:Cr_{35}	L + (Cr) → ~$PtAl_2$ ~Cr_4Al_9
K	~Pt_1:Al_{83}:Cr_{16}	L + ~Cr_4Al_9 + ~$CrAl_4$ → T3
L	~Pt_5:Al_{77}:Cr_{18}	L + T3 → ~Cr_4Al_9 + ~$CrAl_4$
M	~Pt_9:Al_{75}:Cr_{16}	L + ~Cr_4Al_9 → ~$CrAl_4$ + ~$PtAl_2$
N	~Pt_5:Al_{85}:Cr_{10}	L + ~$CrAl_4$ + ~Pt_8Al_{21} → ~Cr_2Al_{13}
O	~Pt_8:Al_{80}:Cr_{12}	L + ~$PtAl_2$ → ~$CrAl_4$ + ~Pt_8Al_{21}
P	~Pt_2:Al_{90}:Cr_8	L + ~$CrAl_4$ → ~$CrAl_5$ + ~Cr_2Al_{13}
Q	~Pt_1:$Al_{98.5}$:$Cr_{0.5}$	L + ~Pt_8Al_{21} → ~Pt_5Al_{21} + (Al)
R	~$Pt_{0.5}$:$Al_{98.5}$:Cr_1	L + ~Cr_2Al_{13} → ~Pt_8Al_{21} + (Al)
Z	~Pt_{60}:Al_{39}:Cr_1	L + ~Pt_3Al → ~Pt_5Al_3 + T1

The following comments can be made regarding the liquidus surface:

- It was assumed that as ~Pt_2Al is formed in the binary system by a solid state reaction from ~Pt_3Al, it does the same in the ternary. Thus, whenever ~Pt_2Al is found in the as-cast state, ~Pt_3Al had actually formed first. In the binary, the transformation occurs on the Al-rich side of ~Pt_3Al. Far into the ternary, however, it consistently occurs in more than one sample apparently from the Pt-rich side. From ~32 at.% Cr upwards (alloys 25 (Pt_{58}:Al_{10}:Cr_{32}), and 12 (Pt_{50}:Al_{10}:Cr_{40})) ~Pt_3Al is no longer formed.
- The eutectic L→(Cr) + Cr_3Pt changes into a peritectic L + (Cr) → Cr_3Pt in the ternary system (alloy 18, Pt_{18}:Al_2:Cr_{80}, § 2.1.18).
- The two eutectic temperatures in the published Pt-Cr system [1990Mas] are the wrong way around. This is shown by alloy 8 (Pt_{10}:Al_{80}:Cr_{10}, § 2.1.4) where ~Cr_3Pt forms peritectically, and then (Pt). This would agree with the experimental phase diagram of Pt-Cr-Ru [2004Süs1, 2006Süs], Cr-Ni-Pt [2005Nzu] as well as the results of NIMS [2004Gu].

- T1 is taken as a ternary phase and not β from the Pt-Al binary that is stabilised by Cr addition. The single phase alloys 11, 37, 24 and 38 (Pt_{40}:Al_{30}:Cr_{30}, Pt_{45}:Al_{35}:Cr_{20}, Pt_{50}:Al_{35}:Cr_{15} and Pt_{52}:Al_{43}:Cr_5) suggest congruent melting, which suggests a ternary phase, rather than a peritectically formed binary phase.
- A maximum temperature is placed on the (Cr)/~PtAl locus because one needs the liquidus to flow down to the ternary eutectic on one side, and the reactions going away from this on the other side. ~PtAl is a high melting point compound and melts congruently in the binary, and so this effect would be expected in a ternary.
- Because Pt_2Al_3 has such a high melting point, the reaction directions are taken as flowing towards (Cr), and this flow can occur with its liquidus surface drawn as it is.
- The dendrites Alloy 16 (Pt_{12}:Al_{18}:Cr_{70}, § 2.1.16) look as though their edges have experienced a peritectic-type reaction. However, the ledges were interpreted to be caused by (Cr) being added on rather than being removed. The resultant sparse ternary eutectic (Cr) + ~PtAl + ~$PtAl_2$ would then be in agreement with that of alloy 9 (Pt_{20}:Al_{40}:Cr_{40}, § 2.1.6).
- The ternary eutectic (Cr) + ~PtAl + ~$PtAl_2$ was identified in alloys 9, 10, 16 and 30 (Pt_{12}:Al_{18}:Cr_{70}, Pt_{20}:Al_{40}:Cr_{40}, Pt_{30}:Al_{50}:Cr_{20} and Pt_{75}:Al_{10}:Cr_{15}).
- The ternary eutectic (Pt) + (Cr) + T1 was identified in alloys 19 and 34 (Pt_{28}:Al_{12}:Cr_{60} and Pt_{15}:Al_5:Cr_{80}).
- There is probably a maximum on the (Cr)/~$PtAl_2$ locus at ~Pt_{12}:Al_{52}:Cr_{36}, which is expected from a high congruently melting binary compound.
- T2≈Cr_3Al_2 is assumed to form by low temperature solid state reactions from (Cr).
- Alloy 17 (Pt_{17}:Al_{68}:Cr_{70}, § 2.1.17) shows that the liquidus surface is shaped so that the liquid composition moves towards the ~$PtAl_2$/~Cr_4Al_9 join, which is consistent with the maximum in the L → (Cr) + ~$PtAl_2$ reaction and the composition of primary ~$PtAl_2$.
- The liquidus surface of T3≈$CrAl_3$ is drawn to accommodate Alloy 31 (Pt_3:Al_{79}:Cr_{18}, § 2.1.30).
- No attempt has been made at this stage to distinguish between the different morphologies of the Al-Cr phases Cr_5Al_8 and Cr_4Al_9.
- Alloys 42 (Pt_8:Al_{89}:Cr_3, § 2.1.42) and 43 (Pt_4:Al_{83}:Cr_{13}, § 2.1.43) are the highest Al-content alloys to date and define the rest of the liquidus surface. It allows the placement of the surprisingly large surface for ~$PtAl_2$, and for

$$L \rightarrow (Al) + Pt_8Al_{21}$$

to be the second last reaction. It should be noted that, strictly speaking, according to the Pt-Al binary system, L $\rightarrow$ (Al) + Pt_5Al_{21} should be the last eutectic. This has not been observed.

2.2. Phase analysis – annealed at 1000°C for 1000 hours

Please note that only alloys that were likely not to start melting at 1000°C were annealed at 1000°C. Except for alloy Pt_{10}:Al_{80}:Cr_{10} (for no particular reason but to see the effect of the annealing and quenching on the as-cast microstructure), none of the alloys that could form L + ~Pt_8Al_{21}/$CrAl_4$/~$CrAl_5$ or any other more Al-rich compounds, were annealed at 1000°C.

2.1.45. Nominal Pt_{10}:Al_{30}:Cr_{60}

Almost identical to its structure in the as-cast condition, alloy Pt_{10}:Al_{30}:Cr_{60} comprised dark dendrites, with an interdendritic eutectic mixture of dark and light that became more sparse during annealing at 1000°C (Figure 2.141). It was even clearer in the annealed sample that light precipitates were present in the dark dendrites. Since the structure hardly changed during annealing, it is likely that 1000 hours was not enough to reach equilibrium at 1000°C. Previous XRD analyses of the as-cast sample showed that the dark phase was (Cr) and the white phase ~$PtAl_2$. The results of the EDX analyses are given in Table 2.46 and shown graphically in Figure 2.142. The standard deviation in overall composition was very large which could mean that the alloy was not very homogeneous. Furthermore, the dark phase and light precipitates were very small (< 3µm beam interaction) and could not be analysed. Even the analyses of the white phase were affected by the surrounding phase because of its small size. Its composition could therefore be extrapolated along the dark/white tie-line to lower levels of Cr, but only subsequent alloys would tell to what extent. An extrapolated tie-line in accordance with that of the as-cast structure for dark/white is shown in Figure 2.143. Considering the position of the measured compositions in Figure 2.142 and the results of alloy Pt_3:Al_{35}:Cr_{62}, of which the microstructure is very similar to that of Pt_{10}:Al_{30}:Cr_{60}, the grey particles could be ~Cr_2Al. XRD analyses (Figure 2.144) confirmed this assessment, with the peaks for ~$PtAl_2$ and (Cr) being an excellent match for the XRD pattern (albeit with some shift to lower angles). The peaks for ~Cr_2Al seem to fit as well. This phase is not stable at 1000°C according to the binary Cr-Al binary diagram, and is probably the remnant of the as-cast state, implying that annealing have not been done long enough and equilibrium has not been reached. The light precipitates will probably dissolve on further annealing since it is likely not to be stable at 1000°C.

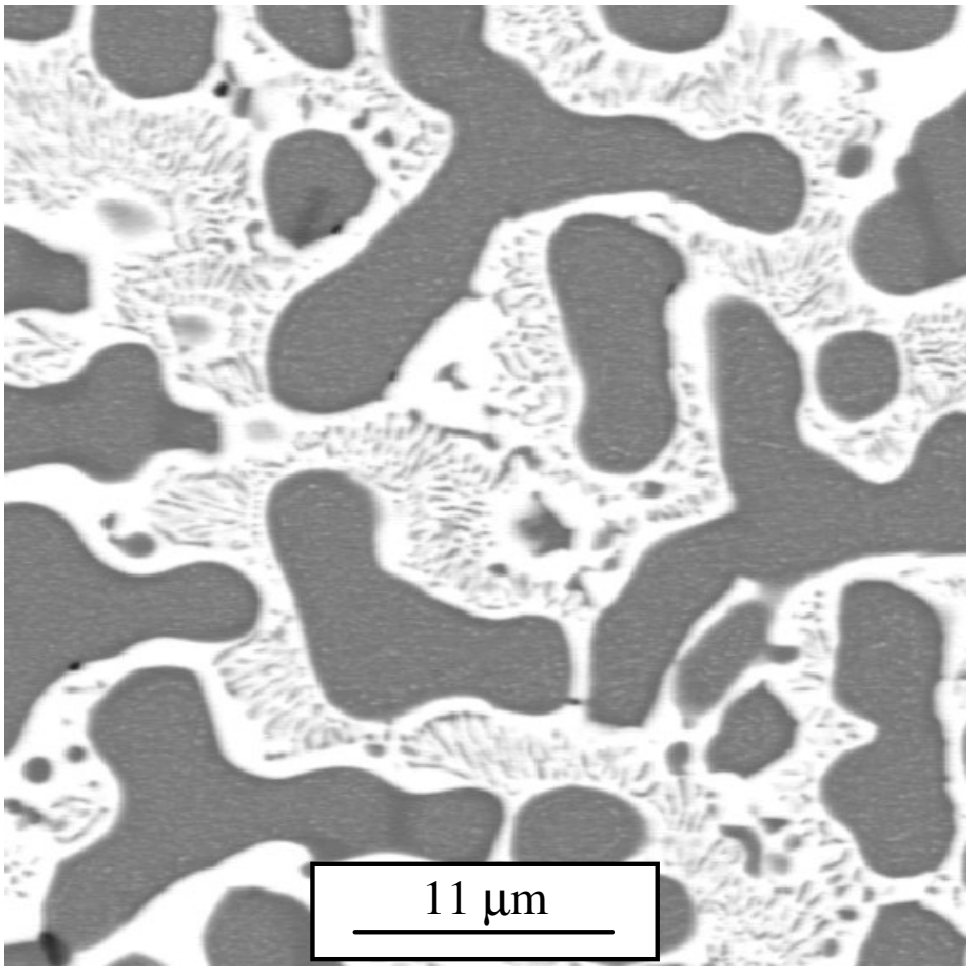

Figure 2.141. BSE-SEM image of nominal $Pt_{10}:Al_{30}:Cr_{60}$ after annealing at 1000 °C: (Cr) dark; ~$PtAl_2$ white; ~Cr_2Al light precipitates.

Table 2.46. Phase analyses for nominal $Pt_{10}:Al_{30}:Cr_{60}$ (at.%) after annealing at 1000 °C.

Phase description	**Pt**	**Al**	**Cr**	**Phase**
Overall	8.3 ± 1.9	27.2 ± 3.9	64.5 ± 5.8	-
Dark	Too small to analyse			(Cr)
White	27.7 ± 0.3	58.6 ± 0.4	13.7 ± 0.7	~$PtAl_2$
Light	Too small to analyse			~Cr_2Al
Dark + light (dendrite)	1.9 ± 0.1	16.3 ± 0.7	81.8 ± 0.6	(Cr) + ~Cr_2Al
Eutectic dark + white	20.2 ± 0.2	47.0 ± 3.3	32.8 ± 5.5	(Cr) + ~$PtAl_2$

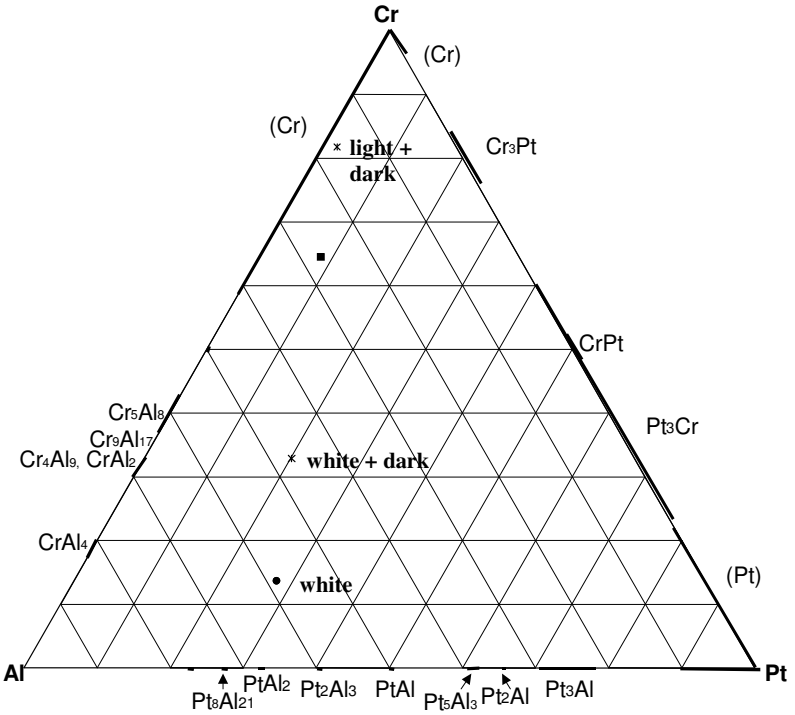

Figure 2.142. EDX analyses of nominal $Pt_{10}:Al_{30}:Cr_{60}$ (at.%) after annealing at 1000 °C.

(■ overall composition; ● phases; ✶ eutectic and two-phase)

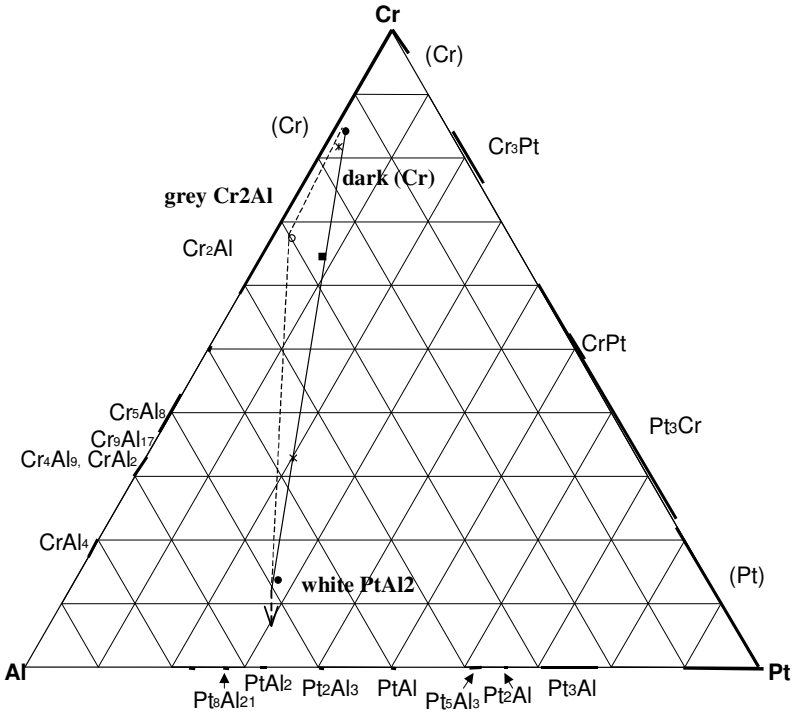

Figure 2.143. EDX analyses of nominal $Pt_{10}:Al_{30}:Cr_{60}$ (at.%) after annealing at 1000 °C.

(■ overall composition; ● phases; ✶ eutectic and two-phase; o extrapolated composition)

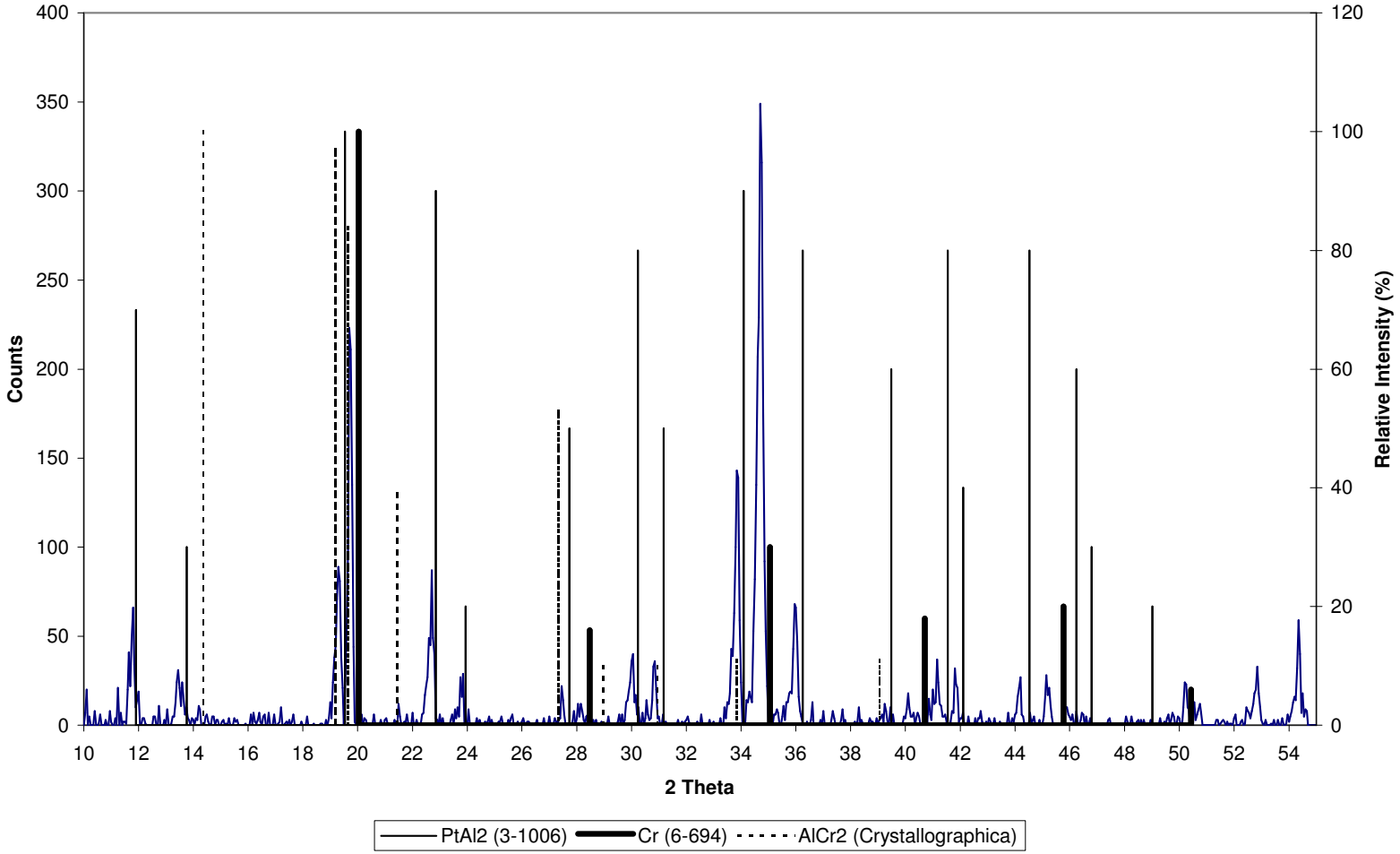

Figure 2.144. XRD pattern for nominal $Pt_{10}:Al_{30}:Cr_{60}$ after annealing at 1000℃.

2.1.46. Nominal $Pt_{10}:Al_{80}:Cr_{10}$

In the as-cast condition, alloy $Pt_{10}:Al_{80}:Cr_{10}$ had had a very complicated structure, comprising four phases (Figure 2.9). Its appearance changed much during annealing with the phases becoming much rounder compared to their more angular appearance in the as-cast condition, and the white phase was much larger and easier to analyse after annealing (Figure 2.145). There was also lots of porosity present (not shown), as well as cracks, indicating brittleness or at least different coefficients of expansion for the phases. The EDX analyses of the alloy and all its phases are given in Table 2.47 and shown graphically in Figure 2.146. Most of the phases had changed compositions, and the black and white phases showed decreased solubility for the components. From Figure 2.146, and considering the as-cast results, the black phase was (Al). Contrary to the as-cast results, the dark grey phase and black phase were very similar in composition. The white phase was probably ~$PtAl_2$. The light grey phase was probably either ~$CrAl_5$ or ~$CrAl_4$. The plot in Figure 2.146 suggests that ~Pt_8Al_{21} disappeared from the structure. XRD analyses (Figure 2.147) confirmed all the above assumptions. (Al) and ~$PtAl_2$ were clearly detected, while ~$CrAl_5$ was a much better fit than the other possibility, ~$CrAl_4$.

The alloy composition relative to the liquid stability range in the Pt-Al and Al-Cr systems, and the fact that the phases did become much rounder and ~$PtAl_2$ appeared dendritic, did suggest that some liquation could have occurred. This was highly likely at 1000°C. It is therefore suggested that the results of this alloy suggest a liquid boundary at 1000°C as indicated by the dashed line in Figure 2.146.

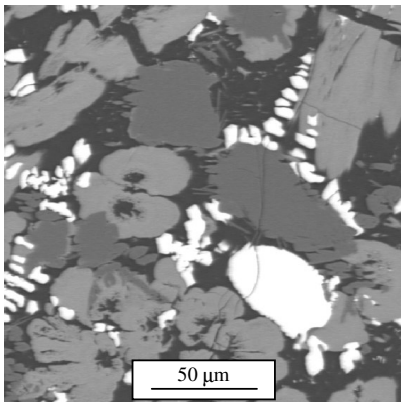

Figure 2.145. BSE-SEM image of nominal $Pt_{10}:Al_{80}:Cr_{10}$ after annealing at 1000°C: (Al) black and dark grey; ~$CrAl_5$ light grey; ~$PtAl_2$ white.

Table 2.47. Phase analyses for nominal $Pt_{10}:Al_{80}:Cr_{10}$ (at.%) after annealing at 1000°C.

Phase description	**Pt**	**Al**	**Cr**	**Phase**
Overall	4.2 ± 0.7	84.9 ± 3.3	10.9 ± 2.7	-
Black	0.1 ± 0.0	99.4± 0.1	0.5 ± 0.1	(Al)
Dark grey	0.2 ± 0.2	99.0 ± 0.8	0.8 ± 0.7	(Al)
Light grey	4.7 ± 0.3	73.9 ± 1.2	21.4 ± 0.9	~$CrAl_5$
White	28.8 ± 0.4	68.1 ± 0.5	3.1 ± 0.4	~$PtAl_2$

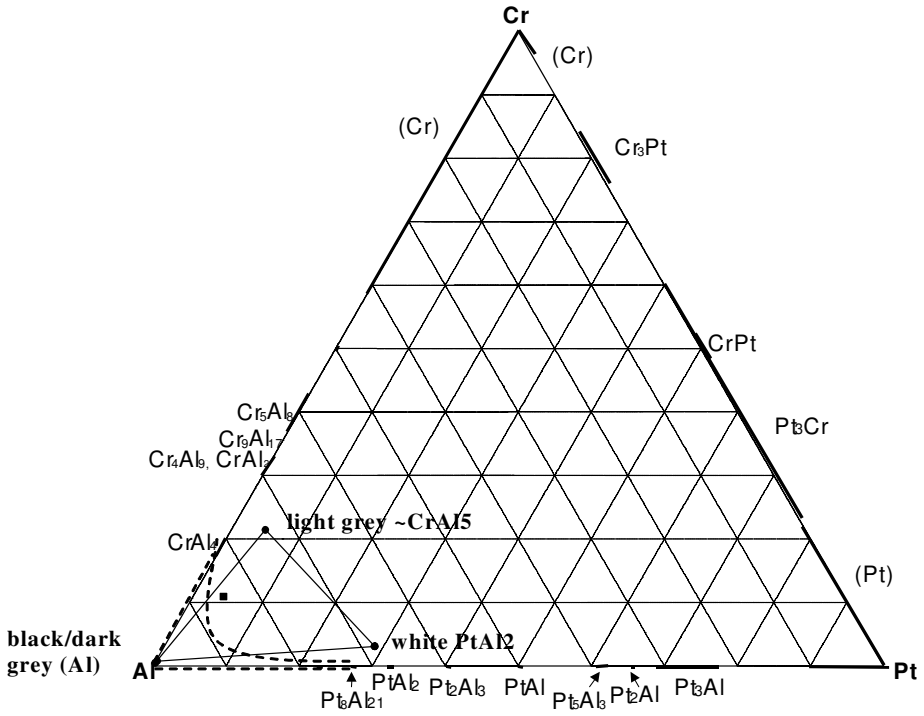

Figure 2.146. EDX analyses of nominal $Pt_{10}:Al_{80}:Cr_{10}$ (at.%) after annealing at 1000°C.

(■ overall composition; ● phases)

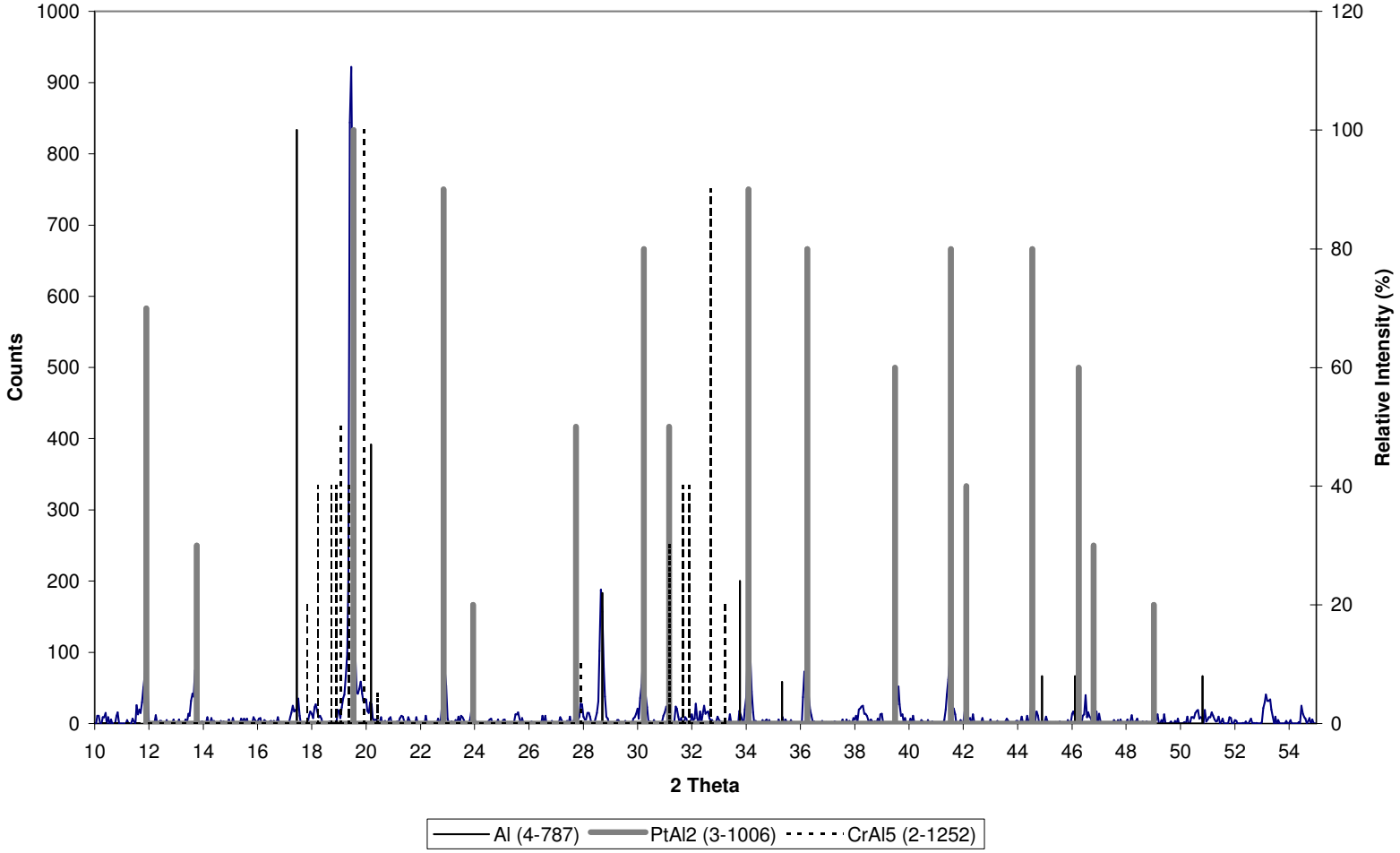

Figure 2.147. XRD pattern for nominal Pt_{10}:Al_{80}:Cr_{10} after annealing at 1000℃.

2.1.47. Nominal $Pt_{30}:Al_{50}:Cr_{20}$

Alloy $Pt_{30}:Al_{50}:Cr_{20}$ comprised primarily grey dendrites with white needles, and interdendritic regions that comprised a ternary eutectic mixture of black + white + grey (Figure 2.148). There was also evidence of black precipitates within the grey phase (Figure 2.148). The general appearance was similar to its as-cast state, but the grey + white eutectic had disappeared and white needles had formed inside the grey dendrites. The EDX analyses of the alloy and its three phases are shown in Table 2.48 and Figure 2.149. The black phase was very small to analyse and its analysis was affected by the surrounding phases (confirmed by the variation of up to ~5.5 at.% Cr in composition (Table 2.48) and it is highly likely that it was much more rich in (Cr), probably up to ~95 at.%. In many cases, the black areas were holes, but analysis under the microprobe confirmed (Cr) being at the bottom of the holes, and the fact that it was not an oxide. Both the grey and white phases were also too small for accurate analysis, although the measurement of grey + white regions should be quite accurate. The black + white + grey eutectic, on the other hand, was very small and only one measurement was taken to get an indication of its composition. However, its composition was lying on the black/white tie-line, while the grey/white composition was far off the grey/white tie-line, probably affected by the small black precipitates in the grey phase. It was obvious that many of the measurements were questionable. It was still possible, however, to identify the likely identity of the phases. Based on the XRD analyses of the as-cast state (Figure 2.21), and the position of the phases on the ternary plot, the grey phase was probably ~$PtAl_2$. Considering its position on the ternary plot, the white phase was probably ~Pt_2Al_3 (and not ~PtAl as in the as-cast state). This assessment was clearly confirmed by XRD analyses of the annealed sample, with the XRD peaks of the named phases fitting perfectly to the measured XRD pattern (Figure 2.150).

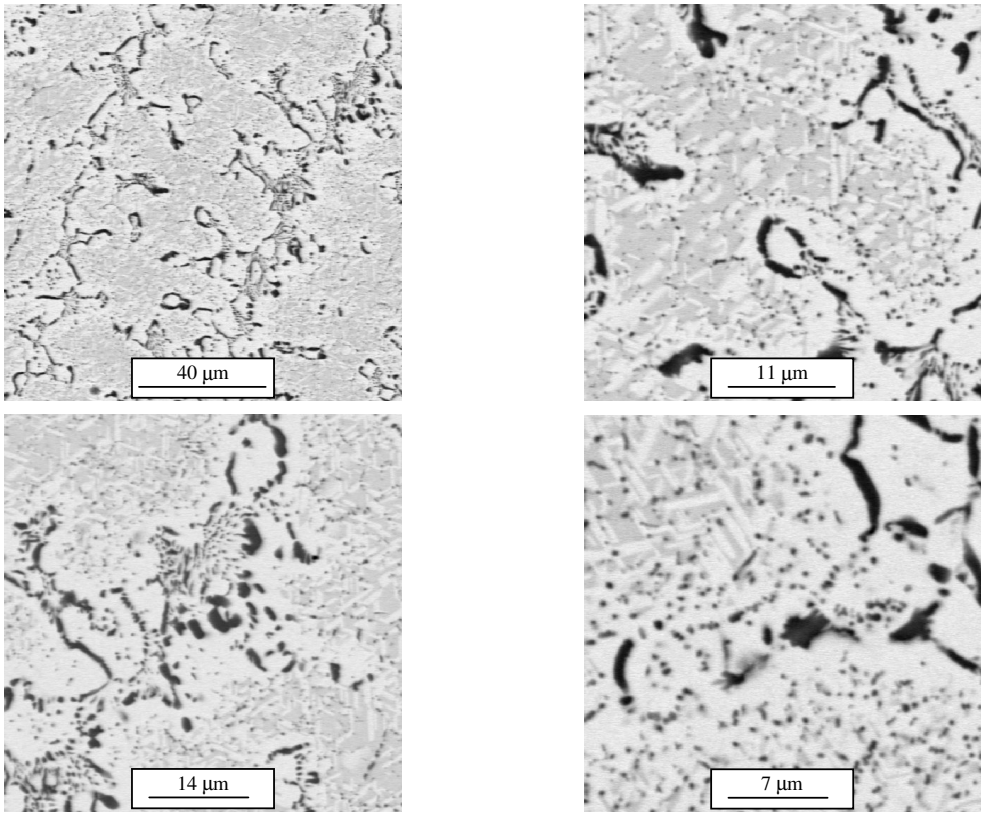

Figure 2.148. BSE-SEM image of nominal Pt_{30}:Al_{50}:Cr_{20} after annealing at 1000°C: (Cr) black; ~$PtAl_2$ grey; ~ Pt_2Al_3 white.

Table 2.48. Phase analyses for nominal Pt_{30}:Al_{50}:Cr_{20} (at.%) after annealing at 1000°C.

Phase description	**Pt**	**Al**	**Cr**	**Phase**
Overall	30.0 ± 0.9	50.4 ± 1.5	19.6 ± 2.4	-
Black	7.1 ± 0.8	11.5 ± 4.4	81.4± 5.2	(Cr)
Grey	30.0 ± 0.2	58.1 ± 0.4	11.9 ± 0.2	~$PtAl_2$
White	39.0 ± 0.6	58.1 ± 0.4	2.9 ± 0.8	~Pt_2Al_3
Eutectic black+white*	25.9	40.1	34.0	(Cr) + ~Pt_2Al_3
Two-phase grey+white	31.6 ± 0.6	51.7 ± 0.7	16.7 ± 0.1	~$PtAl_2$ + ~Pt_2Al_3

* Only one measurement taken due to small size.

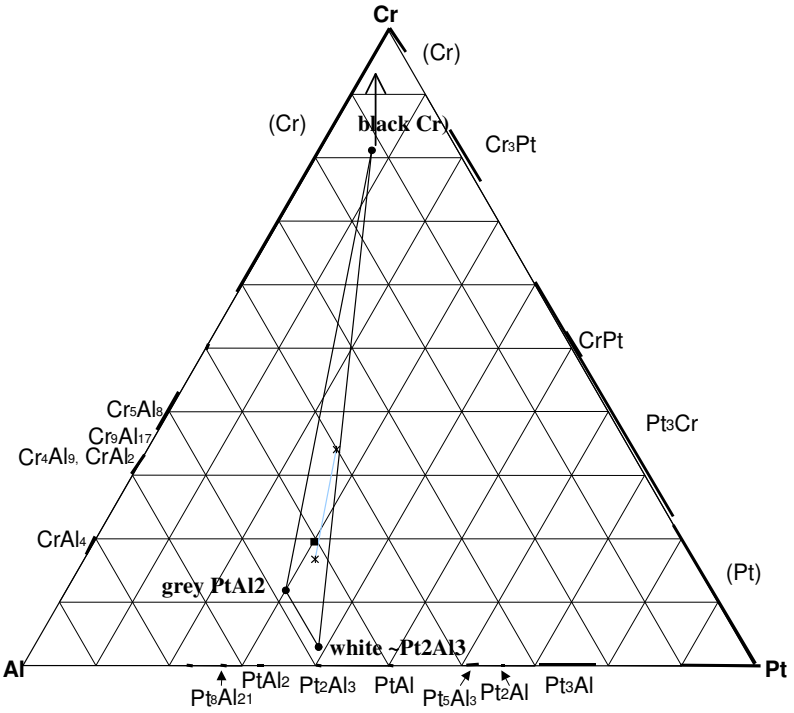

Figure 2.149. EDX analyses of nominal Pt_{30}:Al_{50}:Cr_{20} (at.%) after annealing at 1000 °C. (■ overall composition; ● phases; ✶ eutectic/two-phase; → direction of probable extrapolation)

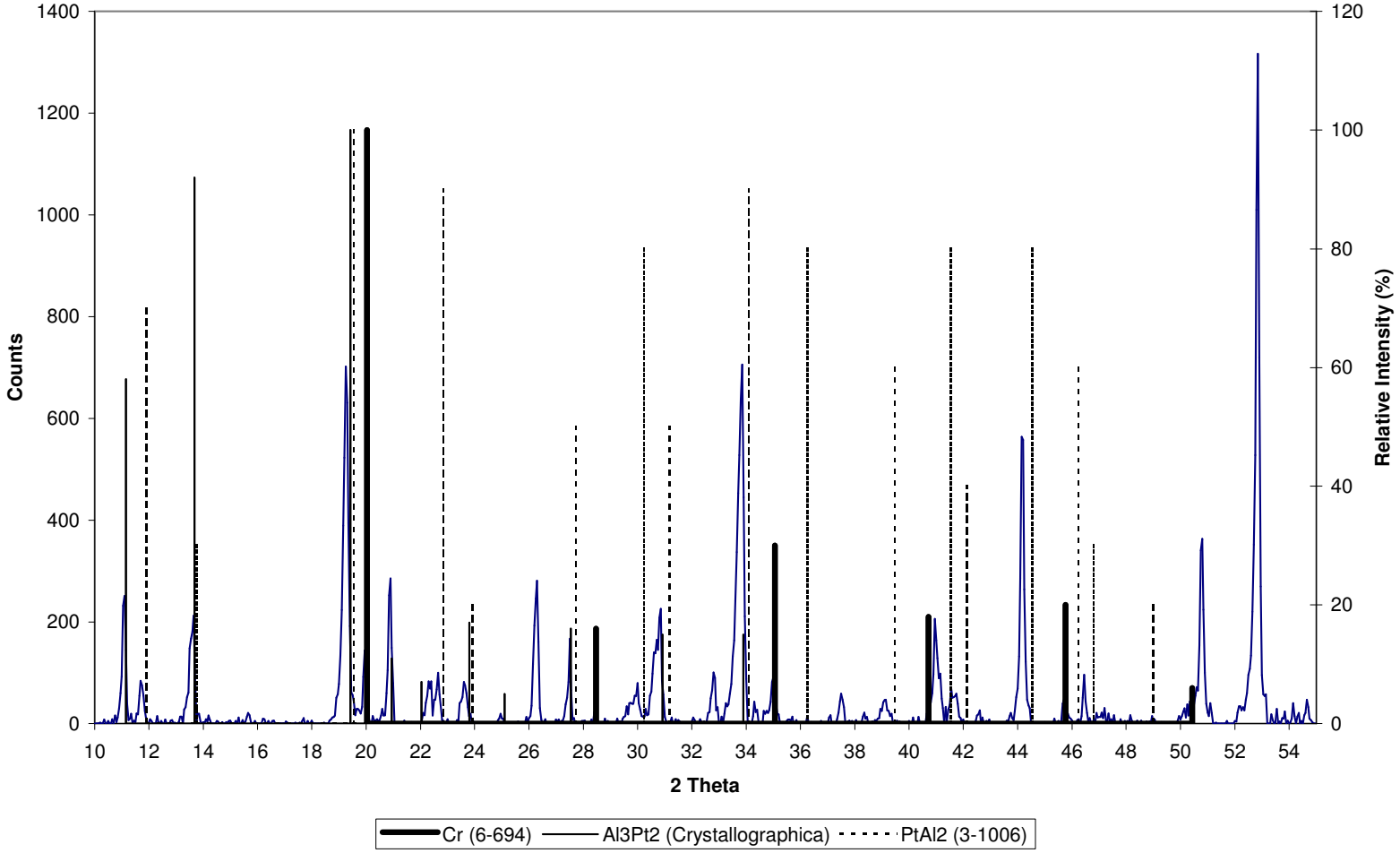

Figure 2.150. XRD pattern for nominal Pt_{30}:Al_{50}:Cr_{20} after annealing at 1000 °C.

2.1.48. Nominal $Pt_{50}:Al_{10}:Cr_{40}$

Alloy $Pt_{50}:Al_{10}:Cr_{40}$ changed from dark ~CrPt dendrites with a light interdendritic phase (Figure 2.36) to a single phase alloy during annealing (Figure 2.151). There was also lots of porosity present (some of it shown in Figure 2.151), which is characteristic of much substitutional diffusion. The EDX (overall area and random spot) analyses are given in Table 2.49 and Figure 2.152. There seems to be a slight discrepancy in composition, probably due to experimental error rather than the suggestion of the presence of a second phase. Taking the as-cast results into account, the phase could be ~CrPt. It was however very difficult to decide which XRD patterns (that of $L1_0$ and/or A1 ~CrPt or $L1_2$ ~Pt_3Al) was the best fit to the measured pattern (Figure 2.153 and insert). Taking into account the results of alloy $Pt_{58}:Al_{10}:Cr_{32}$ where a two-phase ~CrPt + ~Pt_3Al area was identified, alloy $Pt_{50}:Al_{10}:Cr_{40}$ comprised ~CrPt only.

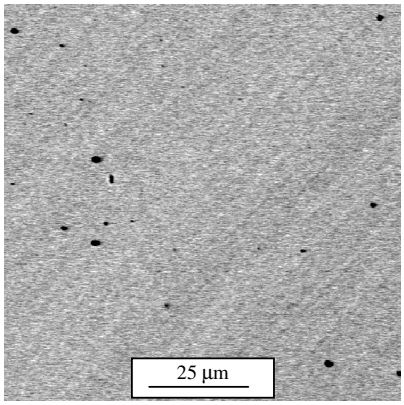

Figure 2.151. BSE-SEM image of nominal $Pt_{50}:Al_{10}:Cr_{40}$ after annealing at 1000°C: ~CrPt grey.

Table 2.49. Phase analyses for nominal $Pt_{50}:Al_{10}:Cr_{40}$ (at.%) after annealing at 1000 °C.

Phase description	**Pt**	**Al**	**Cr**	**Phase**
Overall	50.6 ± 0.1	10.1 ± 0.3	39.3 ± 0.3	-
Dark	52.3 ± 0.5	10.4 ± 0.5	37.3 ± 0.1	~CrPt

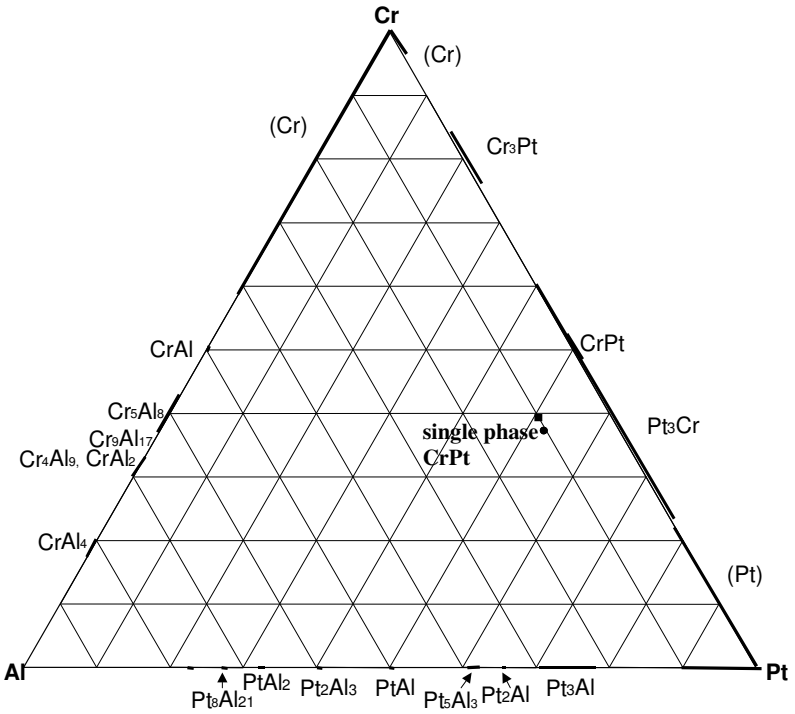

Figure 2.152. EDX analyses of nominal $Pt_{50}:Al_{10}:Cr_{40}$ (at.%) after annealing at 1000 °C.

(■ overall composition; ● phases)

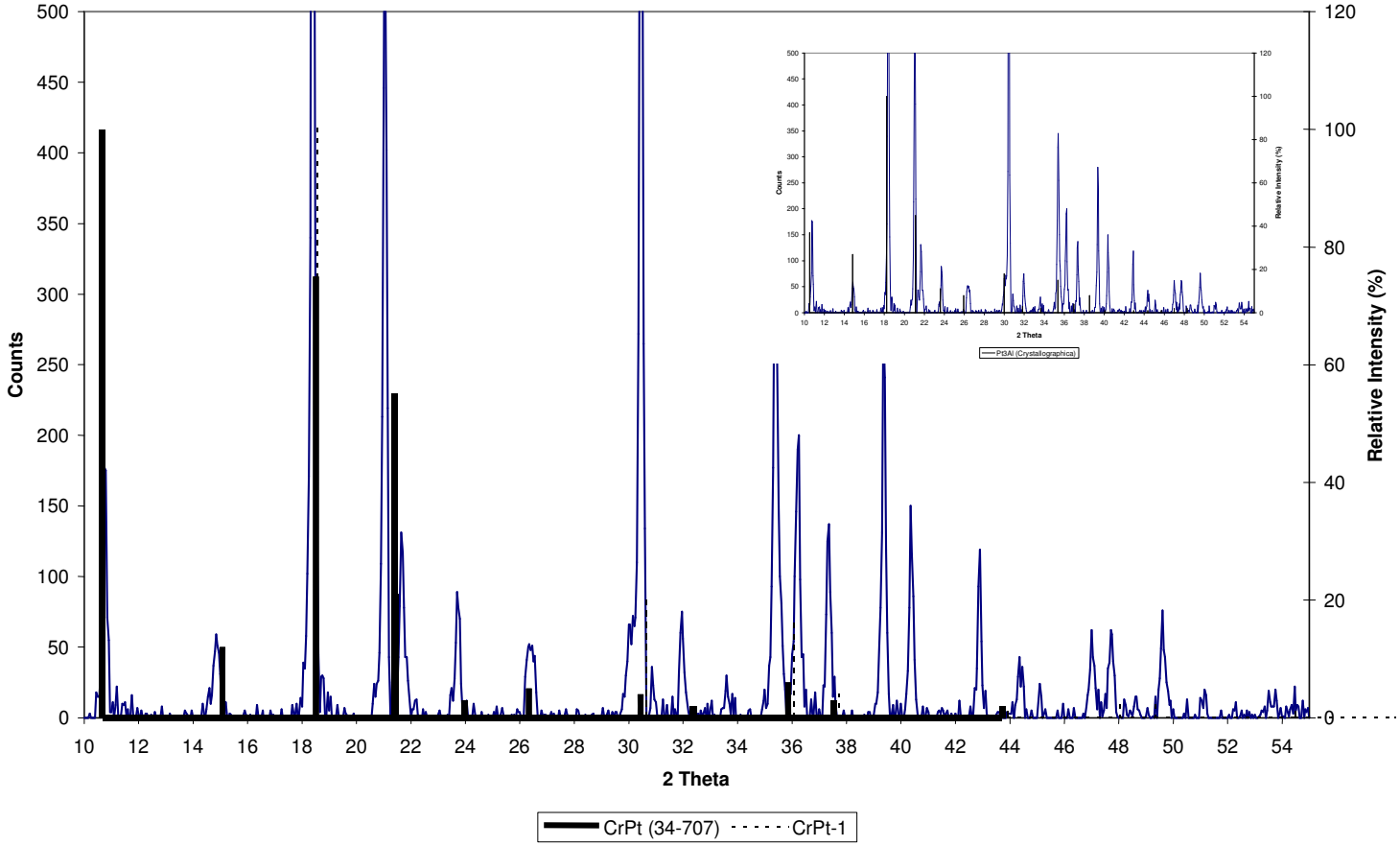

Figure 2.153. XRD patterns for nominal Pt_{50}:Al_{10}:Cr_{40}. after annealing at 1000℃.

2.1.49. Nominal $Pt_{65}:Al_5:Cr_{30}$

The cored appearance of as-cast alloy $Pt_{65}:Al_5:Cr_{30}$ (Figure 2.40) disappeared during annealing to form a clearly single phase alloy (Figure 2.154). The EDX (overall area and random spot) analyses are shown in Table 2.50 and Figure 2.155. There seems to be a slight difference in composition, thought to be due to experimental error rather than the suggestion of the presence of a second phase, since a no second phase could be observed in the sample. Although not shown in Figure 2.154, the alloy was very porous and showed several cracks after polishing, indicating brittleness. XRD analyses clearly identified the phase as $L1_2$ ~Pt_3Al (Figure 2.156). The peaks for ~$CrPt_3$ are also shown, but they did not match several measured peaks (e.g. $2\theta \approx 23.5$, 26 and 30).

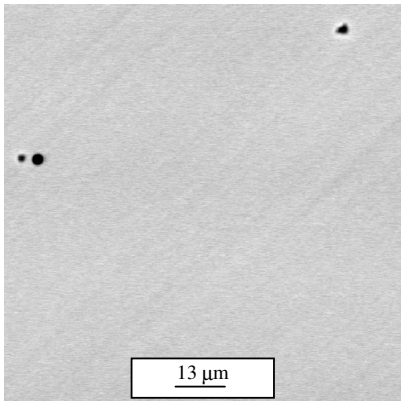

Figure 2.154. BSE-SEM image of nominal $Pt_{65}:Al_5:Cr_{30}$ after annealing at 1000°C: ~Pt_3Al grey.

Table 2.50. Phase analyses for nominal $Pt_{65}:Al_5:Cr_{30}$ (at.%) after annealing at 1000°C.

Phase description	**Pt**	**Al**	**Cr**	**Phase**
Overall	65.0 ± 0.7	5.4 ± 0.6	29.6 ± 0.3	-
Grey	66.3 ± 1.1	5.9 ± 0.4	27.8 ± 0.8	~Pt_3Al

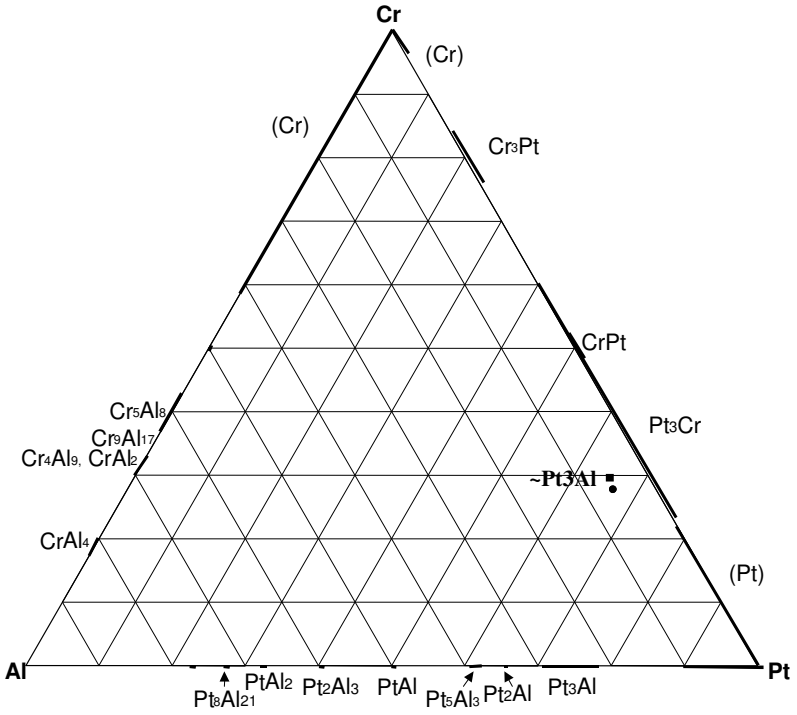

Figure 2.155. EDX analyses of nominal $Pt_{65}:Al_5:Cr_{30}$ (at.%) after annealing at 1000°C.

(■ overall composition; ● phases)

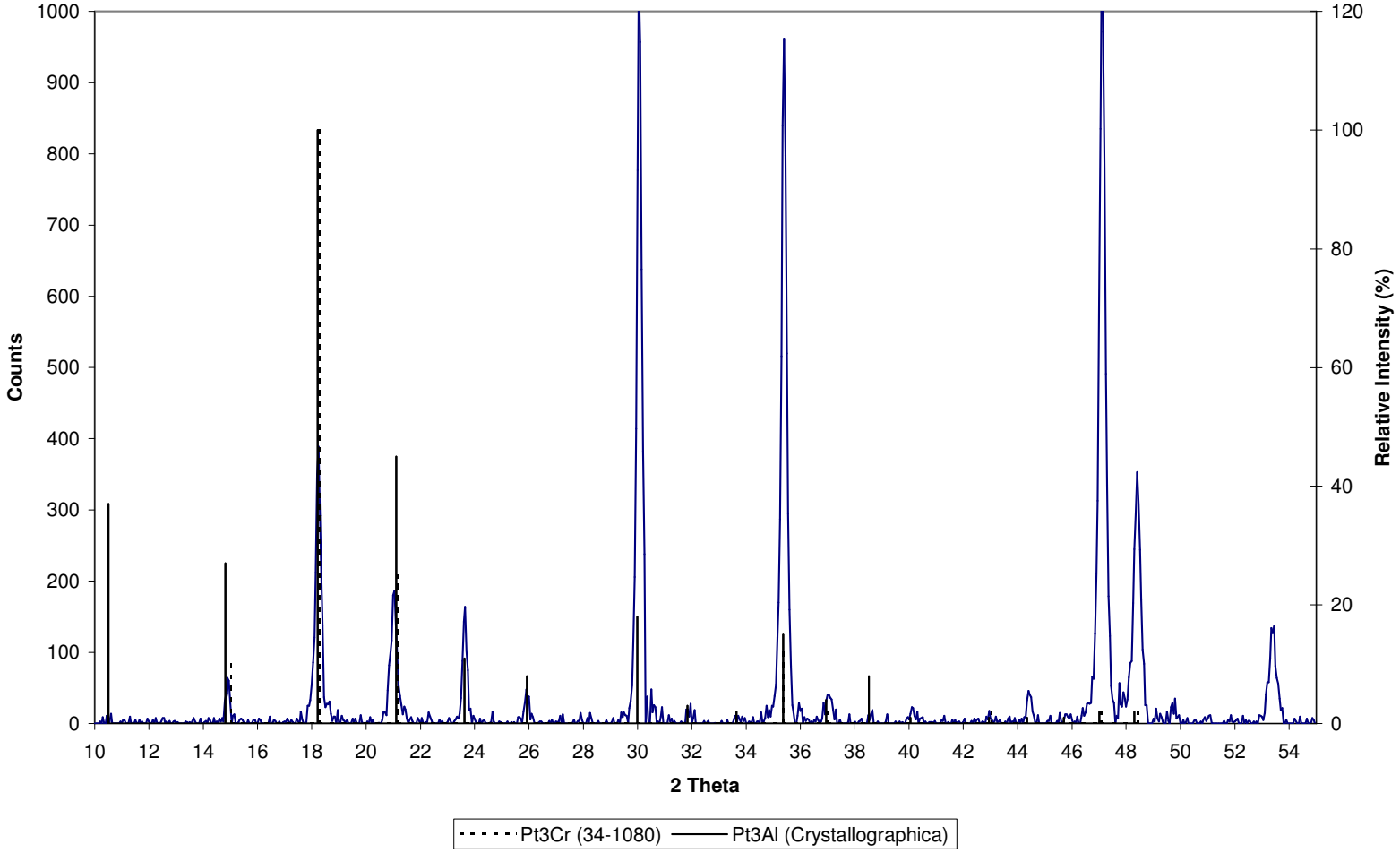

Figure 2.156. XRD patterns for nominal $Pt_{65}:Al_5:Cr_{30}$. after annealing at 1000℃.

2.1.50. Nominal $Pt_3:Al_{65}:Cr_{32}$

In the as-cast state alloy $Pt_3:Al_{65}:Cr_{32}$ comprised dark dendrites with a light interdendritic phase in some areas, while in other areas the interdendritic areas comprised an eutectic mixture of dark and light. During annealing, the dendritic structure disappeared, as well as the eutectic mixture so that the alloy comprised a dark phase with smaller light areas (Figure 2.157). The EDX analyses are given in Table 2.51 and Figure 2.158. XRD analyses could not be performed on the sample since it crumbled during the procedure of breaking it out of its mount after SEM analyses. Assuming that the identity of the phases stayed the same, which was reasonable, considering the position of the phases on the ternary plot, the light phase was probably ~$PtAl_2$ and the dark one ~Cr_4Al_9 (based on the XRD analysis of the as-cast state (Figure 2.45). The solubility of Cr in ~$PtAl_2$ had slightly decreased during annealing.

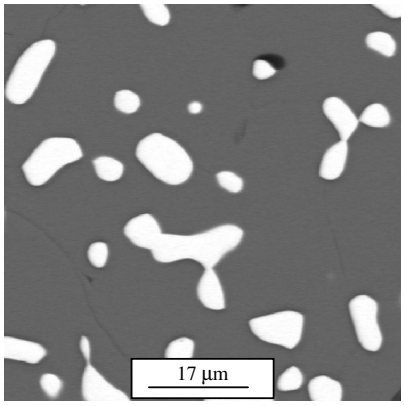

Figure 2.157. BSE-SEM image of nominal $Pt_3:Al_{65}:Cr_{32}$ after annealing at 1000°C: ~Cr_4Al_9 dark; ~$PtAl_2$ light.

Table 2.51. Phase analyses for nominal $Pt_3:Al_{65}:Cr_{32}$ (at.%) after annealing at 1000°C.

Phase description	**Pt**	**Al**	**Cr**	**Phase**
Overall	2.1 ± 0.2	64.3 ± 0.3	33.6 ± 0.4	-
Dark	0.5 ± 0.2	65.0 ± 0.1	34.5 ± 0.2	~Cr_4Al_9
Light	28.5± 0.2	59.5 ± 0.0	12.0 ± 0.2	~$PtAl_2$

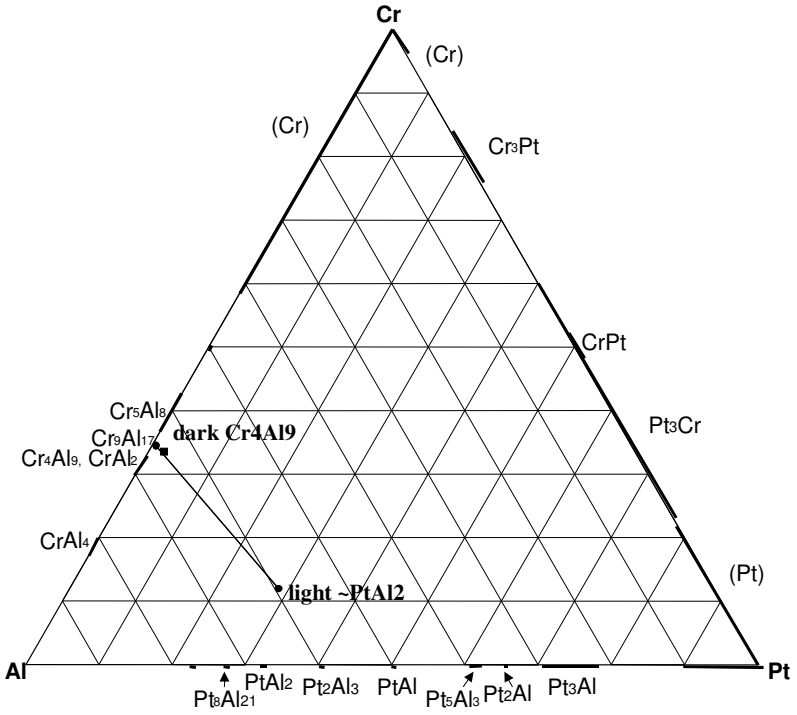

Figure 2.158. EDX analyses of nominal Pt_3:Al_{65}:Cr_{32} (at.%) after annealing at 1000°C. (■ overall composition; ● phases)

2.1.51. Nominal Pt_3:Al_{35}:Cr_{62}

The microstructure of alloy Pt_3:Al_{35}:Cr_{62} changed slightly during annealing. It showed a very rounded dark phase with tiny grey particles inside; a white phase; and a fine eutectic mixture of dark and light (the web-like morphology had changed slightly during annealing) (Figure 2.159). The light phase was analysed in the centre of the biggest white areas, although still too small not be affected by surrounding phase(s), while the black phase was always analysed in areas where the grey particles were not present (also still too small, though). No attempt was made to analyse the grey particles due to their extremely small sizes. The compositions "as-is" (Table 2.52) can be seen graphically in Figure 2.160. However, as already stated, all phases were too small to yield any accurate results. The only compositions that would be accurate in Table 2.52 are the two-phase compositions, i.e. that of the dark + light combination (area analysis of eutectic) and that of the dark + grey combination (area analysis of dendrite interiors).

From Figure 2.160 one would expect that the dark phase was (Cr) and the light phase probably ~$PtAl_2$ (as in the as-cast state) or ~Pt_2Al_3. Considering the results of other annealed alloys, e.g. alloys Pt_{30}:Al_{50}:Cr_{20} (§ 2.2.3) and Pt_{35}:Al_{55}:Cr_{10} (§ 2.2.9), ~$PtAl_2$ seemed more probable. It seemed like the solubility of Cr in ~$PtAl_2$ had decreased. The grey phase was difficult to identify. However, the composition of black+grey and its resulting position on the plot suggests a position for the grey phase near that of ~Cr_2Al or even T2≈Cr_3Al_2 (see the possible extrapolations in Figure 2.160). ~Cr_2Al is only stable up to 910°C according to the Al-Cr phase diagram, and although it could be stabilised to higher temperatures by Pt additions, these grey precipitates could possibly disappear on further annealing. XRD analyses could not be performed on the sample since it crumbled during the procedure of breaking it out of its mount after SEM analyses.

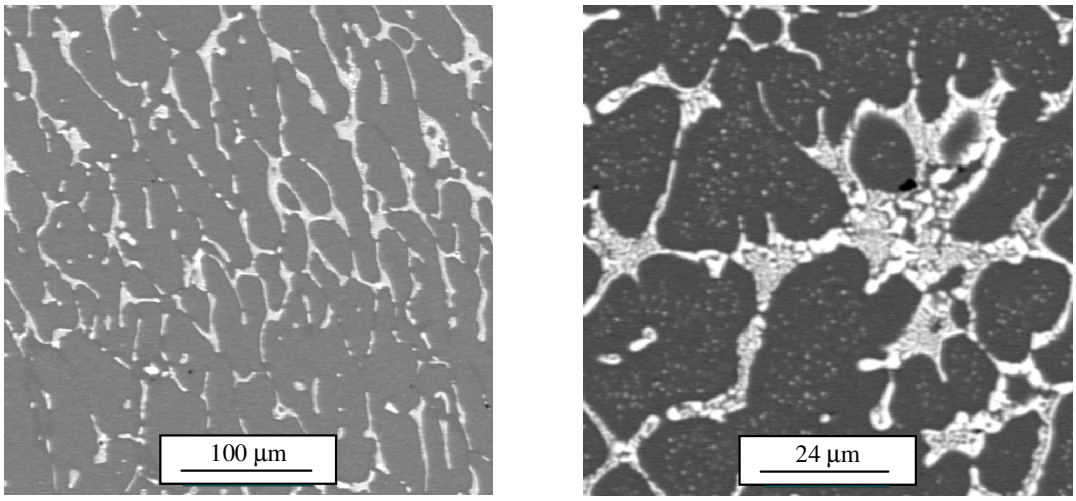

Figure 2.159. BSE-SEM image of nominal Pt_3:Al_{35}:Cr_{62} after annealing at 1000°C: (Cr) dark; ~$PtAl_2$ light; ~Cr_2Al/T2≈Cr_3Al_2 grey.

Table 2.52. Phase analyses for nominal Pt_3:Al_{35}:Cr_{62} (at.%) after annealing at 1000°C.

Phase description	**Pt**	**Al**	**Cr**	**Phase**
Overall	2.8 ± 0.6	33.8 ± 1.0	63.4 ± 1.5	-
Dark	0.2 ± 0.1	33.3 ± 2.0	69.5 ± 1.9	(Cr)
Light	27.7 ± 0.5	56.7 ± 0.3	15.6 ± 0.2	~$PtAl_2$
Eutectic dark + light	14.8 ± 0.8	44.1 ± 0.9	41.1 ± 1.7	(Cr) + ~$PtAl_2$
Two-phase dark + grey	0.7 ± 0.3	30.9 ± 1.2	67.4± 2.6	(Cr) + ~Cr_2Al/T2≈Cr_3Al_2

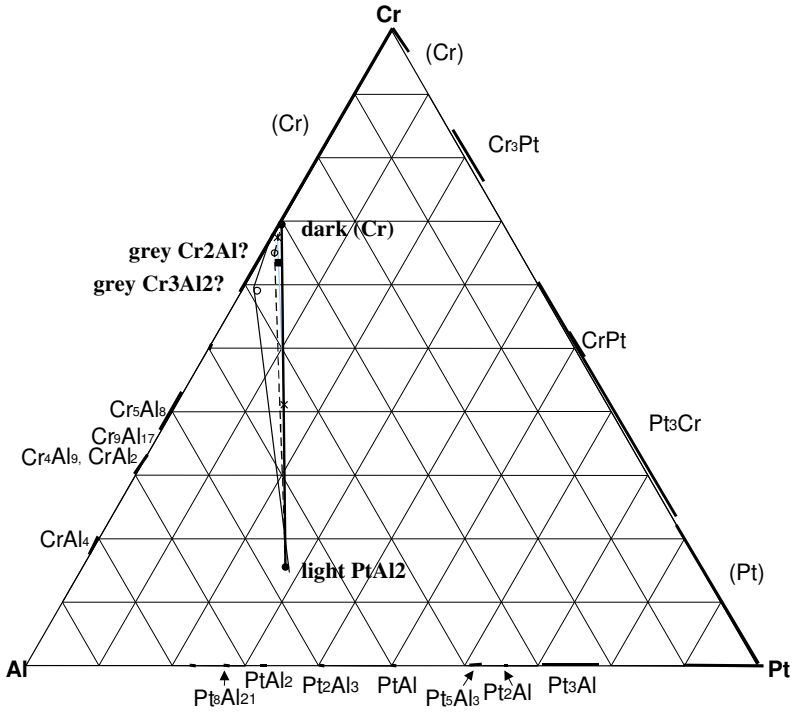

Figure 2.160. EDX analyses of nominal Pt_3:Al_{35}:Cr_{62} (at.%) after annealing at 1000°C. (■ overall composition; ● phases; ✶ eutectic/two-phase; o extrapolated composition)

2.1.52. Nominal Pt_{18}:Al_2:Cr_{80}

Alloy Pt_{18}:Al_2:Cr_{80} comprised three phases: black, grey and white (Figure 2.161). It was similar to its as-cast state, except for the fact that the amount of black and white phase had decreased substantially during annealing. Further annealing would possibly result in a grey single phase alloy. The EDX analyses are shown in Table 2.53 and Figure 2.162. From the as-cast XRD results, the identities were probably black (Cr), grey ~Cr_3Pt and white ~CrPt, although from the ternary plot (compared to the solidification projection) the white phase could possibly be T1 or ~Pt_2Al (Figure 2.162). However, the XRD analyses showed that ~Pt_2Al was not present, and that the diffraction peaks for (Cr), ~Cr_3Pt and T1 (not ~CrPt) fitted the measured pattern very well (Figure 2.163). This was consistent with the results of alloy Pt_{38}:Al_{22}:Cr_{40} (§ 2.2.10).

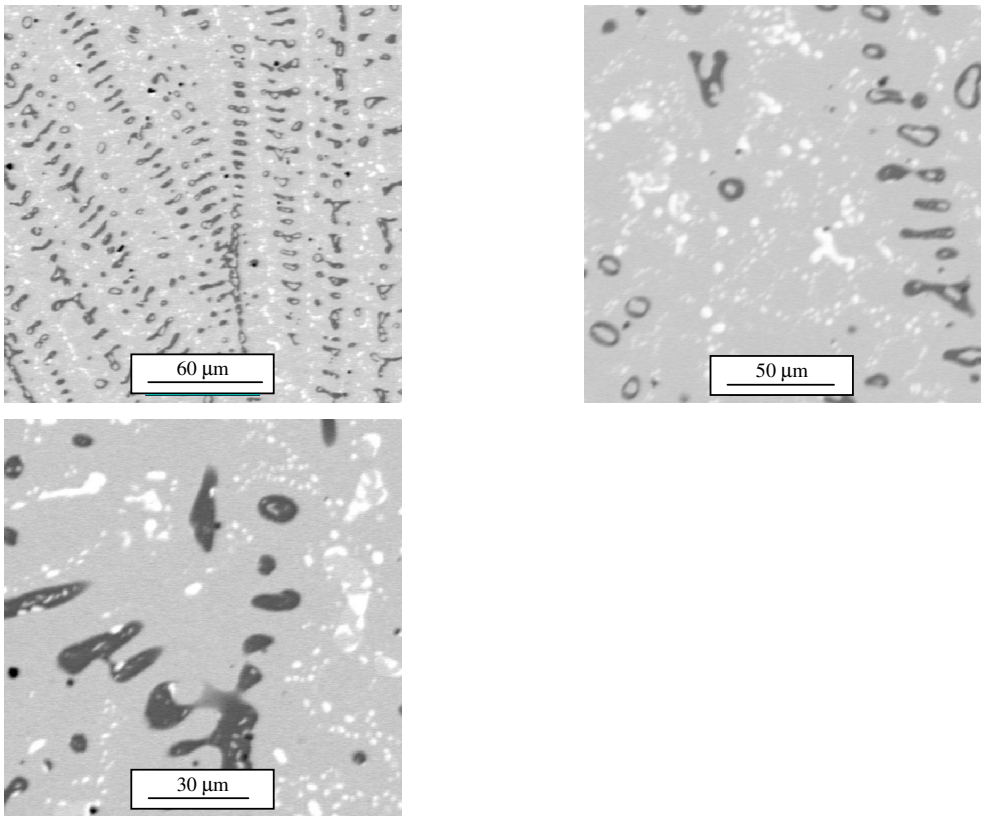

Figure 2.161. BSE-SEM image of nominal $Pt_{18}:Al_2:Cr_{80}$ after annealing at 1000°C: (Cr) black; ~Cr_3Pt grey; T1 white.

Table 2.53. Phase analyses for nominal $Pt_{18}:Al_2:Cr_{80}$ (at.%) after annealing at 1000°C.

Phase description	**Pt**	**Al**	**Cr**	**Phase**
Overall	18.6 ± 1.4	2.3 ± 0.3	79.1 ± 1.6	-
Black*	2.4	0.0	97.6	(Cr)
Grey	19.9 ± 1.0	1.1 ± 0.1	79.0 ± 0.9	~Cr_3Pt
White	43.0 ± 1.8	23.4 ± 1.8	33.6 3.6	T1

* Only one measurement taken due to small size.

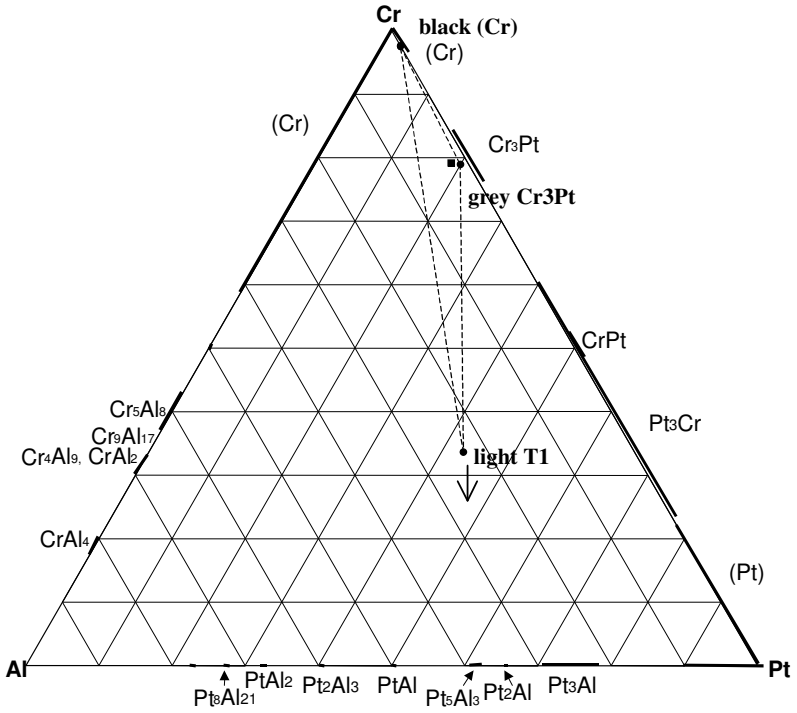

Figure 2.162. EDX analyses of nominal $Pt_{18}:Al_2:Cr_{80}$ (at.%) after annealing at 1000°C.

(■ overall composition; ● phases; → probable extrapolation)

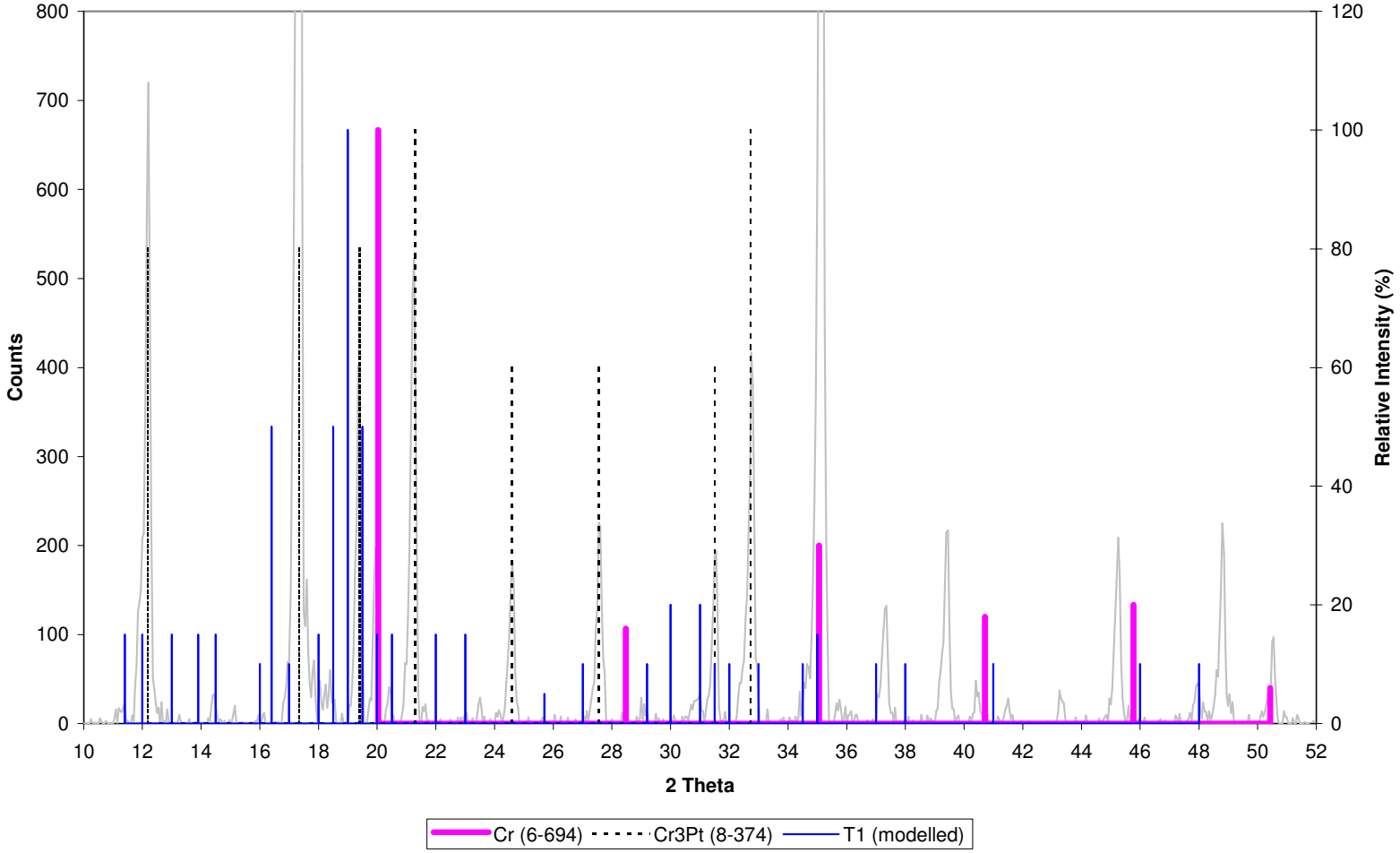

Figure 2.163. XRD pattern for nominal $Pt_{18}:Al_2:Cr_{80}$ after annealing at 1000°C.

2.1.53. Nominal $Pt_{35}:Al_{55}:Cr_{10}$

At low magnification alloy $Pt_{35}:Al_{55}:Cr_{10}$ comprised grey (mostly columnar) grains surrounded by a light interdendritic phase, with black porosity on the grain boundaries (Figure 2.164a). This was very different to the alloy's appearance in the as-cast state (which showed dark dendrites and a majority of a lighter interdendritic phase). At higher magnification, light needles were seen inside the grey phase (Figure 2.164b), as well as black/light and/or light/grey (difficult to distinguish) two phase mixtures at grain junctions (Figure 2.164c). The as-measured EDX analyses of the phases and the alloy are given in Table 2.54 and Figure 2.165. The individual phases were too small for accurate analyses, while the measured two-phase compositions should be accurate. That of light+black was close to the light/black tie-line, and it seemed that the two phase mixture at grain junctions actually comprised only light+black and not light+grey. Considering the results of alloy $Pt_{30}:Al_{50}:Cr_{20}$, and the close similarity of the phase triangles of the alloys' ternary plots (Figure 2.165 vs. Figure 2.149), the black phase was (Cr), the grey phase ~$PtAl_2$ and the light phase ~Pt_2Al_3. This was confirmed by XRD analyses (Figure 2.166), with the peaks for ~Pt_2Al_3 and ~$PtAl_2$ (with some shift) fitting the pattern very well.

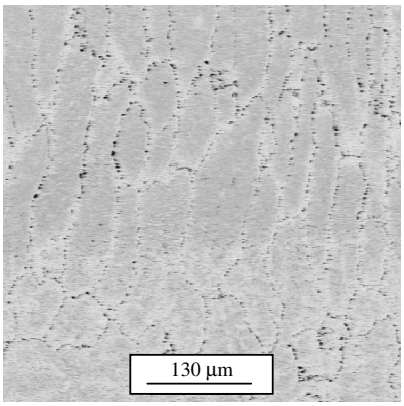

(a)

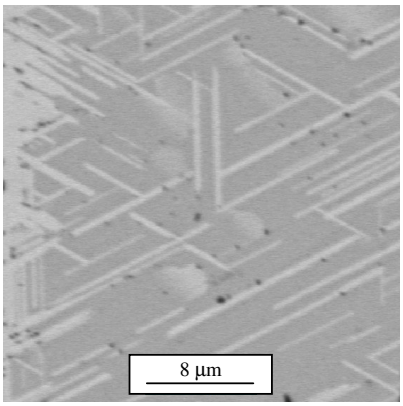

(b)

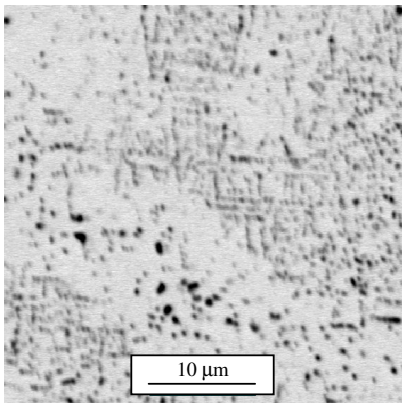

(c)

Figure 2.164. BSE-SEM image of nominal $Pt_{35}:Al_{55}:Cr_{10}$ after annealing at 1000°C: (Cr) black; ~$PtAl_2$ grey; ~Pt_2Al_3 light

Table 2.54. Phase analyses for nominal $Pt_{35}:Al_{55}:Cr_{10}$ at.%) after annealing at 1000°C.

Phase description	**Pt**	**Al**	**Cr**	**Phase**
Overall	35.0 ± 0.4	55.1± 0.8	9.9 ± 0.8	-
Black	3.1 ± 1.6	4.6 ± 1.3	92.3 ± 2.9	(Cr)
Light	39.3± 0.2	59.0 ± 0.1	1.7 ± 0.2	~Pt_2Al_3
Grey*	29.7	57.8	12.5	~ $PtAl_2$
Light needles + grey	32.7 ± 0.4	57.8 ± 0.2	9.5 ± 0.7	~Pt_2Al_3 + ~ $PtAl_2$
Light + dark ppt	35.6 ± 0.3	53.6 ± 0.2	10.8 ± 0.2	~Pt_2Al_3+ (Cr)

* Only one measurement taken due to small size.

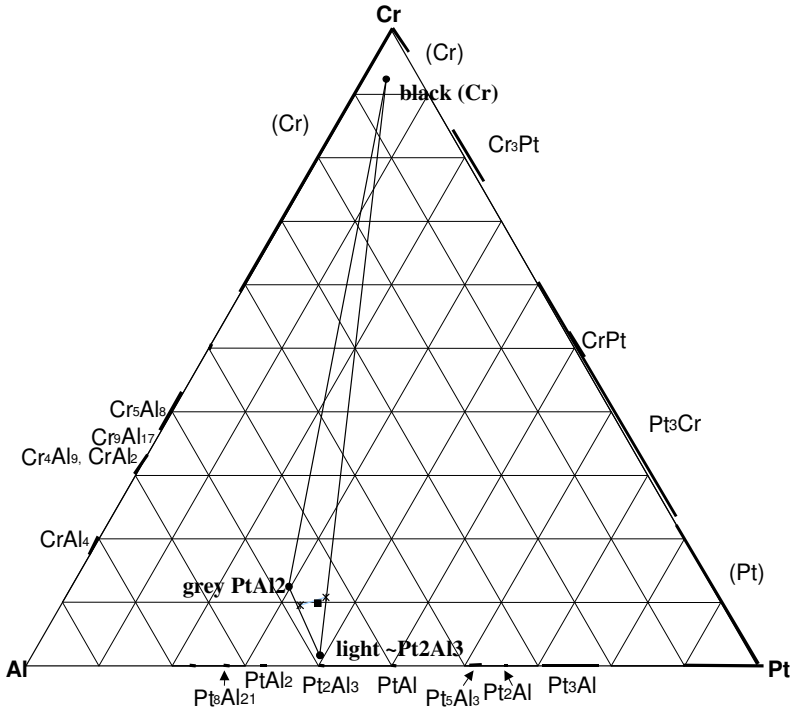

Figure 2.165. EDX analyses of nominal $Pt_{35}:Al_{55}:Cr_{10}$ (at.%) after annealing at 1000°C. (■ overall composition; ● phases; ✶ two-phase)

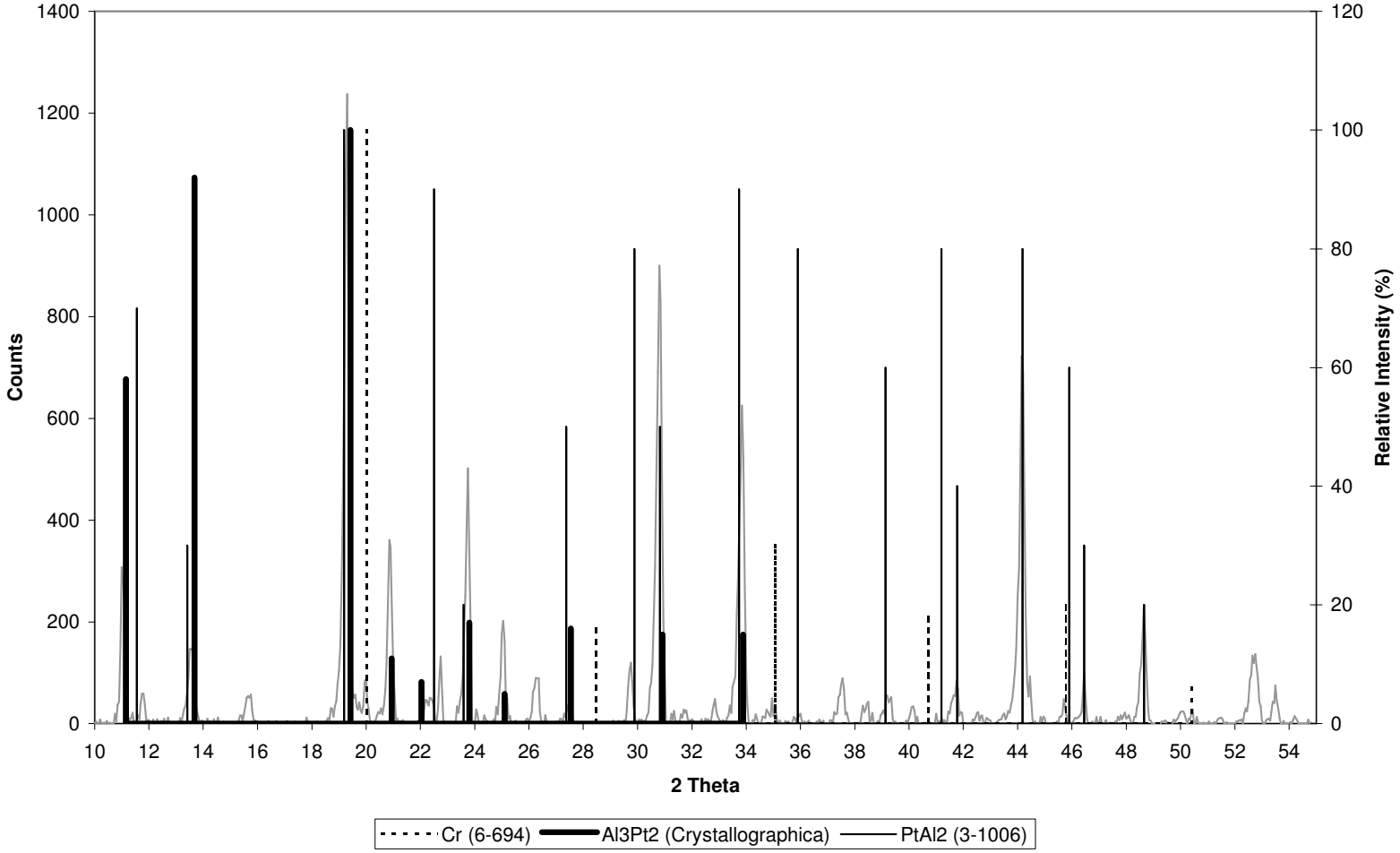

Figure 2.166. XRD pattern for nominal Pt_{35}:Al_{55}:Cr_{10} after annealing at 1000°C.

2.1.54. Nominal $Pt_{38}:Al_{22}:Cr_{40}$

In the as-cast state, alloy $Pt_{38}:Al_{22}:Cr_{40}$ comprised light dendrites with a dark interdendritic phase. During annealing at 1000°C the structure changed totally to that comprising a light phase with a dark grey and black phase dispersed through the structure (Figure 2.167). The EDX analyses are given in Table 2.55 and Figure 2.168. The large standard deviation of the Cr measurements for the overall composition as well as for the black and dark phase would explain why the overall composition was outside the composition triangle. From the position of the black and dark phases on the ternary plot, it seemed that they were (Cr) and ~Cr_3Pt respectively, while the light phase could be ternary phase T1 (as was the case in the as-cast state). XRD analyses did not disprove this assessment (Figure 2.169), with the peaks for (Cr) and ~Cr_3Pt and the modelled peaks for T1 being quite a good fit to the measured pattern. This was in agreement with alloy $Pt_{18}:Al_2:Cr_{80}$.

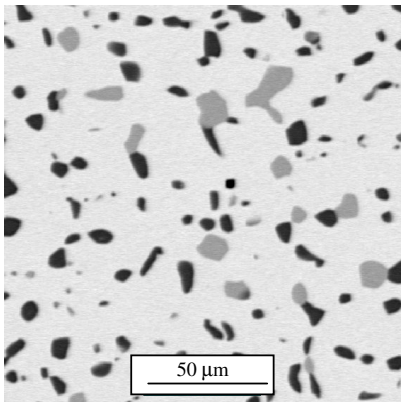

Figure 2.167. BSE-SEM image of nominal $Pt_{38}:Al_{22}:Cr_{40}$ after annealing at 1000°C: (Cr) black; ~Cr_3Pt dark; T1 light.

Table 2.55. Phase analyses for nominal $Pt_{38}:Al_{22}:Cr_{40}$ (at.%) after annealing at 1000°C.

Phase description	**Pt**	**Al**	**Cr**	**Phase**
Overall	38.5 ± 1.2	23.1 ± 0.6	38.4 ± 1.8	-
Black	2.4 ± 0.8	0.6 ± 0.7	97.0 ± 1.4	(Cr)
Dark	20.6 ± 0.8	1.6 ± 0.7	77.8 ± 1.4	~Cr_3Pt
Light	46.3 ± 0.4	26.2 ± 0.3	27.5 ± 0.6	T1

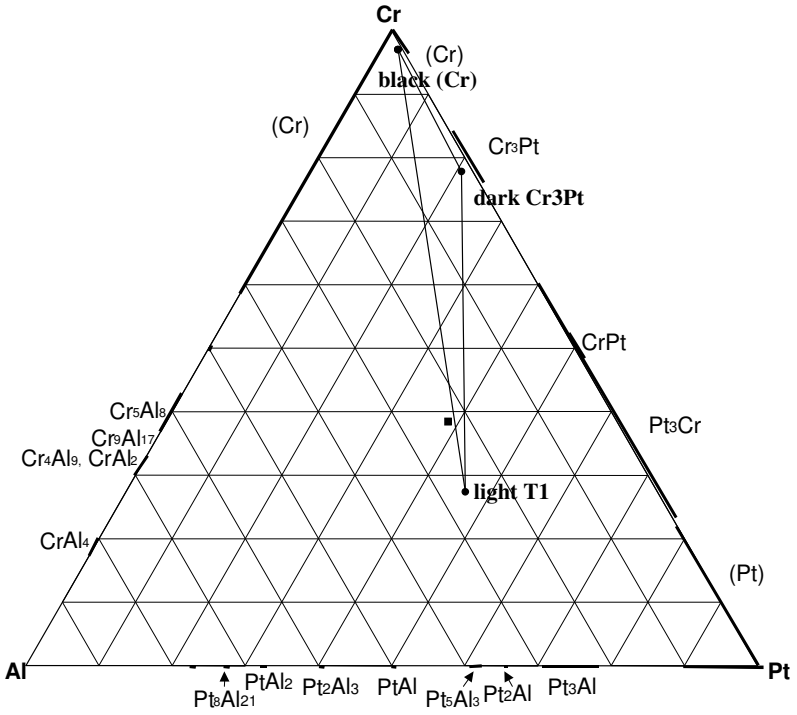

Figure 2.168. EDX analyses of nominal $Pt_{38}:Al_{22}:Cr_{40}$ (at.%) after annealing at 1000 °C.

(■ overall composition; ● phases)

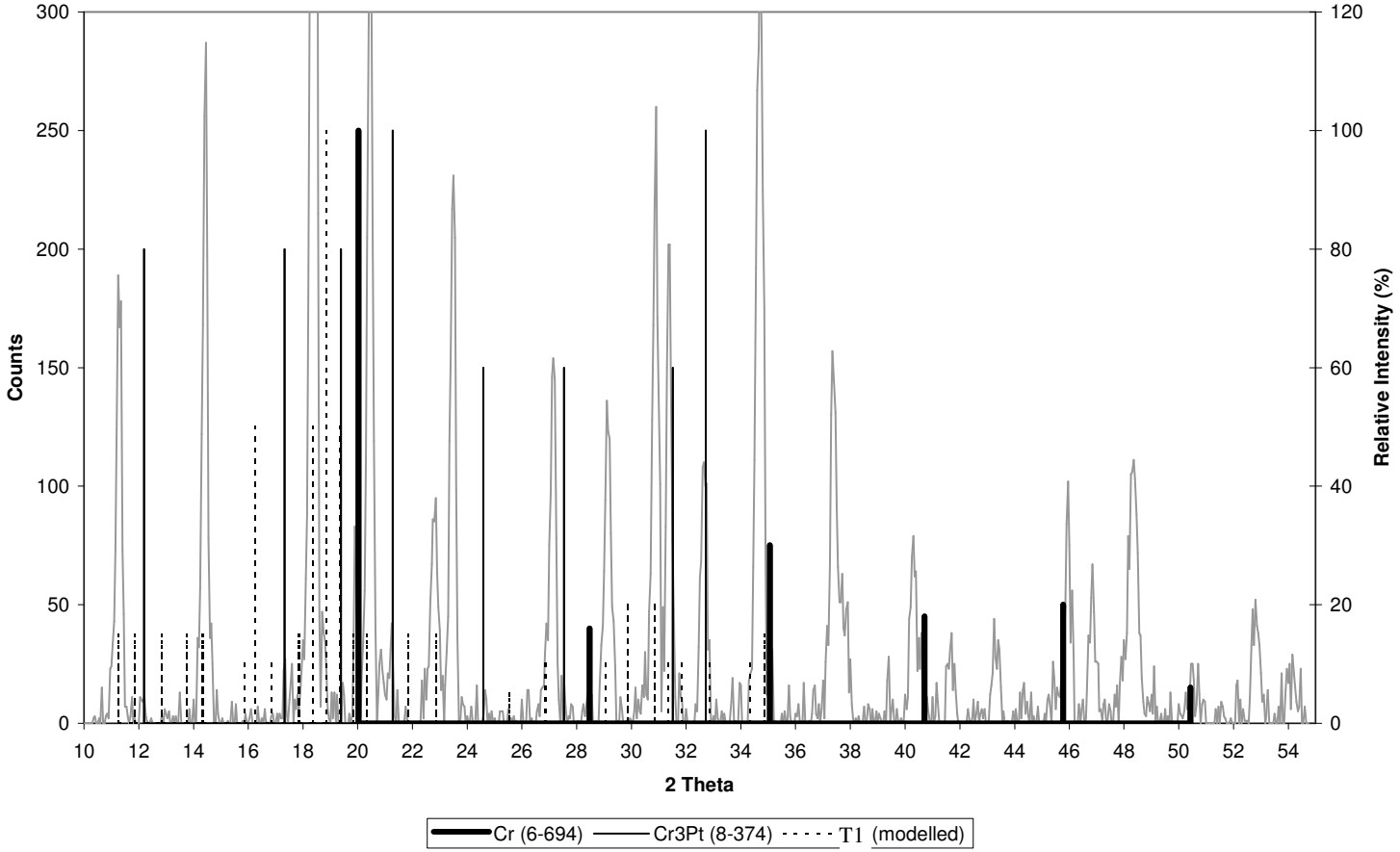

Figure 2.169. XRD pattern for nominal Pt_{38}:Al_{22}:Cr_{40} after annealing at 1000 °C.

2.1.55. Nominal $Pt_{43}:Al_{52}:Cr_5$

Although still comprising a dark and light phase (Figure 2.170), the appearance of alloy $Pt_{43}:Al_{52}:Cr_5$ changed a lot during annealing. The black spots appeared to be porosity, which are often associated with substitutional diffusion. These EDX analyses are given in Table 2.56 and Figure 2.171. Note that the black spots seen are porosity, but that both analysis under SEM and microprobe confirmed a Cr-rich phase being at the bottom of these pores. The microprobe analysis confirmed that no oxide was present. However, it must be noted that the black spots were too small to yield accurate analyses, being smaller than the potential ~3µm size of beam spread on interaction and that their analysed compositions would be affected by the surrounding phases. Considering the position of the phase compositions on the ternary plot and the XRD results of the as-cast state (Figure 2.78), what is observed here is a three-phase equilibrium at 1000°C, with the dark phase probably ~PtAl, the light phase ~Pt_2Al_3, and the black spots (Cr) precipitates in both phases. This would agree well with the position of the overall analysis: a Cr-rich phase had to be present. Unfortunately XRD analyses could not be performed on the sample since it crumbled during the procedure of breaking it out of its mount after SEM analyses, but the assessment was consistent with the results of other alloys ($Pt_{30}:Al_{50}:Cr_{20}$ (§ 2.2.3), $Pt_{35}:Al_{55}:Cr_{10}$ (§ 2.2.9) and $Pt_{50}:Al_{35}:Cr_{15}$ (§ 2.2.12)).

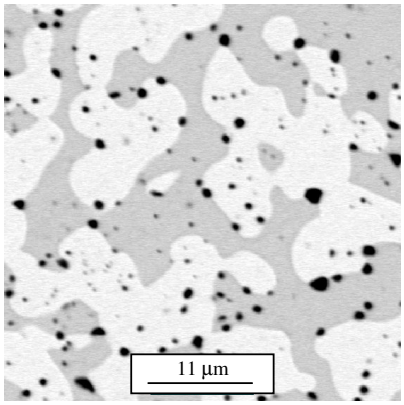

Figure 2.170. BSE-SEM image of nominal $Pt_{43}:Al_{52}:Cr_5$ after annealing at 1000°C: Pores/Cr black; ~ Pt_2Al_3 dark; ~PtAl light.

Table 2.56. Phase analyses for nominal $Pt_{43}:Al_{52}:Cr_5$ (at.%) after annealing at 1000°C.

Phase description	**Pt**	**Al**	**Cr**	**Phase**
Overall	41.4 ± 0.9	53.1 ± 0.3	5.5 ± 0.6	-
Black*	3.7	4.4	91.9	Cr
Dark	39.3 ± 0.3	58.9 ± 0.5	1.8 ± 0.8	~Pt_2Al_3
Light	49.7 ± 0.2	49.6 ± 0.2	0.7 ± 0.4	~PtAl

* Only one measurement taken due to small size.

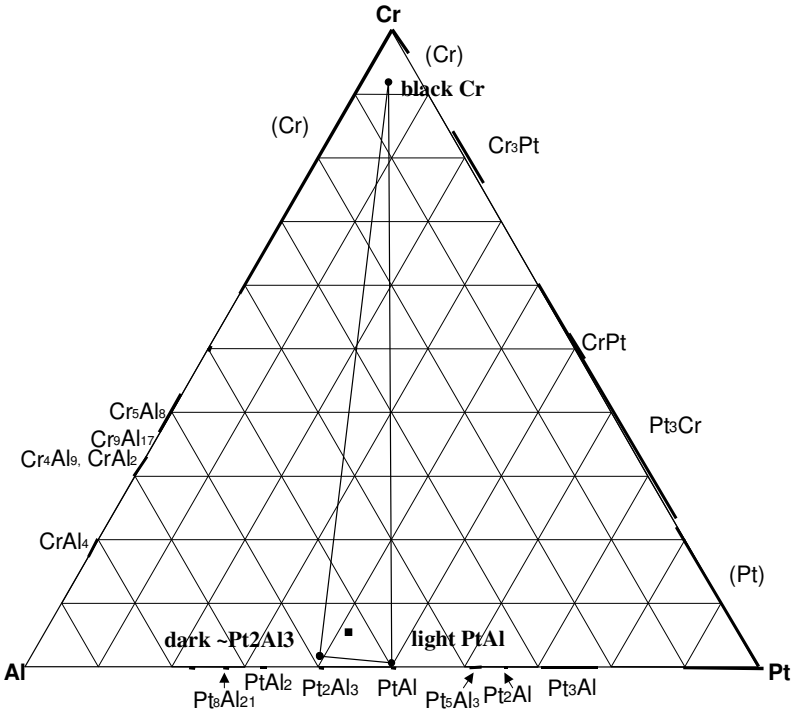

Figure 2.171. EDX analyses of nominal $Pt_{43}:Al_{52}:Cr_5$ (at.%) after annealing at 1000°C. (■ overall composition; ● phases)

2.1.56. Nominal $Pt_{50}:Al_{35}:Cr_{15}$

After annealing at 1000°C, alloy $Pt_{50}:Al_{35}:Cr_{15,}$ clearly had a two-phase structure (Figure 2.172), compared to the cored single phase structure it had in the as-cast state. The EDX analyses showed the difference in composition of the phases (Table 2.57 and Figure 2.173). The large errors in analysis of the overall composition suggested that the alloy was

inhomogeneous, and explained why it did not lie on the tie-line between the phases. Taking into consideration the as-cast results and those of other annealed alloys, the dark phase could be ternary phase T1. The light phase is most probably ~PtAl. XRD analyses clearly detected ~PtAl and T1. Since the XRD pattern is only shown up to 2θ=38 and not the usual 55 (to make the identification of peaks easier), the peaks appear to be broad which is, in fact, not the case, and therefore not indicative of any coring.

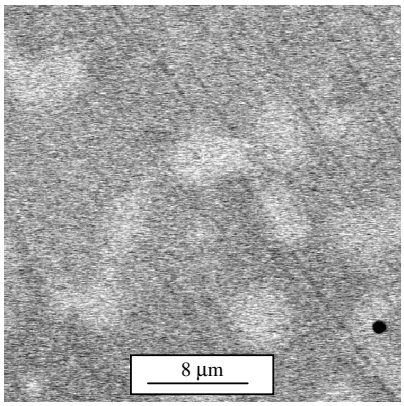

Figure 2.172. BSE-SEM image of nominal Pt_{50}:Al_{35}:Cr_{15} after annealing at 1000°C: T1 dark; ~PtAl light.

Table 2.57. Phase analyses for nominal Pt_{50}:Al_{35}:Cr_{15} (at.%) after annealing at 1000°C.

Phase description	**Pt**	**Al**	**Cr**	**Phase**
Overall	50.0 ± 0.5	36.9 ± 2.0	13.1 ± 1.8	-
Dark	52.2 ± 0.0	29.3 ± 0.1	18.5 ± 0.1	T1
Light	50.0 ± 0.2	49.6 ± 0.2	0.4 ± 0.1	~PtAl

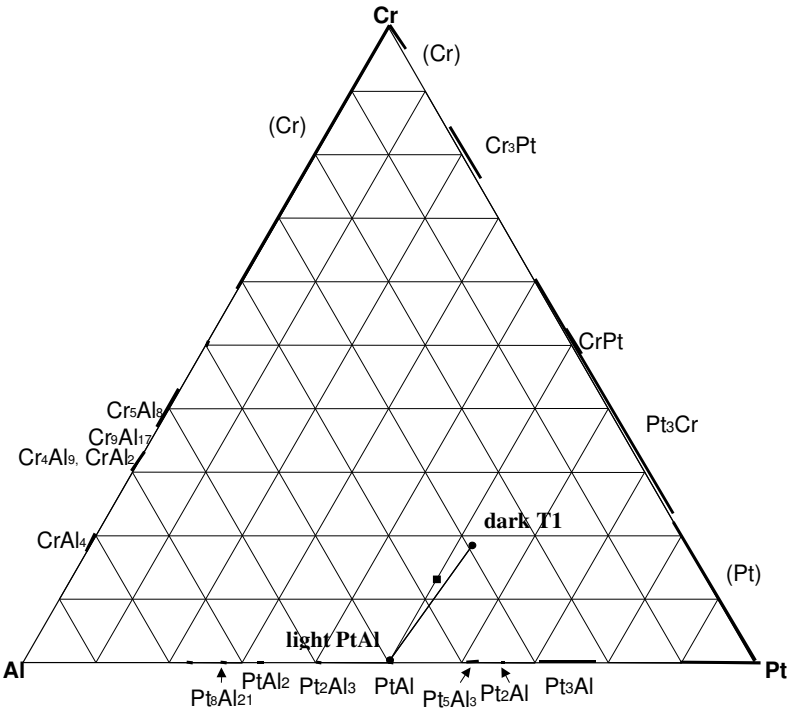

Figure 2.173. EDX analyses of nominal Pt_{50}:Al_{35}:Cr_{15} (at.%) after annealing at 1000 °C.

(■ overall composition; ● phases)

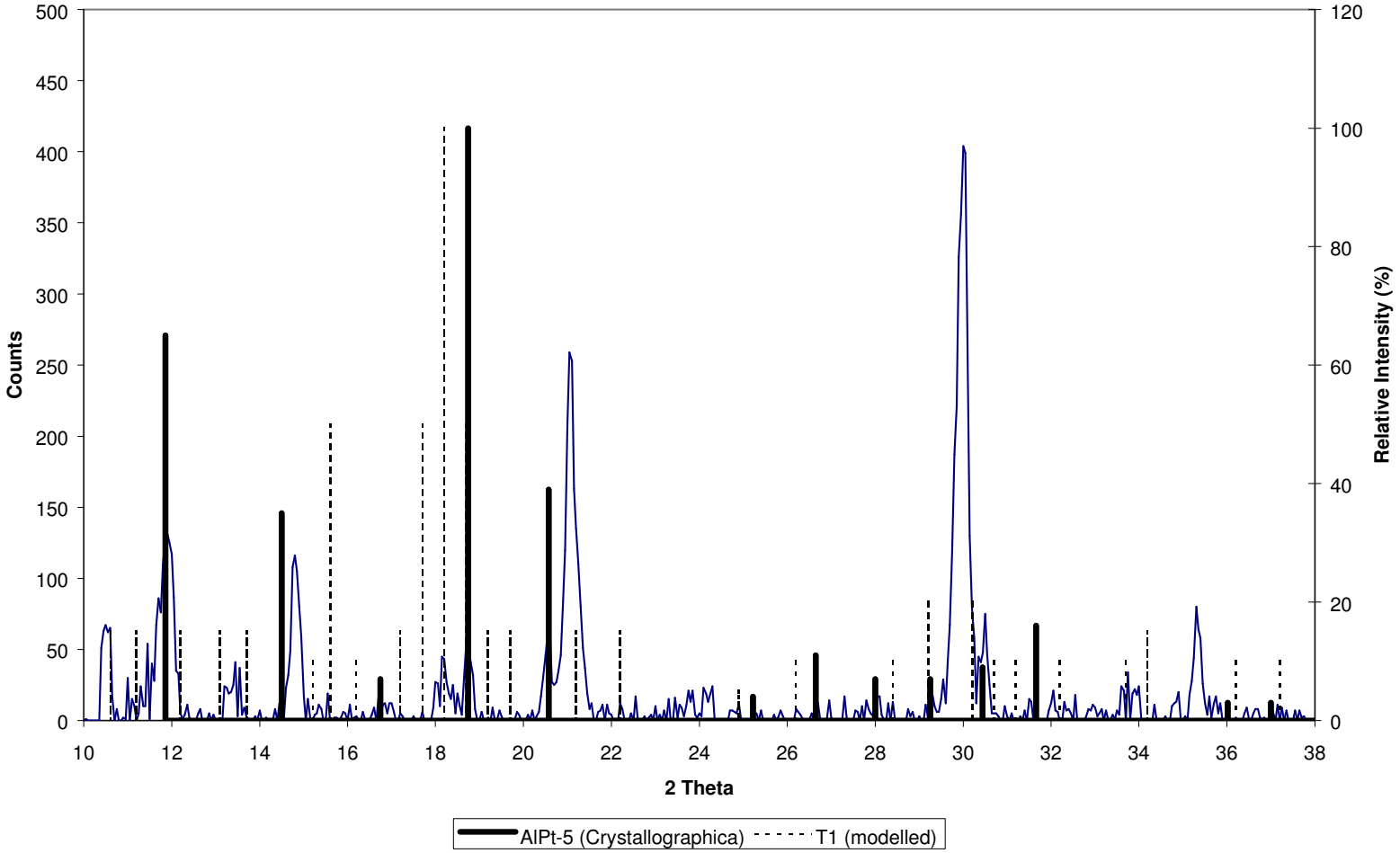

Figure 2.174. XRD pattern for nominal Pt_{50}:Al_{35}:Cr_{15} after annealing at 1000 °C.

2.1.57. Nominal $Pt_{58}:Al_{10}:Cr_{32}$

Like in the as-cast state, alloy $Pt_{58}:Al_{10}:Cr_{32}$ showed a dark and light phase, with the amount of light phase much less than before annealing at 1000°C, but easier to distinguish (Figure 2.175 vs. Figure 2.82). The light phase would probably disappear totally on further annealing. The EDX analyses of the alloy and its phases are shown in Table 2.58 and Figure 2.176. It was interesting to see that the direction of the tie-line had changed compared to that of the as-cast sample (the as-cast sample's overall composition had also been far off the tie-line). XRD analyses of alloy $Pt_{58}:Al_{10}:Cr_{32}$ in the as-cast state (Figure 2.84) showed that the dark and light phases were probably $L1_0$ ~CrPt and ~Pt_3Al respectively. XRD analyses of the annealed alloy showed the same results (Figure 2.177). This would tie in with the results of alloys $Pt_{50}:Al_{10}:Cr_{40}$ (§ 2.2.4) and $Pt_{50}:Al_{10}:Cr_{40}$ (§ 2.2.5).

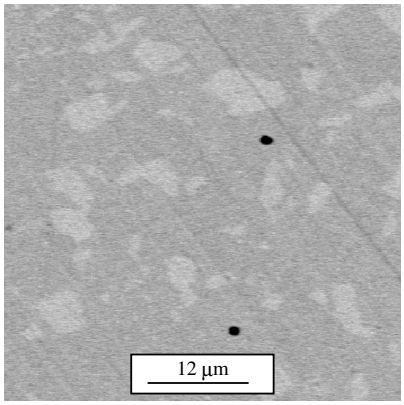

Figure 2.175. BSE-SEM image of nominal $Pt_{58}:Al_{10}:Cr_{32}$ after annealing at 1000°C: ~CrPt dark; ~Pt_3Al light; black porosity.

Table 2.58. Phase analyses for nominal $Pt_{58}:Al_{10}:Cr_{32}$ (at.%) after annealing at 1000°C.

Phase description	**Pt**	**Al**	**Cr**	**Phase**
Overall	58.2 ± 0.3	10.4 ± 0.8	31.4 ± 0.8	-
Dark	59.0 ± 0.3	9.3 ± 1.2	31.7 ± 1.3	~ CrPt
Light	62.5 ± 0.5	10.1 ± 0.4	27.4 ± 0.5	~Pt_3Al

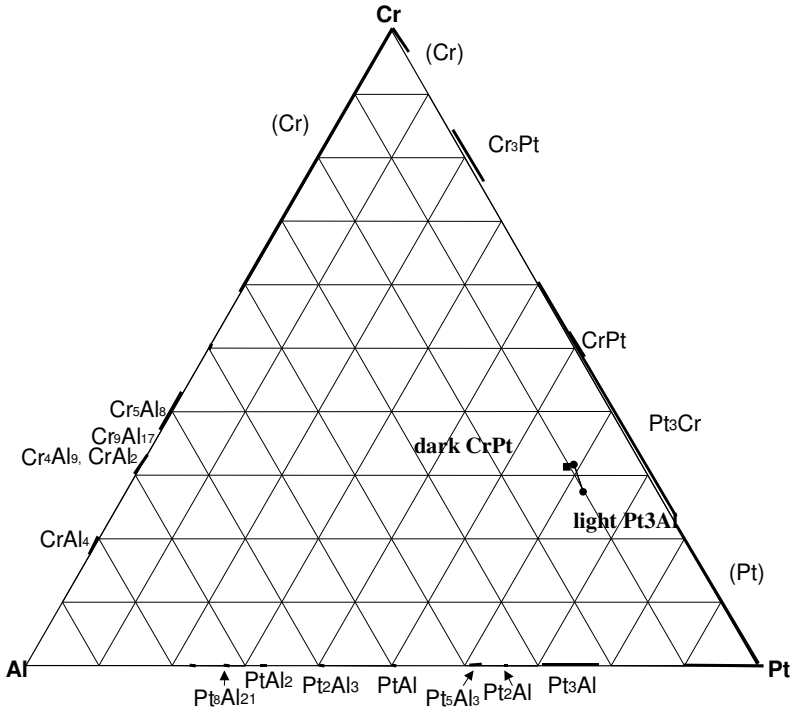

Figure 2.176. EDX analyses of nominal Pt_{58}:Al_{10}:Cr_{32} at.%) after annealing at 1000°C. (■ overall composition; ● phases)

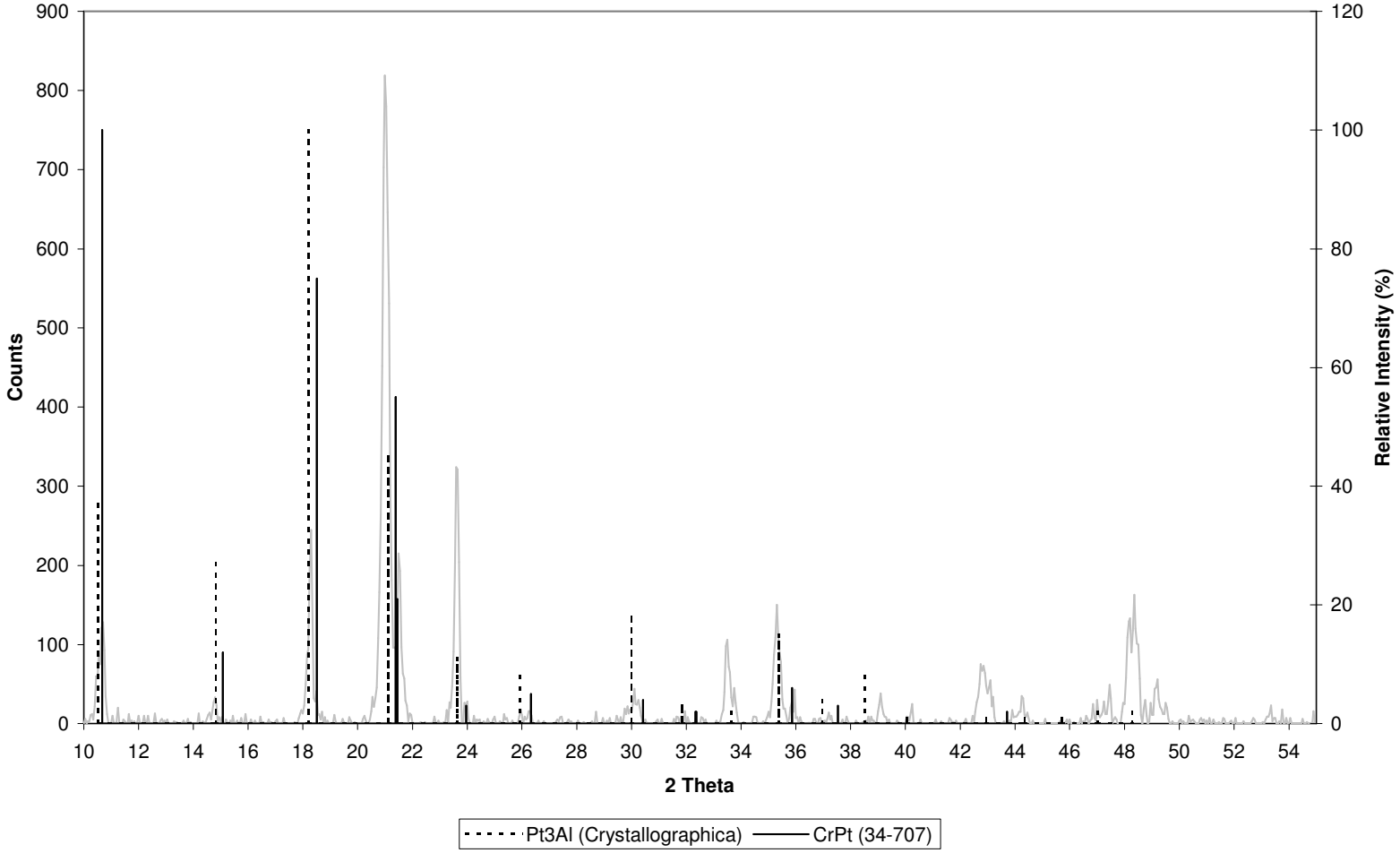

Figure 2.177. XRD pattern for nominal Pt_{58}:Al_{10}:Cr_{32} after annealing at 1000 ℃.

2.1.58. Nominal $Pt_{63}:Al_{32}:Cr_5$

In the as-cast state, alloy $Pt_{63}:Al_{32}:Cr_5$ had appeared single phase, but with image manipulation it had been obvious that more than one phase was present. During annealing at 1000°C though, the second phase disappeared. Figure 2.178 shows a single-phase alloy. The EDX analyses showed that the overall area analyses and random spot analyses were the same (Table 2.59, Figure 2.179). The alloy comprised ~Pt_2Al. The measured XRD pattern did not show as many peaks as the other alloys, indicating that it was single phase. Superposing the XRD peaks of C23 (LT) ~Pt_2Al onto it resulted in an acceptable match, considering the shift expected as a result of the Cr (Figure 2.180).

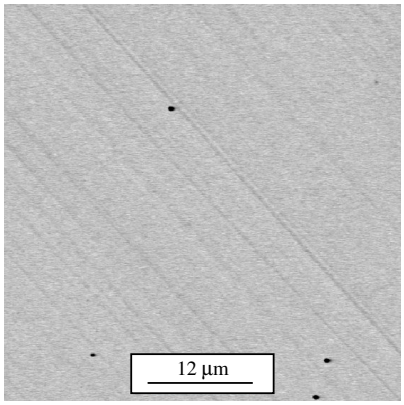

Figure 2.178. BSE-SEM image of nominal $Pt_{63}:Al_{32}:Cr_5$ after annealing at 1000°C: ~Pt_2Al grey.

Table 2.59. Phase analyses for nominal $Pt_{63}:Al_{32}:Cr_5$ (at.%) after annealing at 1000°C.

Phase description	**Pt**	**Al**	**Cr**	**Phase**
Overall	62.2 ± 0.6	33.1 ± 0.7	4.7 ± 0.2	-
Grey	63.7 ± 0.6	32.0 ± 0.8	4.3 ± 0.5	~Pt_2Al

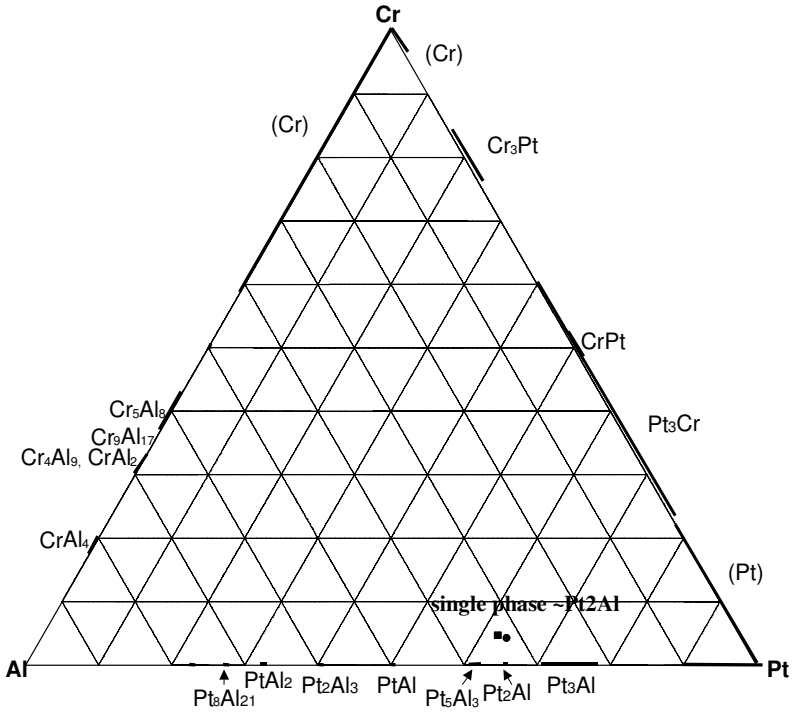

Figure 2.179. EDX analyses of nominal $Pt_{63}:Al_{32}:Cr_5$ (at.%) after annealing at 1000°C.

(■ overall composition; ● phases)

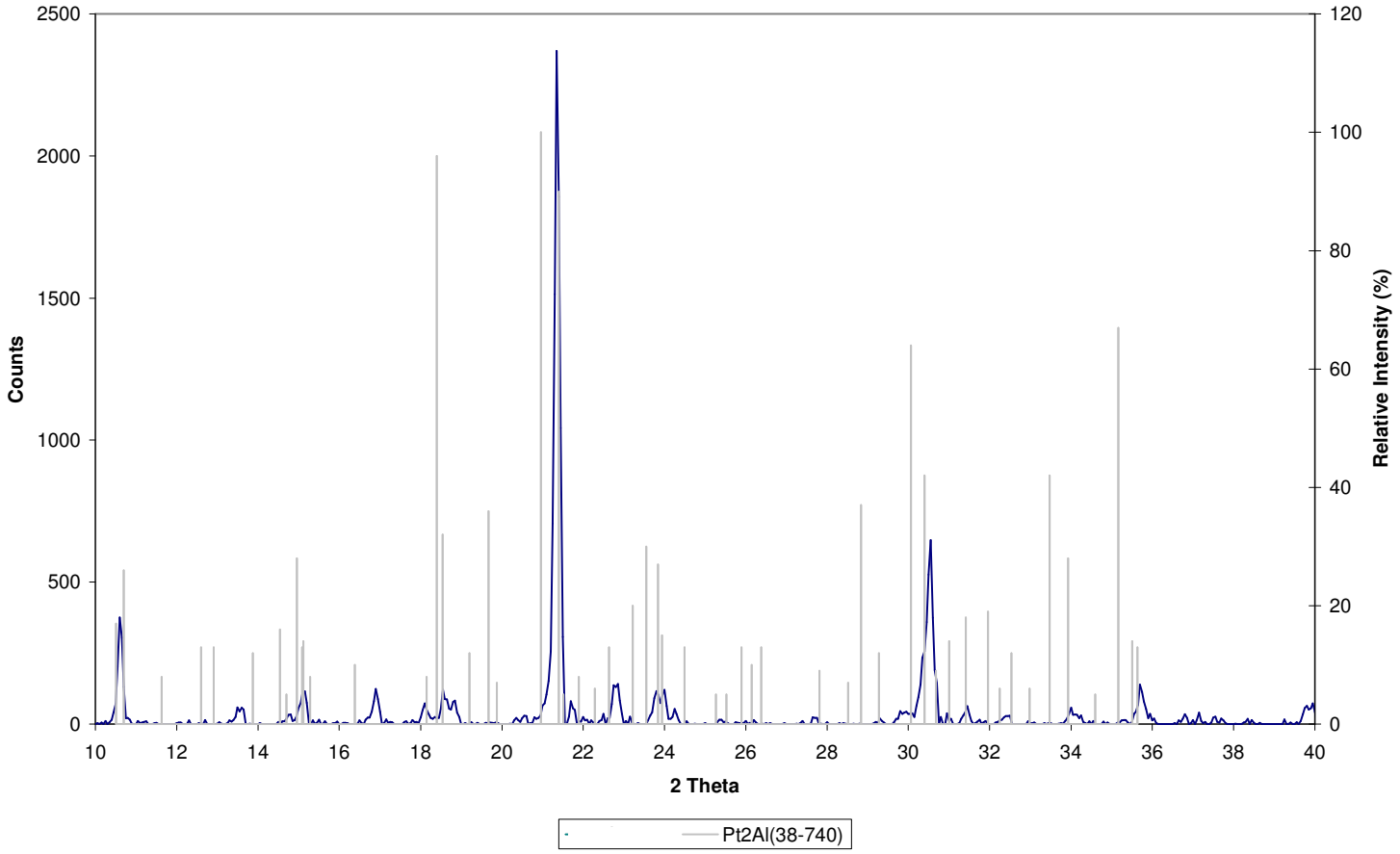

Figure 2.180. XRD pattern for nominal $Pt_{63}:Al_{32}:Cr_5$ after annealing at 1000℃.

2.1.59. Nominal $Pt_{63}:Al_{22}:Cr_{15}$

As was the case for alloy $Pt_{63}:Al_{22}:Cr_{15}$ in the as-cast state (Figure 2.91), it looked like a single phase alloy after annealing at 1000°C, but with digital image manipulation a contrast was obtained between dark and lighter regions, showing a dendritic morphology (Figure 2.171). The image manipulation also revealed a plate-like structure in the dark phase. The tiny particles of white phase seen in the as-cast state had disappeared. The results of the EDX analyses showed that the compositions of the two phases were very different (Table 2.60, Figure 2.182). The overall analyses of the alloy was not on the tie-line, probably due to the fact that the analyses of the light phase, which was difficult to do, was not accurate. The light phase was probably ~Pt_2Al, considering its position on the ternary plot. The dark phase was probably either ~Pt_3Cr or ~Pt_3Al. Superposing the XRD peaks of C23 ~Pt_2Al (LT) (with shift) and $L1_2$ ~Pt_3Al onto the measured XRD pattern resulted in quite a good fit (Figure 2.183). This would agree with alloy $Pt_{58}:Al_{10}:Cr_{32}$ (§ 2.2.13)and $Pt_{65}:Al_5:Cr_{30}$ (§ 2.2.5) containing ~Pt_3Al and not ~Pt_3Cr.

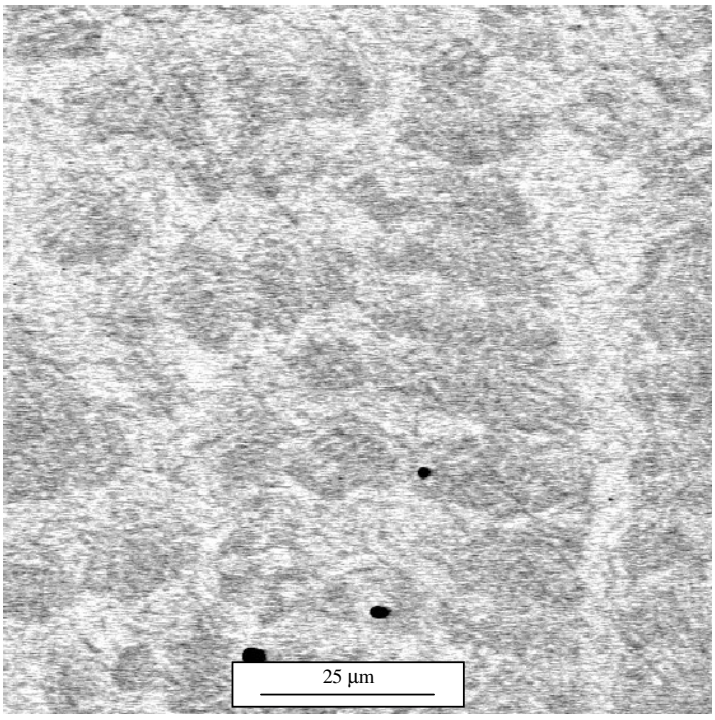

Figure 2.181. BSE-SEM image of nominal $Pt_{63}:Al_{22}:Cr_{15}$ after annealing at 1000°C: ~Pt_2Al light ~Pt_3Al dark.

Table 2.60. Phase analyses for nominal $Pt_{63}:Al_{22}:Cr_{15}$ (at.%) after annealing at 1000°C.

Phase description	**Pt**	**Al**	**Cr**	**Phase**
Overall	63.3 ± 0.8	22.1 ± 1.1	14.6 ± 1.0	-
Dark	64.8 ± 0.3	15.0 ± 0.5	20.2 ± 0.5	~Pt_3Al
Light	64.3 ± 0.2	28.2 ± 0.3	7.5 ± 0.5	~Pt_2Al

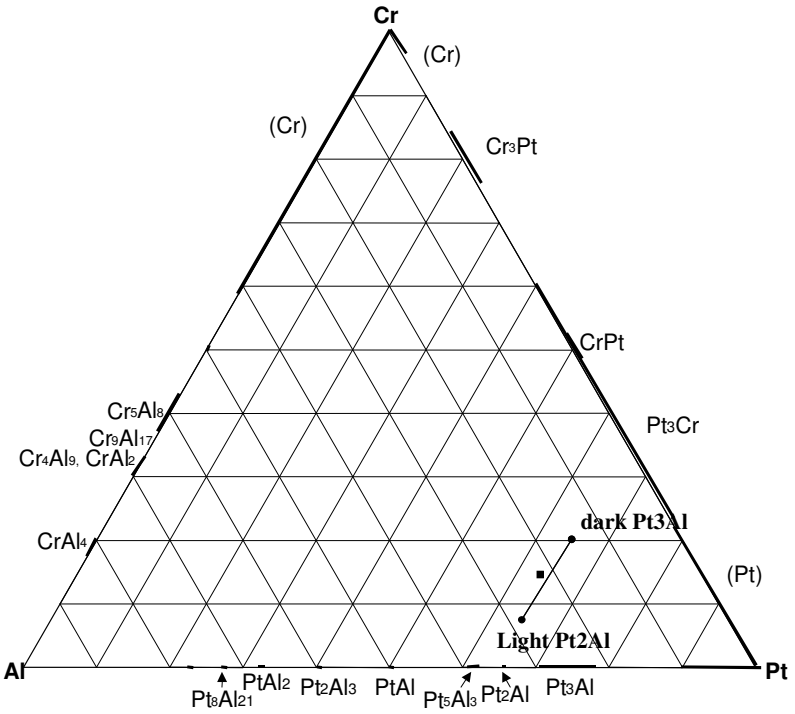

Figure 2.182. EDX analyses of nominal $Pt_{63}:Al_{22}:Cr_{15}$ (at.%) after annealing at 1000°C.

(■ overall composition; ● phases)

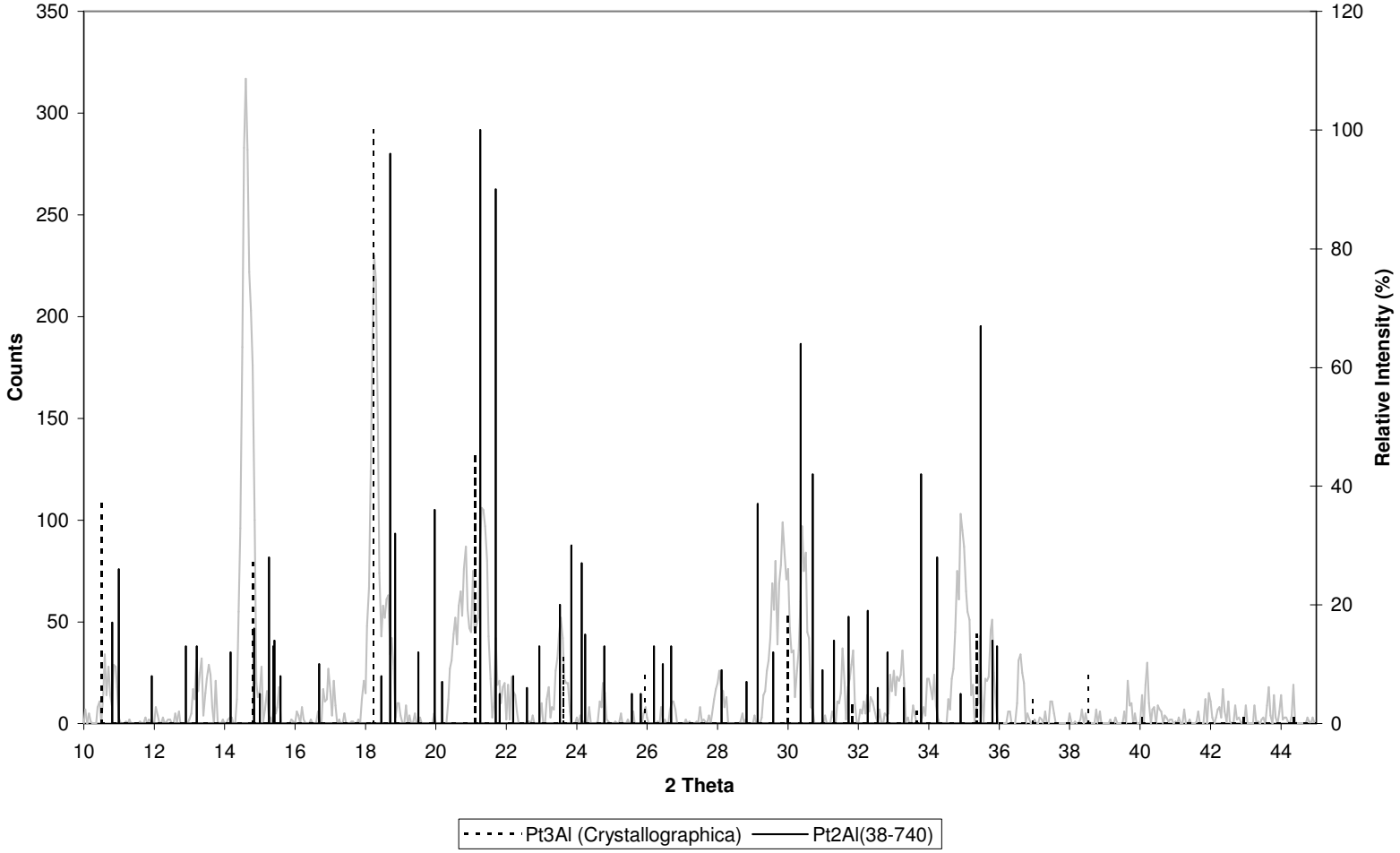

Figure 2.183. XRD pattern for nominal $Pt_{63}:Al_{22}:Cr_{15}$ after annealing at 1000°C.

2.1.60. Nominal $Pt_{75}:Al_{10}:Cr_{15}$

This alloy had previously been shown to be $Pt_{34}:Al_{49}:Cr_{17}$ from Pt losses due to sputtering during melting (§ 2.1.30). Its appearance changed considerably during annealing at 1000°C. It comprised a dark phase (dendrites) with a small amount of interdendritic light phase (Figure 2.184), compared to a large amount of an interdendritic eutectic in the as-cast condition (Figure 2.97). The alloy was similar in appearance to $Pt_{35}:Al_{55}:Cr_{10}$ (§ 2.2.9) and $Pt_{30}:Al_{50}:Cr_{20}$ (§ 2.2.3). The EDX analyses are shown in Table 2.61 and Figure 2.185. The small black spots were confirmed by both SEM and microprobe to be a metallic phase, and not porosity or an oxide. However, they were too small for accurate measurement, and only one was analysed to get an indication of its primary constituent, which was found to be Cr. The black was thus identified as (Cr). The composition of the white phase would suggest that it is probably ~PtAl, while the grey phase could be either ~$PtAl_2$ or ~Pt_2Al_3. Unfortunately, XRD analyses could not be performed on the sample since it crumbled during the procedure of breaking it out of its mount after SEM analyses. However, considering the results of alloys $Pt_{43}:Al_{52}:Cr_5$ (§ 2.2.11), $Pt_{35}:Al_{55}:Cr_{10}$ (§ 2.2.9) and $Pt_{30}:Al_{50}:Cr_{20}$ (§ 2.2.3), the grey phase was likely to be ~Pt_2Al_3 rather than ~$PtAl_2$. Thus, not only had the appearance of the alloy changed during annealing, but also the phase quantities. The standard deviation in measured composition for the grey phase was surprisingly large (especially the Cr-content), considering that the grey areas were large.

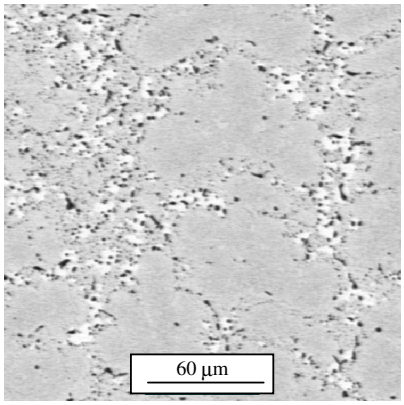

Figure 2.184. BSE-SEM image of nominal $Pt_{34}:Al_{49}Cr_{17}$ after annealing at 1000°C: (Cr) black; ~Pt_2Al_3 grey; ~PtAl white.

Table 2.61. Phase analyses for nominal $Pt_{34}:Al_{49}Cr_{17}$ (at.%) after annealing at 1000°C.

Phase description	**Pt**	**Al**	**Cr**	**Phase**
Overall	33.0 ± 0.7	50.7 ± 0.8	16.3 ± 1.4	-
Black*	2.1	2.6	95.3	(Cr)
White	48.8 ± 0.8	50.0 ± 0.9	1.2 ± 0.1	~PtAl
Grey	34.1 ± 1.1	51.1 ± 1.1	14.8 ± 2.2	~ Pt_2Al_3

* Only one measurement taken due to small size.

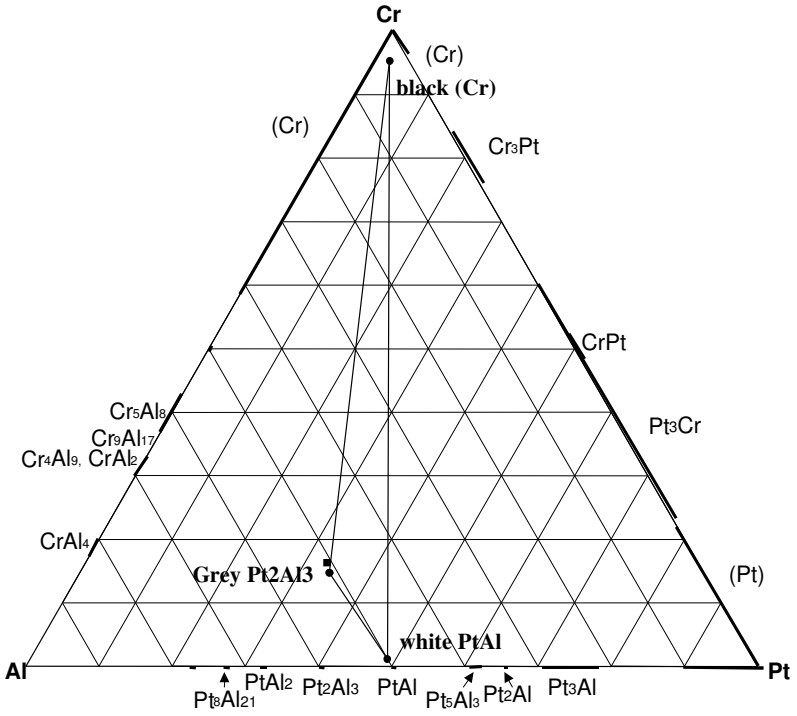

Figure 2.185. EDX analyses of nominal $Pt_{34}:Al_{49}Cr_{17}$ (at.%) after annealing at 1000°C. (■ overall composition; ● phases; ✶ eutectic)

2.1.61. Nominal $Pt_{15}:Al_5:Cr_{80}$

At lower magnification, alloy $Pt_{15}:Al_5:Cr_{80}$ was similar to its as-cast state in the fact that it comprised three phases: dark dendrites, with a medium (grey) interdendritic phase as well as some small light (white) areas (Figure 2.186a). Higher magnification revealed that the white phase was always located in the grey interdendritic phase, as was the case before annealing at 1000°C. However, it was revealed that the dark dendrites were in fact a two-phase mixture of black and grey. The EDX analyses are given in Table 2.62 and Figure 2.187. The microstructure was very fine, and the phase analyses would have been affected by surrounding phases (except for the two-phase regions). However, the ternary plot made the identification of the phases easy, with the black phase most probably (Cr), grey ~Cr_3Pt and white ~PtAl – very different to the phases in the as-cast condition (except for (Cr). Fitting these phases' XRD peaks to the measured XRD pattern for the 1000°C annealed alloy, a reasonably good fit was obtained (especially for ~Cr_3Pt), although some peaks (between 2θ=10 and 11, and at $2\theta \approx 15$) were unidentified (Figure 2.188). It is suspected that the white phase is likely to transform to T1 on further annealing, which would be consistent with the results of alloys $Pt_{18}:Al_2:Cr_{80}$ (§ 2.2.8) and $Pt_{38}:Al_{22}:Cr_{40}$ (§ 2.2.10).

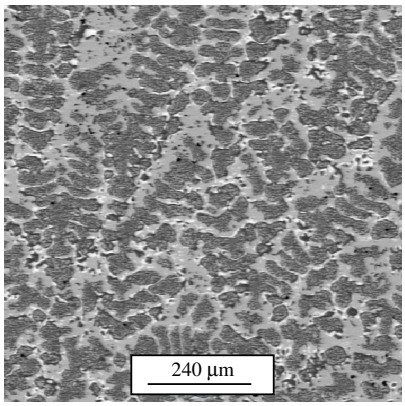

(a)

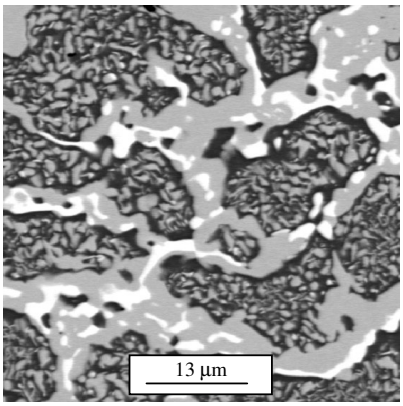

(b)

Figure 2.186. BSE-SEM image of nominal $Pt_{15}:Al_5:Cr_{80}$ after annealing at 1000°C: (Cr) black; ~Cr_3Pt grey; ~PtAl white.

Table 2.62. Phase analyses for nominal $Pt_{15}:Al_5:Cr_{80}$ (at.%) after annealing at 1000°C.

Phase description	**Pt**	**Al**	**Cr**	**Phase**
Overall	13.9 ± 1.1	3.5 ± 0.8	82.6 ± 1.1	-
Black	4.2 ± 2.1	1.1 ± 0.3	94.7 ± 2.4	(Cr)
Grey	24.5 ± 2.8	1.3 ± 0.5	74.2 ± 2.8	~Cr_3Pt
White	47.2 ± 1.2	47.1 ± 1.1	5.7 ± 2.1	~PtAl
Black + grey two-phase	9.1 ± 1.9	1.7 ± 0.5	89.2 ± 2.3	(Cr) + ~Cr_3Pt

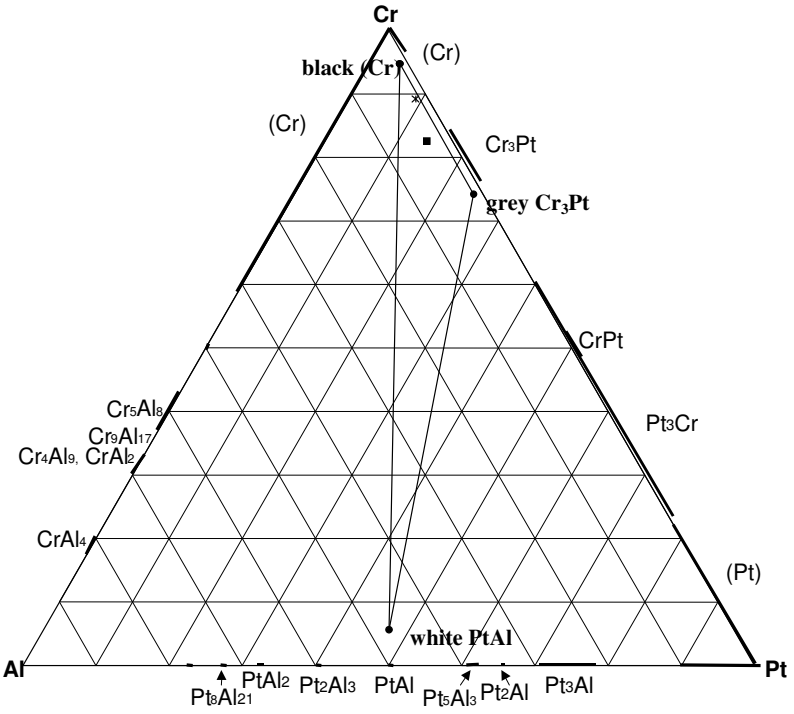

Figure 2.187. EDX analyses of nominal $Pt_{15}:Al_5:Cr_{80}$ (at.%) after annealing at 1000°C. (■ overall composition; ● phases; ✶ two-phase)

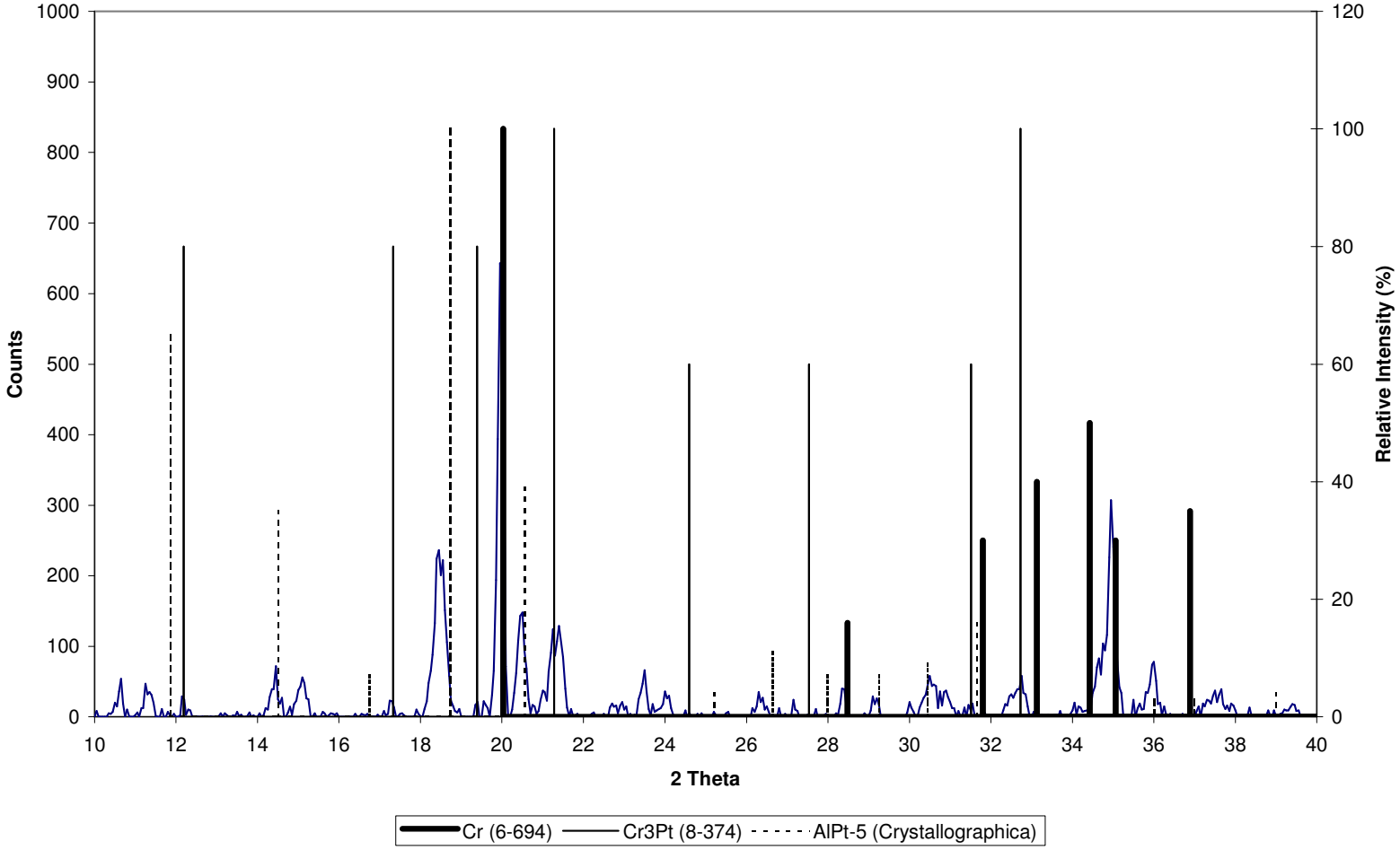

Figure 2.188. XRD pattern for nominal $Pt_{15}:Al_5:Cr_{80}$ after annealing at 1000°C.

2.1.62. Nominal Pt_{55}:Al_{25}:Cr_{20}

Alloy Pt_{55}:Al_{25}:Cr_{20} comprised a dark and a white phase (Figure 2.189) with black porosity. The light phase was much more pronounced than in its as-cast state (Figure 2.124), and the dark phase showed a needle-like structure that had not been observed before annealing at 1000°C (i.e. comprising grey and light). The EDX analyses are given in Table 2.63 and Figure 2.190. The grey component of the dark regions was too fine for analysis, and area analyses were taken of the (grey+light) phases. From the position of the white phase on the ternary diagram, ~Pt_2Al could be a possibility (as in the as-cast state). Since the overall composition does not even lie close to a line connecting the compositions of the white and (grey+light), it suggested that a third phase was present, and also meant that the white phase and light component of the two-phase mixture were not the same phase. The dashed lines in Figure 2.190 show the possible positions of the possible phases. The light phase could be ~Pt_3Al and the grey T1. Another option is to reason that the (grey+white) phase was in fact a single composition and that the morphology was only different due to crystal structural differences after a martensitic-like transformation, but that would not explain why they were different in contrast in back-scattered electron mode. It would still mean that a third phase had to be present to make sense of the overall composition lying so far away from the tie-line. This scenario is sketched in Figure 2.191. It also seemed like the needles actually ran through the white phase as well, which would eliminate the possibility of a martensitic phase change since it is unlikely that the new phase would be able to have a shear relationship with both phases. The first premise is therefore more acceptable. This was confirmed through XRD analyses, which detected C23 ~Pt_2Al (LT), $L1_2$ ~Pt_3Al and T1, with these phases' XRD peaks matching the measured pattern quite well (Figure 2.192). This assessment would agree with that of alloy Pt_{63}:Al_{22}:Cr_{15} (§ 2.2.15).

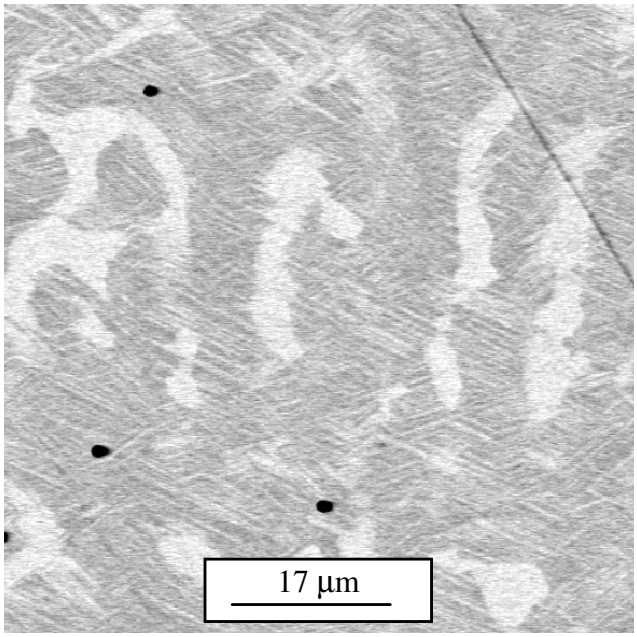

Figure 2.189. BSE-SEM image of nominal $Pt_{55}:Al_{25}:Cr_{20}$ after annealing at 1000°C: (T1 + ~Pt_3Al) dark; ~Pt_2Al white.

Table 2.63. Phase analyses for nominal $Pt_{55}:Al_{25}:Cr_{20}$ (at.%) after annealing at 1000°C.

Phase description	**Pt**	**Al**	**Cr**	**Phase**
Overall	55.6 ± 1.0	27.1 ± 1.1	17.3 ± 0.9	-
Light + grey	58.8 ± 1.1	24.2 ± 0.0	17.0 ± 1.1	~Pt_3Al + T1
White	62.2 ± 1.4	30.7 ± 1.7	7.1 ± 2.3	~Pt_2Al

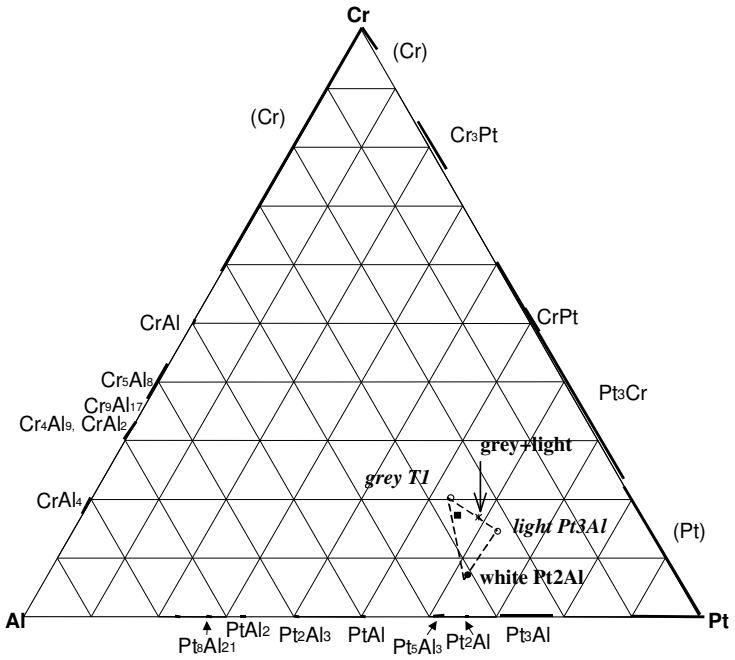

Figure 2.190. EDX analyses of nominal $Pt_{55}:Al_{25}:Cr_{20}$ (at.%) after annealing at 1000°C. (■ overall composition; ● phases; ✶ two-phase; o suggested phase compositions in one possible (preferred) *scenario).*

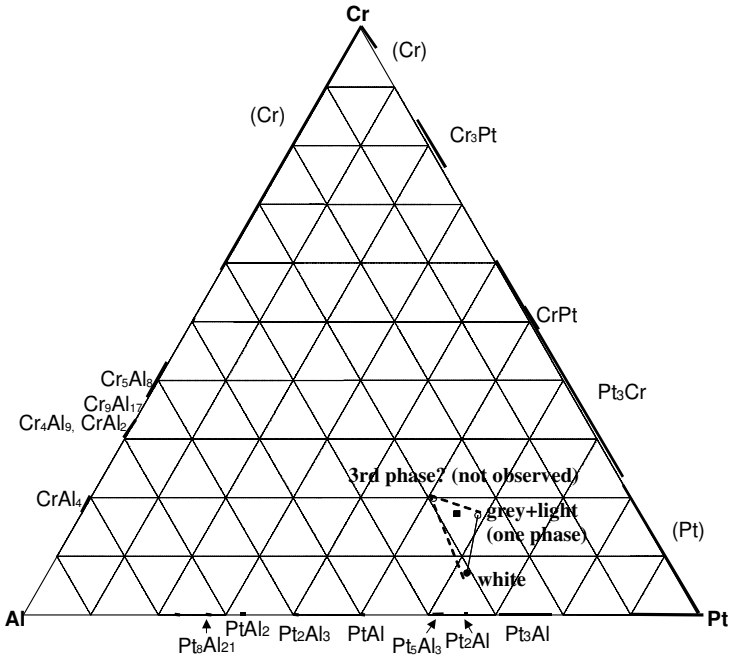

Figure 2.191. EDX analyses of nominal $Pt_{55}:Al_{25}:Cr_{20}$ (at.%) after annealing at 1000°C. (■ overall composition; ● phases; o suggested phase compositions in another possible scenario))

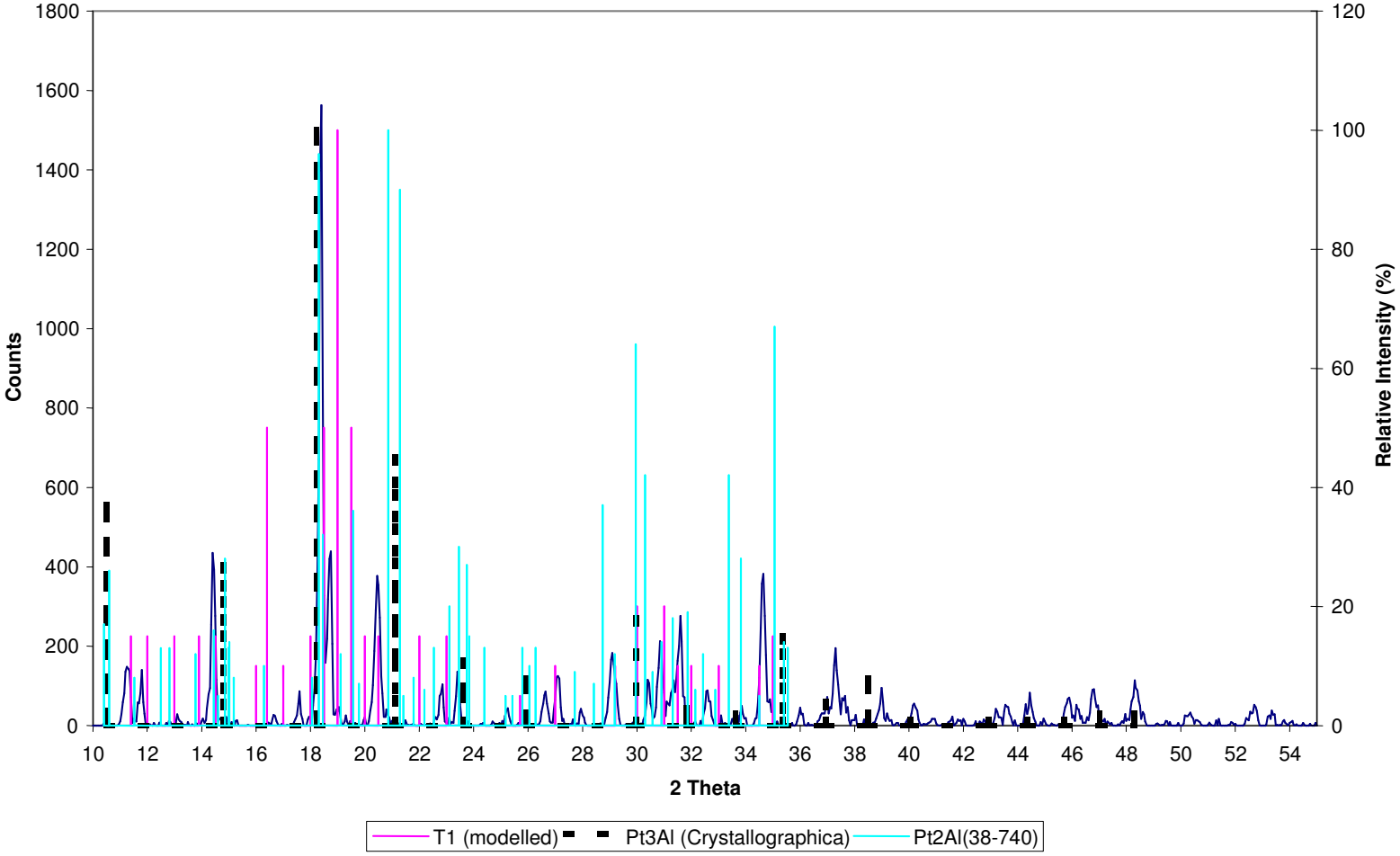

Figure 2.192. XRD pattern for nominal Pt_{55}:Al_{25}:Cr_{20} after annealing at 1000℃.

2.1.63. 1000 ℃ Isothermal Section

An isothermal section at 1000°C was drawn, based on a combination of all the results as discussed in the previous section. The diagram is shown in Figure 2.193. The phase fields of ~Pt_2Al, ~Pt_2Al_3, ~PtAl and especially T1 appeared to have significantly reduced in size due to annealing, which is expected. Tie-lines should not cross in an isothermal section, therefore the ~Cr_3Pt/~PtAl tie-line of alloy Pt_{15}:Al_5:Cr_{80} (§ 2.2.17) that would have cut across those of other alloys, is probably the result of non-equilibrium of that alloy, and shows that the white ~PtAl phase would probably transform to T1, as supported by alloys Pt_{18}:Al_2:Cr_{80} (§ 2.2.8) and Pt_{38}:Al_{22}:Cr_{40} (§ 2.2.10). The isothermal section also shows that the structure of laths in alloy ~Pt_{55}:Al_{25}:Cr_{20} is unlikely to be a single composition since it would be inconsistent with the rest of the data. Furthermore, the composition of the grey phase that is thought to be ~Pt_2Al_3 (Pt_{34}:$Al_{51}Cr_{15}$) in alloy Pt_{34}:$Al_{49}Cr_{17}$ (§ 2.2.16) seems to be inconsistent with the results of other alloys, but the EDX did show large errors in analysis. The lower Cr content values for ~Pt_2Al_3 of alloys Pt_{30}:$Al_{50}Cr_{20}$ and Pt_{35}:$Al_{55}Cr_{10}$ were rather taken. The measured XRD patterns of many of the alloys with phases containing more than 50% at.% Pt have been complicated.

Since (Al) would not be stable at 1000°C, and taking into account the highly probable liquation that occurred in alloy Pt_{10}:Al_{80}:Cr_{10} (§ 2.2.2), a liquid boundary at 1000°C is suggested as indicated by the dashed line in Figure 2.193, based on the results of alloy Pt_{10}:Al_{80}:Cr_{10}.

Similar to the solidification projection, a ~CrPt/~Pt_3Cr boundary is shown as a dashed line. Around this boundary it will be difficult to predict whether the ~Pt_3Cr will order to form $L1_0$ ~CrPt at lower temperatures (below ~700°C) or not. None of the alloys that were annealed at 1000°C showed either ~Pt_3Cr or (Pt), and the position of the boundary is based on the still generally accepted binary Pt-Cr phase diagram given Massalski [1990Mas]. If the diagram of Zhao et al. is correct [2005Zhao], the dashed line in Figure 2.193 would not denote an actual phase boundary, but the estimated position of the ~CrPt/~Pt_3Cr two-phase region shown in Figure 1.2.

Much of the data were re-assessed to check consistency, and the current interpretation as seen in Figure 2.193 seems to be the most sensible and the diagram is self-consistent and reasonably complete.

The extensions of the phases were determined to be:

- (Cr): ~ 40 at.% Al max., ~4 at.% Pt max.;
- ~Cr_3Pt: ~ 3 at.% Al;
- ~CrPt [$L1_0$]: ~ 12 at.% Al;
- (Pt): ~11 at.% Al max., ~ 20-30 at.% Cr depending on where ordering occurs;
- ~Pt_3Al [$L1_2$]: ~31 at.% Cr;
- ~Pt_2Al [HT & LT]: ~9 at.% Cr;
- ~PtAl [B20]: ~ 1 at.% Cr;
- ~Pt_2Al_3: ~3 at.% Cr;
- ~$PtAl_2$: ~15 at.% Cr;
- ~$CrAl_5$: ~ 5 at.% Pt;
- T1: ~Pt_3Al_2Cr with ~6 at.% stability range.

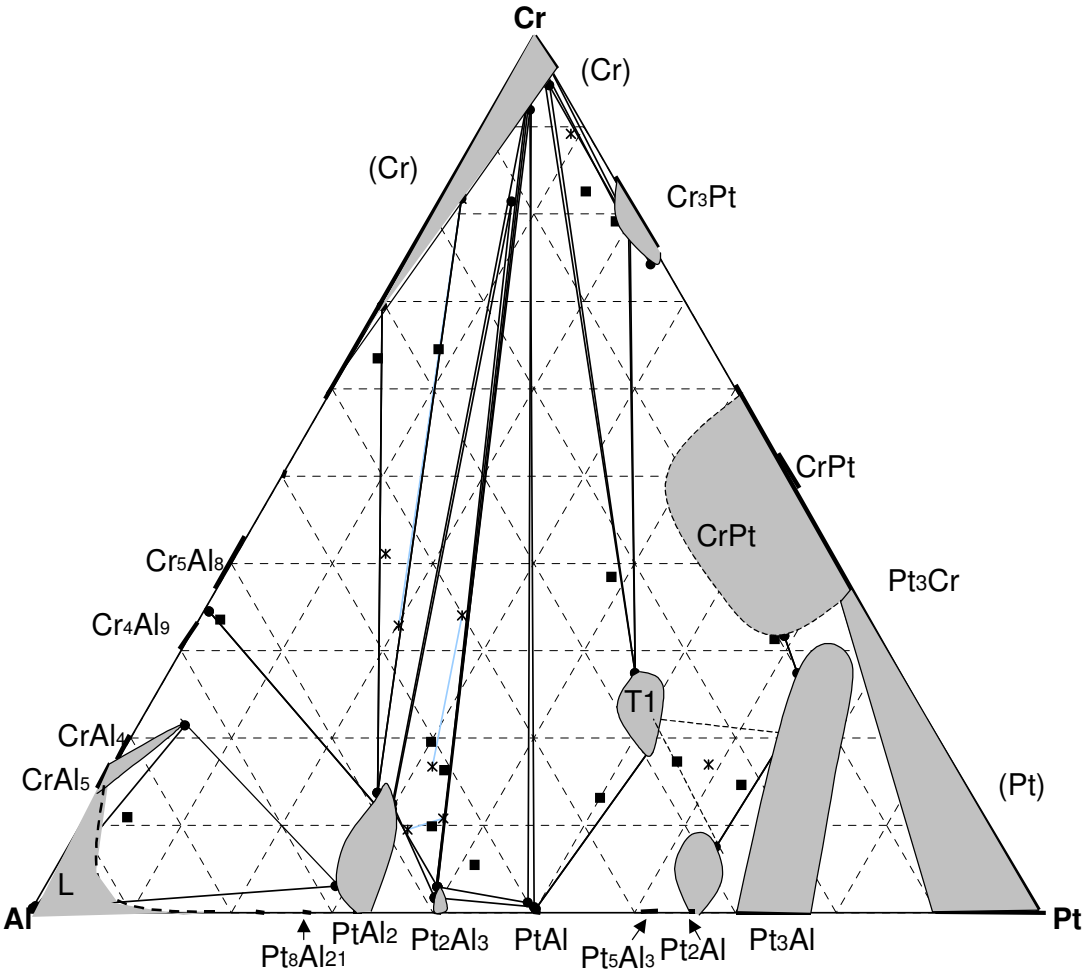

Figure 2.193. 1000 °C isothermal section for Pt-Al-Cr.

2.3. Phase analysis – annealed at 600°C for 2500 hours

Please note that none of the alloys with more than ~75 at.% Al were annealed at 600°C because all these alloys were brittle in the as-cast condition and shattered during the process of breaking them out of the mount for further experimentation.

2.1.64. Nominal Pt_{10}:Al_{30}:Cr_{60}

Almost identical to its structure in the as-cast and 1000°C annealed conditions, alloy Pt_{10}:Al_{30}:Cr_{60} comprised dark dendrites, with an interdendritic eutectic mixture of dark and light phases (Figure 2.194). Unlike in the other conditions, light precipitates were not present in the dark dendrites after annealing at 600°C. Since the structure hardly changed during annealing, it is probable that 2500 hours were not enough to reach equilibrium at 600°C (while 1000 hours had been enough at 1000°C). The results of the EDX analyses are given in Table 2.64 and shown graphically in Figure 2.195. The analyses of the white phase could be affected by the surrounding phase because of its small size, but areas with ~3µm cross-sections were chosen for analyses. XRD analyses of the as-cast and 1000°C annealed samples showed that the dark phase was (Cr) and the white phase ~$PtAl_2$, and the positions of the phase compositions at 600°C on the ternary diagram would concur with that. The XRD analyses of the 600°C annealed sample confirmed that the identities of the phases have not changed (Figure 2.196), with both these phases' shifted XRD peaks being a very good fit to the measured XRD pattern.

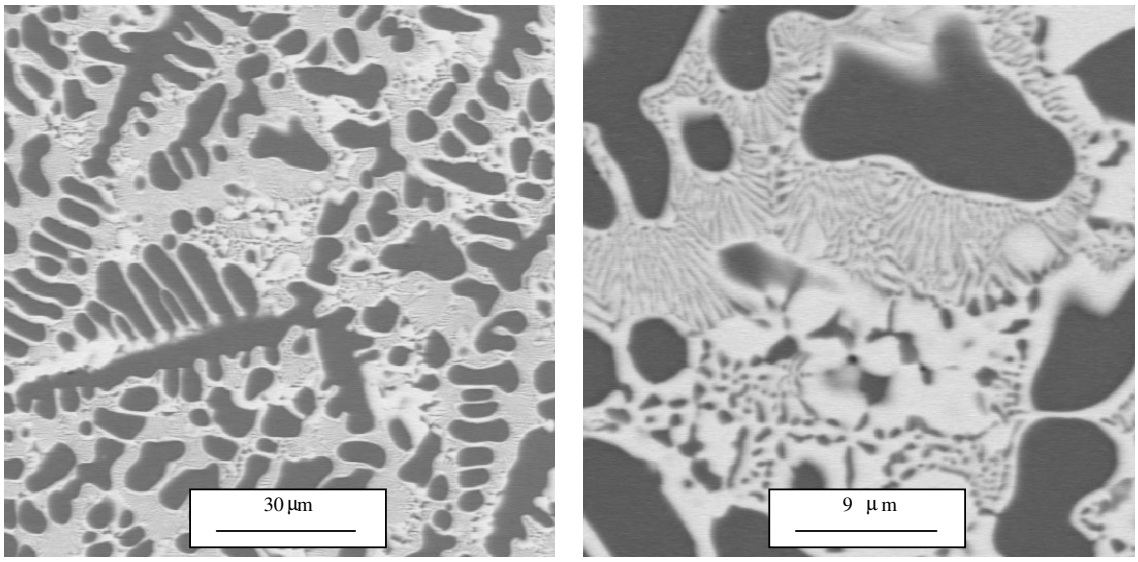

Figure 2.194. BSE-SEM image of nominal $Pt_{10}:Al_{30}:Cr_{60}$ after annealing at 600°C: (Cr) dark; ~$PtAl_2$ light.

Table 2.64. Phase analyses for nominal $Pt_{10}:Al_{30}:Cr_{60}$ (at.%) after annealing at 600°C.

Phase description	**Pt**	**Al**	**Cr**	**Phase**
Overall	10.0 ± 0.8	31.3 ± 1.4	58.7 ± 2.1	-
Dark	1.9 ± 0.1	19.1 ± 0.4	79.0 ± 0.5	(Cr)
Light	25.3 ± 0.1	54.1 ± 0.2	20.6 ± 0.2	~$PtAl_2$
Dark + light	19.1 ± 0.6	43.6 ± 1.2	37.3 ± 1.8	(Cr) + ~$PtAl_2$

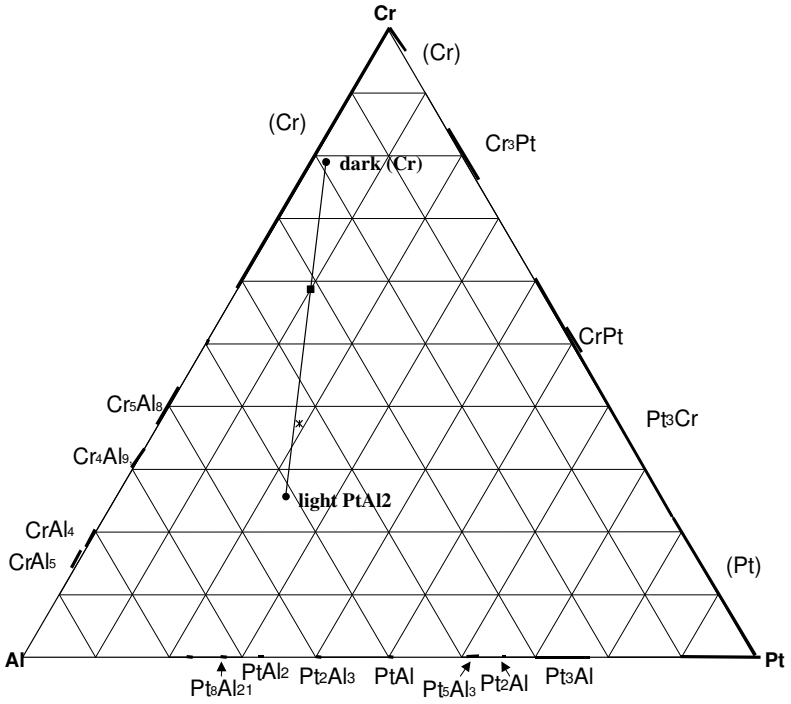

Figure 2.195. EDX analyses of nominal $Pt_{10}:Al_{30}:Cr_{60}$ (at.%) after annealing at 600°C.

(■ overall composition; ● phases; ✶ two-phase)

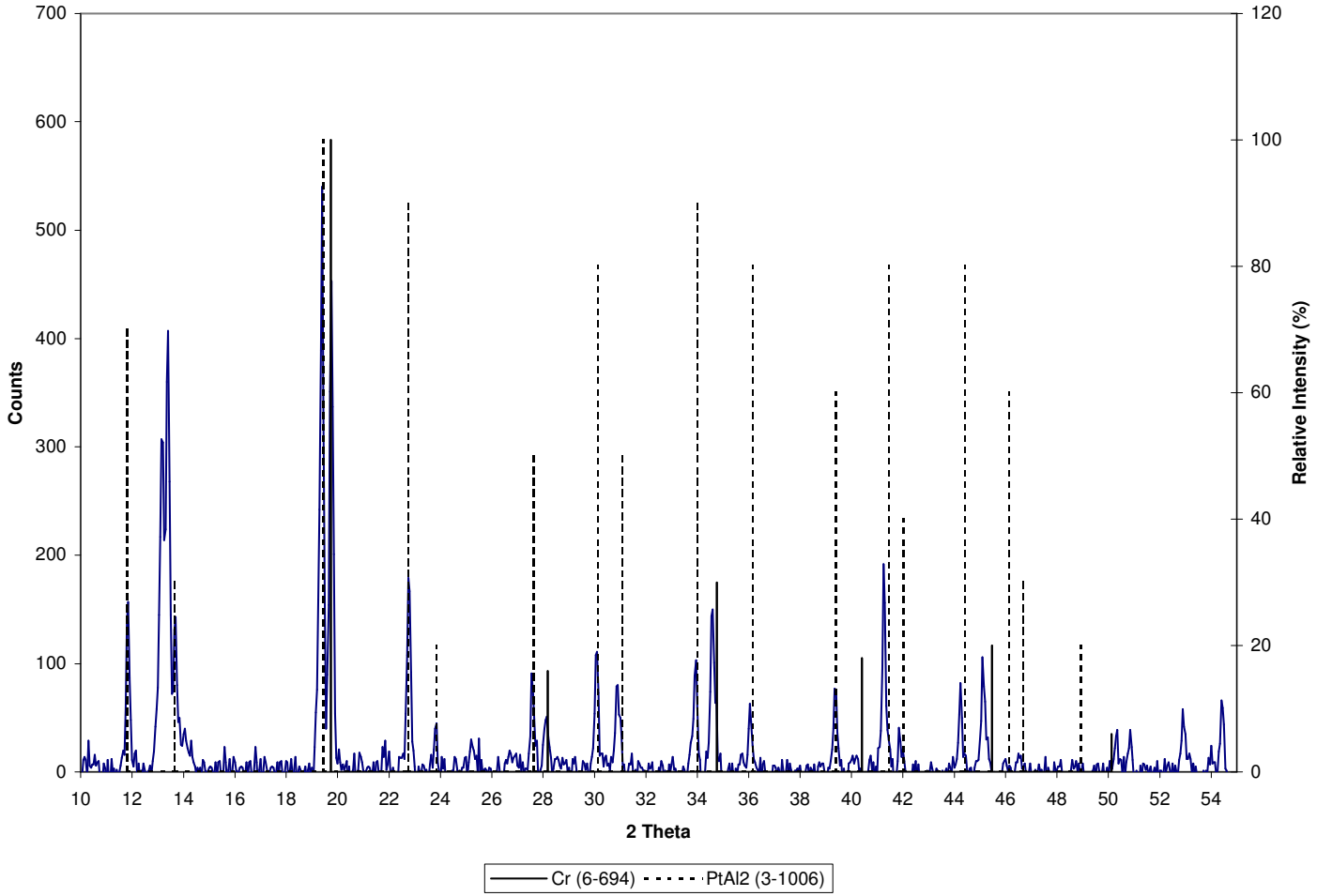

Figure 2.196. XRD pattern for nominal Pt_{10}:Al_{30}:Cr_{60} after annealing at 600 ℃.

2.1.65. Nominal $Pt_{10}:Al_{60}:Cr_{30}$

Similar to the as-cast state (Figure 2.6), alloy $Pt_{10}:Al_{60}:Cr_{30}$ after annealing at 600°C comprised light dendrites with a dark interdendritic phase in some areas, while in other areas the interdendritic areas comprised an sparse eutectic mixture of dark and light (Figure 2.197). The eutectic coarsened during annealing. At higher magnification the dark phase showed a grey phase within, which was not present in the as-cast state. The EDX analyses are given in Table 2.65 and Figure 2.198. The dark and grey phases were too small for accurate analyses and therefore only area analyses were taken. In the as-cast condition, XRD analysis clearly confirmed that the one phase – the light one – was ~$PtAl_2$ (Figure 2.8). This was once again the case when studying the measured XRD pattern for the 600°C annealed sample (Figure 2.199). Taking into account the position of the two-phase composition on the ternary diagram (Figure 2.198), one would expect that the grey phase was ~Cr_5Al_8, and the black phase another phase richer in Al, like ~Cr_4Al_9. The latter's peaks were a reasonable fit for some of the measured peaks (Figure 2.199), while ~Cr_5Al_8 was a less obvious fit, but not inconceivable. Previous results, the position of the two-phase composition on the ternary diagram, and the XRD results would suggest that the proposed identities of these three phases are the most likely to be true. The presence of ~Cr_4Al_9 was confirmed by 600°C annealed alloy $Pt_3:Al_{65}:Cr_{32}$ (§ 2.3.6).

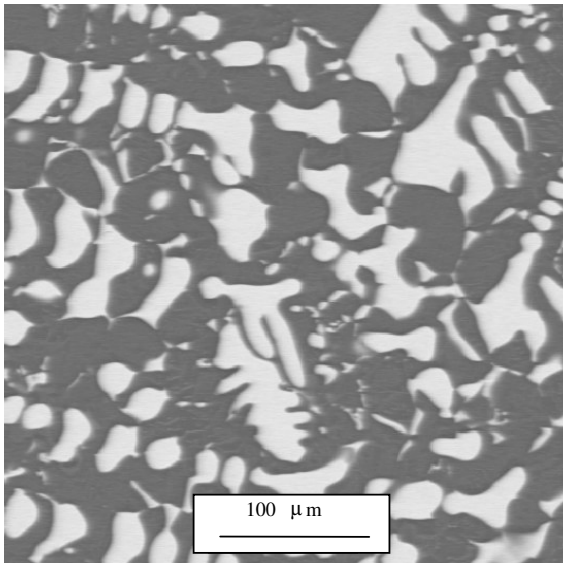

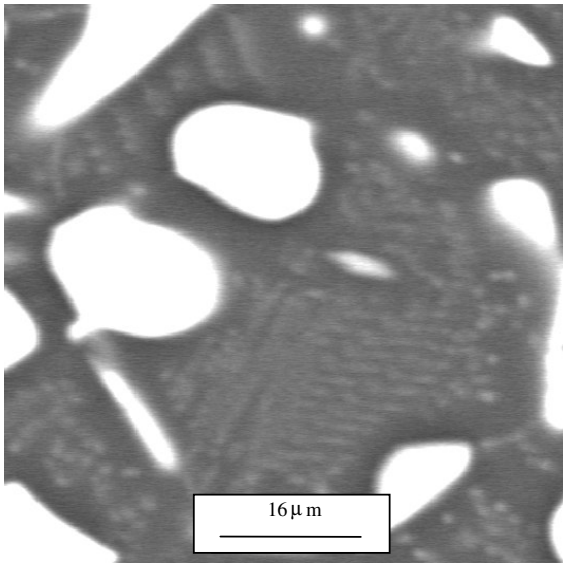

Figure 2.197. BSE-SEM image of nominal $Pt_{10}:Al_{60}:Cr_{30}$ after annealing at 600°C: black ~Cr_4Al_9 ; grey ~Cr_5Al_8; ~$PtAl_2$ white.

Table 2.65. Phase analyses for nominal $Pt_{10}:Al_{60}:Cr_{30}$ (at.%) after annealing at 600°C.

Phase description	**Pt**	**Al**	**Cr**	**Phase**
Overall	7.5 ± 0.2	60.6 ± 0.1	31.9 ± 0.1	-
Black+grey	27.6 ± 0.3	59.2 ± 0.1	13.2 ± 0.1	~Cr_4Al_9 + Cr_5Al_8
White	1.1 ± 0.1	61.4 ± 0.7	37.5 ± 0.7	~$PtAl_2$

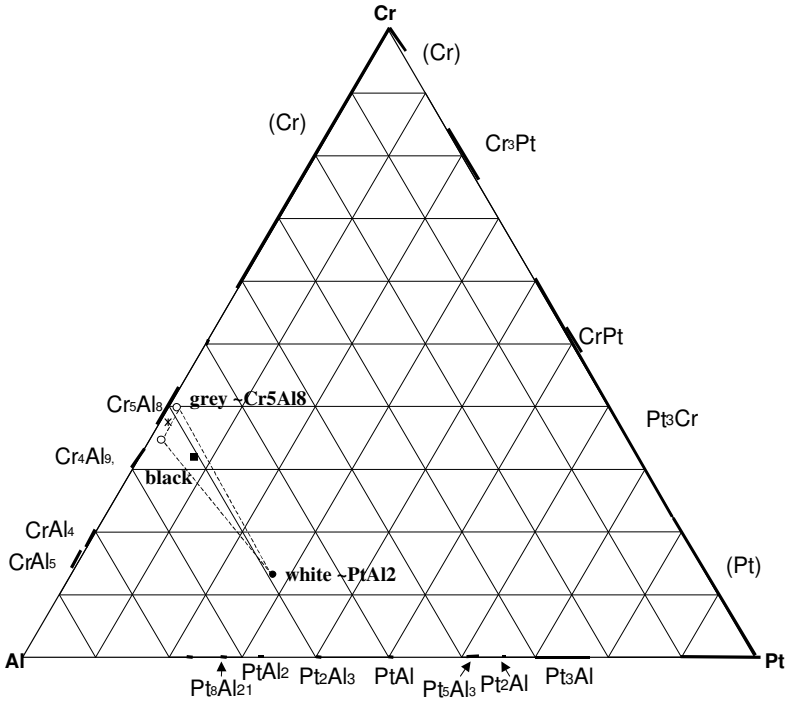

Figure 2.198. EDX analyses of nominal $Pt_{10}:Al_{60}:Cr_{30}$ (at.%) after annealing at 600°C.

(■ overall composition; ● phases; two-phase; o presumed phases)

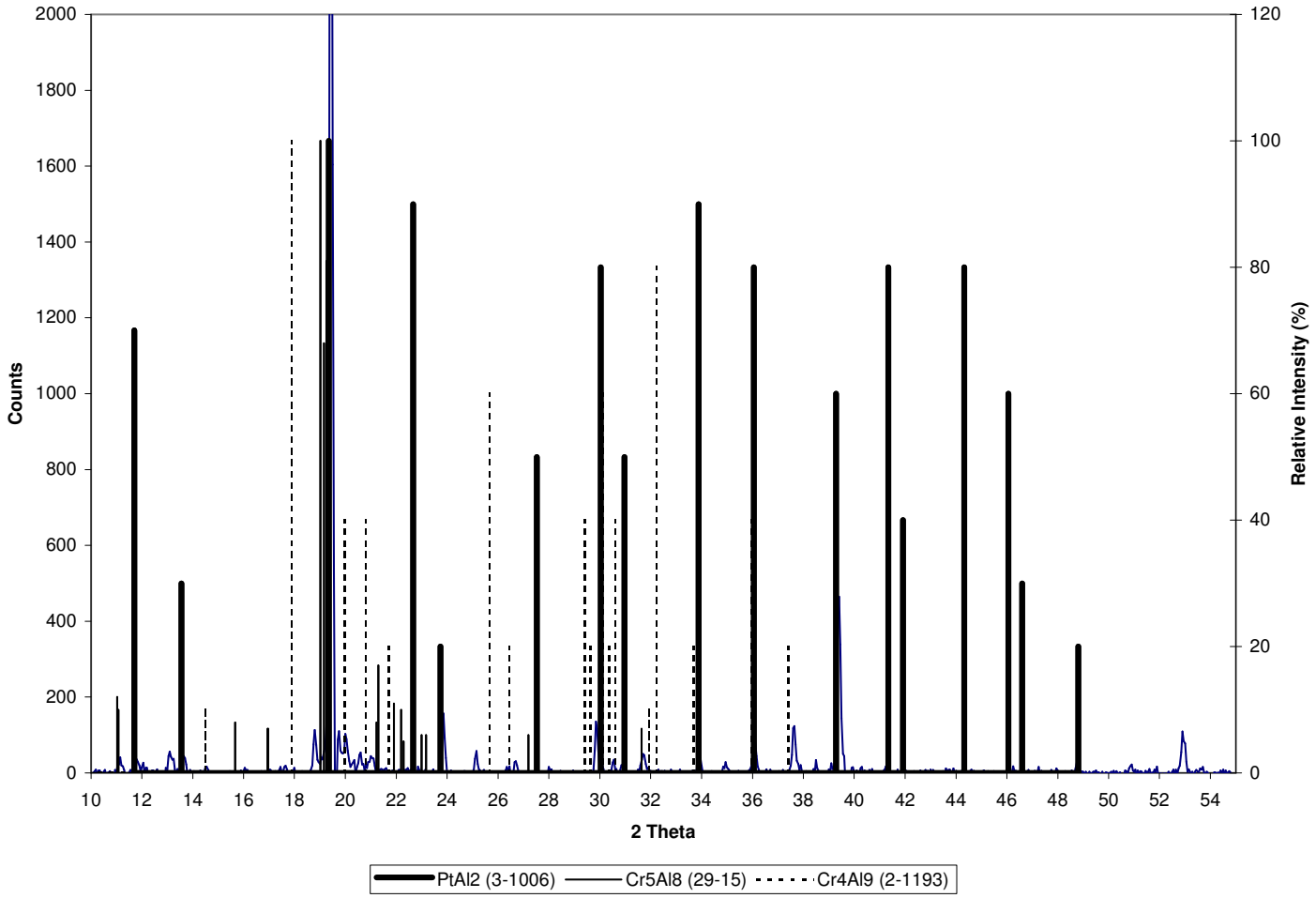

Figure 2.199. XRD pattern for nominal Pt_{10}:Al_{60}:Cr_{30} after annealing at 600℃.

2.1.66. Nominal Pt_{30}:Al_{50}:Cr_{20}

Alloy Pt_{30}:Al_{50}:Cr_{20} (as in the as-cast state) comprised primarily large grey areas with regions in between that comprised two different mixtures: binary: grey + white; and ternary: black + white + grey (Figure 2.200). There was also evidence of black precipitates within the grey phase. In some areas (Figure 2.200a) the black phase appeared to precipitate within an apparent binary eutectic, whereas in other areas (Figure 2.200c), there was clearly an appearance of a ternary eutectic. The grey component of the binary grey/white mixture had coarsened compared to the as-cast condition (Figure 2.200 vs. Figure 2.19). The EDX analyses of the alloy and its three phases are shown in Table 2.66 and Figure 2.201. The black phase was too small to analyse, although it is highly likely that it was much more rich in Cr, and an extrapolated value is given in Figure 2.201, assuming that it was probably (Cr), which would make sense considering the position of the two- and three-phase regions. The white phase was also very small and its analyses would have been affected by the surrounding phase and was therefore inaccurate. Considering the position of the compositions on the ternary diagram, the white phase was probably ~Pt_2Al_3 or ~PtAl and the grey phase ~$PtAl_2$ or ~Pt_2Al_3. However, the XRD analyses were difficult to interpret. Both sets of peaks for ~$PtAl_2$ and ~Pt_2Al_3 were good fits to the measured pattern's peaks (Figure 2.202), the peaks for ~Pt_2Al_3 showing some negative shift. The peaks for Cr were not such a good fit, probably because the volume fraction (Cr) was too low for proper detection. There was, however, also definitely a suggestion of the presence of ~PtAl by the XRD results. Taking into consideration the results of 600°C annealed alloys Pt_{35}:Al_{55}:Cr_{10} (§ 2.3.9), Pt_{75}:Al_{10}:Cr_{15} (actual Pt_{33}:Al_{51}:Cr_{16}) (§ 2.3.16) and Pt_{43}:Al_{52}:Cr_5 (§ 2.3.11), it was more likely that the grey phase was ~$PtAl_2$ and the white phase ~PtAl. The interpretation of the phase identities was different to that of the 1000°C annealed alloy.

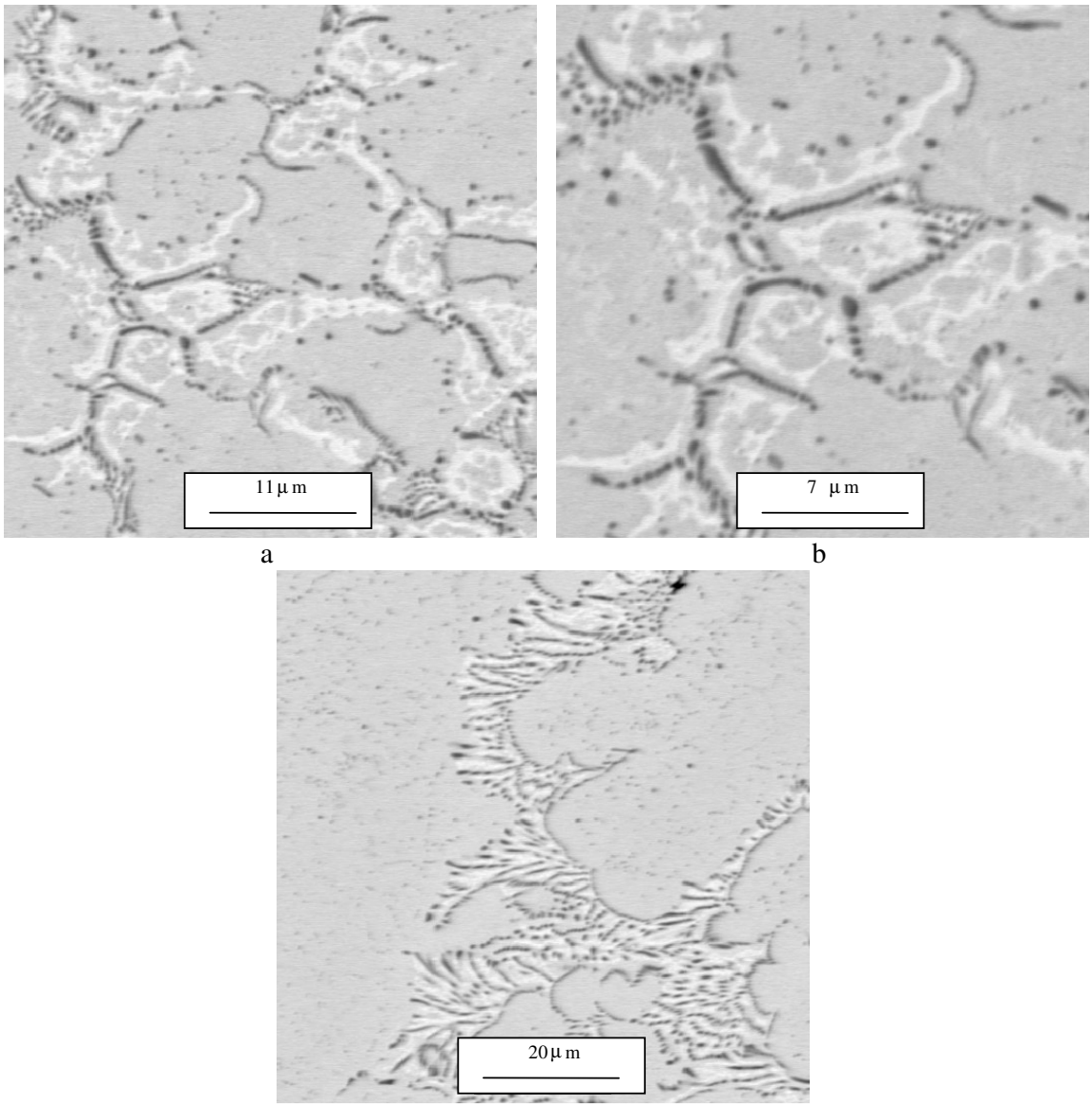

a b

c

Figure 2.200. BSE-SEM image of nominal $Pt_{30}:Al_{50}:Cr_{20}$ after annealing at 600°C: (Cr) black; ~$PtAl_2$ grey; ~ PtAl white.

Table 2.66. Phase analyses for nominal $Pt_{30}:Al_{50}:Cr_{20}$ (at.%) after annealing at 600°C.

Phase description	**Pt**	**Al**	**Cr**	**Phase**
Overall	29.8 ± 0.2	50.5 ± 1.0	19.7 ± 1.1	-
Black*	-	-	-	(Cr)
Grey	31.3 ± 0.2	51.4 ± 0.9	17.3 ± 0.9	~$PtAl_2$
White	36.8 ± 2.1	46.3 ± 0.2	16.9 ± 2.2	~PtAl
Two-phase: grey+white**	32.5	46.2	21.3	~$PtAl_2$ + ~PtAl
Three-phase: grey+white+black	27.9 ± 2.6	42.0 ± 3.9	30.1 ± 6.5	(Cr) + ~$PtAl_2$ + ~PtAl

* Too small too analyse ** Only one measurement due to small size

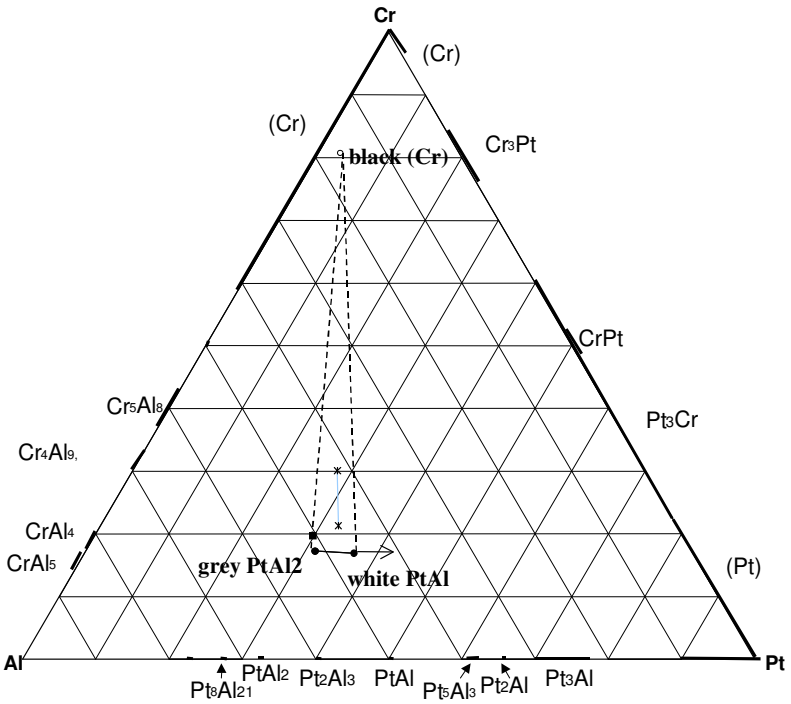

Figure 2.201. EDX analyses of nominal Pt_{30}:Al_{50}:Cr_{20} (at.%) after annealing at 600°C. (■ overall composition; ● phases; → probable direction of extrapolation for white phase; ✶(top) three-phase; ✶(bottom) two-phase; o presumed phase composition)

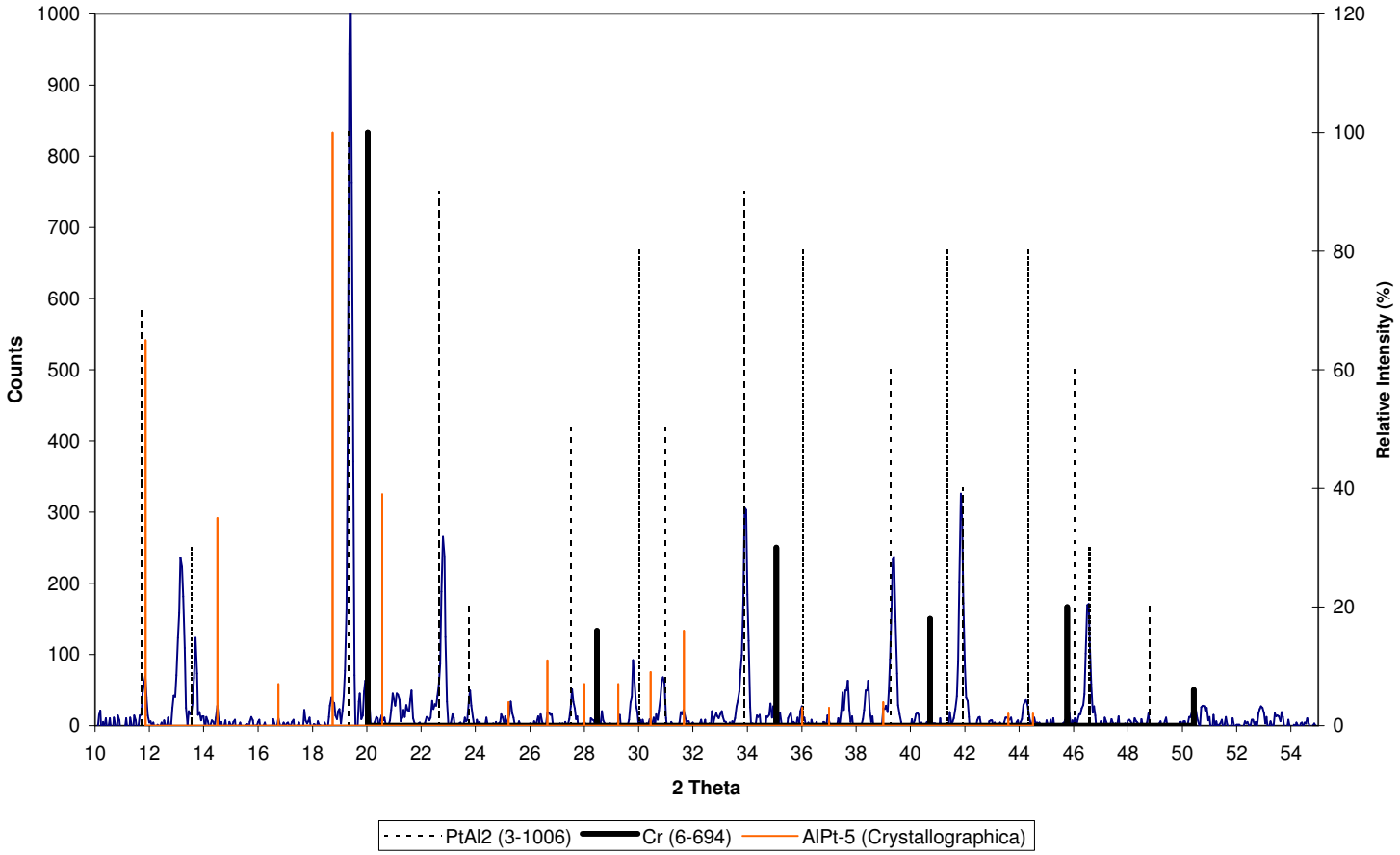

Figure 2.202. XRD pattern for nominal Pt_{30}:Al_{50}:Cr_{20} after annealing at 600℃.

2.1.67. Nominal $Pt_{50}:Al_{10}:Cr_{40}$

The microstructure of alloy $Pt_{50}:Al_{10}:Cr_{40}$ hardly changed during annealing at 600°C (Figure 2.203 vs. Figure 2.36). The EDX analyses are given in Table 2.67 and Figure 2.204. $L1_0$ ~CrPt's XRD peaks showed a good match to some of the measured peaks, and well as those of C23 ~Pt_2Al (LT) (Figure 2.205). An attempt to match Pt_3Al's XRD peaks to the measured pattern failed, while the peaks for T1 yielded reasonable results as well (Figure 2.205 insert). It was decided that the phases were probably ~CrPt and ~Pt_2Al, the latter with a high Cr content. This would agree with the as-cast results, especially since the phase compositions had also hardly changed.

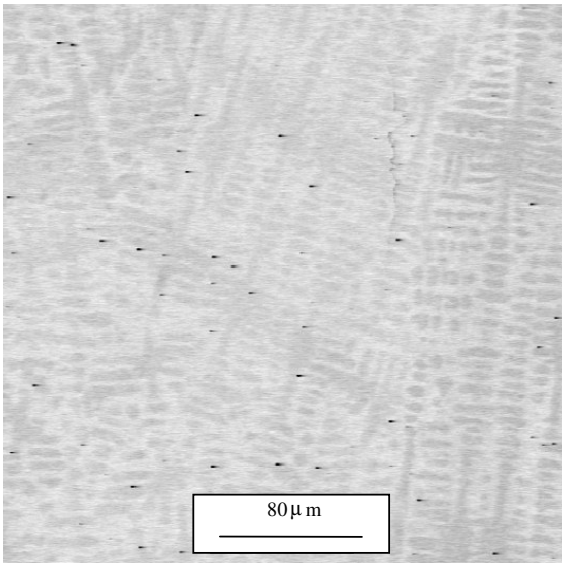

Figure 2.203. BSE-SEM image of nominal $Pt_{50}:Al_{10}:Cr_{40}$ after annealing at 600°C: dark ~CrPt; light ~Pt_2Al.

Table 2.67. Phase analyses for nominal $Pt_{50}:Al_{10}:Cr_{40}$ (at.%) after annealing at 600°C.

Phase description	**Pt**	**Al**	**Cr**	**Phase**
Overall	50.6 ± 0.4	10.7 ± 0.7	38.7 ± 0.4	-
Dark	51.1 ± 0.5	6.0 ± 0.8	42.9 ± 0.8	~CrPt
Light	51.7 ± 0.3	14.0 ± 0.9	34.3 ± 0.8	~Pt_2Al

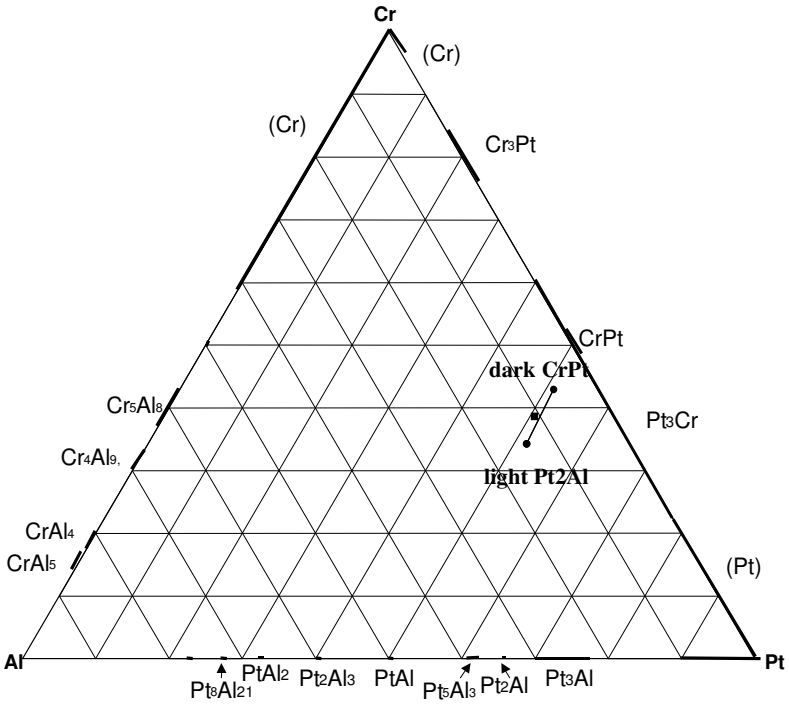

Figure 2.204. EDX analyses of nominal Pt_{50}:Al_{10}:Cr_{40} (at.%) after annealing at 600℃.

(■ overall composition; ● phases)

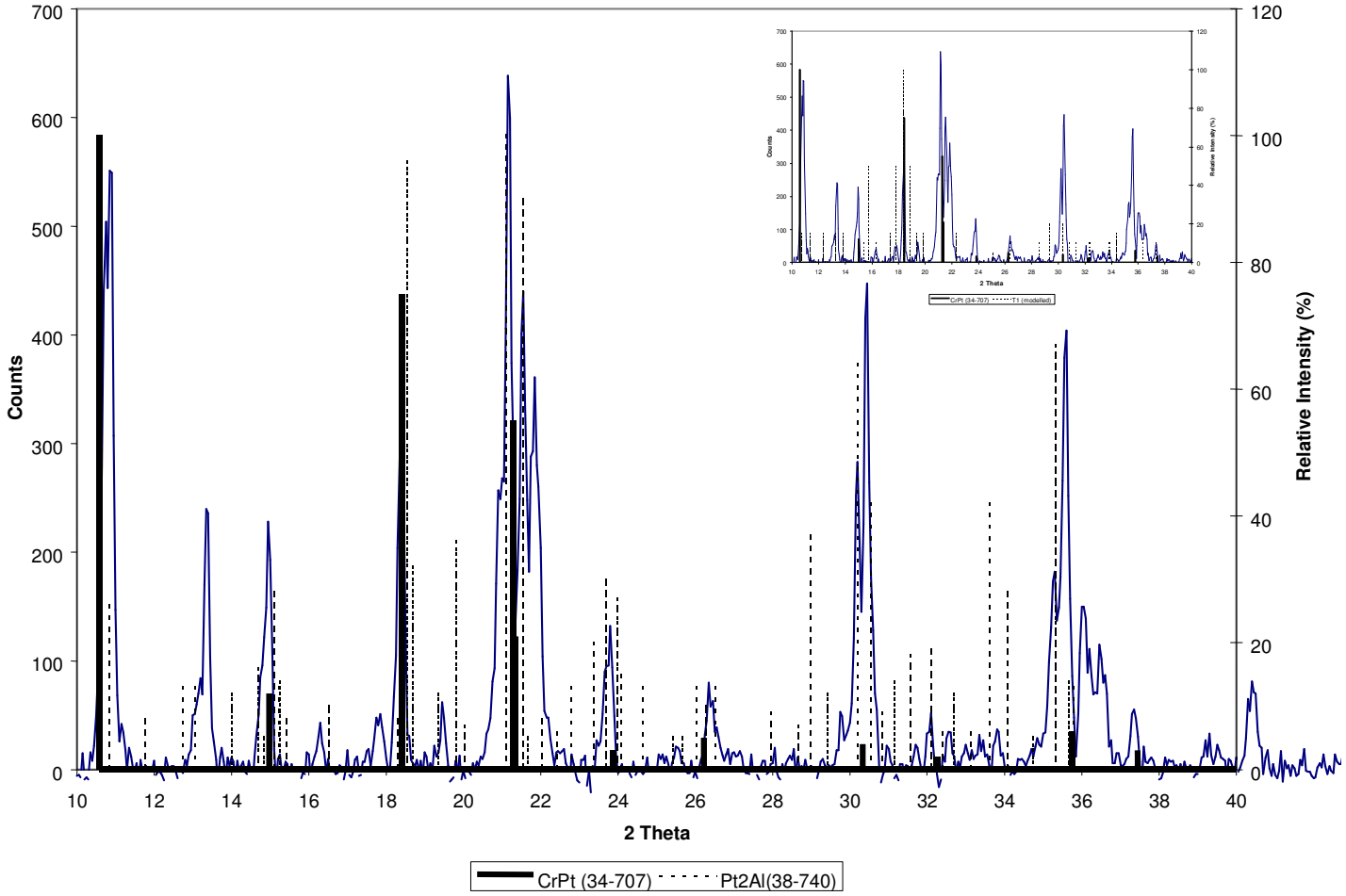

Figure 2.205. XRD patterns for nominal Pt_{50}:Al_{10}:Cr_{40}. after annealing at 600℃.

2.1.68. Nominal $Pt_{65}:Al_5:Cr_{30}$

The cored appearance of the as-cast alloy $Pt_{65}:Al_5:Cr_{30}$ (Figure 2.40) disappeared during annealing at 600°C to form what appeared to be two phases (Figure 2.206). The EDX analyses are shown in Table 2.68 and Figure 2.207. Considering the results from the as-cast sample, the two phases would be ~Pt_3Cr (dark) and ~Pt_3Al (light), which would be plausible looking at their positions of the phases on the ternary diagram (Figure 2.207). This was clearly confirmed by XRD analyses (Figure 2.208). At 1000°C, the alloy turned into single-phase ~Pt_3Al (§ 2.2.5).

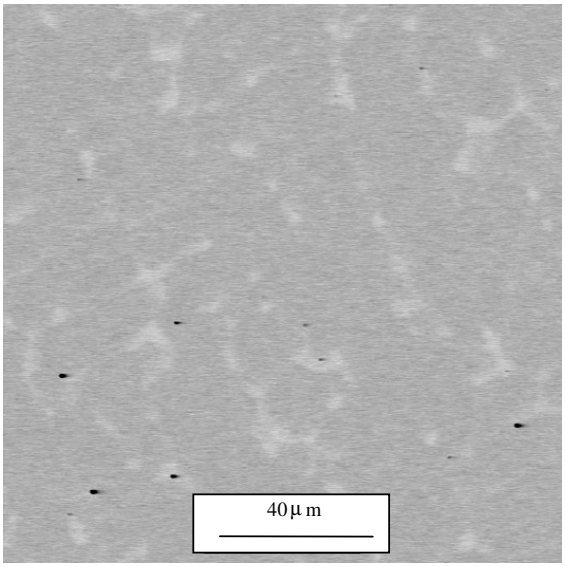

Figure 2.206. BSE-SEM image of nominal $Pt_{65}:Al_5:Cr_{30}$ after annealing at 600°C: ~Pt_3Cr dark; ~Pt_3Al light.

Table 2.68. Phase analyses for nominal $Pt_{65}:Al_5:Cr_{30}$ (at.%) after annealing at 600°C.

Phase description	**Pt**	**Al**	**Cr**	**Phase**
Overall	65.4 ± 0.3	5.2 ± 0.6	29.4 ± 0.5	-
Dark	65.2 ± 0.2	3.1 ± 0.5	31.7 ± 0.6	~Pt_3Cr
Light	65.0 ± 0.3	14.4 ± 1.5	20.6 ± 1.7	~Pt_3Al

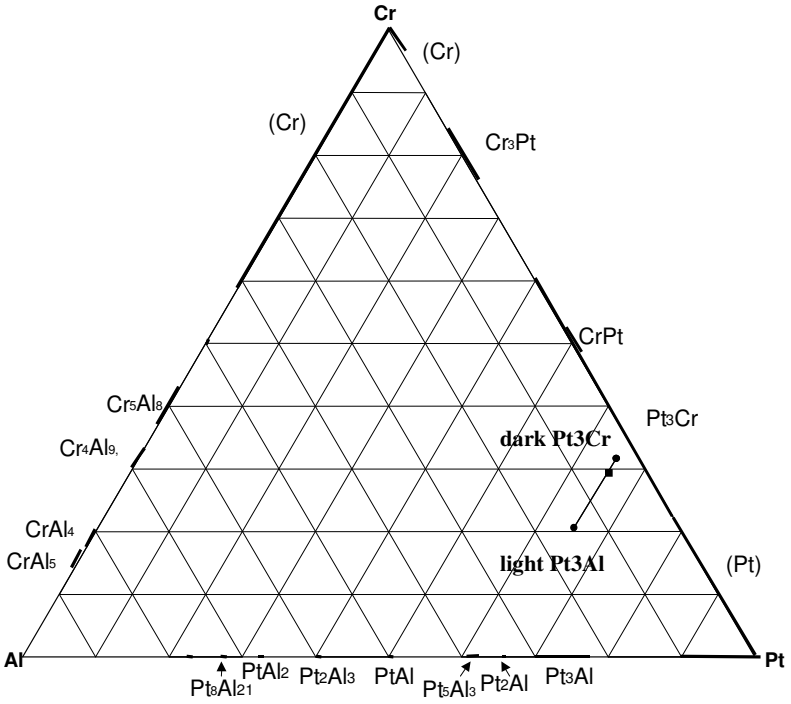

Figure 2.207. EDX analyses of nominal $Pt_{65}:Al_5:Cr_{30}$ (at.%) after annealing at 600°C.

(■ overall composition; ● phases)

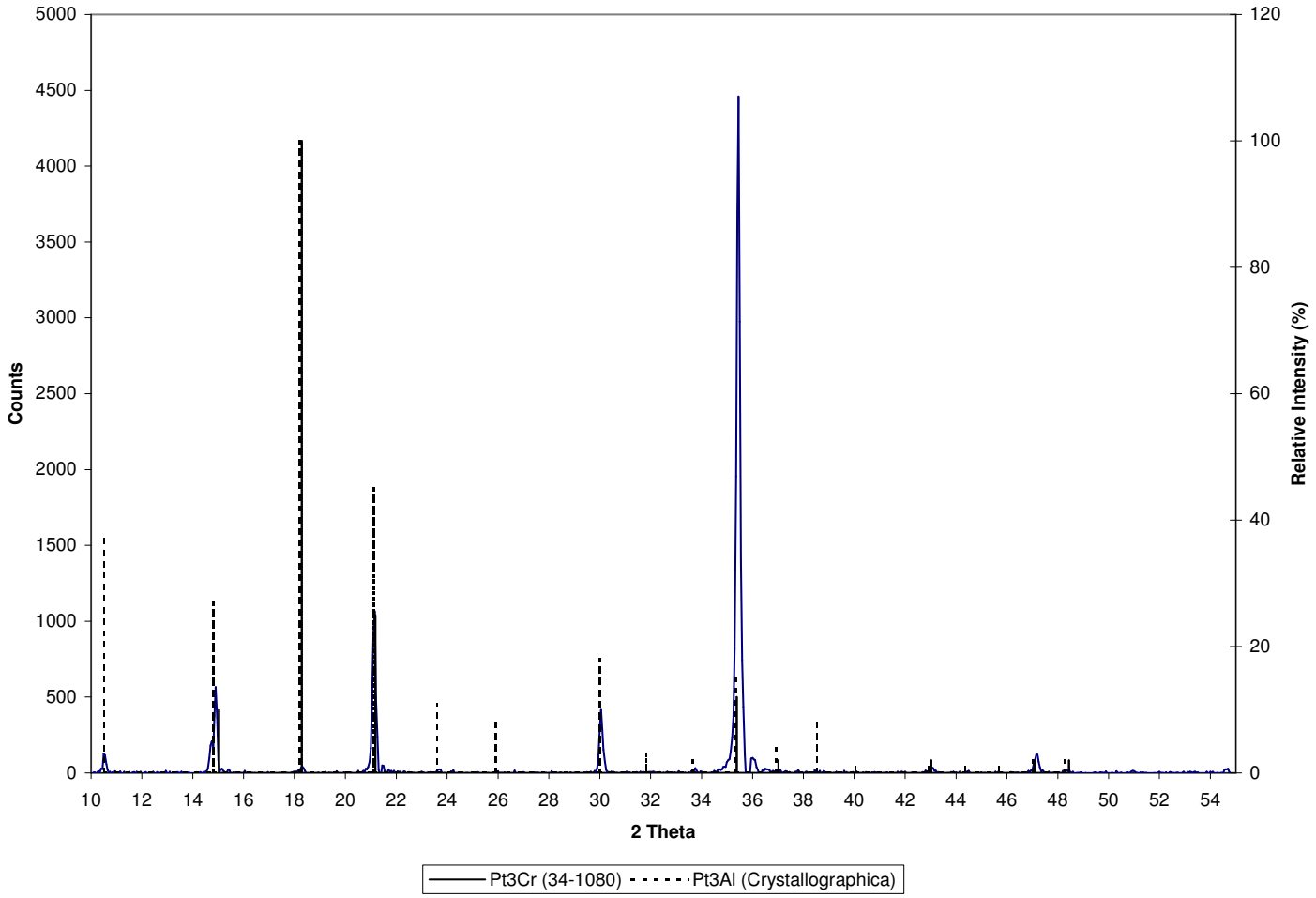

Figure 2.208. XRD patterns for nominal $Pt_{65}:Al_5:Cr_{30}$. after annealing at 600℃.

2.1.69. Nominal $Pt_3:Al_{65}:Cr_{32}$

As-cast alloy $Pt_3:Al_{65}:Cr_{32}$ comprised dark dendrites with a light interdendritic phase in some areas. The structure did not change during annealing at 600°C (Figure 2.209) as it had changed during annealing at 1000°C. The EDX analyses are given in Table 2.69 and Figure 2.210, and the phase compositions have not changed. Annealing at 2500 hours at 600°C was not enough to induce any change, unlike a 1000°C heat treatment. Assuming that the identity of the phases stayed the same, and considering the position of the phases on the ternary plot, the light phase was ~$PtAl_2$ and the dark one ~Cr_4Al_9 (based on the XRD analysis of the as-cast state). This was confirmed by XRD analyses of the 600°C annealed sample (Figure 2.209). The micrograph (Figure 2.11) shows some dark regions which appear as if the light ~$PtAl_2$ phase had been removed on sample preparation. If so, this shows that ~$PtAl_2$ is brittle.

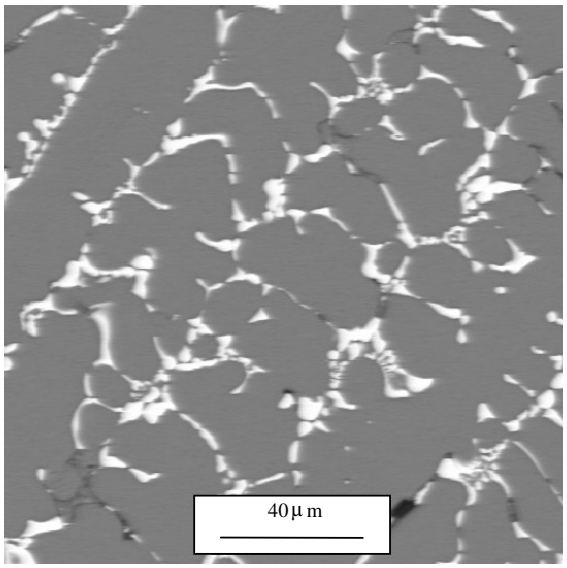

Figure 2.209. BSE-SEM image of nominal $Pt_3:Al_{65}:Cr_{32}$ after annealing at 600°C: ~Cr_4Al_9 dark; ~$PtAl_2$ light.

Table 2.69. Phase analyses for nominal $Pt_3:Al_{65}:Cr_{32}$ (at.%) after annealing at 600°C.

Phase description	**Pt**	**Al**	**Cr**	**Phase**
Overall	2.4 ± 0.3	65.4 ± 0.3	32.2 ± 0.1	-
Dark	0.7 ± 0.1	65.3 ± 0.1	34.0 ± 0.2	~Cr_4Al_9
Light	27.3 ± 0.2	60.5 ± 0.1	12.2 ± 0.2	~$PtAl_2$

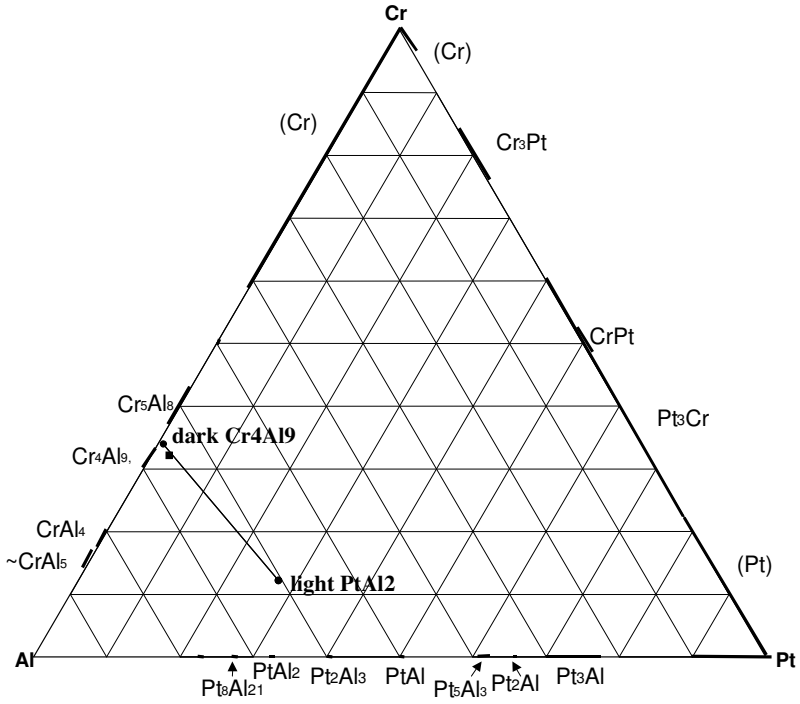

Figure 2.210. EDX analyses of nominal Pt_3:Al_{65}:Cr_{32} (at.%) after annealing at 600°C. (■ overall composition; ● phases)

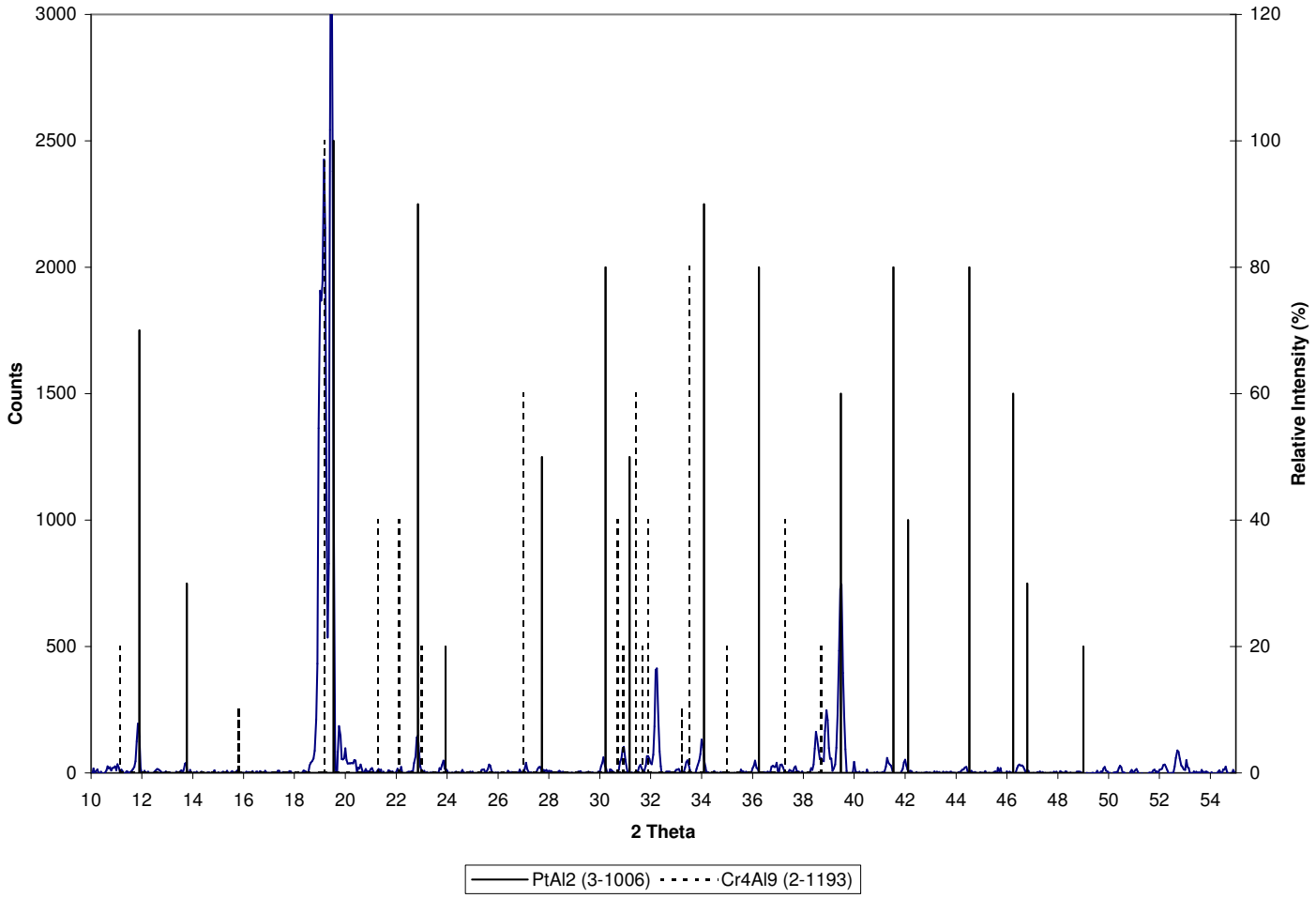

Figure 2.211. XRD patterns for nominal Pt_3:Al_{65}:Cr_{32}. after annealing at 600 ℃.

2.1.70. Nominal $Pt_3:Al_{35}:Cr_{62}$

The microstructure of alloy $Pt_3:Al_{35}:Cr_{62}$ had not changed during annealing at 600°C: it showed a dark phase with tiny grey particles inside; a white phase; and a fine eutectic-like mixture of dark and light with a web-like appearance (Figure 2.212) (which had changed its morphology during annealing at 1000°C, which was probably cellular precipitation). The light phase was analysed in the centre of the largest white areas, although still too small not be affected by surrounding phase(s), while the black phase was always analysed in areas where the grey particles were not present (also still too small, though). No attempt was made to analyse the grey particles due to their extremely small sizes. The compositions "as-is" (Table 2.70) can be seen graphically in Figure 2.213. However, as already stated, all phases were too small to yield any accurate results. The only compositions that would be accurate in Table 2.70 are the two-phase compositions, i.e. that of the dark + light combination (area analysis of eutectic) and that of the dark + grey combination (area analysis of dendrite interiors).

From Figure 2.14, one would expect that the dark phase was (Cr) and the light phase probably ~$PtAl_2$ (as in the as-cast state) or ~Pt_2Al_3. Considering the results of other annealed alloys ($Pt_3:Al_{65}:Cr_{32}$, § 2.3.6 and $Pt_{10}:Al_{60}:Cr_{30}$, § 2.3.2), ~$PtAl_2$ seemed more probable. The grey phase was difficult to identify. However, the composition of black+grey and its resulting position on the plot suggests a position for the grey phase near that of ~Cr_2Al (as in the extrapolation in Figure 2.213).

The XRD analyses clearly showed that the three phases present were indeed ~$PtAl_2$, ~Cr_2Al and (Cr) (Figure 2.214). This agreed with the 1000°C annealed condition (§ 2.2.7). The change in phase compositions correlated with a change in phase identities during annealing, although the appearance of the microstructure hardly changed.

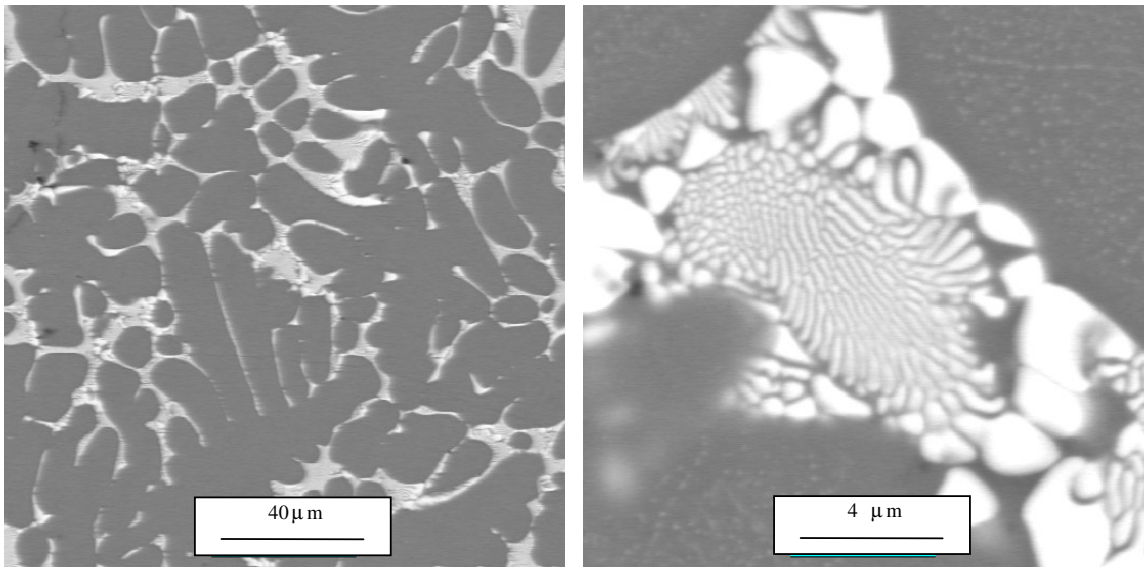

Figure 2.212. BSE-SEM image of nominal $Pt_3:Al_{35}:Cr_{62}$ after annealing at 600°C: (Cr) black; ~$PtAl_2$ white; ~Cr_2Al grey.

Table 2.70. Phase analyses for nominal $Pt_3:Al_{35}:Cr_{62}$ (at.%) after annealing at 600°C.

Phase description	**Pt**	**Al**	**Cr**	**Phase**
Overall	4.1 ± 1.3	36.3 ± 2.6	59.6 ± 3.8	-
Black	1.0 ± 0.1	31.9 ± 0.4	67.1 ± 0.3	(Cr)
White	24.5 ± 2.3	54.6 ± 2.1	20.9 ± 4.4	~$PtAl_2$
Grey (inside dendrite)*	-	-	-	~Cr_2Al
Eutectic Black + white	14.4 ± 0.7	46.1 ± 0.9	39.5 ± 1.6	(Cr) + ~$PtAl_2$
Two-phase black + grey	0.8 ± 0.0	33.1 ± 0.9	66.1 ± 0.9	(Cr) + ~Cr_2Al

* Too small for analysis.

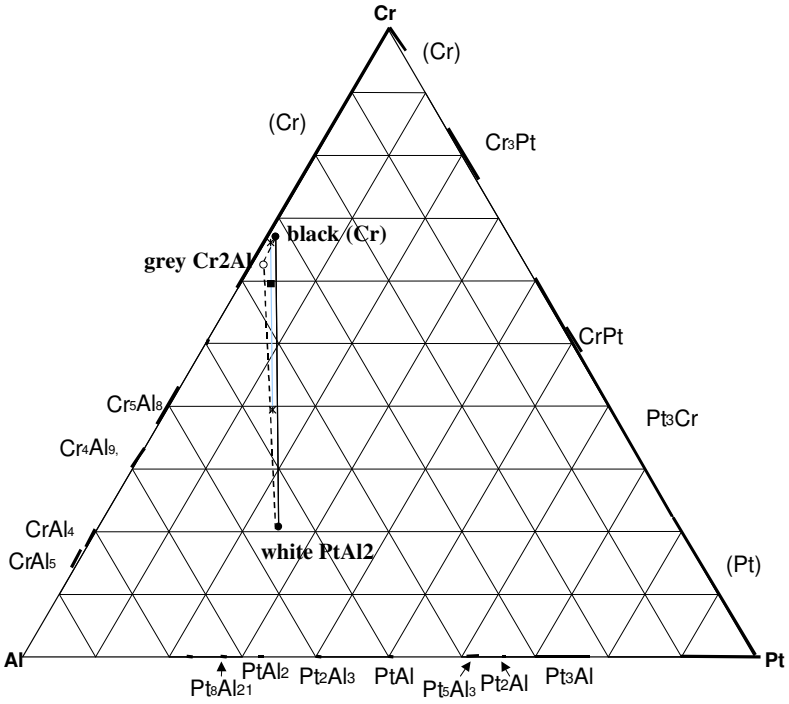

Figure 2.213. EDX analyses of nominal Pt_3:Al_{35}:Cr_{62} (at.%) after annealing at 600°C. (■ overall composition; ● phases; ✶ eutectic/two-phase; o presumed phase)

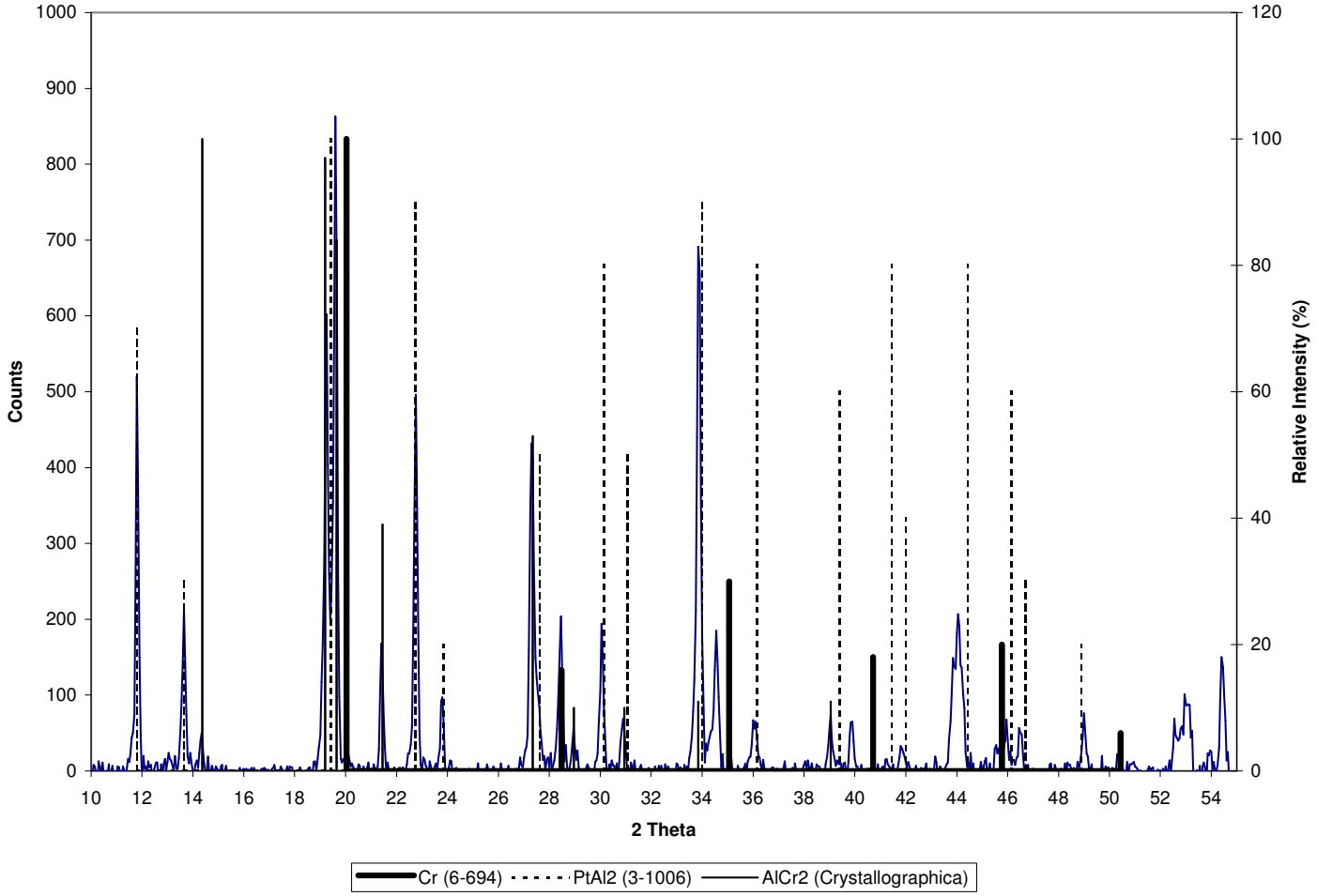

Figure 2.214. XRD patterns for nominal $Pt_3:Al_{35}:Cr_{62}$ after annealing at 600℃.

2.1.71. Nominal $Pt_{18}:Al_2:Cr_{80}$

After annealing at 600°C, alloy $Pt_{18}:Al_2:Cr_{80}$ comprised three phases: dark, medium and light (Figure 2.215). It was similar to its as-cast state, and the amount of dark and light phase had not decreased substantially as they had during annealing at 1000°C (Figure 2.161). Much further long-term annealing would probably result in a medium grey single-phase alloy. The EDX analyses are shown in Table 2.71 and Figure 2.216. The dark phase was small and its analyses probably compromised by the surrounding medium phase, and is likely to be richer in Cr. From earlier XRD results, the identities of the phases were probably black (Cr), grey ~Cr_3Pt and white ~CrPt ($L1_0$). XRD analyses of the 600°C annealed sample confirmed this assessment (Figure 2.217), with very good fits.

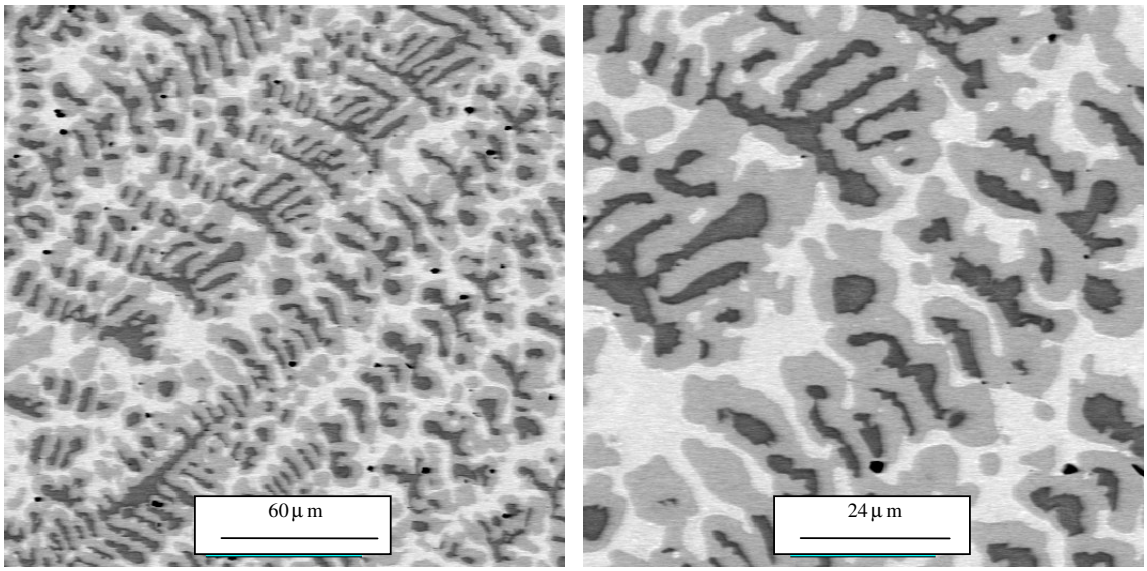

Figure 2.215. BSE-SEM image of nominal $Pt_{18}:Al_2:Cr_{80}$ after annealing at 600°C: (Cr) black; ~Cr_3Pt grey; ~CrPt white.

Table 2.71. Phase analyses for nominal $Pt_{18}:Al_2:Cr_{80}$ (at.%) after annealing at 600°C.

Phase description	**Pt**	**Al**	**Cr**	**Phase**
Overall	18.4 ± 0.5	2.3 ± 0.4	79.3 ± 0.6	-
Black	11.0 ± 0.2	0.7 ± 0.1	88.3 ± 0.2	(Cr)
Grey	18.4 ± 0.2	1.0 ± 0.1	80.6 ± 0.2	~Cr_3Pt
White	27.0 ± 0.2	3.6 ± 0.5	69.4 ± 0.7	~CrPt

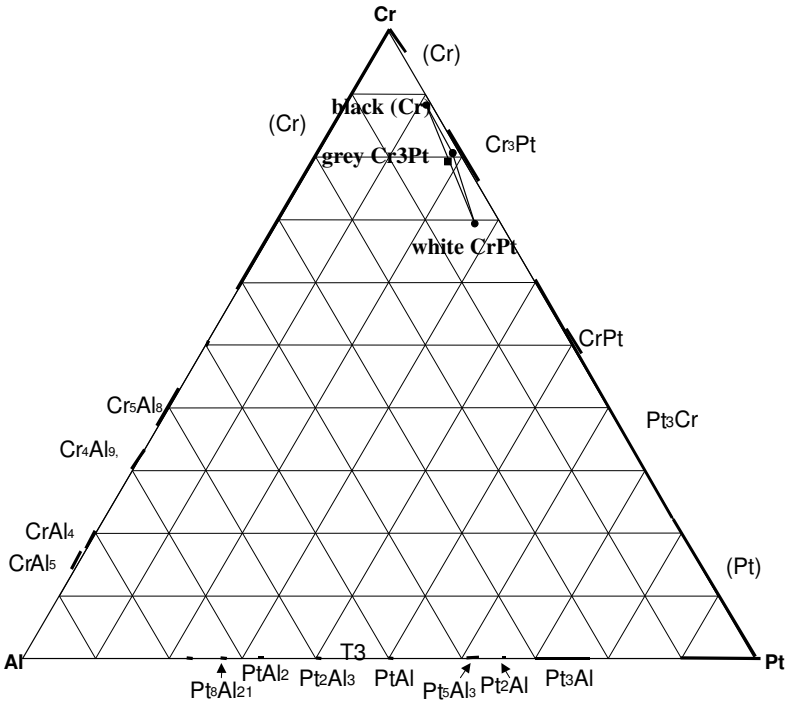

Figure 2.216. EDX analyses of nominal $Pt_{18}:Al_2:Cr_{80}$ (at.%) after annealing at 600°C.

(■ overall composition; ● phases)

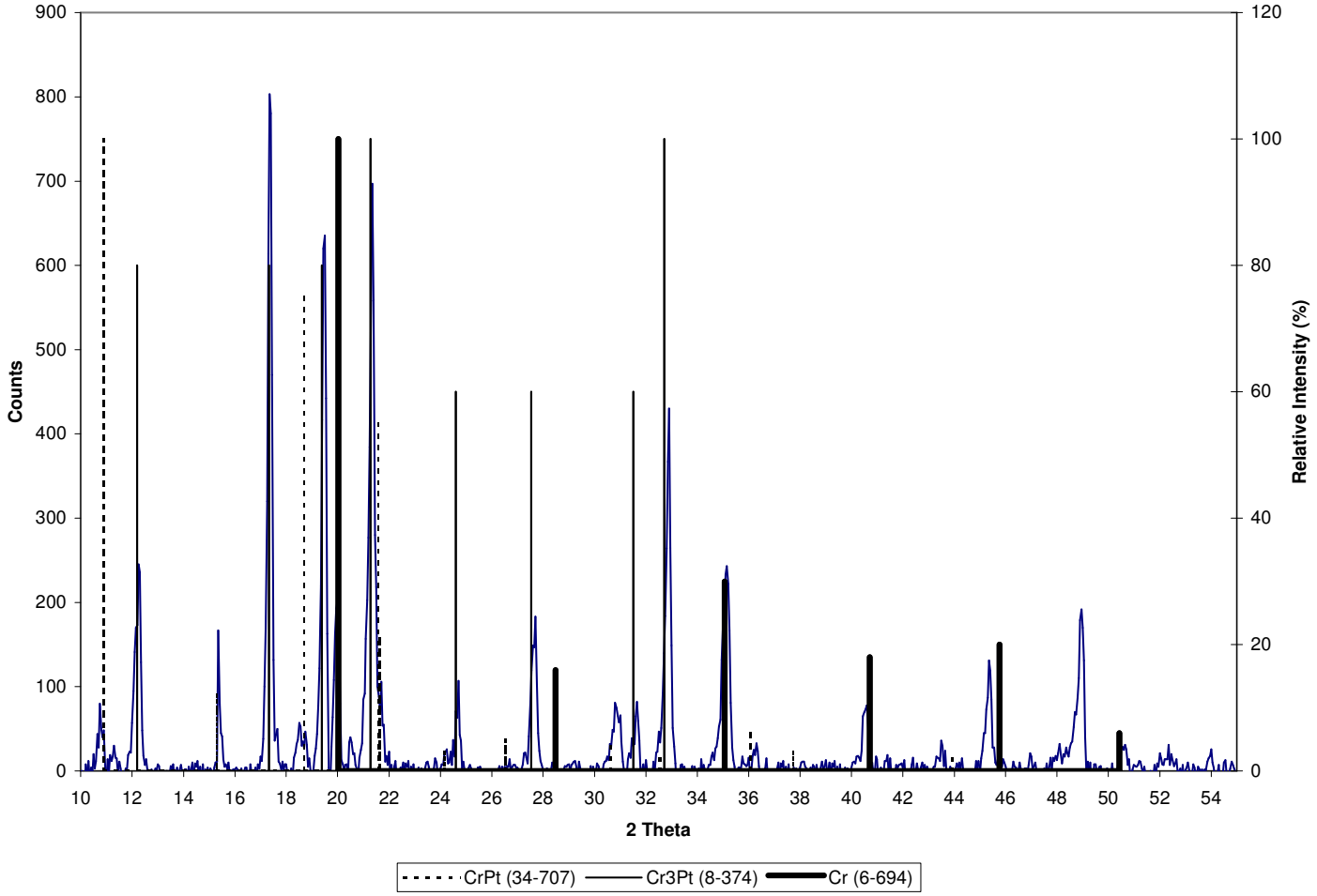

Figure 2.217. XRD pattern for nominal Pt_{18}:Al_2:Cr_{80} after annealing at 600°C.

2.1.72. Nominal $Pt_{35}:Al_{55}:Cr_{10}$

Unlike after annealing at 1000°C, the appearance of alloy $Pt_{35}:Al_{55}:Cr_{10}$ annealed at 600°C was identical to the alloy's appearance in the as-cast state, showing dark dendrites and a majority of a lighter interdendritic phase (Figure 2.218). The EDX analyses of the phases and the alloy are given in Table 2.72 and Figure 2.219. Again, the overall composition of the alloy was slightly off the tie-line between the two phases, suggesting that the light phase as seen in Figure 2.218 is actually a mixture of phases, which could indeed be possible when looking at the slight contrast found there. Assuming the phase identities stayed the same, the phases would be dark ~$PtAl_2$, and a light ~Pt_2Al_3 + ~PtAl two-phase. Unfortunately, the sample fractured when being broken out from its mount, and no XRD analyses could be performed. The assessment would however agree with that of the as-cast state (§ 2.1.20).

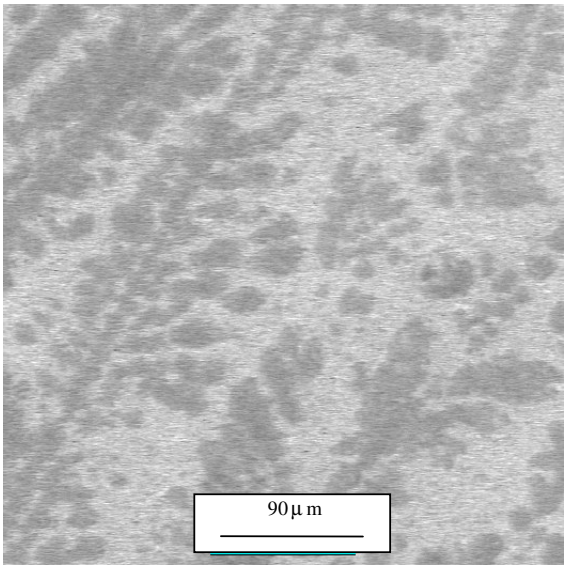

Figure 2.218. BSE-SEM image of nominal $Pt_{35}:Al_{55}:Cr_{10}$ after annealing at 600°C: ~$PtAl_2$ dark; ~Pt_2Al_3 + ~PtAl light.

Table 2.72. Phase analyses for nominal $Pt_{35}:Al_{55}:Cr_{10}$ at.%) after annealing at 600℃.

Phase description	**Pt**	**Al**	**Cr**	**Phase**
Overall	35.1 ± 0.4	55.1 ± 0.5	9.8 ± 0.3	-
Dark	32.4 ± 0.1	57.2 ± 0.2	10.4 ± 0.3	~$PtAl_2$
Light	37.5 ± 0.8	50.4 ± 1.3	12.1 ± 1.5	~Pt_2Al_3 + ~PtAl

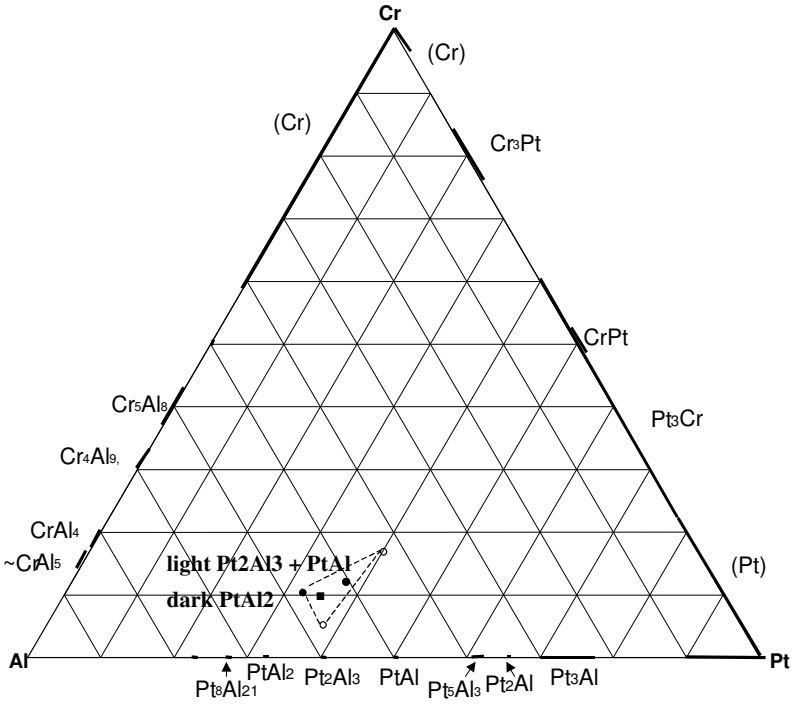

Figure 2.219. EDX analyses of nominal $Pt_{35}:Al_{55}:Cr_{10}$ (at.%) after annealing at 600℃.

(■ overall composition; ● phases; o suggested phases)

2.1.73. Nominal $Pt_{38}:Al_{22}:Cr_{40}$

In the as-cast state, alloy $Pt_{38}:Al_{22}:Cr_{40}$ comprised light dendrites with a dark interdendritic phase (Figure 2.73). During annealing at 600°C the structure stayed the same (Figure 2.220) (unlike the significant changes that transpired during annealing at 1000°C (§ 2.2.10)). Close examination of the light phase showed that it actually comprised two phases (contrary to the as-cast state). Even the dark phase could in fact be two phases (one precipitated in another), albeit very similar in composition. The EDX analyses are given in Table 2.73, with the as-measured compositions given in Figure 2.221. Precipitation would be expected after annealing as-cast samples at relatively low temperatures because the solubilities are likely to decrease. Considering that the dark composition could be richer in Cr due to the analyses being affected by the surrounding phase, it was probably (Cr) (or (Cr) and ~Cr_3Pt), while the light phase could be ~Pt_2Al, or ternary phase T1, as had been the case in the as-cast and 1000°C annealed states. The identity of the grey precipitates inside the light phase is unknown, but it could be ~Cr_3Pt or CrPt. XRD analyses confirmed the presence of T1 and $L1_0$ ~CrPt (Figure 2.223). XRD peak matches of ~Cr_3Pt and (Cr) seemed less likely. Although the latter could be the result of a small volume percentage present that is below the detection limit of the XRD scan, it is more likely that (Cr), which normally appears a black phase in lower Al-content alloys, was not present. Note that only 2θ values up to 40 degrees are shown, because there no peak matches above this due to lack of JCPDS XRD data at higher angles.

A more sensible assessment would therefore be that T1, ~CrPt and ~Cr_3Pt are present. Figure 2.222 shows a hypothetical ternary diagram. It is assumed that that the "dark" analyses were wrong and affected by surrounding phases, and is therefore shown as more Cr-rich. The composition of ~Cr_3Pt was taken from alloy $Pt_{18}:Al_2:Cr_{80}$ (§ 2.3.8) and that of ~CrPt from alloy $Pt_{15}:Al_5:Cr_{80}$ (§ 2.3.17).

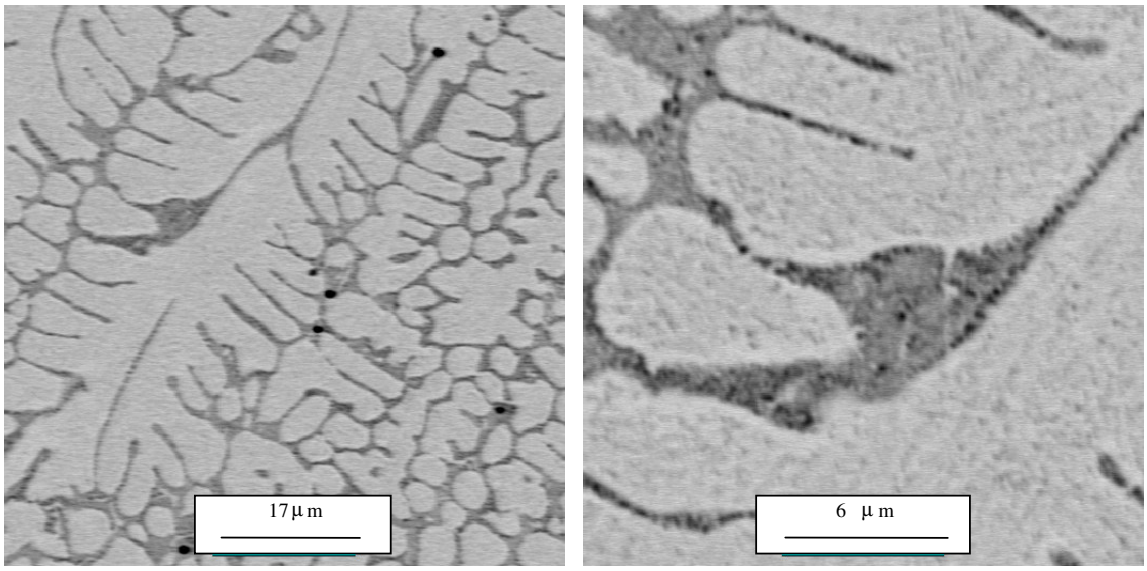

Figure 2.220. BSE-SEM image of nominal $Pt_{38}:Al_{22}:Cr_{40}$ after annealing at 600°C: ~Cr_3Pt dark; T1 light; ~CrPt grey

Table 2.73. Phase analyses for nominal $Pt_{38}:Al_{22}:Cr_{40}$ (at.%) after annealing at 600°C.

Phase description	**Pt**	**Al**	**Cr**	**Phase**
Overall	39.5 ± 0.3	23.5 ± 0.2	37.0 ± 0.4	-
Dark two-phase	31.3 ± 0.8	12.1 ± 1.4	56.6 ± 0.7	~Cr_3Pt + ~CrPt
Light + grey two-phase	42.7 ± 0.4	26.8 ± 0.3	30.5 ± 0.5	T1 + ~CrPt

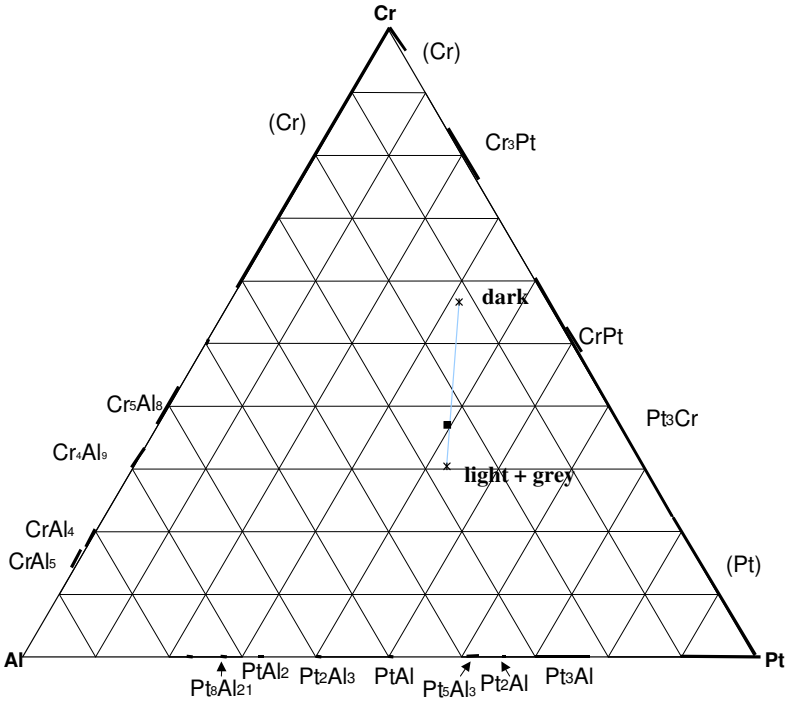

Figure 2.221. EDX analyses of nominal $Pt_{38}:Al_{22}:Cr_{40}$ (at.%) after annealing at 600°C.

(■ overall composition; ✶ two-phase)

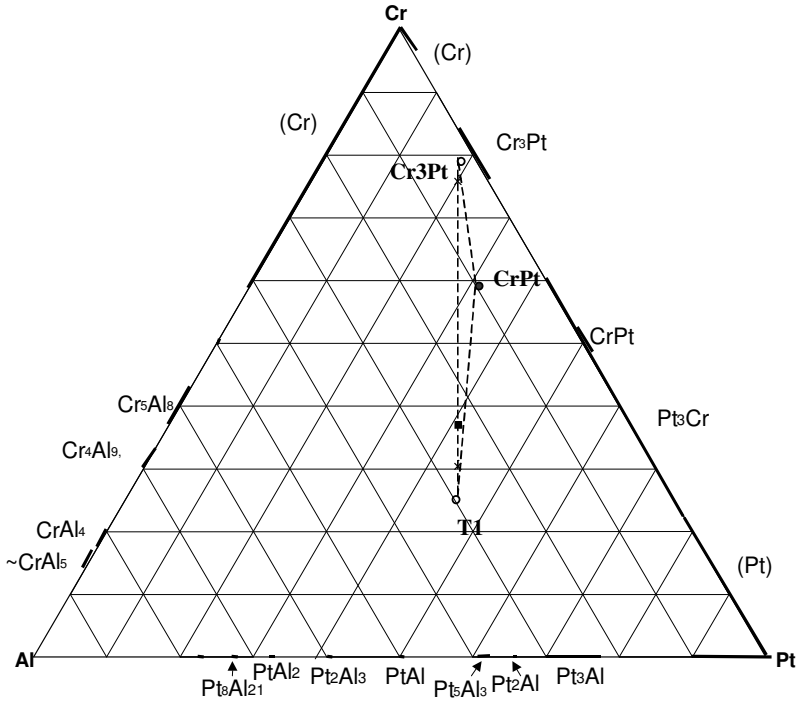

Figure 2.222. Hypothetical equilibrium triangle for the phases in nominal $Pt_{38}:Al_{22}:Cr_{40}$.

(■ overall composition; o presumed phase compositions; ✶ two-phase)

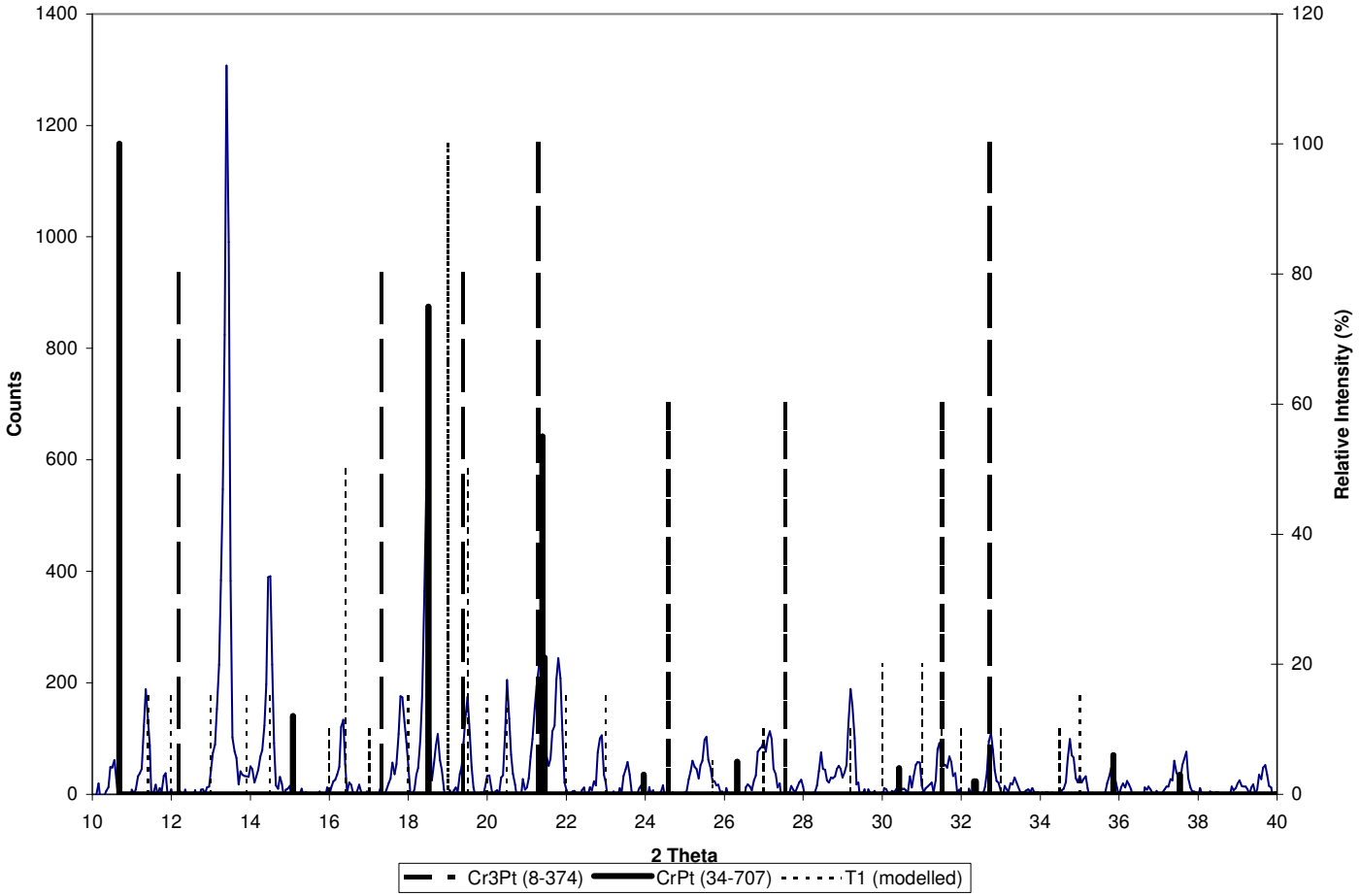

Figure 2.223. XRD pattern for nominal Pt_{38}:Al_{22}:Cr_{40} after annealing at 600℃.

2.1.74. Nominal $Pt_{43}:Al_{52}:Cr_5$

The appearance of alloy $Pt_{43}:Al_{52}:Cr_5$ did not change much during annealing at 600°C apart from coarsening, still comprising a dark and light phase (Figure 2.224). The EDX analyses are given in Table 2.74 and Figure 2.225. Once again, the phases were very small to yield accurate analyses. Considering the position of the phase compositions on the ternary plot and the XRD results of the as-cast state (Figure 2.78), the phases were clearly ~PtAl and ~Pt_2Al_3 (~Pt_2Al_3 and ~PtAl were present after annealing at 1000°C as well (§ 2.2.11)). The XRD pattern for the 600°C sample could not be determined because of severe sample fracture during the process of removing it from its mount after SEM examination.

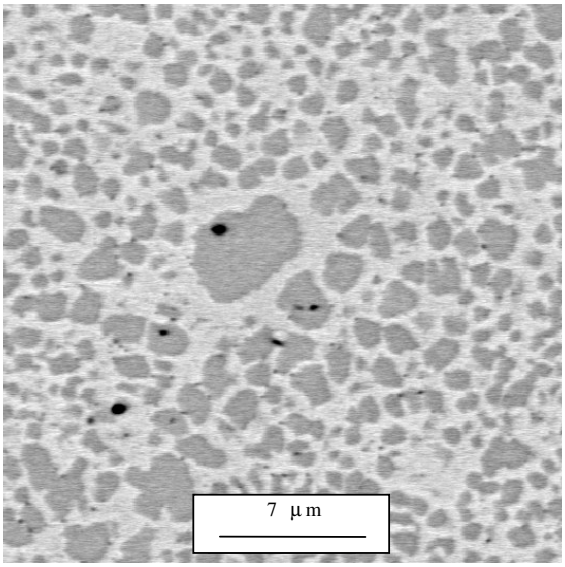

Figure 2.224. BSE-SEM image of nominal $Pt_{43}:Al_{52}:Cr_5$ after annealing at 600°C: Pores black; ~Pt_2Al_3 dark; ~PtAl light.

Table 2.74. Phase analyses for nominal $Pt_{43}:Al_{52}:Cr_5$ (at.%) after annealing at 600°C.

Phase description	**Pt**	**Al**	**Cr**	**Phase**
Overall	42.1 ± 0.3	53.0 ± 0.2	4.8 ± 0.3	-
Dark	39.2 ± 0.5	58.7 ± 0.5	2.0 ± 0.4	~Pt_2Al_3
Light	44.8 ± 0.4	46.8 ± 0.2	8.3 ± 0.2	~PtAl

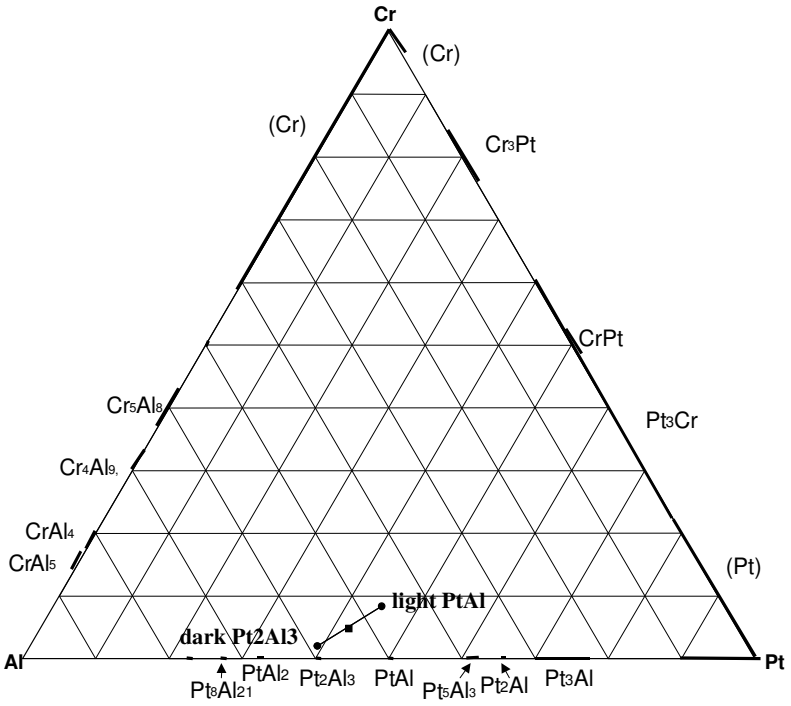

Figure 2.225. EDX analyses of nominal Pt_{43}:Al_{52}:Cr_5 (at.%) after annealing at 600°C. (■ overall composition; ● phases)

2.1.75. Nominal Pt_{50}:Al_{35}:Cr_{15}

After annealing at 600°C, alloy Pt_{50}:Al_{35}:Cr_{15} clearly had a two-phase structure with Widmanstätten-type needles (Figure 2.226), compared to the cored single-phase structure it had in the as-cast state (Figure 2.79). The EDX analyses are shown in Table 2.75 and Figure 2.227. Taking into consideration the as-cast results, the dark phase could be ternary phase T1, although, looking at its composition and the results of the alloy's 1000°C annealed state, ~PtAl would be a better option, with the light phase (which was too small to analyse) being either ~Pt_2Al or T1. For consistency with the position of phases as derived from other samples, T1 would be more applicable. The results of the XRD analyses concurred with this assessment (Figure 2.228). Only 2θ values up to 40 degrees are shown, because there no peak matches above this due to lack of XRD data at higher angles. The peaks for both ~PtAl and T1 were shifted to get a reasonably good fit. A hypothetical extrapolated composition is given for T1 in Figure 2.227.

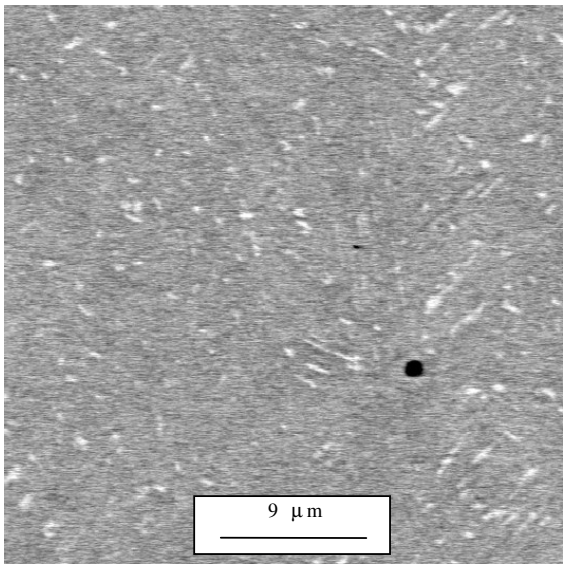

Figure 2.226. BSE-SEM image of nominal $Pt_{50}:Al_{35}:Cr_{15}$ after annealing at 600°C: ~PtAl dark; ~Pt_2Al light.

Table 2.75. Phase analyses for nominal $Pt_{50}:Al_{35}:Cr_{15}$ (at.%) after annealing at 600°C.

Phase description	**Pt**	**Al**	**Cr**	**Phase**
Overall	51.0 ± 0.5	34.9 ± 0.4	14.1 ± 0.1	-
Dark	50.5 ± 0.2	37.1 ± 0.9	12.4 ± 0.7	~PtAl
Light*	-	-	-	T1

** Too small to analyse.*

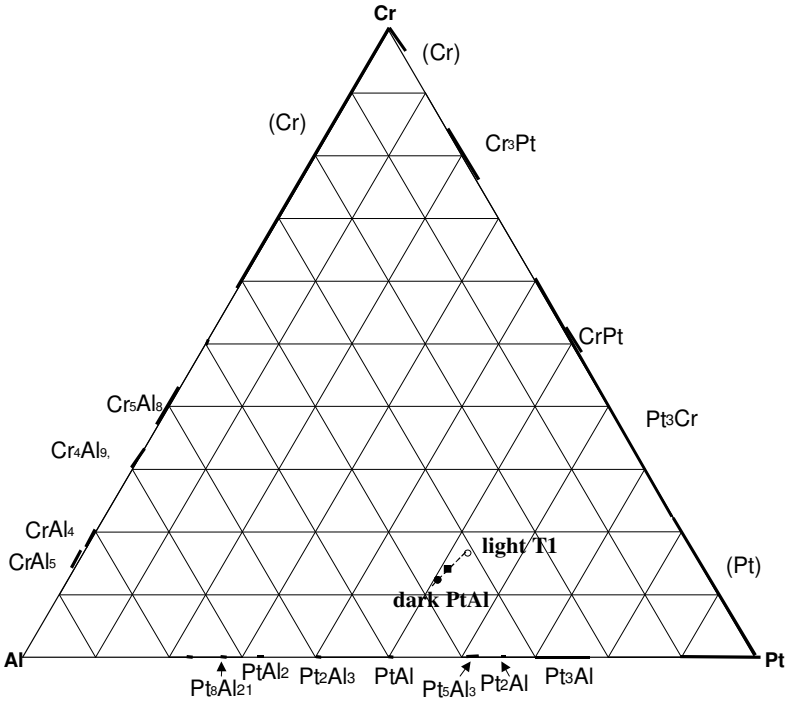

Figure 2.227. EDX analyses of nominal Pt_{50}:Al_{35}:Cr_{15} (at.%) after annealing at 600°C.

(■ overall composition; ● phases; o presumed phase composition)

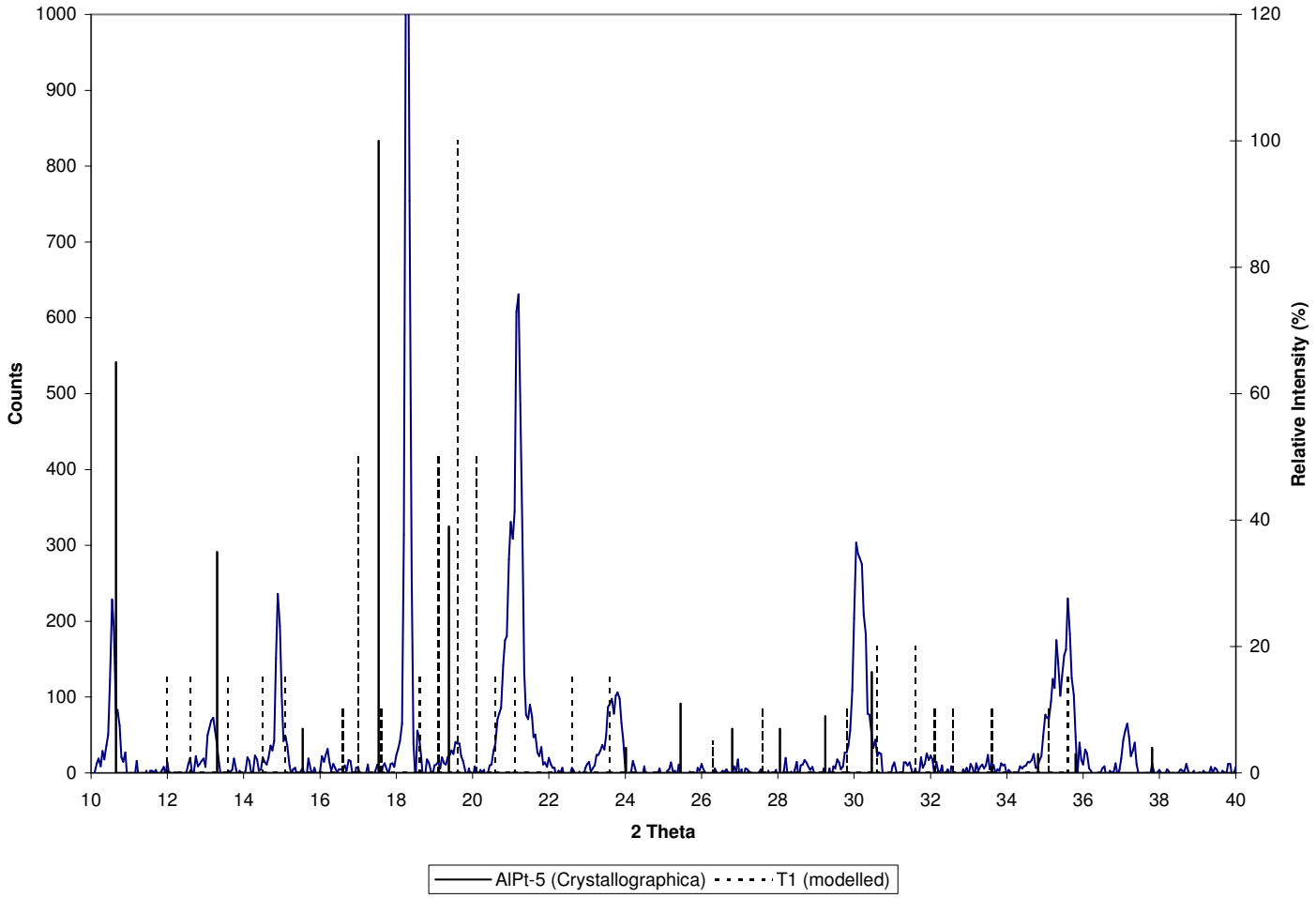

Figure 2.228. XRD pattern for nominal $Pt_{50}:Al_{35}:Cr_{15}$ after annealing at 600℃.

2.1.76. Nominal $Pt_{58}:Al_{10}:Cr_{32}$

Like in the as-cast state, alloy $Pt_{58}:Al_{10}:Cr_{32}$ showed a dark and a light phase (after digital manipulation of the image) (Figure 2.229). There seemed to be a bigger proportion of dark phase. The EDX analyses of the alloy and its phases are shown in Table 2.76 and Figure 2.230. The light phase was small and difficult to analyse. The standard deviation in composition of the dark phase was very large. The uncertainty in analyses explains why the overall composition does not fall on the tie-line between the two phases. XRD analyses of alloy $Pt_{58}:Al_{10}:Cr_{32}$ in the as-cast state (Figure 2.84), as well as the 600°C annealed state (Figure 2.231), showed that the dark and light phases were probably $L1_0$ ~CrPt and $L1_2$ ~Pt_3Al respectively. This agreed with the results of the 1000°C annealed sample of alloy $Pt_{58}:Al_{10}:Cr_{32}$. The XRD suggested the presence of ~Pt_3Cr, probably the remnants of an incomplete ordering reaction ~$Pt_3Cr \rightarrow$~CrPt. The results of alloy $Pt_{50}:Al_{10}:Cr_{40}$ (§ 2.3.4) suggested that that the dark phase could perhaps be ~Pt_2Al, but the match between the peaks and the measured pattern were unsatisfactory. A hypothetical tie-line (dashed) is consequently shown in Figure 2.230 based on an extrapolated composition for the dark phase.

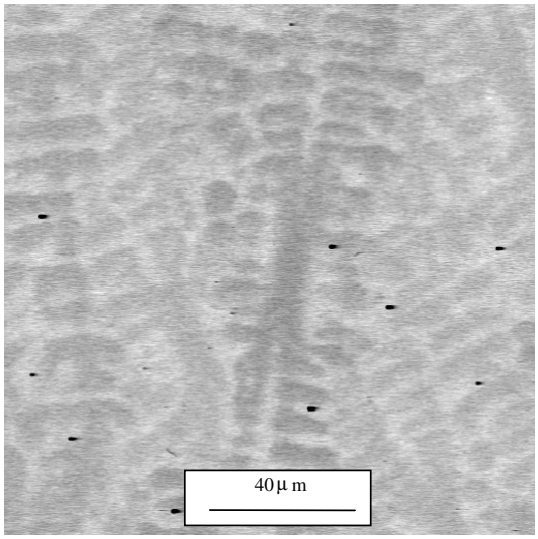

Figure 2.229. BSE-SEM image of nominal $Pt_{58}:Al_{10}:Cr_{32}$ after annealing at 600°C: ~CrPt/~Pt_3Cr dark; ~Pt_3Al light; black porosity.

Table 2.76. Phase analyses for nominal $Pt_{58}:Al_{10}:Cr_{32}$ (at.%) after annealing at 600°C.

Phase description	**Pt**	**Al**	**Cr**	**Phase**
Overall	58.4 ± 0.2	9.4 ± 0.5	32.2 ± 0.6	-
Dark	59.0 ± 0.2	12.9 ± 6.4	28.1± 6.5	~CrPt/~Pt_3Cr
Light	59.4± 0.6	16.8 ± 1.1	23.8 ± 1.6	~Pt_3Al

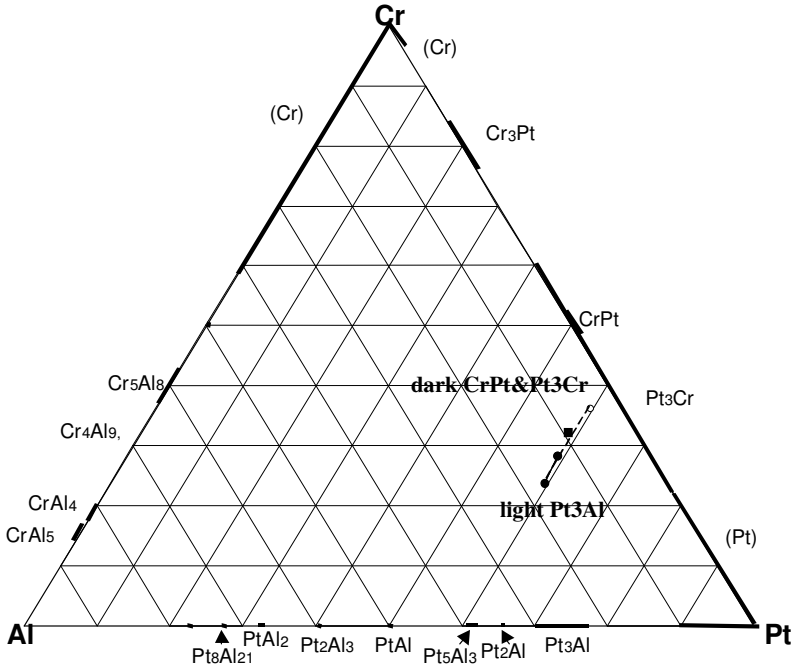

Figure 2.230. EDX analyses of nominal $Pt_{58}:Al_{10}:Cr_{32}$ at.%) after annealing at 600°C.
(■ overall composition; ● phases; o presumed phase composition)

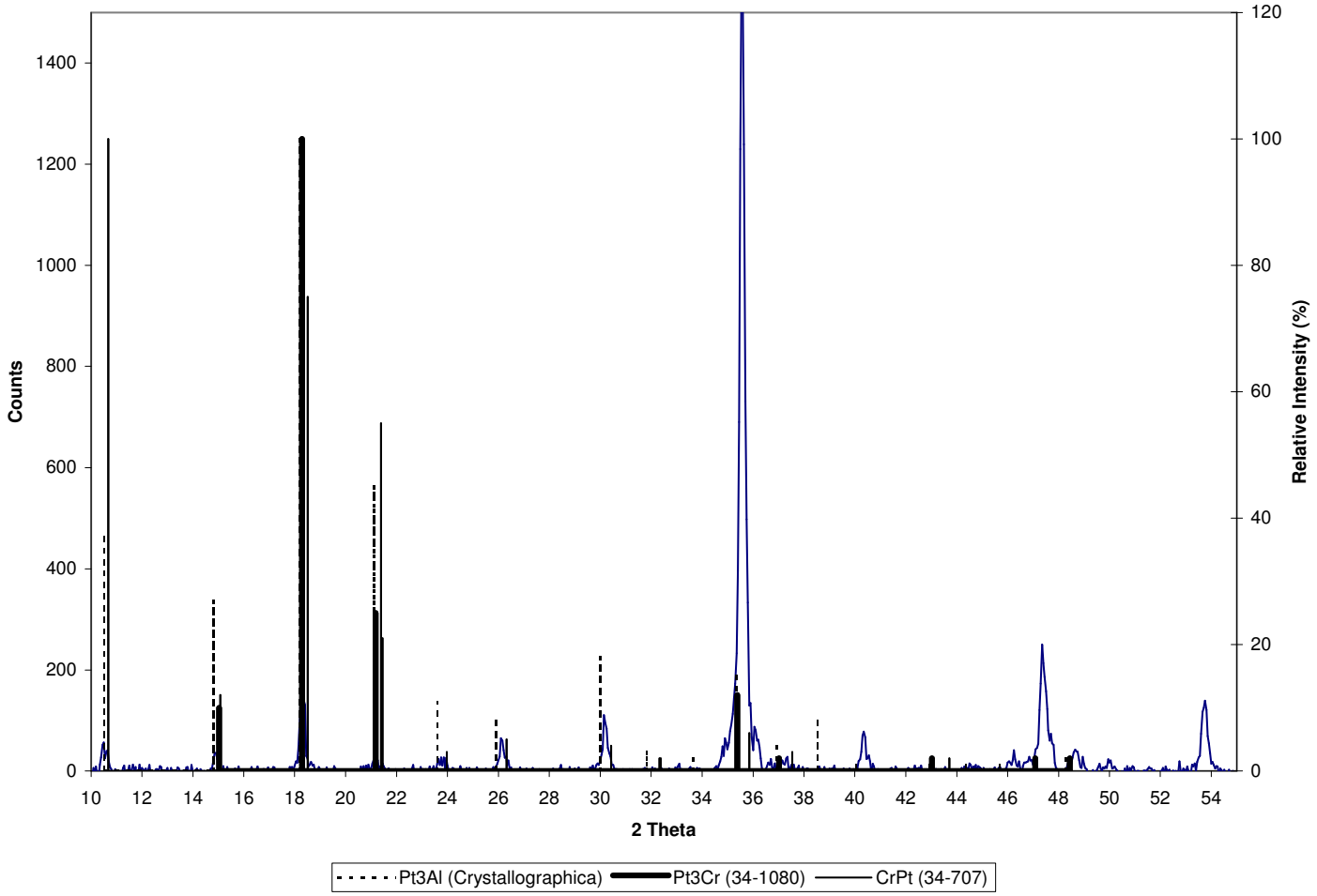

Figure 2.231. XRD pattern for nominal $Pt_{58}:Al_{10}:Cr_{32}$ after annealing at 600℃.

2.1.77. Nominal $Pt_{63}:Al_{32}:Cr_5$

Like the as-cast state (Figure 2.88), alloy $Pt_{63}:Al_{32}:Cr_5$ had appeared single-phase but with image manipulation it had been obvious that more than one phase was present (Figure 2.232). During annealing at 1000°C, the second phase had disappeared (Figure 2.178). Annealing at 600°C resulted in an alloy which was primarily single-phase, but localised second phase was observed (Figure 2.232) The EDX analyses are shown in Table 2.77 and Figure 2.233. The dark phase was very small and its analyses would have been affected by the surrounding phase. The light phase was probably ~Pt_2Al. XRD analyses confirmed this (Figure 2.234), and also showed that the dark phase was T1. The XRD peaks of both phases exhibited some shift.

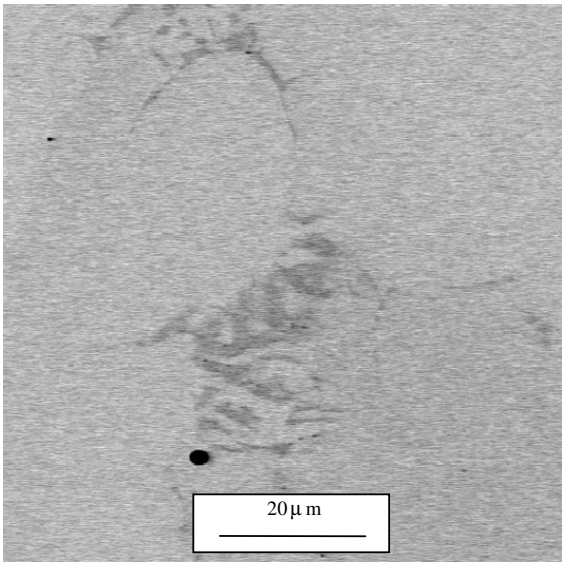

Figure 2.232. BSE-SEM image of nominal $Pt_{63}:Al_{32}:Cr_5$ after annealing at 600°C: ~Pt_2Al light; T2 dark.

Table 2.77. Phase analyses for nominal $Pt_{63}:Al_{32}:Cr_5$ (at.%) after annealing at 600°C.

Phase description	**Pt**	**Al**	**Cr**	**Phase**
Overall	63.5 ± 0.5	32.1 ± 0.6	4.4 ± 0.2	-
Dark	57.2 ± 0.0	30.9 ± 1.9	11.9 ± 1.9	T1
Light	63.7 ± 0.7	32.2 ± 0.2	4.1 ± 0.7	~Pt_2Al

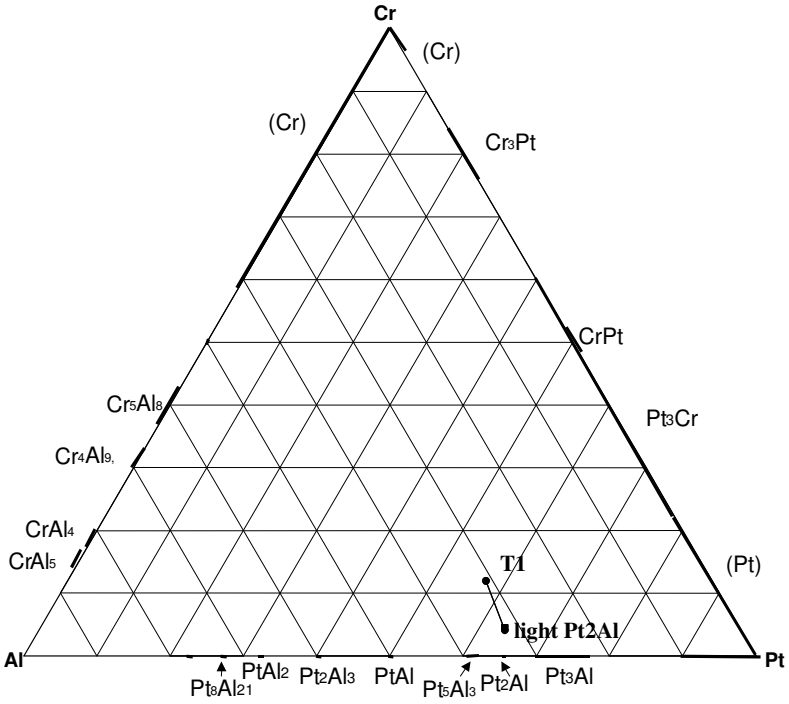

Figure 2.233. EDX analyses of nominal Pt_{63}:Al_{32}:Cr_5 (at.%) after annealing at 600°C. (■ overall composition; ● phases)

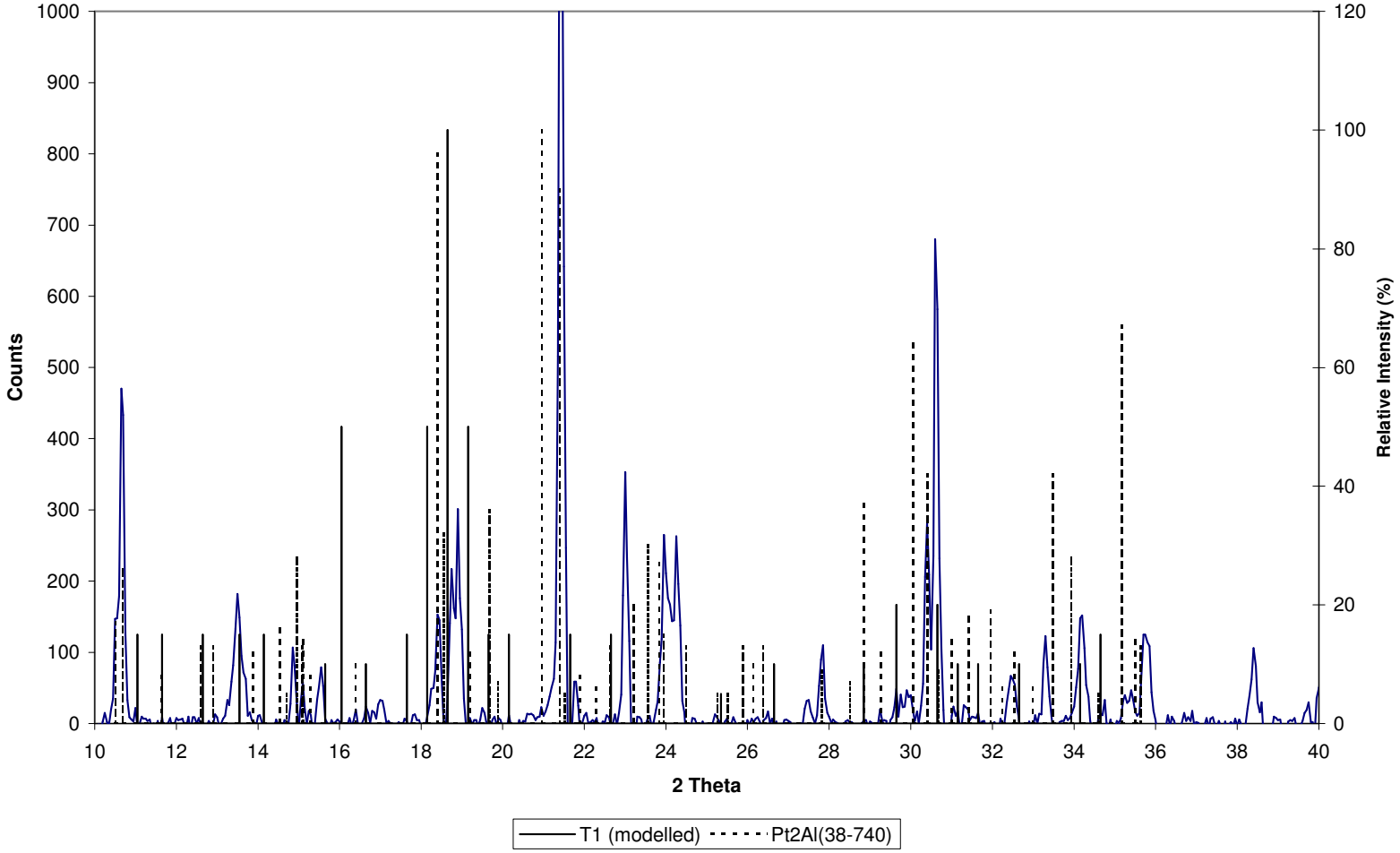

Figure 2.234. XRD pattern for nominal Pt_{63}:Al_{32}:Cr_5 after annealing at 600℃.

2.1.78. Nominal $Pt_{63}:Al_{22}:Cr_{15}$

As was the case for alloy $Pt_{63}:Al_{22}:Cr_{15}$ in the as-cast state (Figure 2.91), it looked like a single-phase alloy after annealing at 600°C, but with digital image manipulation, a contrast was obtained between dark and lighter regions, showing a dendritic morphology (Figure 2.30). The results of the EDX analyses showed that the compositions of the two phases were different (Table 2.78, Figure 2.236). Based on earlier results, the two phases were probably ~Pt_2Al and ~Pt_3Al. The presence of ~Pt_3Al ($L1_2$) was confirmed by XRD analyses (Figure 2.237), while the XRD peaks for ~Pt_2Al (C23, LT) seemed to be a reasonable fit to many of the small peaks observed in the measured pattern.

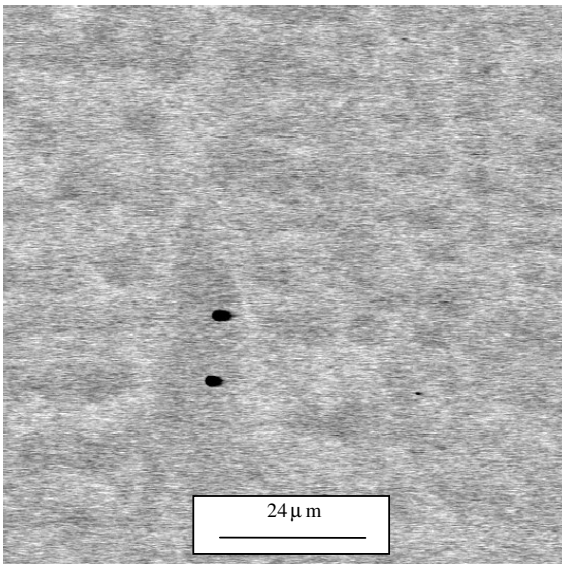

Figure 2.235. BSE-SEM image of nominal $Pt_{63}:Al_{22}:Cr_{15}$ after annealing at 600°C: ~Pt_2Al light ~Pt_3Al dark.

Table 2.78. Phase analyses for nominal $Pt_{63}:Al_{22}:Cr_{15}$ (at.%) after annealing at 600°C.

Phase description	**Pt**	**Al**	**Cr**	**Phase**
Overall	64.0 ± 0.7	21.4 ± 1.0	14.6 ± 0.4	-
Dark	64.8 ± 0.6	17.6 ± 0.1	17.6 ± 0.6	~Pt_3Al
Light	63.3 ± 0.9	23.9 ± 2.6	12.8 ± 1.6	~Pt_2Al

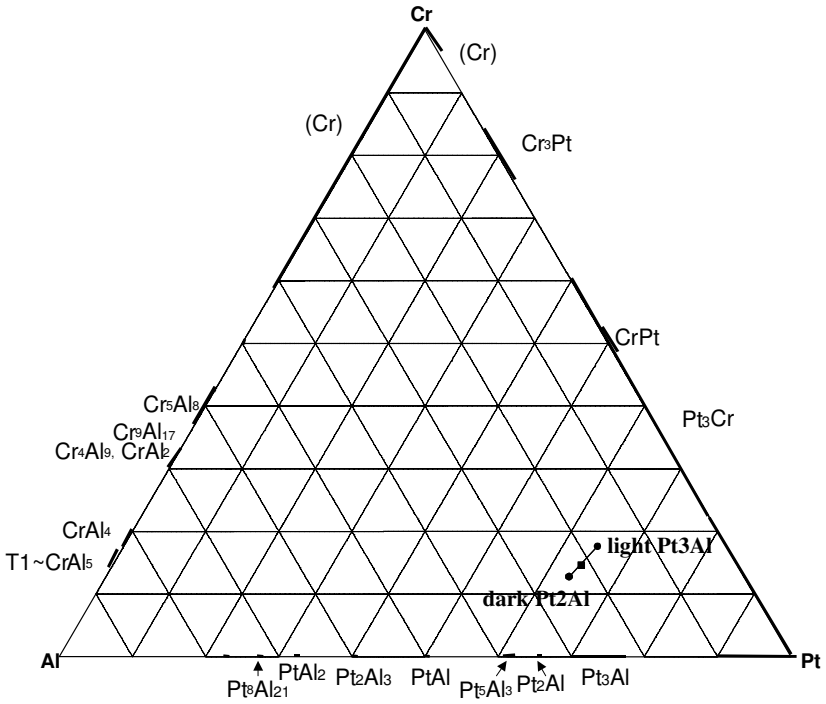

Figure 2.236. EDX analyses of nominal Pt_{63}:Al_{22}:Cr_{15} (at.%) after annealing at 600°C. (■ overall composition; ● phases)

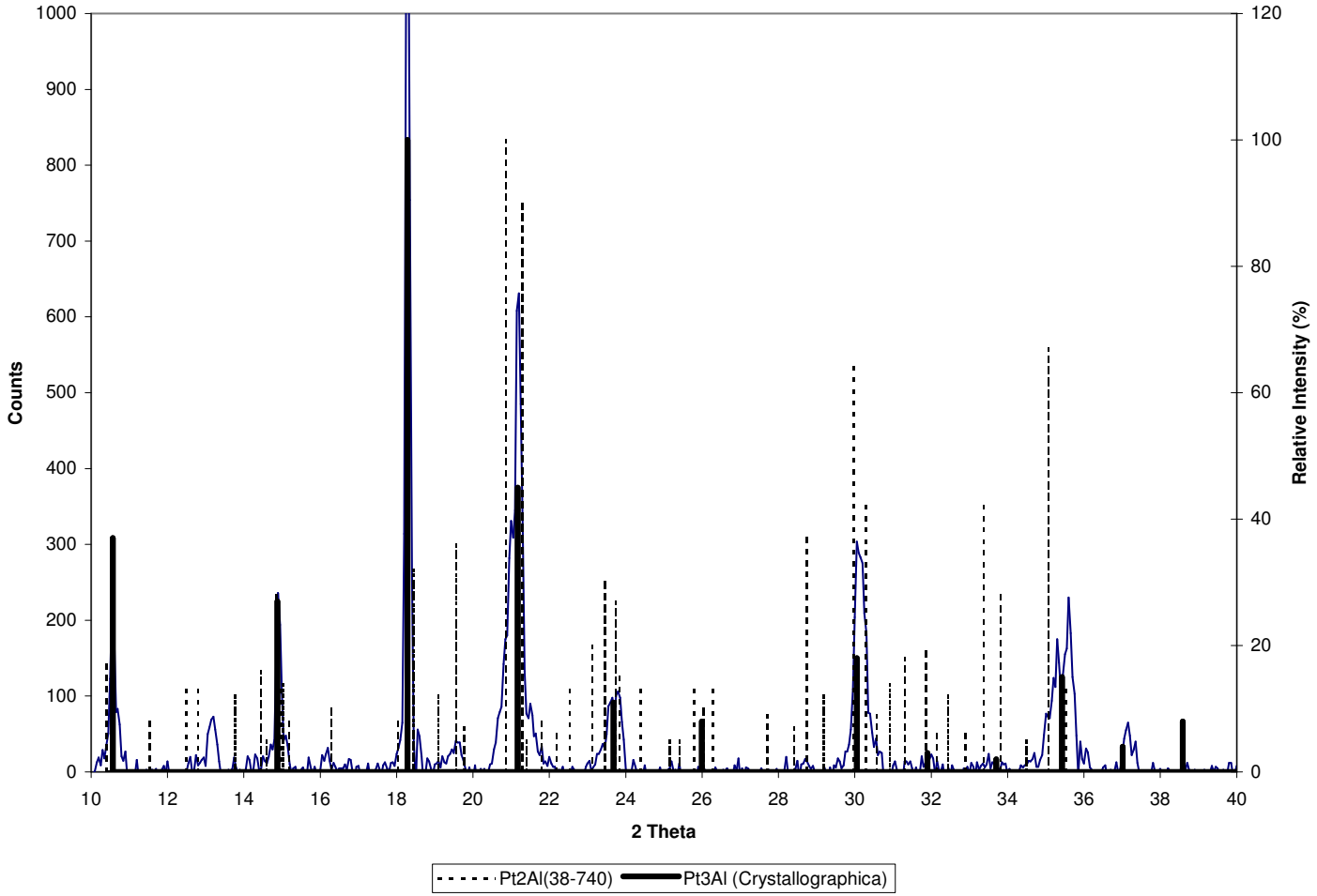

Figure 2.237. XRD pattern for nominal $Pt_{63}:Al_{22}:Cr_{15}$ after annealing at 600℃.

2.1.79. Nominal $Pt_{75}:Al_{10}:Cr_{15}$ (Actual $Pt_{33}:Al_{51}:Cr_{16}$)

This alloy had previously been shown to be $Pt_{34}:Al_{49}:Cr_{17}$ from Pt losses due to sputtering during melting. Its appearance changed considerably during annealing at 1000°C (Figure 2.184), but not during annealing at 600°C. It comprised a dark phase (dendrites) with possible precipitation within (difficult to distinguish), and a two-phase mixture of grey and light in between (Figure 2.238). The black spots were porosity in all cases, and neither (Cr) nor oxides. The as-measured EDX analyses are shown in Table 2.79, and graphically in Figure 2.239 for the scenario where the dark phase is single-phase. The compositions of the phases would suggest that the light phase is probably ~PtAl/~Pt_2Al_3 or even something richer in Pt, while the dark phase could be either ~Pt_2Al_3/~$PtAl_2$. If the dark phase is in fact a two-phase mixture, any triangle (as shown in Figure 2.240) could fit as long as the multi-phase compositions lie on the legs of the triangle. XRD analyses detected the three mentioned phases, as their peaks seemed to match the measured pattern well (Figure 2.241). Measured peaks at $2\theta \approx 28.5$ and 35 suggested the presence of some (Cr) (Figure 2.241 insert) that might have been remnant from the as-cast condition, although this was not observed. The phase identities given in Figure 2.240 seemed to be highly likely, considering the results of alloys $Pt_{43}:Al_{52}:Cr_5$ (§ 2.3.11) and $Pt_{35}:Al_{55}:Cr_{10}$ (§ 2.3.9).

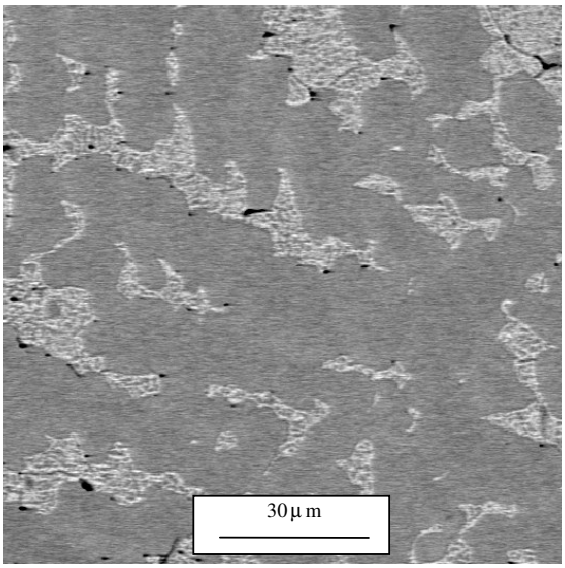

Figure 2.238. BSE-SEM image of $Pt_{34}:Al_{49}:Cr_{17}$ after annealing at 600°C: dark ~Pt_2Al_3 (+$PtAl_2$); ~PtAl+ ~Pt_2Al_3 light.

Table 2.79. Phase analyses for $Pt_{34}:Al_{49}Cr_{17}$ (at.%) after annealing at 600°C.

Phase description	**Pt**	**Al**	**Cr**	**Phase**
Overall	33.3 ± 0.2	50.4 ± 0.5	16.3 ± 0.3	-
Dark (+very dark two-phase?)	31.9 ± 0.2	53.5 ± 0.6	14.6 ± 0.6	~Pt_2Al_3 (+$PtAl_2$)
Dark+light two-phase	35.3 ± 0.4	46.7 ± 0.5	18.0 ± 0.8	~Pt_2Al_3 + ~PtAl

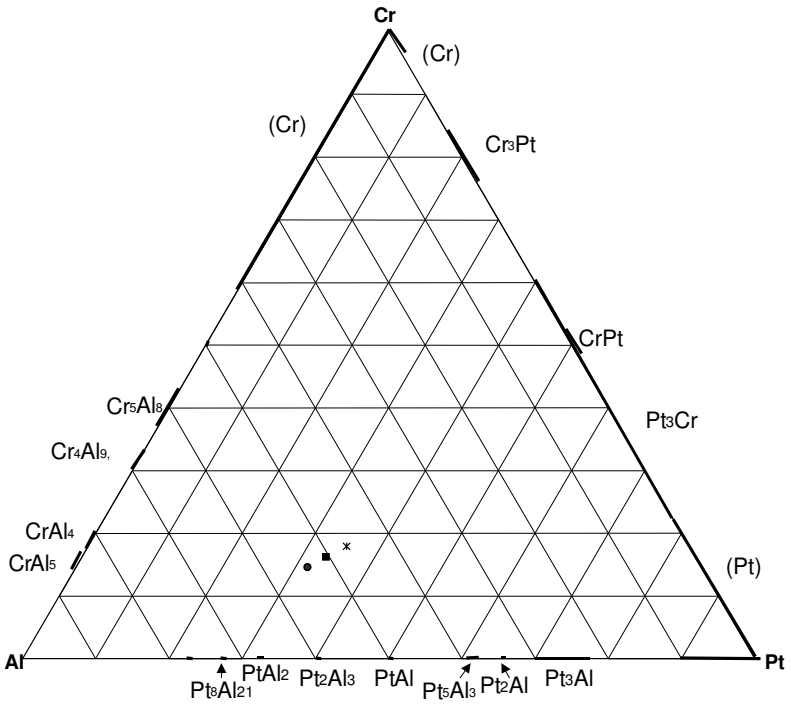

Figure 2.239. EDX analyses of $Pt_{34}:Al_{49}Cr_{17}$ (at.%) after annealing at 600°C. (■ overall composition; ● phases; ✶ eutectic/two-phase)

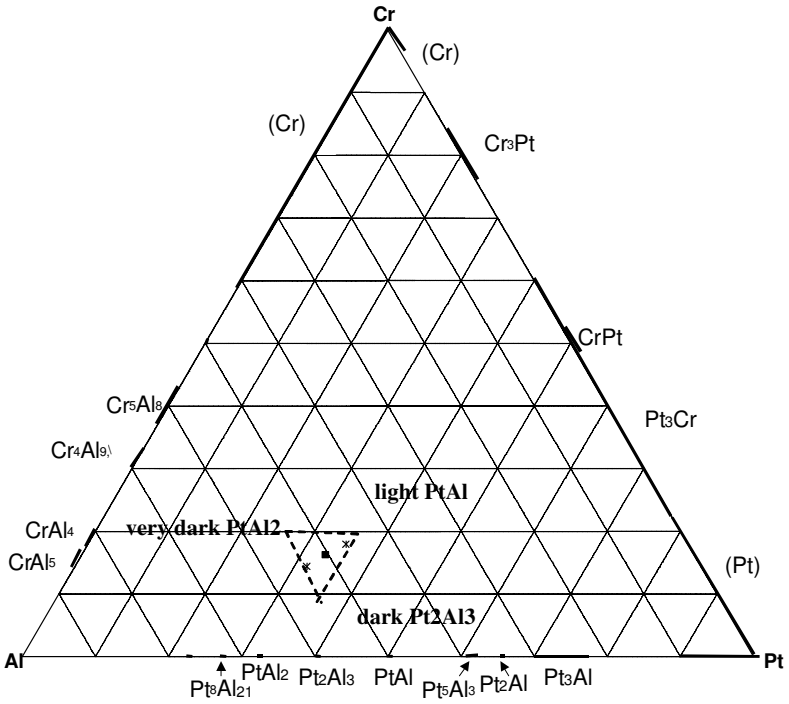

Figure 2.240. EDX analyses of $Pt_{34}:Al_{49}Cr_{17}$ (at.%) after annealing at 600°C. (■ overall composition; ---likely three-phase triangle)

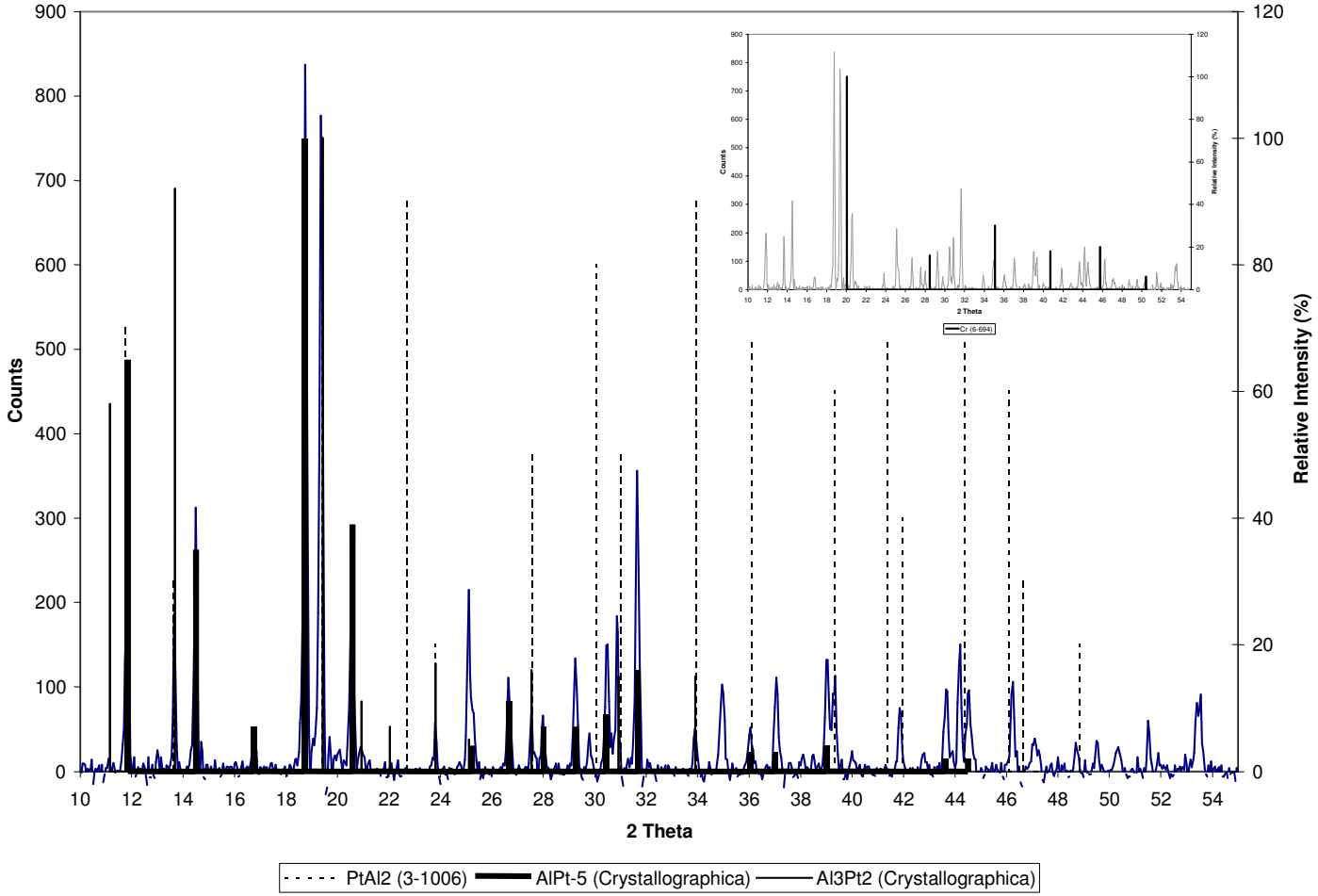

Figure 2.241. XRD pattern for Pt_{34}:$Al_{49}Cr_{17}$ after annealing at 600℃.

2.1.80. Nominal $Pt_{15}:Al_5:Cr_{80}$

Alloy $Pt_{15}:Al_5:Cr_{80}$, similar to its as-cast state in general appearance (Figure 2.110), comprised three phases: dark dendrites with grey Widmanstätten needles within (previously not observed), with a medium (grey) interdendritic phase and some small light (white) areas (Figure 2.242). The EDX analyses are given in Table 2.80, with Figure 2.243 showing the as-measured results of the EDX analyses. The white phase was too small to analyse accurately. Only area analyses were taken of the dark+grey phases. From earlier results, the white phase could possibly be ternary T1, while the dark phase was (Cr) and the grey phase either ~CrPt or ~Cr_3Pt. Unfortunately, this 600°C sample also broke during removal from the mount, and no XRD analyses could be performed. Considering all the other results, the grey phase was most likely ~CrPt. This would be in agreement with the as-cast condition, since the phase compositions had hardly changed, compared to the sample of alloy $Pt_{15}:Al_5:Cr_{80}$ annealed at 1000°C where the compositions had changed. However, it is proposed that the grey needles and the grey bulk phase were in fact not the same phase. It was found in the Pt-Cr-Ru system [2006Süs1] that grey Cr_3Pt Widmanstätten needles typically to precipitate in the (Cr) phase. This is what probably occurred here as well. Probable equilibrium tie-lines are shown in Figure 2.243 as well as a possible compositions for the dark (Cr) and white T1 phases. These tie-lines fit in very well with those of alloy $Pt_{38}:Al_{22}:Cr_{40}$ (§ 2.3.10).

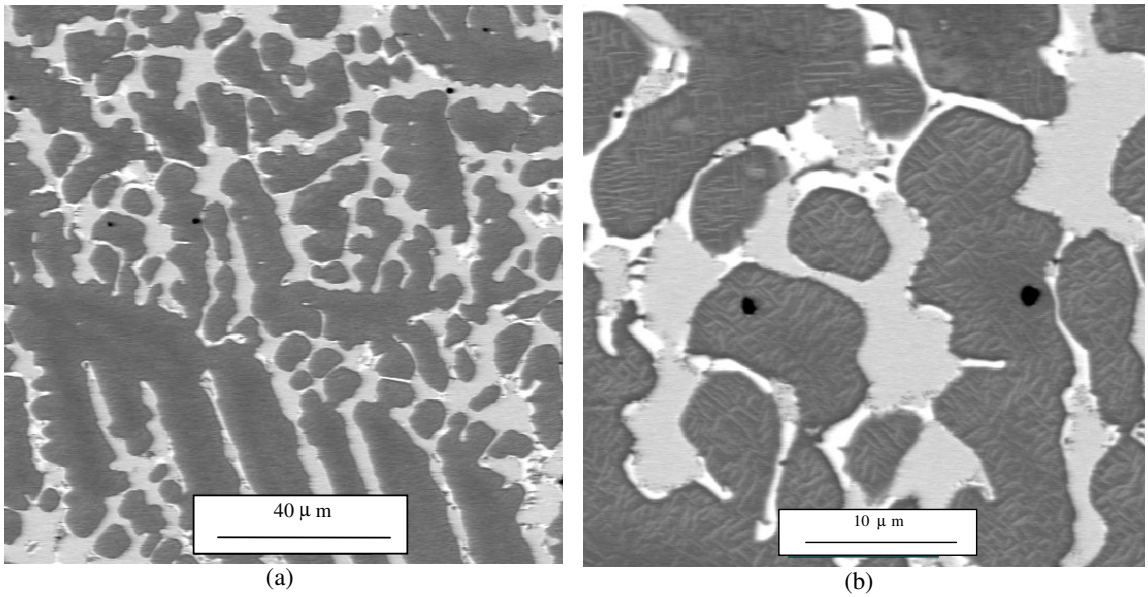

(a) (b)

Figure 2.242. BSE-SEM image of nominal $Pt_{15}:Al_5:Cr_{80}$ after annealing at 600°C: (Cr) black; ~CrPt grey bulk; ~Cr_3Pt grey needles ~T1 white.

Table 2.80. Phase analyses for nominal $Pt_{15}:Al_5:Cr_{80}$ (at.%) after annealing at 600°C.

Phase description	**Pt**	**Al**	**Cr**	**Phase**
Overall	14.6 ± 1.0	4.8 ± 0.8	80.6 ± 1.8	-
Dark*	-	-	-	(Cr)
White*	-	-	-	T1
Grey	27.5 ± 0.6	9.3 ± 0.3	63.2 ± 0.9	~CrPt
Dark + grey two-phase?	9.3 ± 0.3	2.3 ± 0.4	88.4 ± 0.6	(Cr) + ~CrPt

* Too small for analysis.

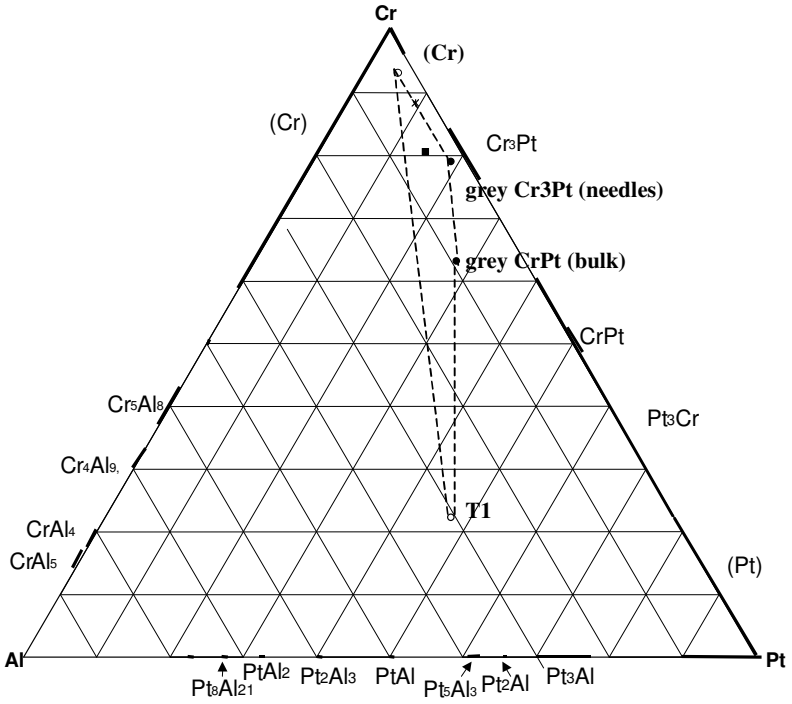

Figure 2.243. EDX analyses of nominal $Pt_{15}:Al_5:Cr_{80}$ (at.%) after annealing at 600°C. (■ overall composition; ● phases; ✶ two-phase; o presumed phase compositions)

2.1.81. Nominal $Pt_{55}:Al_{25}:Cr_{20}$

After annealing at 600°C, alloy $Pt_{55}:Al_{25}:Cr_{20}$ comprised a dark and a light phase (Figure 2.244) with black porosity, and a suggestion of very small even lighter regions within the light phase. The light phase was much more pronounced than in its as-cast state (Figure 2.124), and the dark phase did not show a needle-like structure that had been observed after annealing at 1000°C (i.e. comprising grey and light) (Figure 2.189). The EDX analyses are given in Table 2.81 and Figure 2.245. From the position of the light phase on the ternary diagram, ~Pt_2Al could be a possibility (as in the as-cast state). The dark phase could either be ~Pt_3Al or T1. The XRD results suggested that the dark phase was more likely to be T1 (Figure 2.246). ~Pt_2Al (*C*23) also seemed to be a reasonable fit for many of the measured peaks. This assessment would concur with other alloys in the same region of the ternary diagram. The presence of an even lighter phase would be inconsistent, and would suggest that if present, it was not at equilibrium.

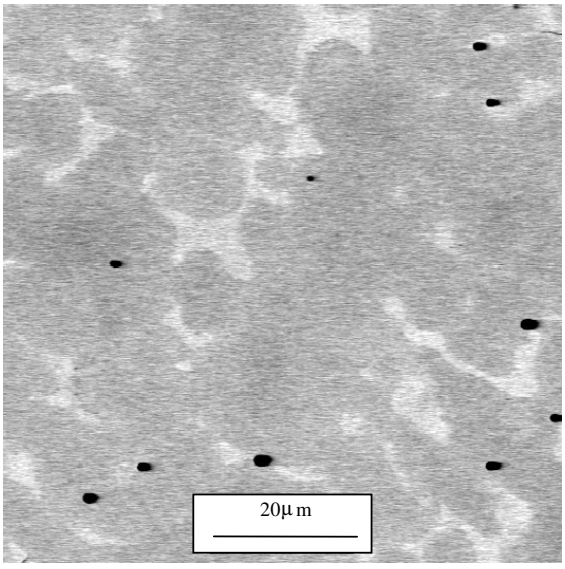

Figure 2.244. BSE-SEM image of nominal $Pt_{55}:Al_{25}:Cr_{20}$ after annealing at 600°C: T1/ ~Pt_3Al dark; ~Pt_2Al light.

Table 2.81. Phase analyses for nominal $Pt_{55}:Al_{25}:Cr_{20}$ (at.%) after annealing at 600°C.

Phase description	**Pt**	**Al**	**Cr**	**Phase**
Overall	57.3 ± 0.7	25.3 ± 0.6	17.4 ± 1.1	-
Dark	56.5 ± 1.1	23.6 ± 1.3	19.9 ± 1.5	T1
Light	60.8 ± 0.3	30.6 ± 0.4	8.6 ± 0.7	~Pt_2Al

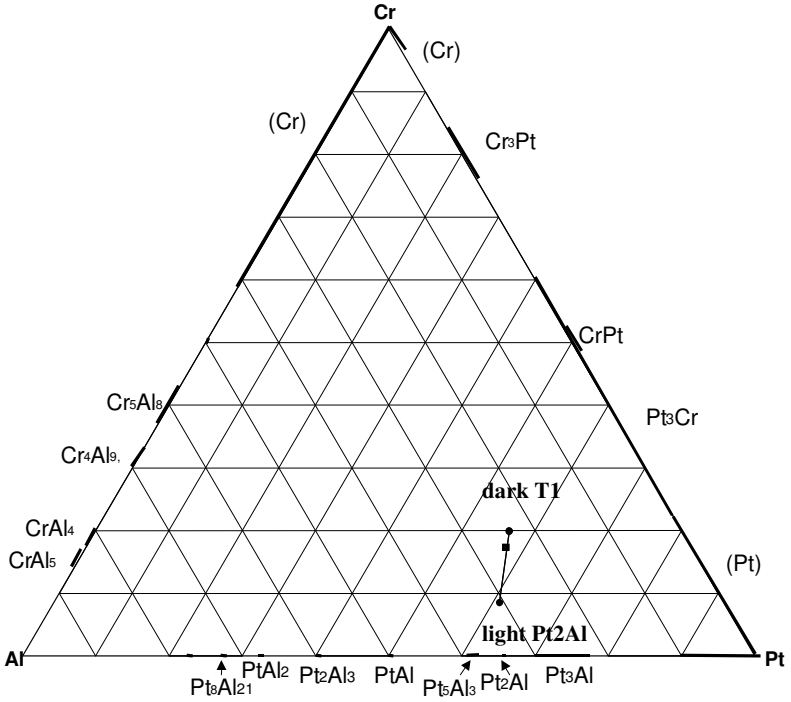

Figure 2.245. EDX analyses of nominal $Pt_{55}:Al_{25}:Cr_{20}$ (at.%) after annealing at 600°C.

(■ overall composition; ● phases)

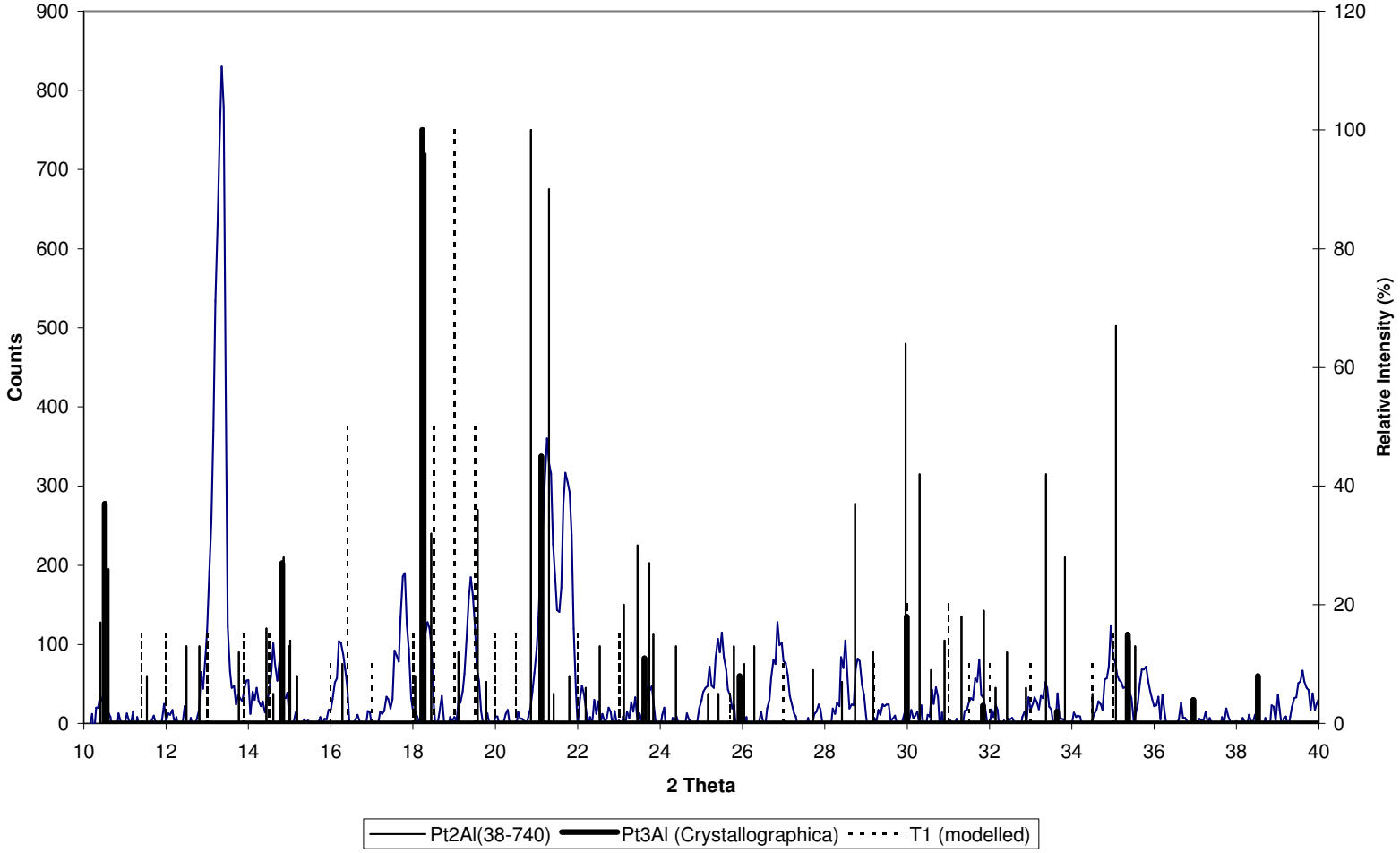

Figure 2.246. XRD pattern for nominal Pt_{55}:Al_{25}:Cr_{20} after annealing at 600℃.

2.1.82. 600 ℃ isothermal section

An isothermal section at 600°C was drawn, based on a combination of all the results as discussed in the previous section. The diagram is shown in Figure 2.247. The current interpretation seems to be the most sensible and the diagram seems to be reasonably complete and self-consistent.

The phase fields of ~Pt_3Al and T1 appeared to have reduced in size due to annealing. The homogeneity range of T1 is a mere estimation based on the results of alloys Pt_{15}:Al_5:Cr_{80} (§ 2.3.17), Pt_{50}:Al_{35}:Cr_{15} (§2.3.12), Pt_{38}:Al_{22}:Cr_{40} (§ 2.3.10) and Pt_{63}:Al_{32}:Cr_5 (§ 2.3.14). In all these cases T1 was very small, and its analyses probably compromised by interaction with surrounding phases, which, through extrapolation, would result in a smaller phase field. One would expect the phase field to be smaller at 600°C than at 1000°C.

The extension of ~Pt_3Al, ~$PtAl_2$ and ~PtAl have increased. Unlike in the 1000°C annealed condition, the microstructural and XRD evidence suggest that the slope of the ~Pt_2Al field is similar to that in the solidification projection.

The (Cr)-~$PtAl_2$ and (Cr)-~PtAl tie-lines (based on alloy Pt_{30}:Al_{50}:Cr_{20}, § 2.3.3) are drawn in dashed lines since it is not clear whether the alloy was at equilibrium or not (the (Cr) will probably disappear on further annealing). The same is true for the (Cr)-Cr_3Pt-CrPt tie-lines of alloys Pt_{18}:Al_2:Cr_{80} (§ 2.3.8) which will probably turn into single-phase ~Cr_3Pt on prolonged annealing.

The ~$PtAl_2$-~PtAl and ~$PtAl_2$-~Pt_2Al_3-~PtAl tie-lines were taken from alloys Pt_{30}:Al_{50}:Cr_{20} and Pt_{35}:Al_{55}:Cr_{10} (§ 2.3.9). Although not shown on the diagram due to uncertain compositions, the three-phase equilibria for alloy Pt_{75}:Al_{10}:Cr_{15} (Pt_{34}:Al_{49}:Cr_{17}) should also be satisfied by this configuration, suggesting an extension of PtAl up to ~20 at.%Cr.

As was the case with the solidification projection, the ~CrPt/~Pt_3Cr and ~Pt_3Cr/(Pt) boundaries are shown as dashed lines. Around the former boundary, it will be difficult to predict whether the solidified (Pt) will order to form ~Pt_3Cr or not, and around the latter it will be difficult to say and whether the ~Pt_3Cr will order to form $L1_0$ ~CrPt at lower

temperatures (below ~700°C) or not. This is based on the still generally accepted diagram given by Massalski [1990Mas]. If the diagram of Zhao et al. is correct [2005Zhao], the dashed lines in Figure 2.247 would not denote actual phase boundaries, but the estimated positions of the ~CrPt/~Pt_3Cr and ~Pt_3Cr/(Pt) two-phase regions shown in Figure 1.2.

Since no alloys with > 70 at.% Al were annealed at 600°C, the phase fields above 70 at.% Al in Figure 2.247 are based on those in the solidification projection. This should be a reasonable approximation.

To summarise, the extensions of the phases were determined to be:

- (Cr): ~ 33 at.% Al max., ~3 at.% Pt max.;
- ~Cr_3Pt: ~ 1.3 at.% Al;
- ~CrPt [$L1_0$]: ~ 9 at.% Al;
- (Pt): ~11 at.% Al max., ~ 15 at.% Cr depending on where ordering occurs;
- ~Pt_3Al [$L1_2$]: ~24 at.% Cr;
- ~Pt_2Al [HT & LT]: ~33 at.% Cr;
- ~PtAl [B20]: ~ 20 at.% Cr;
- ~Pt_2Al_3: ~5 at.% Cr;
- ~$PtAl_2$: ~26 at.% Cr;
- (Al): <1 at.% Cr and Pt;
- ~$CrAl_4$: ~ 5 at.% Pt (assumed from solidification projection);
- ~$CrAl_5$: ~ 5 at.% Pt (assumed from solidification projection);
- ~Pt_8Al_{21}: ~ 5 at.% Cr (assumed from solidification projection);
- T1: ~Pt_3Al_2Cr with ~8 at.% stability range.

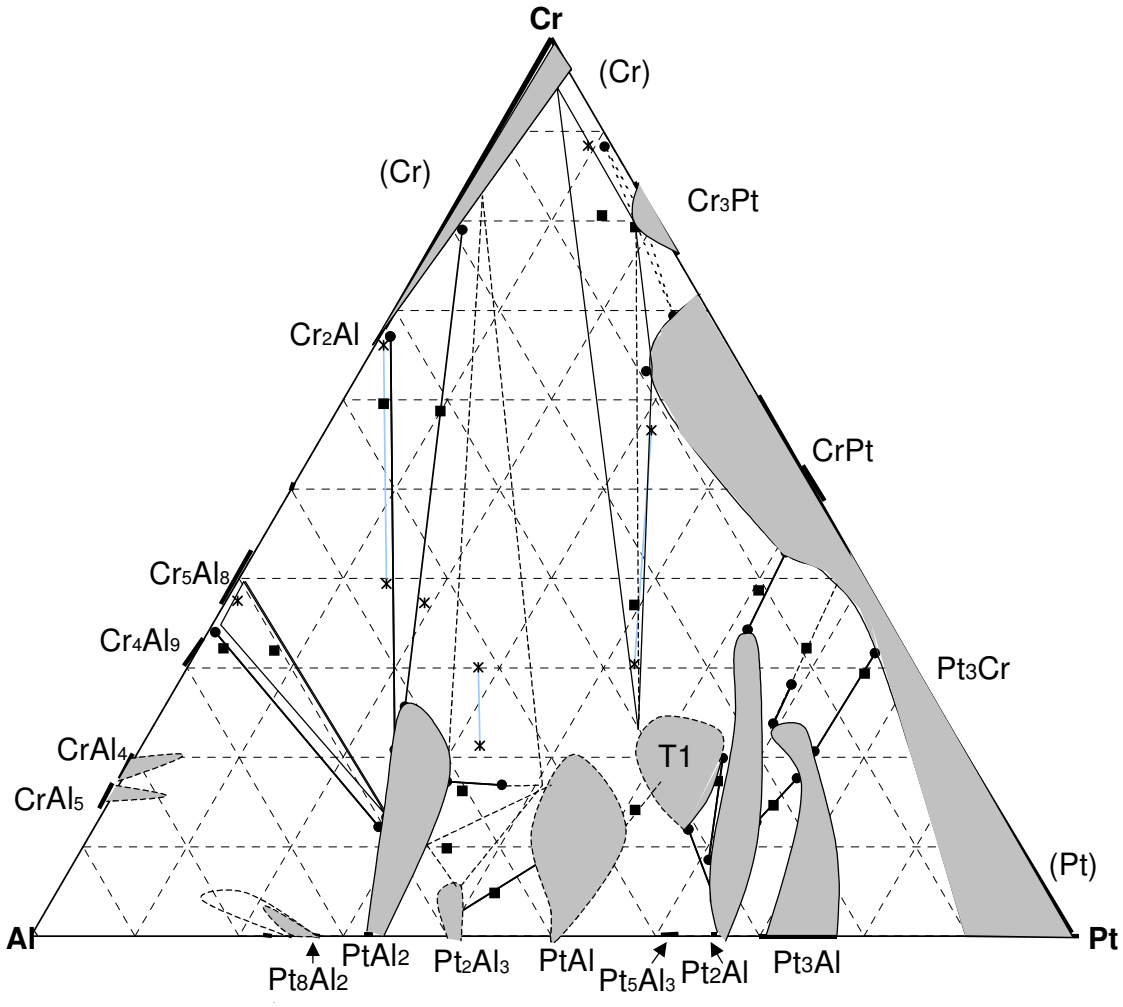

Figure 2.247. 600℃ isothermal section for Pt-Al-Cr.

3. CONCLUSIONS

- After using SEM with EDX, and XRD on a selection of alloys, the following diagrams were successfully constructed for the Pt-Al-Cr system:
  - solidification projection
  - liquidus surface projection
  - isothermal sections at 600°C and 1000°C.
- It was concluded that all phase regions were identified correctly since the results were self-consistent.
- None of the diagrams were dominated by any particular phase.

- The extension of the Pt-Al intermetallic compounds (~$PtAl_2$, ~PtAl and especially ~Pt_2Al and ~Pt_3Al) were surprisingly significant, compared to those of the Cr-Al system. ~20-30% solubility of Cr in was found in most cases except for ~Pt_8Al_{21} and ~Pt_2Al_3.
- Three ternary phases were found:
  - T1: A true ternary phase for which none of the XRD patterns of the phases in the three binary phases was a good match to its measured pattern.
  - T2: A phase with crystal structure similar to that of ~Cr_3Al_2 (a compound listed by the JCPDS database).
  - T3: A phase with crystal structure similar to that of ~$CrAl_3$ (a compound listed in Pearson's Handbook [1985Vil] and modelled accordingly with *Crystallographica*).
- The ~CrPt/~Pt_3Cr and ~Pt_3Cr/(Pt) boundaries were shown as a dashed lines, indicating the uncertainty of where the ordering reactions according to the binary Cr-Pt phase diagram given by Massalski [1990Mas], occur. According to the new proposed diagram by Zhao et al. [2005Zhao], the ordering reaction

  $$(Pt) \rightarrow Pt_3Cr \rightarrow CrPt$$

  does not occur, but fcc (Pt) orders to either CrPt or Pt_3Cr depending on the composition. If this was the case, the dashed lines would not denote actual phase boundaries, but the estimated positions of the ~CrPt/~Pt_3Cr and ~Pt_3Cr/(Pt) two-phase regions shown by Zhao et al. in Figure 1.2.
- As many as 19 ternary invariant reactions were identified in the Pt-Al-Cr system.
- In agreement with the experimental phase diagram of Pt-Cr-Ru [2004Süs1, 2005Süs, 2006Süs1], Cr-Ni-Pt [2005Nzu] as well as the results of NIMS [2004Gu], the two eutectic temperatures in the published Pt-Cr system [1990Mas] are the wrong way around. This was shown by alloy Pt_{10}:Al_{80}:Cr_{10} (§ 2.1.4) where ~Cr_3Pt formed peritectically, and then (Pt).
- Single-phase alloys suggested the congruent melting of T1, which confirmed a ternary phase, rather than a peritectically formed binary phase. The primary phase field of T1 in the liquidus projection was significant in size.
- For the purpose of this thesis the XRD pattern for T1 was merely approximated by identifying the obvious peaks that several alloys containing T1 had in common (Figures 2.31 and 2.32 in § 2.1.9). Work is being done to get more precise crystallographic data for the phase [2007Ngw].